ORNL-3153
Chemical Separations Processes for
Plutonium and Uranium
TID-4500 (16th ed., Rev.)

CHEMICAL TECHNOLOGY DIVISION

ANNUAL PROGRESS REPORT

FOR PERIOD ENDING MAY 31, 1961

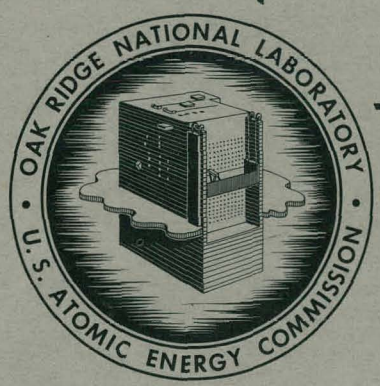

OAK RIDGE NATIONAL LABORATORY
operated by
UNION CARBIDE CORPORATION
for the
U.S. ATOMIC ENERGY COMMISSION

DISCLAIMER

Printed in USA. Price $2.75. Available from the
Office of Technical Services
Department of Commerce
Washington 25, D.C.

ORNL-3153

Contract No. W-7405-eng-26

CHEMICAL TECHNOLOGY DIVISION

ANNUAL PROGRESS REPORT

for Period Ending May 31, 1961

F. L. Culler – Division Director
D. E. Ferguson – Chemical Development Section A Chief
R. E. Blanco – Chemical Development Section B Chief
K. B. Brown – Chemical Development Section C Chief
M. E. Whatley – Unit Operations Section Chief
H. E. Goeller – Process Design Section Chief
J. C. Bresee – Pilot Plant Section Chief

DATE ISSUED

SEP 21 1961

OAK RIDGE NATIONAL LABORATORY
Oak Ridge, Tennessee
operated by
UNION CARBIDE CORPORATION
for the
U. S. ATOMIC ENERGY COMMISSION

THIS PAGE

WAS INTENTIONALLY

LEFT BLANK

SUMMARY

1. POWER REACTOR FUEL PROCESSING

Chemical Processes for Stainless Steel–Containing Fuels

Cold laboratory and engineering-scale development of the Darex process for stainless steel–containing reactor fuels was completed except for final refinement of the room-temperature NO_2 sparging method of chloride removal from Darex solutions and possibly additional studies of off-gas composition. In decladding tests with stainless steel–clad ThO_2-UO_2 fuel samples irradiated to 25,000 Mwd/ton the uranium loss increased with burnup, to ~3%; the thorium loss was 0.1% at all burnups. These results show that Darex cannot be used as a decladding method for ThO_2-UO_2 fuels.

Uranium losses to initial decladding solutions resulting from Co^{60} gamma radiation were twice the oxidation losses, 0.30 vs. 0.15%, but in final Darex solutions oxidation was controlling, 0.90 vs. 0.25% for 3 hr exposure.

Removal of chloride from Darex solutions by NO_2 sparging at ~25°C produced solutions containing ~40 ppm chloride when 2000% excess NO_2 was used; better contacting methods are being studied to decrease the amount of NO_2 required.

Cold laboratory and engineering-scale development of the Sulfex process was also completed. In Sulfex decladding of UO_2-ThO_2 samples irradiated to 20,000 Mwd/ton, uranium and thorium losses were less than 0.4 and 0.2%, respectively. Losses were independent of burnup. In initial solution, uranium losses were increased 5-fold by Co^{60} gamma irradiation and 17-fold by oxidation, to 0.86 and 0.29%, respectively; losses in final solution were not materially affected by either oxidation or radiation.

Dissolution studies with high-density UO_2–6% ThO_2 pellets in Thorex dissolvent showed that 35 hr is required for a cyclic dissolution process operated with 5% oxide heel.

Modified Zirflex Process for Zirconium-Containing Fuels

The modified Zirflex process, in which uranium-zirconium alloy fuel is dissolved in 6 *M* NH_4F–1 *M* NH_4NO_3–H_2O_2, was demonstrated with unirradiated fuel, on a small engineering scale. The optimum H_2O_2 concentration was 0.01 *M*, continuous addition being required to prevent uranium precipitation. A dissolution flowsheet for the TRIGA fuel (8% U–91% Zr–1% H) was demonstrated, 11 hr being required for core dissolution with an initial dissolution rate of 30 mg cm^{-2} min^{-1}. The off-gas contained 10% H_2 and 88% NH_3. The dissolution of the PWR Seed 3, 34% UO_2–65% ZrO_2, was unsatisfactory, 0.04 mg cm^{-2} min^{-1} in 12 *M* NH_4F–1 *M* H_2O_2. The rate in boiling 12 *M* HF was 3.3 mg cm^{-2} min^{-1}.

Anhydrous Hydrochlorination Processes

A Zircex flowsheet for processing the TRIGA fuel (8% U–91% Zr–1% H) was developed. The aluminum cladding is reacted with HCl-N_2 at 300°C to produce volatile $AlCl_3$, and the U-Zr-H is reacted with HCl at 600°C and then with CCl_4-N_2 at 550°C. The uranium chloride residue can be either dissolved in 13 *M* HNO_3 to produce 0.1 *M* uranium solution or fluorinated at 200°C to UF_6. The graphite end plugs are burned in oxygen at 750°C.

An oxyhydrochlorination process developed for the U–10% Mo fuel of the CPPD Core 1 provides for mechanical decladding and washing free the Na bond. Ninety percent of the molybdenum is removed by 15% HCl–air at 400°C, another 3 to 6% is removed by pure HCl at 400°C, and chloride is removed by converting the uranium to U_3O_8 with 0.6% H_2O in air at 100 to 400°C. The U_3O_8 is dissolved in nitric acid to produce a 1 *M* uranium solution containing 175 ppm of chloride.

Processes for Graphite-Based and Uranium Carbide Fuels

In tests on the 90% HNO_3 disintegration-leach process for graphite-uranium fuels with fuel containing 3 to 12% uranium, 0.001% burnup, 44, 30,

and 20% of the Ce^{144}, Zr^{95}, and Ru^{106}, respectively, were not leached from the graphite in two 4-hr digestions. The amount of Cs^{137} retained varied from 7 to 81%. The uranium loss at boiling for 12% uranium fuel was 0.03% and for 3% uranium fuel was 0.7%, the same as for unirradiated fuel. Losses at 25°C were about twice these values. The mean particle size of the residue was 200 to 400 μ, with ~0.25% <10 μ after 1 day's contact and ~1% <10 μ after 4 days' contact. In filtration studies the filtration rate, with >6 in. Hg vacuum, was 60 gal ft^{-2} hr^{-1} with a 1-ft-deep graphite cake.

Combustion of 0.001% burned up graphite-uranium fuel in oxygen at 900°C volatilized most of the Ru^{106}; however, that which did not plate out in cool parts of the equipment was quantitatively absorbed in NaOH solution. No Zr^{95}, Cs^{137}, or Ce^{144} was volatilized. The 90% HNO_3 process is not applicable to graphite fuel containing Al_2O_3-coated UO_2 particles; <1% of the uranium was leachable. Combustion of this fuel resulted in a uranium recovery of only 10% when the ash was treated 8 hr in boiling 10 *M* HNO_3. Combustion of fuel with coated Si-SiC was more satisfactory; losses varied from 0.35 to 2% as the coating thickness was varied from 3 to 30 mils.

The off-gas from dissolution of uranium monocarbide in 4 *M* HNO_3 was principally NO and CO_2 and no H_2 or hydrocarbons were produced. Dissolution of uranium carbide in water and HCl produced ~85% methane and 10% H_2.

Process Studies on Advanced Mixed Oxide and Metal Fuels

Hastelloy X, which may be used as a cladding material for the GCRE and MGCR fuels, dissolved at a rate of 28 mg cm^{-2} min^{-1} in 2 *M* HNO_3–4 *M* HCl. Boiling 6 to 13 *M* HNO_3 dissolved 99.8% of the UO_2 and 50% of the BeO from 30% BeO–70% UO_2 GCRE fuel pellets in 6 to 7 hr; however, 50 hr was required to dissolve all the BeO. In 6 *M* HNO_3–3 to 7 *M* H_2SO_4, 80% of the BeO dissolved in 6 to 7 hr. With the MGCR fuel, 61% UO_2–39% BeO, 24 hr leaching in 8 *M* HNO_3 was required to recover the uranium quantitatively. The UO_2-BeO fuels containing <10% UO_2 dissolved much more slowly, the highest rate being 1.7 mg cm^{-2} min^{-1} with boiling 5.8 *M* NH_4HF_2.

The uranium leaching rate from sintered UO_2-Al_2O_3 pellets by nitric acid was feasible for high-UO_2-content fuel but too low for low-UO_2-content fuel. The uranium loss for UO_2–4% Al_2O_3 was 0.002%, but 88% for a fuel containing 61% Al_2O_3. Hydrofluoric acid and 5 *M* HNO_3–5 *M* HCl were equally ineffective for high Al_2O_3 contents.

Beryllium metal dissolved in boiling 4 *M* H_2SO_4, 6 *M* NaOH, and 6 *M* HNO_3–0.1 *M* NaF at rates varying from 2 to 63 mg cm^{-2} min^{-1}. Niobium metal reacted with anhydrous chlorine at 360°C at a rate of 28 mg cm^{-2} min^{-1} and with 9 *M* HF–3 *M* HNO_3 at a rate of 35 mg cm^{-2} min^{-1}; rates in other reagents generally were low.

Corrosion Studies

Final corrosion tests indicated that titanium is satisfactory for dissolution of thorium fuels but cannot be used in the condenser for continuous refluxing. Under modified Zirflex conditions, LCNA was corroded at an over-all rate of 1.15 mils/month and was superior to Hastelloy F and types 304L and 309 SNb stainless steel.

In Zircex tests in which specimens of Haynes 25, Inor-8, Nichrome V, and Pyroceram were exposed to 15% HCl–85% air at 400°C and to HCl at 350°C, all the above alloys were satisfactory.

Tests to determine the best material for handling Darex, Zirflex, Thorex, and Purex solutions at room temperature, such as might be required for a universal centrifuge, indicated that Hastelloy F with a maximum rate of 0.7 mil/month in Purex service was superior to Titanium-45A, Hastelloy C, LCNA, and Carpenter 20 SNb.

In corrosion tests on glass Raschig rings, for possible use in criticality control during storage of uranium and plutonium solutions, 4% boron glass samples exposed to 2 and 6 *M* HNO_3 at 23 and 65°C were satisfactory but 5.8% boron glass and titania-coated 5.8% boron glass were unsuitable.

Solvent Extraction Studies

In a large number of 2-in.-dia pulsed column runs to determine optimum operating conditions for the acid Thorex flowsheet, with both sieve and nozzle plates and with both a top and a bottom interface, losses, HETS data, and flooding values were obtained for extraction, partitioning, and stripping. A uranium product concentration of 20 g/liter was achieved by refluxing uranium in the stripping column and top of the partitioning column. The uranium loss to the thorium product was 0.054%, and the thorium loss was 0.03%. It was found that

plant capacity can be increased with no sacrifice in fission product decontamination by increasing the thorium feed concentration from 260 to 325 g/liter and increasing either the TBP volume or concentration.

The optimum point for addition of 14 *M* HNO_3 for salting was found to be four stages below the feed addition point. Addition at this point rather than at the feed point gave a 10-fold increase in ruthenium, zirconium, and niobium decontamination and an 8-fold decrease in thorium loss.

The use of dibasic aluminum nitrate for partitioning the uranium from the thorium was demonstrated. This innovation simplifies the subsequent thorium second cycle feed adjustment and results in a more concentrated uranium product.

Irradiation of the feed in a Co^{60} gamma field to 5 whr/liter decreased the over-all decontamination factor by <2, and irradiation to 65 whr/liter increased decontamination by ~4.

Both boron and cadium, which are being considered as soluble poisons for criticality control, were satisfactorily removed by solvent extraction. The boron and cadmium contents of the extraction product were <7.8 and <0.4 ppm, respectively.

The first cycle raffinate was satisfactorily concentrated to 6% of its original volume by evaporation to 1.3% for HNO_3 recovery and dilution with water back to 6%. This is equivalent to 0.2 liter per kilogram of thorium processed and is a 10-fold improvement over the aluminum-salted Thorex flowsheet.

Tests with the second uranium solvent extraction cycle demonstrated that, due to increase in solvent saturation, decontamination from fission products does not decrease between 2.5 and 15% TBP when nitric acid is the salting agent. About 99% of the thorium in the concentrated U^{233} product was removed on Dowex 50W resin.

In high-activity tests, 0.1% of the CETR fuel activity (25,000 Mwd/t), decontamination factors for ruthenium, zirconium-niobium, and rare earths were 10^4, 5×10^3, and 2×10^5, respectively.

In studies on the chemistry of zirconium and niobium extraction, it was found that at least two species of zirconium are present in 2 *M* HNO_3 and that the distribution coefficient of 0.12 for the more extractable form in 30% TBP in dodecane is constant for contact times of 5 to 60 min. More than 90% of the niobium was adsorbed on Vycor glass powder from zirconium solutions containing zirconium-niobium tracer.

Mechanical Processing

The mechanical dejacketing facility for the SRE Core 1 fuel was completed and tested with unirradiated fuel, and operation with irradiated fuel was started. The fuel was removed from the stainless steel jackets at a rate of 2 to 3 kg/hr, washed free of NaK, and recanned in aluminum for shipment off-site for subsequent processing. The interior surfaces of the empty jackets were scraped free of NaK with a plastic rabbit, flattened, rolled into coils, and removed to the burial ground. The processing rate attained thus far is about 30% of that expected.

The 250-ton fuel shear was installed with the leacher and auxiliary equipment in Bldg. 3019, and testing with nonirradiated material was started. In a large number of laboratory countercurrent dissolving experiments with UO_2 pellets to simulate leaching, 3 to 4 stages were required to attain steady-state operation. At steady state the product solution uranium concentration varied from 300 to 500 g/liter and the acidity from 1.2 to 3.2 *M* H^+, composite values being 410 g/liter and 2.3 *M*.

Engineering Studies

A critically safe shipping cask for U^{233} was designed and constructed which permits shipment of up to about 30 kg of U^{233} at a uranium concentration of 225 g/liter. A neutron multiplication test performed during filling gave a maximum source multiplication of 4 to 5, which indicates an effective multiplication constant of <0.8. A conventional tank containing boron-glass Raschig rings is being installed which permits storage of 60 kg of U^{233} at a uranium concentration up to 200 g/liter.

2. FLUORIDE VOLATILITY PROCESS

Processing of Uranium-Zirconium Alloy Fuel

Seven complete batch flowsheet runs, including dissolution of zirconium-uranium alloy, 400 to 600 g of uranium per batch, in molten $NaF\text{-}LiF\text{-}ZrF_4$ with HF, and fluorination to UF_6, were made in the Fluoride Volatility Pilot Plant. Dissolution rates were >3.5 kg/hr with an HF flow rate of 150 g/min. Nonrecoverable uranium losses averaged less than 0.8 g per run, and total cation impurities in the UF_6 product were less than 320 ppm. Corrosion in

the dissolver in 14 runs was ~20 mils overall.

NaF sorption bed studies indicated that the film and solid phase diffusions of UF_6 and the heat transfer rates between the solid and the gas stream are sorption rate-controlling processes. The mass transfer film coefficient for UF_6 has a value of ~0.05 cm/sec and the solid phase diffusivity of UF_6 is $\sim 10^{-5}$ cm^{-2} sec^{-1}. Average zirconium dissolution rates in the Inor-8 prototype dissolver were correlated satisfactorily by the equation $r = k\nu^{-1/3} \ln (W/0.40)$ where ν is the kinematic viscosity and W the HF flow rate.

Application to Stainless Steel–Containing Fuel and Pu Recovery

Laboratory studies on dissolution of stainless steel and of various oxides in fused fluorides and on volatilization of PuF_6 as well as of UF_6 from such melts indicated the feasibility of fluoride-volatility processing of a wide variety of reactor fuels.

3. MOLTEN SALT REACTOR FUEL PROCESSING

Fluorination

Uranium recoveries of ~98% were obtained from NaF-ZrF_4-UF_4 salts containing 1 and 0.2 wt % uranium by fluorination in a one-stage laboratory-scale steady-state fluorinator. The carrier salt (63-37 mole % LiF-BeF_2) dissolved in stirred, boiling 90% HF–10% UO_2 at an initial rate of $\geq$50 mils/hr, but the rate decreased to <10 mils/hr as a layer of undissolved BeF_2 was left on the surface.

Carrier Salt Recovery

Solvents of SbF_5 in HF were investigated for blanket salt decontamination. With LiF the compound $LiSbF_6$ was formed, with a solubility of 0.23 mole per liter of HF. Rare earths formed a complex with SbF_5 that was soluble to the extent of 200 to 300 g of rare earths per liter of HF, but ThF_4 was insoluble.

4. HOMOGENEOUS REACTOR FUEL PROCESSING

Multiclone System Studies

Development work on aqueous homogeneous reactor fuel processing was concluded with termination of the Homogeneous Reactor Project.

Hydroclone performance studies, in both out-of-pile tests and at the HRT Chemical Plant, demonstrated that multiple hydroclone units could not be operated satisfactorily with induced underflow. A significant lowering of the efficiency offset all gains. When the fuel was processed through hydroclones on a 10-min cycle, solids collection rates were as high as production rates from corrosion, but with large reactors such short cycles necessitate a large and complex processing system. Periodic, infrequent descaling of heat exchanger surfaces may be a more attractive processing scheme than rapid, continuous hydroclone processing. For either method, nuclear poisons are controlled at very low levels by solubility effects and mechanisms which deposit solids on pipe walls outside the reactor core.

Fuel Processing by Uranyl Peroxide Precipitation

Rapid processing of reactor fuel to limit the accumulation of nickel by batch precipitation of uranyl peroxide was tested in the laboratory and demonstrated in full-scale, 4-kg engineering tests. The 4-kg batches of natural uranium were processed in geometrically safe equipment with uranium losses of 3% and decontamination factors of 100. The process may be carried out in an ordinary fuel–D_2O system without addition of potential contaminants. The engineering system was on the scale required for large power stations.

Related Systems

The charcoal off-gas absorber beds were satisfactorily operated with the system below atmospheric pressure to decrease the potential hazard of a leak in the off-gas system.

5. WASTE TREATMENT AND DISPOSAL

High-Activity Waste Treatment

Synthetic nonradioactive Purex, Darex, and TBP-25 wastes were successfully evaporated and calcined in both bench-scale (18- by 4-in.-dia) and engineering scale (82- by 8-in.-dia) pots. Sulfate volatility from Purex waste was only 0.2 to 0.7% when 10% excess sodium, magnesium, or calcium was added to form thermally stable sulfate salts. The nitrate content of the calcined solid varied from 60 to 500 ppm. Control of a 25-liter continuous evaporator with direct feeding of the pot

calciner was satisfactorily demonstrated in two runs. In the bench-scale equipment, ruthenium volatility from Purex waste was decreased to background counting levels, 0.03%, by making the waste 1.5 *M* in phosphite.

Glasses were prepared from Purex waste by adding borate and phosphate as fluxing agents in addition to sodium and magnesium or calcium to prevent sulfate volatility. The best product contained 22.2, 30, 5, and 8.9 wt %, respectively, of SO_3, P_2O_5, B_2O_3, and MgO and had a density of 2.7 g/cc. About 5.5 gal of this glass would contain the waste oxide from 1 ton of uranium. The initial leach rate in water was less than 10^{-5} g cm^{-2} day^{-1} after 1 week in spite of the high sulfate content. The phosphate can be formed by adding phosphite to the nitrate waste, thus achieving control of ruthenium volatility at the same time.

Conceptual design of a pot calcination pilot plant indicates an initial cost of $1,000,000 for purchase and installation of equipment in existing cells at Idaho. A cost of $1,500,000 was estimated for construction of a new building for installation of this equipment at ORNL.

Low-Activity Waste Treatment

Bench-scale tests of a scavenging-ion exchange process using phenolic resins showed that ORNL low-activity wastes can be decontaminated to the maximum permissible concentration recommended for populations in the neighborhood of atomic energy installations. More than 99.9% of the cesium and strontium were removed from 1500 resin bed volumes of waste by sorption on either sulfonic-phenolic or carboxylic-phenolic ion exchange resins; these resins were regenerated with 10 resin bed volumes of 5 *M* HCl or 0.5 *M* HNO_3, respectively. A small test unit (60 liters/hr) was started up to determine the efficiency of the system on actual waste. A pilot plant (10 gal/min) is scheduled for startup in August.

A study of interim waste storage costs for tanks showed that for storage times of 0.5 to 30 years, costs ranged from 2×10^{-3} to 9.3×10^{-3} mil/kwh_e for acidic wastes, and from 1.5×10^{-3} to 4.7×10^{-3} mill/kwh_e for neutralized wastes.

6. PILOT PLANT DECONTAMINATION

The activity level in the Radiochemical Processing Pilot Plant, following an explosion in November 1959, was decreased to an average level of from 80 to 20,000 d/m/100 cm^2 prior to bonding the activity with paint. A total of 1.5 kg of plutonium was flushed from the processing equipment, of which 1.1 kg was recovered.

7. GCR COOLANT PURIFICATION STUDIES

Oxidation by O_2 or CuO

Kinetic studies of the oxidation of contaminants in a simulated helium coolant stream resulted in design data for either a catalytic oxidizer or a copper oxide oxidizer. Data from the catalytic studies were empirically correlated to give reactor design equations, and the copper oxide oxidizer data were fitted to a theoretical model which can be used in reactor bed design. The theoretical model for the heterogeneous reaction with copper oxide was postulated to be a combination of gas film and molecular diffusion in the porous solid.

Design of Helium Purification System

A purification system was designed for the proposed Pebble Bed Reactor Experiment coolant gas, consisting of a delay trap for fission product gases, an oxidizer for chemical contaminants, an adsorber for the oxidation products, and an absolute filter for particulate removal.

8. EQUIPMENT DECONTAMINATION

Several improvements in stability and effectiveness were made in the oxalate-peroxide solution recommended as a general decontaminant and UO_2 solvent for the GCR charge and service machines. Peroxide, 0.1 *M*, was shown to be a corrosion inhibitor for stainless steel in fluoride, sulfate, oxalate, and citrate solutions. Homogeneous reactor scale was dissolved from a rupture disk of the HRT by inhibited phosphoric acid, and further decontaminated to its Co^{60} background radiation by oxalic acid–hydrogen peroxide.

9. HRP THORIA BLANKET DEVELOPMENT

Preparation of ThO_2 Pellets

Strains leading to cracking in rounded thoria pellets, fabricated by automatic pressing and calcination of ThO_2 powder, were decreased by prefiring the powders to 1200°C prior to granulation, minimizing the curvature of the punch face, and holding the pressed pellets at 1200 to 1300°C for

1.5 to 2 hr before final firing at 1750°C. Weight losses in attrition tests on thoria particles prepared by the sol-gel process were due to grinding off of edges and sharp points. Slight, but consistent increases in density were observed in ThO_2 gels fired in hydrogen over those fired in air. Firing at 1150 to 1200°C increased the ThO_2 density slightly more than at 1200 to 1250°C.

Development of Gas Recombination Catalyst

The catalytic activity of the sol-prepared palladium catalyst is more than sufficient to recombine the radiolytic gas (at 100 psi D_2 partial pressure) produced in a thoria-urania blanket slurry at the 10-kw/liter power level expected in a breeder blanket. Out-of-pile tests with a slurry (782 g Th/kg D_2O, 1460 ppm Pd/Th) proposed for an in-pile slurry corrosion experiment at 26 watts/ml power level indicate a catalytic activity sufficient to maintain the radiolytic D_2 gas pressure at <100 psi at 280°C. Gas recombination data obtained with palladium-containing slurries at oxygen partial pressures greater than 200 psi agreed with a kinetic expression showing a first-order dependence on hydrogen and a 0.5 order dependence on the oxygen partial pressure. At lower oxygen partial pressures or H_2/O_2 ratios >1 the kinetic expression did not hold and catalytic activity was enhanced.

Calibration of the gas injection apparatus used in the gas recombination catalyst development studies showed unsuspected gas holdup in the capillary tubing connecting the gas charging system to the reaction autoclave. Re-evaluation of previous rate data obtained in this system prior to calibration with slurries containing the sol-prepared palladium catalyst showed little or no deactivation of the catalyst by excess oxygen and complete reaction of deuterium (or hydrogen) and oxygen in the presence of the slurry-catalyst.

Thorium Oxide Irradiations

Examination of a settled bed of 50 thoria pellets irradiated 2900 hr in D_2O in the LITR at 250°C and a thermal flux of $\sim 2 \times 10^{13}$ n cm^{-2} sec^{-1} showed 20 of the pellets broken into fragments and fines. The remainder had essentially the same bulk density as the original material but showed some damage from chipping out of surface fragments and breaking off of spherical segments. All surfaces were porous, and a black, carbonaceous, vitreous-appearing substance, about 1 wt % of the recovered solids, was found in the upper half of the irradiation autoclave. This was probably a carbon residue from the polyvinyl alcohol binder used in the pellet fabrication.

A D_2O slurry of classified thorium–0.4% U^{235} oxide irradiated in a settled condition at 280°C in the LITR to a total nvt of 5×10^{19} n/cm^2 showed pronounced particle damage. Twelve percent of the irradiated material (initially 2.1 μ average size and 0.5% <1 μ) was recovered as a dispersed suspension with an average particle size of 2500 A. A portion of the material (≧6%) that had settled to the bottom of the autoclave and been resuspended by stirring had an average size of 1.6 μ but a very steep size distribution curve, indicating that nearly all the original material had suffered particle damage.

A review of the particle size information obtained in 18 slurry irradiations over the past several years suggests pronounced particle damage in some cases; some oxide preparations have greater radiation damage resistance than others.

10. FUEL CYCLE DEVELOPMENT

Sol-Gel Process for ThO_2-UO_2 and ThO_2

Thoria-urania particles containing 4.4 wt % of 93% enriched uranium prepared by the sol-gel process had a particle density of 9.93 g/cc, compared to the theoretical 10.035 g/cc and were compacted in tubes by air vibration to bulk densities of 8.7 g/cc. The tubes were sealed and placed in the NRX reactor in March. A method for preparing sols from oxides derived by steam denitration of thorium nitrate gave high-density thoria-urania particles. Thoria particles were prepared similarly.

Material suitable for dispersion to a sol was prepared on an engineering scale in an agitated-trough steam stripper. The density of the final particles increased as the N/Th mole ratio of the denitration product increased from 0.05 to 0.10.

Modified Sol-Gel Process for UO_2

Ten grams of dense (10.6 g/cc) urania gel particles was prepared by evaporation and calcination of a hydrous uranous oxide precipitate from uranous formate solution.

11. TRANSURANIUM ELEMENT STUDIES

Isotope Production Calculations

Irradiation calculations for production of Cf^{252} have shown that the High Flux Isotope Reactor (HFIR)–Transuranium Facility (TrU) complex will produce ~1.3 g of Cf^{252} per year at steady state. Milligram amounts will be produced by December 1965.

Basis for Shielding Design

The bulk shielding requirements for the TrU Facility have been revised because of a more conservative estimate of the production of Cf^{254}, which has a 55 day-half-life for spontaneous fission. The shielding, carrier, and chemical operations are now designed for processing 1 g of Cf^{252} irradiated 30 days at 5×10^{15} n cm^{-2} sec^{-1} and decayed for 1 day.

Chemical Process Development

Two feasible chemical separation methods, one based on solvent extraction with a tertiary amine, and the other on anion exchange were developed at tracer levels for most of the required steps in the Transuranium Program. In batch countercurrent tests with synthetic feed containing americium and cerium, americium was selectively extracted into 30% Alamine from 11 *M* LiCl containing <0.1 *M* HCl with >99.99% recovery and a decontamination factor from rare earths of $>10^4$. Tests of the anion exchange process with synthetic solutions traced with americium and cerium on a column 2.5 cm dia and 60 cm high gave >99.99% americium recovery and a decontamination factor from rare earths of $>10^6$.

The proposed flowsheet for High Flux Isotope Reactor target processing includes dissolution in hydrochloric acid and selective extraction of actinides into tertiary amine from 11 *M* LiCl followed by berkelium-californium extraction from 1.5 *M* HCl into 1 *M* mono-2-ethylhexyl phenylphosphonic acid. In a miniature batch countercurrent extraction, californium recovery was 99 ± 1%, and the decontamination factor from curium was 10^3. Preliminary measurement of einsteinium distribution coefficients indicate that neither tertiary amine nor phenylphosphonic acid extraction can be used to separate californium and einsteinium. The only method available is chromatographic elution from a cation exchange column with α-hydroxy-isobutyrate. Berkelium-californium separation factors of 10^5 per stage were obtained by extracting Bk(IV) into 1 *M* di-2-ethylhexyl phosphoric acid from 10 *M* HNO_3–0.1 *M* $KBrO_3$.

HFIR Target Fabrication Development and Design Features of the TRU Facility

The design of The Transuranium Facility is in progress. Cold development work, as a joint program with the Metallurgy Division, on target fabrication has started and design and installation have started for a sealed manipulator-served box located in a 4.5-ft-concrete-shielded cell for higher activity tests of process chemistry. Two cells have been added, along with four additional cold laboratories, to do special separations for isotopes such as Bk^{249} milking for Cf^{249}, Bk^{250} decay to Cm^{250} followed by separation, Es and Fm separations, and others. Construction is scheduled for completion in April 1964 and full-scale operation by June 1965.

12. PRODUCTION OF URANIUM-232

Pure U^{232} is to be prepared for nuclear cross-section measurements. Calculations showed that 10 mg of U^{232} containing <100 ppm of U^{233} can be prepared by irradiating 50 g of Pa^{231} for 5 hr at a flux of 1×10^{14} n cm^{-2} sec^{-1} and processing after 20 to 120 hr decay. Irradiation for 200 hr and processing after 65 to >140 hr decay yields 1 g of U^{232} containing <1% U^{233}. In preliminary tests on a chemical flowsheet for recovering uranium and protactinium from irradiated Pa_2O_5-Al by anion exchange <0.3% of the protactinium and <3% of the uranium, the limits of detection, were lost. The protactinium product contained <10% of the uranium and the uranium product 0.04% of the protactinium.

13. URANIUM PROCESSING

A solvent extraction process for purifying uranium concentrates, which uses a phosphonate as extractant and ammonium carbonate as stripping agent, was demonstrated successfully in continuous equipment. The use of a phosphonate allows extraction with low-nitrate salting in the aqueous phase, and the product from the ammonium carbonate stripping circuit is converted to UO_3 more easily than is uranyl nitrate from the conventional tributyl phosphate circuit.

A method was developed for recovering nitric acid from refinery waste streams by extraction with a secondary amine.

14. FISSION PRODUCT RECOVERY

Solvent Extraction

In a continuous run of the di(2-ethylhexyl) phosphoric acid (D2EHPA) extraction process for recovering strontium from Purex wastes in miniature mixer-settlers with nonradioactive feed, both chemical and physical performance were satisfactory. In laboratory experiments cesium was extracted from Purex waste, adjusted to pH 5, by sodium tetraphenyl boron and stripped with dilute acid. However, such a process will be economically attractive only if the extractant can be obtained at a price considerably below current quotations. Zirconium and niobium were extracted from acidic Purex waste with 0.3 *M* D2EHPA in hydrocarbon diluent and stripped with 1 *M* oxalic acid.

Precipitation

Strontium was recovered from a Purex waste concentrate by precipitation with NH_3, Na_2CO_3, NaOH, and Na_2CO_3, in sequence; iron, lead, and calcium impurities in the final product were <3 wt % of the strontium.

Ion Exchange

In laboratory studies on pre-ion exchange treatment of Purex waste, >85% of the sulfate ion present was precipitated by addition of excess ferric ion and dilution with fuming nitric acid to 50–55% HNO_3.

15. THORIUM RECOVERY FROM GRANITE

Sample Collection

Study of thorium reserves and recovery costs from various large-tonnage sources was continued with the principal effort centered on granitic rock. Of ~200 rock samples collected, Conway granite from New Hampshire showed the highest average thorium content, 47 ppm, and this formation may represent an important thorium reserve.

Acid Leach–Solvent Extraction Method

Thorium recoveries in acid leaching of granite were similar with sulfuric, nitric, and hydrochloric acids and were not improved by grinding smaller than −48 mesh. Thorium was extracted from sulfate liquors with primary amines.

Cost Studies

Preliminary estimates of mining and granite-treating costs were $3.61 to 5.30 per ton. Estimated costs for recovery of 1 lb of thorium plus uranium ranged from $31 to $510 for the 16 samples studied.

16. SOLVENT EXTRACTION TECHNOLOGY

Final Cycle Plutonium Recovery by Amine Extraction

A chemical flowsheet was developed for final-cycle plutonium purification by tertiary amine extraction and reductive or complexing stripping. A Purex partitioning-cycle plutonium-product stream can be used as feed with no adjustment other than reoxidation of plutonium to Pu(IV). Sulfate can be tolerated at the levels expected from ferrous sulfamate reductive stripping in the Purex cycle. Several amine-diluent combinations at 0.3 *M* concentration showed stable plutonium loading to above 15 g/liter, sufficient to concentrate plutonium from 0.5–2 g/liter in the feed to 20–60 g/liter in the product.

Metal Nitrate Extraction by Amines

Continued studies on amine extraction of fission product and corrosion-product metal nitrates showed extraction coefficients, with ~0.3 *M* amine from 2–8 *M* HNO_3, of <0.01 for zirconium, <0.02 for Ce(III), $<10^{-3}$ for Cr(III), Fe(III), Ni(II), and Co(II). Extraction coefficients for zirconium and for excess nitric acid decreased slightly but regularly with increasing temperature, ~20 and <15%, respectively between 25 and 55°C.

Technetium-Neptunium-Uranium Recovery

Laboratory development was completed of the tertiary amine single-cycle process for recovery and separation of technetium, neptunium, and uranium from fluorination plant residues. Elimination of nitrate from the technetium can be included in the single-cycle process, in contrast to the typical need for a separate cycle, because of the high separation factor for technetium from nitrate together with a control test developed to monitor 98 ± 1% hydrolysis of the amine salt. Estimates indicate essentially complete elimination of nitrate in perhaps only 12 ideal stages.

Extraction Performance and Cleanup of Degraded Process Extractants

Infrared measurements as well as several different extraction tests have shown nitrohydrocarbons (RNO_2) to be the most likely diluent degradation products formed during radiochemical processing of nitrate solutions. The chemical properties of these compounds are such that they can react in combination with TBP to give strong, synergistically enhanced, extraction of fission-product zirconium-niobium. The only effective method found for removing the nitrohydrocarbons from the solvent has been their sorption on activated solids such as alumina or manganese dioxide. The amounts of solid required, however, are impractical for process use. In view of this, attention has turned to new diluents which are less susceptible to nitration. Encouraging results have been obtained with monoalkylbenzenes such as butylbenzene. In addition to greater resistance to degradation these aromatic diluents also have other advantages, as compared to aliphatic diluents. They impart greater radiation stability to the extractant such as TBP, provide better separation of uranium and fission products, and permit greater organic phase solubility of extracted metal-complex salts.

Suppression of Zr-Nb and Ru Extraction by TBP-Amsco from Feeds Pretreated with Keto-Oximes

An improvement in decontamination of uranium from zirconium-niobium and ruthenium has been noted when aqueous nitrate feed solutions were treated with nitrous acid and acetone before solvent extraction with phosphates or phosphonates. A plausible explanation has been based on the fact that acetone (as well as certain other ketones) can react with nitrous acid to form keto-oximes which are potential complexing agents for metal. Diacetyl monoxime, a commercially available keto-oxime, decreased Zr-Nb and Ru extraction by severely degraded TBP-Amsco extractants. A keto-dioxime also suppressed Zr-Nb extraction. The bifunctionality of these keto-oximes has been shown to be essential to suppression of Zr-Nb and Ru extraction.

Alkaline Earth Extraction by Di(2-ethylhexyl) Phosphate

The equilibria between aqueous hydrogen ion in 4 *M* $NaNO_3$ and 0.1 *M* di-2-ethylhexyl phosphoric acid plus sodium di-2-ethylhexyl phosphate mixtures in benzene were established over the range $10^{-1} \geq [H^+]_{aq} \geq 10^{-13}$. The extractant became 1% Na at $[H^+]_{aq} = 1.3 \times 10^{-4}$, and 99% Na at $[H^+]_{aq} = 3.0 \times 10^{-6}$. Strontium extraction coefficients varied with the aqueous acidity according to the expected inverse square relation in some cases and with continuously varying power dependences in others. The first power dependence on the organophosphate concentration suggests extraction by dimeric D2EHPA.

Uranyl Sulfate Diffusion in Solvent Extraction

A preliminary study of the diffusion of uranium in acidic aqueous sulfate solutions indicated that the diffusivity of the uranyl ion is about 10 times that of either the monosulfate complex or the disulfate complex, in reasonable agreement with the factor of 6 derived from measurements of the extraction kinetics with similar aqueous systems.

Solvent Extraction System Activity Coefficients

The vapor pressures of a series of water-saturated solutions of tri-*n*-octylamine in benzene indicated that this system obeys Raoult's law up to about 0.2 *M*, in confirmation of the hypothesis used previously in deriving equilibrium constants for the system $TOA-C_6H_6:H_2O-H_2SO_4$.

17. MECHANISMS OF SEPARATIONS PROCESSES

In studies on the distribution of nitric acid between aqueous and 5 to 100% TBP in Amsco 125-82, the concentration-activity quotient for extraction was found to be a simple function of the nitric acid concentration in the organic phase when the aqueous acidity was <5 *M*.

The $G(-HNO_3)$ value in the radiolysis of $TBP-Amsco\ 125\text{-}82-H_2O-HNO_3$ was found to be 4 to 11 molecules/100 ev at a dose of 45 whr/liter as the organic phase acidity increased from 0.1 to 0.7 *M*. Corresponding values for dibutyl phosphoric acid formation, *G*(HDBP), were 1.2 to 3 molecules/100 ev. Both $G(-HNO_3)$ and *G*(HDBP) decreased as the irradiation increased to 405 whr/liter.

A model of the foam separation process combining the Gibbs and Langmuir equations accurately summarized and correlated measurements of surface tensions and surface radioactivities of solutions of surface-active agents and with the separation attained in a total-recycle single-stage foam column.

In tests on solubilities, critical micelle concentrations, foamabilities, and separation of cesium, strontium, and cerium at pH 1, 7, or 12 with a hundred commercial surfactants, at least one surfactant was found that gave good separation for each element.

18. RADIATION EFFECTS ON CATALYSTS

Conversion of Cyclohexanol to Cyclohexene with $MgSO_4$-Na_2SO_4 as Catalyst

Irradiation of the $MgSO_4$-Na_2SO_4 catalyst in the conversion of cyclohexanol to cyclohexene at rates of 13 rad/min did not effect the activity of the catalyst.

Dehydrogenation of Methylcyclohexane on Promoted Chromia-Alumina Catalysts

Incorporation of up to 51 mc of Pm^{147} per gram of chromia-alumina catalyst had no measurable effect on the catalytic dehydrogenation of methylcyclohexane to toluene.

19. ION EXCHANGE TECHNOLOGY

Irradiation of Dowex 50W X-8 (20–50 mesh) resin, in a circulating system of demineralized water, in a 10,000-curie Co^{60} source to 0.85×10^9 r decreased the resin specific capacity 30%, the volume 20%, and the moisture content from its original 42.7% to 38.6%. A dose of 3.9×10^9 r decreased the specific capacity 60% and the volume 85%, but increased the moisture content to 55.1%.

Uranium, sulfate, and chloride self-diffusion rates and uranyl sulfate loading and elution rates measured with various size fractions of Dowex 21K confirmed a mathematical model that was based on the assumption that only one significant uranium species exists within the resin. The model accurately predicted uranyl sulfate loading rates on sulfate-equilibrated resin when the uranium species was considered to be $UO_2(SO_4)_2^{=}$.

About 99% of the thorium and only 2.5% of the U^{233} were sorbed by Dowex 50W resin from a 0.1 *M* HNO_3 solution containing 100 and 1 g per liter, respectively, of uranium and thorium.

Plutonium was recovered from spent decontaminating solutions with <1% loss by sorption on Permutit SK resin and elution with nitric acid.

20. CHEMICAL ENGINEERING RESEARCH

Bottom Interface Control for Pulsed Column

A bottom interface control based on differential levels in water-purged head pots was satisfactorily demonstrated on a 24-ft-high nozzle-plate pulsed column. It can be operated remotely.

Interfacial Viscosimeter

An interfacial viscosimeter, essentially a modified two-dimensional Brookfield viscosimeter, was designed for use in measuring transport of molecules across an interface, the rate of which is a function of interfacial viscosity.

Stacked-Clone Contactor

A stacked-clone solvent extraction contactor larger than the Mark I was designed. The capacity of Mark II for both phases was quintupled to 6 liters per minute compared to 1.2 liters per minute for Mark I, while the actual clone stage volume exclusive of recycle pumps and lines was only doubled. The total volume of a typical stage including pumps and lines was only 10% greater than that of Mark I. While the tested stage efficiencies of Mark II range up to 56% compared to 90% for Mark I, contact times still compared favorably because of the high throughput to stage volume ratio. Mark II exhibited a much more sharply delineated organic-rich vortex region and much cleaner pump streams. The favorable operating characteristics of Mark I of short half-time to steady state of about ten seconds per stage, stable control of inventory and throughput, simple start-up and shutdown, and trouble-free operation over 300 hr have been maintained in Mark II.

Thermal Diffusion

Thermal diffusion studies of uranyl sulfate solutions showed very small Soret coefficients, with no or very small concentration at the cold wall. Large Soret coefficients measured for zirconyl and hafnyl nitrates may be due to spurious thermal osmotic effects in the experiments.

Intermediate-Scale Mixer-Settler Performance

The intermediate-scale mixer settler performed satisfactorily in extensive tests.

21. INSTRUMENTATION

A method based on x-ray determinations of the position of the liquid-vapor interface in a calibrated

pressure vessel was devised for measuring liquid densities at measured high temperatures and pressures.

22. HIGH-TEMPERATURE CHEMISTRY

A high-temperature high-pressure spectrophotometer system suitable for use with solutions containing α emitters at temperatures up to 330°C and pressures up to 3000 psi was designed.. The system includes a digital output of wavelength and absorbency information on IBM computer punch cards.

23. CHEMICAL APPLICATIONS OF NUCLEAR EXPLOSIONS (CANE)

Calcium and magnesium sulfates were reduced by hydrogen at 800 to 900°C to a solid containing about 15% CaO and 85% CaS, and pure MgO, respectively. The instantaneous reduction rate for $CaSO_4$ at 700°C was 2.43×10^{-7} mole m^{-2} min^{-1}, and the apparent activation energy was 39 kcal/mole. Tritium exchange from HTO to H_2 over $CaSO_4$ was slow at 400 to 700°C, the highest value being 25% at 600°C for a flowing mixture of 6.5×10^{-3} mole H_2 min^{-1}, 4.5×10^{-4} mole H_2O min^{-1}, and 4.1×10^{-11} mole HTO min^{-1} and a gas-solid contact time of 45 sec. The apparent activation energy for the exchange was 8.8 kcal $mole^{-1}$.

A sequenced sampler for the Project Gnome detonation was designed, and a hypervelocity jet sampler was developed in co-operation with Frankford Arsenal.

24. REACTOR EVALUATION STUDIES

Heat Transfer from Spent Fuels during Shipping

Experimental measurements of the temperature rise in simulated spent fuel elements and shipping carriers were started to evaluate the limitations that heat transfer considerations will place on shipping carrier design and economics. Initial results indicated that $\geq$30% of the heat transfer will be by radiation.

Shielding Design Calculation Code

A code was written for the IBM 7090 which will perform $\geq$90% of the basic shielding calculations for fuel-handling facilities.

25. ASSISTANCE PROGRAMS

Eurochemic Assistance

ORNL coordinated the Eurochemic assistance program, with review and exchange of information on radiochemical processing of irradiated fuel. The Eurochemic preproject study has been completed.

O^{17} Pilot Plant

Design of the O^{17} Separations Pilot Plant was completed. The facility includes small-scale distillation equipment for preliminary separation of oxygen isotopes and two thermal diffusion cascades for final enrichment of the O^{17} isotope product.

U^{233} Metallurgical Development Laboratory

Design criteria and a preliminary cost estimate for a laboratory for fabricating U^{233} were started. The design includes three cells shielded by 4 ft of normal concrete. Master-slave and rectilinear operators will be provided.

High Radiation Level Analytical Laboratory

Design criteria were provided for the HRLAL, which will have two storage cells of 4-ft-thick barytes concrete plus laboratories and supporting areas.

Building 4507 Addition

An addition to Bldg. 4507 was designed with work cells for demonstrating radiochemical processes on a small but full-activity-level scale.

Containment Modifications

Containment changes made in the Volatility Pilot Plant included sealing of the cells and installation of filters and backflow preventers on the air inlets, of a scrubber on the cell off-gas system to remove HF and F_2, and of appropriate ventilation and radiation instruments and controls. Similar changes were made in Bldg. 4507, and the area above the cells was provided with secondary containment by construction of an 18-ft-high roof-cover. Building 3026 was also similarly contained.

Plant Aqueous Waste System

Preliminary design was made for a new waste system for Melton Valley. Design of a new 600-gal/min intermediate-activity-level waste evaporator and of two new high-activity-level waste tanks was completed.

THIS PAGE

WAS INTENTIONALLY

LEFT BLANK

CONTENTS

1. POWER REACTOR FUEL PROCESSING

Laboratory- and engineering-scale development work is being done on processes for recovering fissionable and fertile material from irradiated fuel elements. Dissolution and feed-preparation methods for power reactor fuels containing stainless steel and zirconium are being investigated. Processing by new chemical and mechanical methods is being studied for the power reactor fuels of current importance; chemical and cold engineering studies for advanced reactor fuels such as graphite loaded with uranium and/or thorium oxide or carbide and beryllia-UO_2 are in progress.

1.1 CHEMICAL PROCESSES FOR STAINLESS STEEL–CONTAINING FUELS

Two processes being developed for recovering uranium and thorium from stainless steel–containing fuels are Darex and Sulfex. The chief effort has been applied to the Consolidated Edison (CETR) fuel, stainless steel–clad ThO_2-UO_2, which appears to be the most difficult to handle in either process. Development of the Darex and Sulfex dissolution processes is now complete except for radioactive verification tests with a high level of radioactivity and certain engineering-scale tests on chloride removal from Darex solutions by NO_2 sparging.

In the Darex process stainless steel and uranium (or UO_2) are totally dissolved in boiling 5 *M* HNO_3–2 *M* HCl in titanium equipment. Chloride ion is quantitatively distilled from the dissolver solution, which has been acidified to 10 to 12 *M* HNO_3, and the chloride-free solution is adjusted to correct metal and nitric acid concentrations for Purex or TBP-25 solvent extraction. For highly irradiated ThO_2-UO_2 fuels a two-step procedure is required. First, stainless steel cladding is dissolved in 5 *M* HNO_3–2 *M* HCl, which also dissolves 2 to 3% of the uranium from the mixed oxide core. Chloride ion is distilled from the decladding solution, acidified to ~12 *M* HNO_3, and the ThO_2-UO_2 core is dissolved in the decladding solution to which 0.4 *M* NaF and 0.1 *M* Al^{3+} have been added. The core solution, containing stainless steel, thorium, and uranium, would then be evaporated and steam stripped to 0.1 *M* acid deficiency for acid Thorex solvent extraction.

In the Sulfex process the stainless steel cladding is dissolved in boiling 4 to 6 *M* H_2SO_4, and the solution is discarded. Undissolved UO_2 cores are washed free of residual sulfuric acid and then dissolved in 8 to 12 *M* HNO_3; washed ThO_2-UO_2 cores must be dissolved in Thorex dissolvent, 13 *M* HNO_3–0.04 *M* NaF–0 to 0.1 *M* $Al(NO_3)_3$.

Darex Process

Decladding. – Uranium losses to boiling 5 *M* HNO_3–2 *M* HCl were too high for the Darex process to be applicable as a decladding method.[1] In a series of tests on prototype CETR fuel pins under flowsheet conditions,[2] uranium losses in 1 hr increased with irradiation, from 0.04 to 3% as the burnup increased from 0 to 25,000 Mwd per ton of fuel (Table 1.1a). Losses varied inversely with the density of the fuel pellets and directly with the exposed surface area of the oxide. With high-density unshattered fuel pellets, thorium losses were usually <0.1%, even at very high burnup. However, many pellets in irradiated test pins with burnup >500 Mwd/ton were severely shattered, a condition which probably is representative of the spent fuel elements from an actual power reactor.

The uranium loss from 6% UO_2-ThO_2 pellets in contact for 3 hr with a final Darex decladding solution (5 *M* H^+, 47 g of stainless steel per liter) was 0.25% in the absence of air. Irradiation of a similar sample in a 1-watt/liter Co^{60} gamma field

[1] Work done by Battelle Memorial Institute under subcontract 1381.

[2] L. M. Ferris and A. H. Klibbey, *Sulfex-Thorex and Darex-Thorex Processes for Dissolution of Consolidated Edison Power Reactor Fuel: Laboratory Development*, ORNL-2934 (Oct. 26, 1960).

Table 1.1. Uranium and Thorium Losses in Decladding of Irradiated Prototype CETR Fuel Pins*

Pin No.	Pellet Composition			Burnup (Mwd/ton of core)	Decladding Time (hr)	Losses (%)	
	UO_2 (%)	O/U Ratio	Density (g/cc)			U	Th
				(a) Darex Decladding (5 *M* HNO_3–2 *M* HCl)			
1	4.5	2.7	8.0–8.5	0	2	0.63	0.09
2	4.5	2.7	8.0–8.5	0	1	0.23	0.10
3**	5.0	2.7	8.0–8.5	190	1	2.1	1.1
					4	3.7	2.6
4	5.0	2.7	8.0–8.5	275	1	0.06	0.03
					4	0.15	0.06
5	9.1	2.0	9.5	0	1	0.04	0.01
					16	0.17	0.02
6**	9.1	2.0	9.5	875	1	0.32	0.16
					8	0.90	0.40
7**	4.2	2.0	9.5	21,800	1	2.1	0.07
					3	3.2	0.09
8**	4.2	2.0	9.5	~25,000	1.5	3.0	0.07
					3	4.6	0.12
				(b) Sulfex Decladding (4–6 *M* H_2SO_4)			
9	4.5	2.7	8.0–8.5	0	3	0.31	0.05
10	4.5	2.7	8.0–8.5	0	4	0.35	0.03
11	4.5	2.7	8.0–8.5	0	6	0.39	0.04
12**	5.0	2.7	8.0–8.5	200	3	0.26	0.12
					6	1.6	0.70
13	9.1	2.0	9.5	0	3	0.008	0.006
					16	0.008	0.01
14**	9.1	2.0	9.5	620	1	0.04	0.04
					8	0.07	0.04
15**	9.1	2.0	9.5	740	1	0.07	0.11
					5	0.26	0.18
16**	6.5	2.0	9.1	~ 6,000	3	0.03	0.03
17**	6.5	2.0	9.1	~12,000	3	0.30	0.29
18**	4.2	2.0	9.5	19,600	3	0.09	0.02

* Specimens comprised of sintered ThO_2-UO_2 pellets encased in type 304 stainless steel.

** Fuel pellets severely shattered.

did not increase the loss.[3] However, with air present, the loss increased to 0.90%. Losses were higher with fragmented irradiated pellets than predicted from tests on unirradiated powdered samples.[2]

Chloride Removal. – Chloride ion can be removed adequately from dissolver solutions by distillation from strong nitric acid. In tests on an attractive alternative chloride removal method, sparging with NO_2, the chloride concentration of adjusted Darex dissolver product was decreased from 0.75 *M* to 40 ppm in 3 hr (Fig. 1.1). However, the amount of NO_2 used was 2000% of the stoichiometric requirement for the reaction $2NO_2 + Cl^- \rightarrow NOCl + NO_3^-$, and better contacting methods are being sought to decrease the quantity of NO_2 required.

[3]T. A. Gens, *Consolidated Edison Fuel Losses on Exposure to Irradiated and Aerated Sulfex and Darex Decladding Solutions*, ORNL-3023 (Apr. 18, 1961).

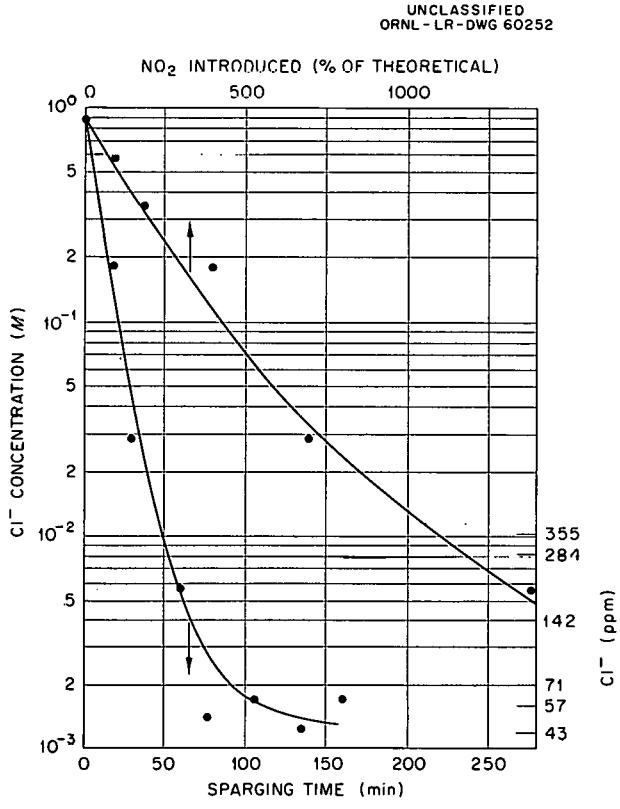

Fig. 1.1. Removal of Chloride from Adjusted Darex Dissolution Product by Sparging with NO_2 (0.077 mole/min) at 60°C: Effect on Chloride Concentration of Time and Amount of NO_2 Used. Solution composition: 8.5 *M* HNO_3–0.75 *M* Cl^-, 30 g of stainless steel per liter.

Sulfex Process

In contrast to prototype CETR fuel losses to Darex decladding solutions, losses to Sulfex decladding solutions, 4 to 6 *M* H_2SO_4, were not greatly affected by reactor burnup over the range studied, 0 to 20,000 Mwd per ton of fuel.[1] In general, uranium losses were less than 0.4% in 6 hr decladding time with pellets containing 5 to 10% UO_2 and with densities greater than 9 g/cc (Table 1.1b). Losses were higher from low-density pellets with O/U > 2.3. Thorium losses were generally less than 0.2%.

Cobalt-60 irradiation increased the loss of uranium from 6% UO_2–ThO_2 pellets in contact with final Sulfex decladding solution (2.8 *M* H_2SO_4, 56 g of stainless steel per liter).[3] Exposure of pellets in the clad solution for 1 hr to a 1-watt/liter Co^{60} gamma field in the absence of air resulted in a uranium loss of about 0.1%, which, while not significant, was 1.5 times higher than losses without irradiation.

Stainless steel exposed to high-temperature reactor cooling water develops an oxide film[4,5] that is resistant to attack by sulfuric acid in the concentration range 6 to 8 *M*. The passive film can be broken by contact with a less noble metal, as is done in the KAPL-developed SIR process.[6] Chemical methods for breaking this film have been investigated,[7] and the reaction potentials and dissolution rates of passivated stainless steel in sulfuric acid were studied. At temperatures of 73 to 110°C, the protective film was attacked rapidly by 6 *M* H_2SO_4, particularly at the higher temperatures. At all temperatures tested above 73°C, the passivated stainless steel was less

[4]T. A. Gens, *Investigation of Depassivation of 304 Stainless Steel in 6 M H_2SO_4 by EMF Measurements*, ORNL-CF-60-1-22 (Jan. 14, 1960).

[5]*Chem. Tech. Div. Ann. Prog. Rep. Aug. 31, 1960*, ORNL-2993.

[6]M. E. Brennan et al., *Fuel Recovery Process for the SIR Mark A*, KAPL-933 (July 17, 1953) (classified).

[7]T. A. Gens, *Sulfex Process: Depassivation of Stainless Steel*, ORNL-2785 (Nov. 6, 1959).

noble than platinum (Fig. 1.2). When the oxide film was completely penetrated, active dissolution of the stainless steel started, with hydrogen evolution, and the potential rose sharply. The logarithm of the depassivation time was a linear function of reciprocal temperature (Fig. 1.3), indicating that the reaction is zero order. The activation energy determined from the slope of the Arrhenius plot was 37 kcal/mole.

UO_2-ThO_2 Pellet Dissolution

Unirradiated UO_2-ThO_2 dissolution rates, both initial and at various stages of dissolution of individual pellets, were determined for use in design of a processing plant. Most of the tests were made with 4.4% UO_2 pellets that were ~95% of theoretical density. The dissolvents contained 8 to 18 *M* HNO_3, 0.04 *M* NaF, 0.1 *M* $Al(NO_3)_3$, and 0.02 to 1.0 *M* Th, and the U/Th ratio was 0.05.

The empirical correlation obtained,

$$R = 0.627\left(\frac{M_{HNO_3}}{10}\right)^3 - 0.336\left(\frac{M_{HNO_3}}{10}\right)^4 - 0.12\left(\frac{M_{HNO_3}}{10}\right)^3 M_{Th}$$

(R = reaction rate, mg g^{-1} min^{-1}, M_{HNO_3} and M_{Th} = molarities of nitric acid and thorium in dissolvent) was reported previously.[5] The average deviation between predicted (C) and experimental (E) initial dissolution rates,

$$\sum_{i=1}^{i=n} C_i - E_i = -0.0036 \text{ mg g}^{-1} \text{ min}^{-1}$$

showed very nearly equal plus and minus variations from the correlation values. The average mean square deviation,

$$\sqrt{\frac{\sum_{i=1}^{i=n}\left(\frac{C-E}{C}\right)_i - \left(\frac{C-E}{C}\right)^2}{n}} = 0.22$$

showed that, although there is scattering of the data, any experimental value should fall in the interval C ± 0.5C with >95% certainity.

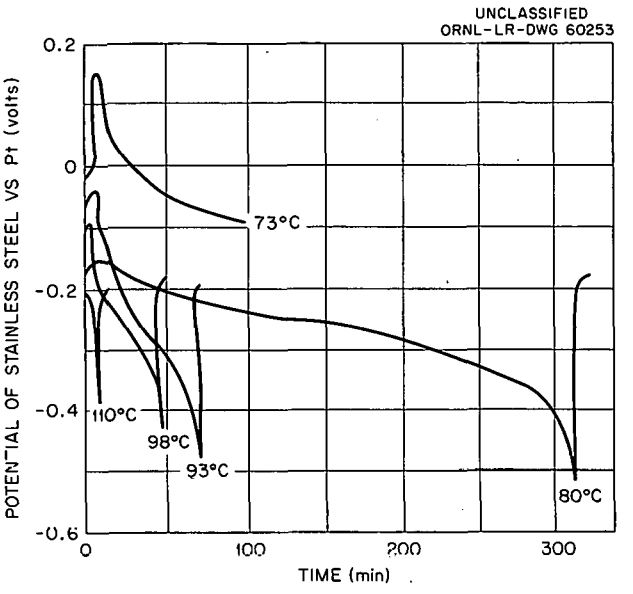

Fig. 1.2. EMF Differences Between Passivated Type 304 Stainless Steel and a Platinum Wire in 6.0 *M* H_2SO_4. Passivation produced by refluxing 1 hr in 15.8 *M* HNO_3–0.025 *M* Cr(III).

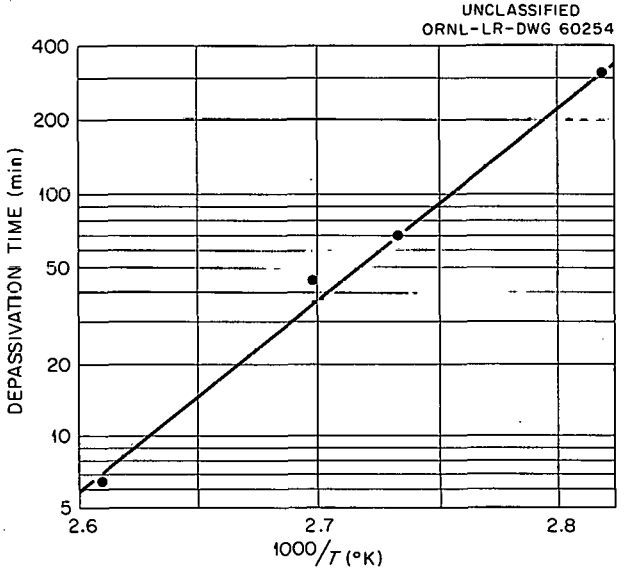

Fig. 1.3. Effect of Temperature on Depassivation Time of Type 304 Stainless Steel in 6.0 *M* H_2SO_4. Passivation treatment: 1 hr in refluxing 15.8 *M* HNO_3–0.025 *M* Cr(III).

As pellets dissolve, roughness and porosity increase with an attendant increase in both the surface/weight ratio and dissolution rate. In more than 300 measurements of instantaneous dissolution rates of pellets that had been 0 to 87% dissolved, an intermediate maximum rate was observed when 10 to 15% had dissolved. This may be due to the release of small particles of UO_2-ThO_2 from the pellet surface, resulting in an apparent weight loss without dissolution having actually occurred.

The variability of dissolution rates increased as the percentage dissolution increased (Fig. 1.4). Rates of fresh pellets in modified Thorex dissolvent, 12 *M* HNO_3–0.04 *M* F–0.10 *M* $Al(NO_3)_3$–0.2 *M* Th–0.01 *M* U varied from 0.28 to 0.37 mg g^{-1} min^{-1} and for 50% dissolved pellets from 0.54 to 1.17 mg g^{-1} min^{-1}. The mean rates and standard deviations for the two sets of pellets were 0.325 and 0.022 mg g^{-1} min^{-1} for fresh and 0.772 and 0.164 mg g^{-1} min^{-1} for 50% dissolved pellets, respectively. Normal distributions were approximated in both cases.

Because total dissolution required >48 hr, the time for cyclic operation with a 5% ThO_2-UO_2 heel was determined. In two runs with 660-g charges of UO_2-ThO_2 the steady-state dissolution time was ~35 hr with 5% or less initial heel (Table 1.2). In the first run no initial heel was involved, and less time was required to dissolve the oxide than in the second run with a 4.5% heel. If the number of pellets for subsequent runs were the same, the heel buildup for a dissolution time of ~35 hr should not exceed 5%.

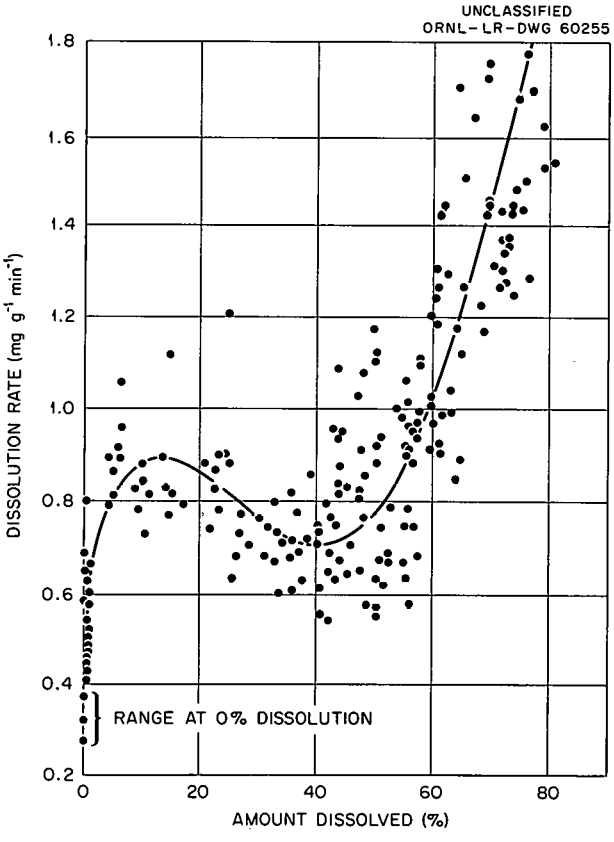

Fig. 1.4. Dissolution Rate of Single UO_2-ThO_2 Pellets in 12 *M* HNO_3–0.4 *M* NaF–0.02 *M* Th–0.1 *M* $Al(NO_3)_3$, Th/U = 20, as a Function of Fraction Dissolved. Pellets: 95.6% ThO_2-UO_2, O/U = 2.0; density 9.5 g/cc, wt 5.0 to 5.5 g, dia 0.264 in., length 0.60 to 0.65 in.

Table 1.2. Thorex Batch Recycle Dissolution Runs

Charge: 125–130 UO_2-ThO_2 pellets (Universal Match Co.)
Dissolution temperature: 120–2°C
Dissolvent: 15.8 *M* HNO_3–0.04 *M* NaF–0.1 *M* $Al(NO_3)_3$, recirculated; 3.30 liters per run

	Run 1	Run 2
UO_2-ThO_2 charged (g)	659.1	661.1
Total UO_2-ThO_2 in dissolver (g)	659.1	690.6
Recycling time (hr)	31.5	40.0
Final dissolvent vol (liters)	3.20	3.18
Final Th dissolvent loading (g/liter)	164.8	178.3
UO_2-ThO_2 heel (g)	29.5	12.4
UO_2-ThO_2 heel (% of charge)	4.5	1.9

Effect of Irradiation on Core Dissolution. – After either Darex or Sulfex decladding of irradiated fuel,[1] the residual ThO_2-UO_2 core (8 to 20 mesh) was dissolved in 200% excess boiling 13 *M* HNO_3–0.04 *M* NaF–0.1 *M* $Al(NO_3)_3$. The rate of dissolution was essentially the same as that of unirradiated material[2] of approximately the same particle size; cores were completely dissolved after two 5-hr digestions with fresh reagent.

1.2 MODIFIED ZIRFLEX PROCESS FOR ZIRCONIUM-CONTAINING FUEL

The Zirflex process, an aqueous head-end process for decladding zirconium-clad UO_2 fuel with

NH_4F-NH_4NO_3 solutions, was modified and extended to the complete dissolution of zirconium-clad U-Zr and U-Zr-Nb alloy fuels by addition of H_2O_2 during dissolution.

A modified Zirflex flowsheet (Fig. 1.5)[8,9] was developed for TRIGA fuel, which is aluminum-clad 8% U–91% Zr–1% H alloy containing graphite end plugs and Al-Sm neutron poison wafers. The aluminum is removed with 2 *M* NaOH–1.8 *M* $NaNO_3$, the graphite is disintegrated in 19 *M* HNO_3–2 *M* H_2SO_4, and the alloy core is finally dissolved in 5.4 *M* NH_4F–0.3 *M* NH_4NO_3. Decladding and graphite disintegration require 3 hr and core dissolution requires 11 hr. The initial core dissolution rate is 30 mg cm^{-2} min^{-1}. The average composition of the gas evolved during core dissolution is 10% H_2, 2% N_2, 0.5% O_2, and 87.5% NH_3. The dissolver solution is adjusted to 1.6 *M* HNO_3 and 1.4 *M* $Al(NO_3)_3$ for solvent extraction. After the HNO_3-$Al(NO_3)_3$ addition the solvent extraction feed contains 0.0085 *M* U.

Uranium-zirconium alloys containing up to 10% uranium were successfully dissolved in 6 *M* NH_4F–1 *M* NH_4NO_3 by continuous addition of H_2O_2 to the dissolvent to oxidize U(IV) to the more

[8] T. A. Gens, *Zircex and Modified Zirflex Processes for 8% U–91% Zr–1% H TRIGA Reactor Fuel*, ORNL-3065 (in press).

[9] T. A. Gens, *Nuclear Sci. Eng.* 9, 488 (1961).

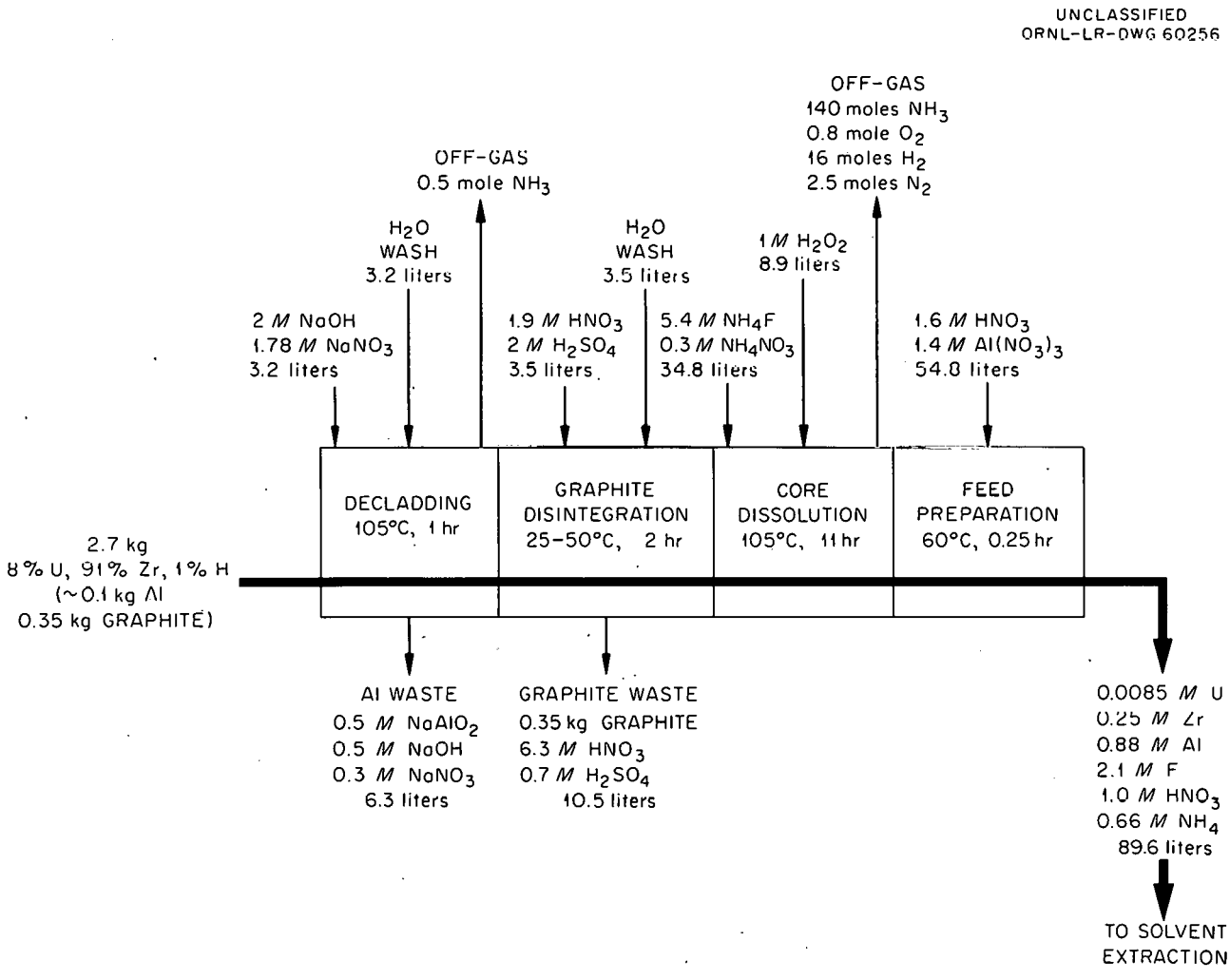

Fig. 1.5. Modified Zirflex Process for Dissolution of TRIGA (8% U–91% Zr–1% H) Fuel in 5.4 *M* NH_4F–0.3 *M* NH_4NO_3–H_2O_2.

soluble U(VI). In four runs in engineering-scale batch equipment, uranium-zirconium-tin multiplate assemblies (1.24 to 2.73% uranium and 0 to 1.6% tin) were dissolved in 6.65 *M* NH_4F. An H_2O_2 addition rate of $\sim 0.5 \times 10^{-5}$ mole cm^{-2} min^{-1} prevented UF_4 precipitation, and excess H_2O_2 had little effect on the stability of the adjusted solvent extraction feed. With a dissolvent boilup rate at 100°C of 0.07 ml cm^{-2} min^{-1} the Zircaloy dissolution rate was acceptable. Foaming presented no problem and no solids remained on the walls of the dissolver. The product solution had to be maintained at ~90°C until HNO_3-$Al(NO_3)_3$ solution was added to form solvent extraction feed in order to prevent fluorozirconate precipitation. Hydrogen was a major component of the off-gas after HNO_3 scrubbing, but the amount decreased to <0.1 mole per mole of zirconium dissolved when the ammonium nitrate concentration in the dissolvent was increased to 0.67 *M*. The ammonia evolution rate was 4.7 ± 0.16 moles per mole of zirconium disolved.

The PWR Seed-3 contains wafers of 40-mil-thick 34% UO_2–66% ZrO_2 ceramic clad in Zircaloy-4. Ammonium fluoride solutions, which dissolved the Zircaloy cladding, attacked the wafers only slowly, the penetration rate in 12 *M* NH_4F being only 0.03 mg cm^{-2} min^{-1} and in 9 *M* NH_4F–1 *M* H_2O_2 only 0.04 mg cm^{-2} min^{-1}. This dissolution rate in refluxing hydrofluoric acid increased from 0.3 to 3.3 mg cm^{-2} min^{-1} as the hydrofluoric acid concentration was increased from 3 to 12 *M*.

Laboratory tests to determine the mechanism of H_2O_2 decomposition, for use in optimizing the H_2O_2 concentration and addition rate, showed three decomposition mechanisms in boiling 5.4 *M* NH_4F, 0.1 *M* NaOH, and 1 *M* HNO_3: (1) a very fast reaction, which probably occurred before the hydrogen peroxide became well mixed with the solution; (2) a slightly slower reaction which continued until the peroxide concentration reached about 0.01 *M*; and (3) a relatively slow decomposition of the remaining peroxide. The second reaction was decidely faster in 1 *M* NaOH and in modified Zirflex solution containing dissolved Zircaloy-2 than in 1 *M* HNO_3. In fresh modified Zirflex solution this reaction occurred at an intermediate rate, and was not affected by the presence of ammonium nitrate (Fig. 1.6). Data on decomposition of 5 *M* H_2O_2 in boiling 1 *M* HNO_3 (Fig. 1.7) indicated that the intermediate reaction is not first order, but that the subsequent slow reaction, which starts when the hydrogen peroxide concentration goes below 0.01 *M*, is. The specific rate constant measured for the latter reaction was 0.033 hr^{-1}.

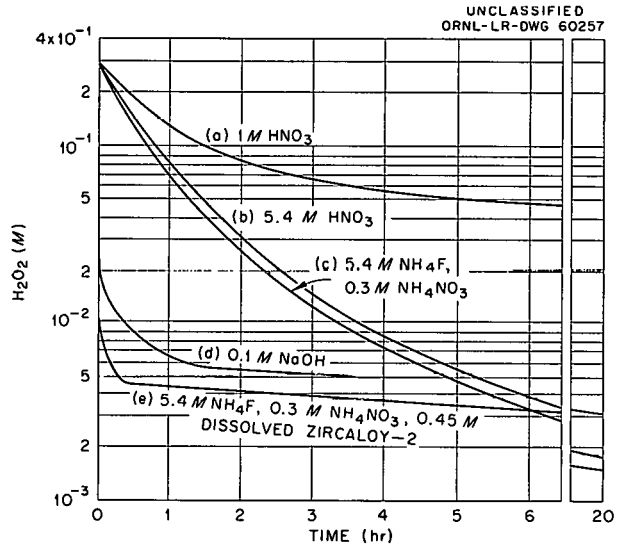

Fig. 1.6. Decomposition of Hydrogen Peroxide in Various Boiling Solutions Initially 1 *M* in H_2O_2.

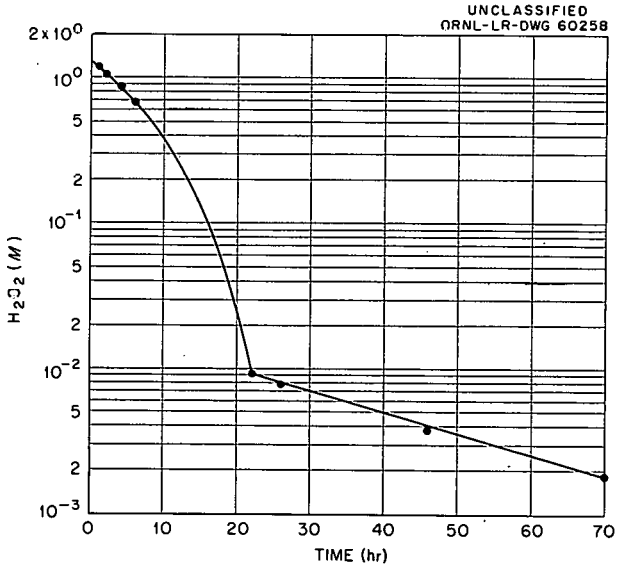

Fig. 1.7. Decomposition of Hydrogen Peroxide in Boiling 1 *M* HNO_3–5 *M* H_2O_2.

1.3 ANHYDROUS HYDROCHLORINATION PROCESSES

The Zircex process is a hydrochlorination process for zirconium-clad UO_2 and uranium-zirconium alloy, including U-Zr-H, fuels. In a similar process for uranium-molybdenum fuels, the fuel is reacted with HCl, HCl-air, Cl_2, or CCl_4-N_2 gas at 400 to 600°C to produce a mixture of metal chlorides, which are water- or nitric acid-soluble and can be processed further by standard techniques. Zirconium, niobium, molybdenum, and perhaps other fuel diluents can be partially or totally separated as volatile chlorides from the less volatile uranium chlorides.

Zircex Process for U-Zr Fuels

A Zircex process (Fig. 1.8) was developed for the TRIGA fuel,[8] which is 8% U–91% Zr–1% H alloy clad with aluminum and contains graphite end plugs and Al-Sm neutron poison wafers. The aluminum cladding is removed as volatile $AlCl_3$ by HCl-N_2 gas at 300°C, at a rate of 11 mg cm^{-2} min^{-1}. The core is then reacted with HCl at 600°C, at a rate of 20 mg cm^{-2} min^{-1}, and the residue is contacted with CCl_4-N_2 at 550°C. In both the two latter steps uranium chloride is selectively condensed and is subsequently dissolved in 13 *M* HNO_3. The chloride is removed as in the Darex process, and the solution is further processed by solvent extraction. The final uranium concentration in the solvent extraction feed, after chloride removal, is 0.1 *M*. The graphite end plugs are burned in O_2 at 750°C or could be removed mechanically. Alternatively, the uranium chloride product can be fluorinated[10]

[10] T. A. Gens and R. L. Jolley, *New Laboratory Developments in the Zircex Process*, ORNL-2922 (Apr. 10, 1961).

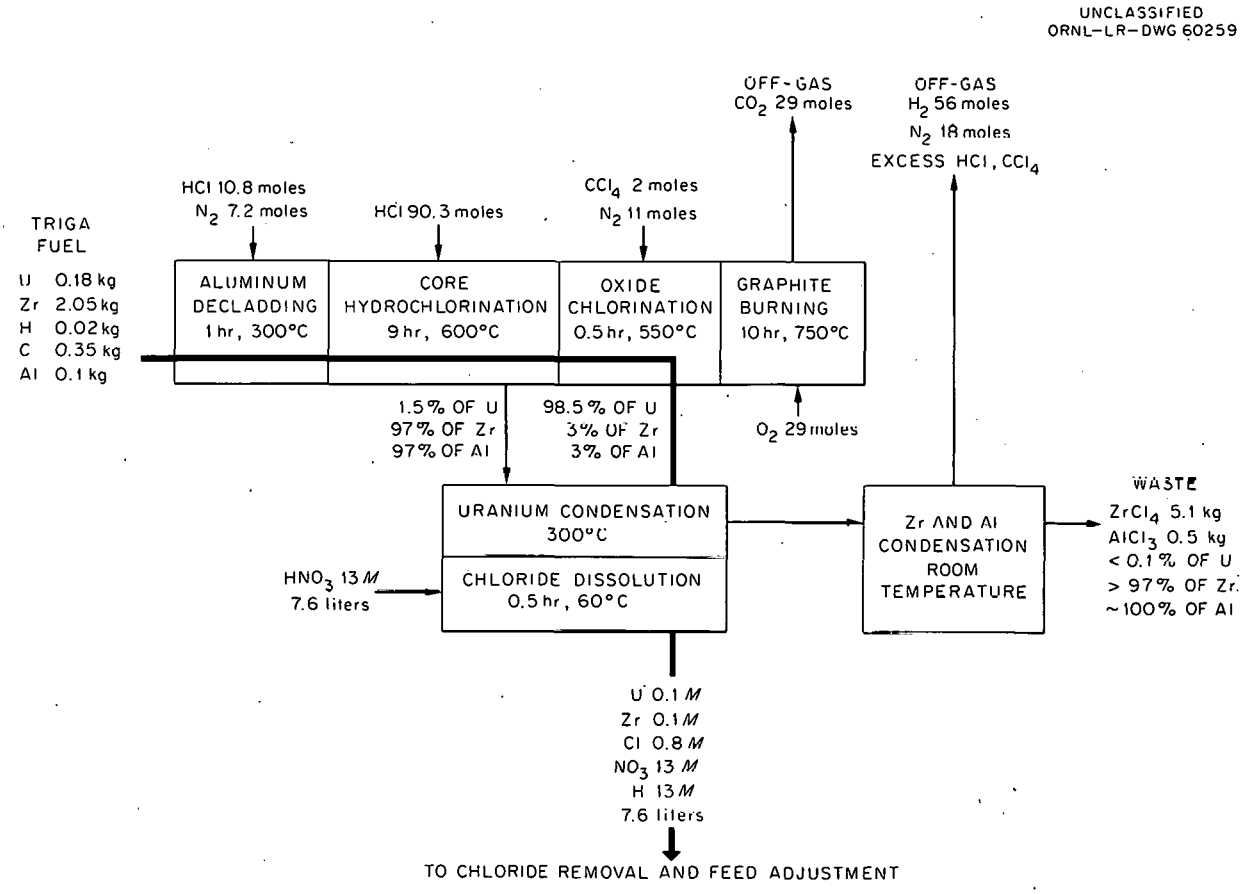

Fig. 1.8. Zircex Process for Recovering Uranium from TRIGA (8% U–91% Zr–1% H) Fuel.

at 200°C to produce UF_6, which could be processed further by the Fluoride Volatility process (Chap 2).

The aqueous dissolution rates of 34% UO_2–66% ZrO_2 wafers (PWR Seed-3) in either 9 to 12 *M* NH_4F or 3 to 12 *M* HF were unsuitably slow (Sect. 1.2), but the reaction rate with CCl_4 vapor was 0.4 to 0.6 mg cm^{-2} min^{-1} at 300 to 550°C and 3 mg cm^{-2} min^{-1} at 595°C.

Oxyhydrochlorination Process for U-Mo Fuels

An oxyhydrochlorination process (Fig. 1.9) was developed on a laboratory scale for 90% U–10% Mo alloy from the CPPD Core 1 fuel.[11] It was assumed that the fuel would first be mechanically declad to remove the stainless steel cladding and residual Na bonding agent and that the uranium-molybdenum alloy rods would be recanned in aluminum. The chemical processing then consists in removing the aluminum cans by hydrochlorination at 300°C and reaction of the core with 15% HCl in air at 400°C to remove 90% of the molybdenum and with pure HCl to remove another 5%. The residual uranium oxide is reacted with 0.6% H_2O in air at 100 to 400°C to strip the chloride. The residual U_3O_8 is dissolved in 4 *M* HNO_3 to produce a solvent extraction feed 1 *M* in uranium, containing only 175 ppm chloride. Reaction rates of 90% U–10% Mo with 15% HCl in air were >5 mg cm^{-2} min^{-1} above 400°C (Fig. 1.10a), and up to 90% of the molybdenum volatilized (Fig. 1.10b).

[11] T. A. Gens, *An Oxyhydrochlorination Process for Preparing Uranium-Molybdenum Reactor Fuels for Solvent Extraction: Laboratory Development*, ORNL-3019 (May 8, 1961).

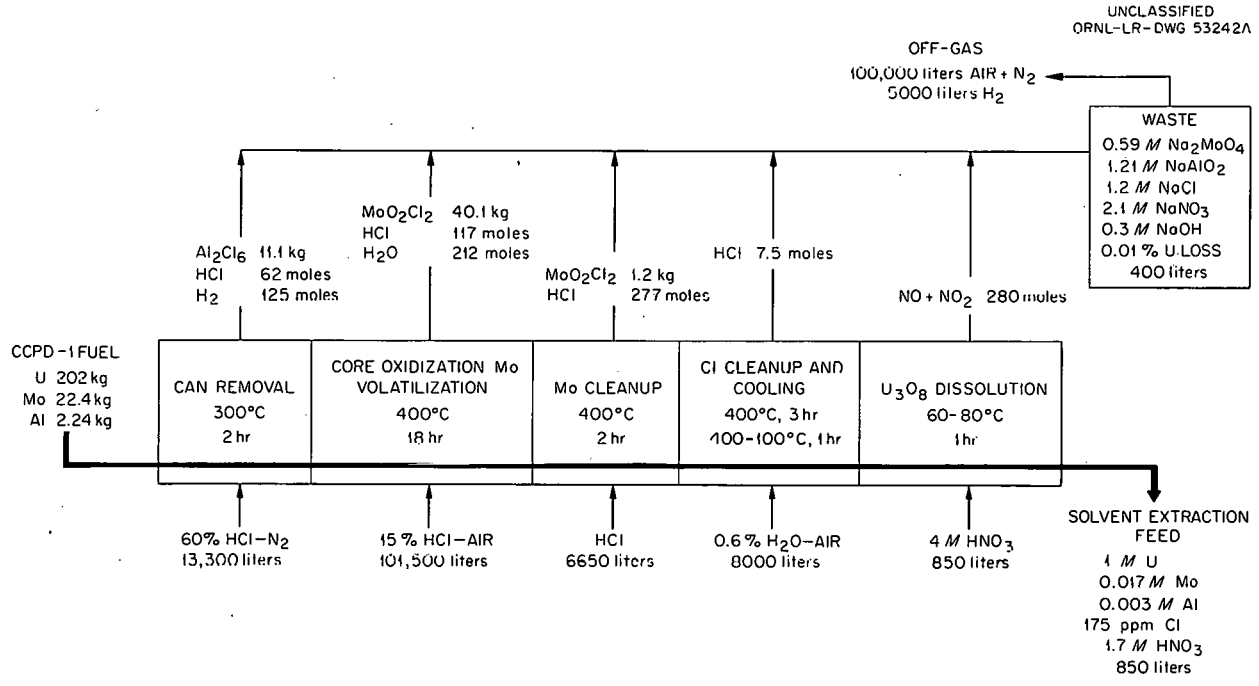

Fig. 1.9. Oxyhydrochlorination Process for Removing the Aluminum Can and Processing the CPPD Core, 90% U–10% Mo Alloy.

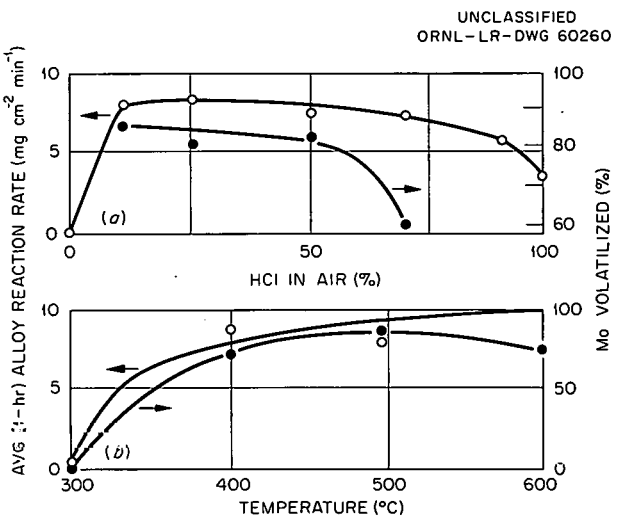

Fig. 1.10. Oxyhydrochlorination Rates and Molybdenum Volatilization from 90% U–10% Mo as a Function of (*a*) Percentage HCl in air at 500°C; (*b*) Temperature with 15% HCl in air.

1.4 PROCESSES FOR GRAPHITE-BASED AND URANIUM CARBIDE FUELS

Development of processes for uranium-graphite fuels included investigation of 90% nitric acid to disintegrate and leach the fuel and of burning the fuel and leaching the uranium-bearing ash. Studies on processing of uranium carbide fuels included work on the stoichiometry of dissolution in water and various acids.

Graphite-Based Fuel

The 90% HNO_3 treatment[12] consists of two successive 4-hr leaches of the fuel with 90% HNO_3 at either 25°C or the boiling point. Each leach is followed by thorough water-washing of the graphite residue. Under flowsheet conditions with fuel specimens irradiated to about 0.001% burnup and containing either 3 or 12% uranium, a significant fraction of the long-lived fission products remained in the graphite residue even when uranium recovery was essentially quantitative (Table 1.3). Minimums of 44% of the Ce^{144}, 30% of the Zr^{95}, and 20% of the Ru^{106} were retained by the graphite residue; the amount of Cs^{137} retained varied from 7 to 81%. A larger fraction of the fission products was solubilized in two 24-hr leaches than in the standard 4-hr treatment. Uranium losses were essentially those expected from experiments with unirradiated samples,[12] being about 0.7 and 0.03%, respectively, from specimens containing 3 and 12% uranium with boiling acid and about twice as high with acid at 25°C. Inert graphite accessories will require special consideration. Exposure of 2.25-in. cubes of AGOT graphite to 90% HNO_3 for 48 hr at 93°C plus 48 hr at 25°C reduced the material to only 15% <20 mesh.

Particle size analyses of the graphite residues from the leaching of the irradiated samples were best correlated by assuming a log-normal distribution. The geometric mean particle size varied with both leaching temperature and time. After two 4-hr leaches of specimens containing either 3 or 12% uranium, the geometric mean particle sizes of the residue were 300 to 400 and 200 to 300 μ when leaching was conducted at 25 and 93°C, respectively. Two 24-hr leaches with boiling acid decreased the geometric mean particle size of the residue to 100-190 μ.

On an engineering scale, with kilogram quantities of 3% uranium-graphite, swelling and disintegration of $\frac{5}{8}$-in.-thick slabs in 90% HNO_3 were complete in 30 to 60 min. Less than 0.25% of the graphite particles in material leached 24 hr was <10 μ; 4-day leaching followed by water washing produced ~1.0% <10-μ particles. Material leached either 24 hr at 60°C or 4 days at 25°C contained 560 to 670 ppm undissolved uranium. The amount of undissolved uranium was not strongly dependent on particle size for a single batch leaching. Neutron-activation analysis of samples taken by the Andreasen pipet method for particle size distribution indicated undissolved uranium contents of 600 and 200 ppm for particles less than 175 and 15 μ, respectively. A settled bed, 6 in. dia × 5 in. deep, of 24-hr leached material was readily transferred through a $\frac{3}{4}$-in.-dia tube by vacuum.

The permeability of disintegrated graphite to the flow of water was low, with a filtration rate of ~60 gal ft^{-2} hr^{-1} for a 1-ft-thick cake at 21 in. Hg differential pressure. Water flow rates through the cake were practically constant over the range 6 to 21 in. Hg vacuum in a 2-in.-dia

[12] M. J. Bradley and L. M. Ferris, *Ind. Eng. Chem.* 53, 279 (1961)

Table 1.3. Disintegration and Leaching of Slightly Irradiated Uranium-Graphite Fuel

Fuel burnup: ~0.001%

Leaching procedure: two successive leaches with 90% HNO_3, each followed by water-washing of residue

Nominal U in Fuel (%)	Leaching Conditions		Amount in Graphite Residue (% of original)				
	Temperature (°C)	Time (hr)	U	Zr^{95}	Ru^{106}	Cs^{137}	Ce^{144}
3	25	4	1.1	38.2	46.3	80.7	75.7
	93*	4	0.62	40.0	36.0	31.4	62.1
	25	4	1.3	81.9	41.2	8.1	69.1
	93*	4	0.66	54.2	43.6	22.4	55.3
	93*	24	0.15	20.5	22.7	13.0	26.8
12	25	4	0.11	46.2	63.2	28.0	74.4
	93*	4	0.03	59.5	36.7	21.1	61.3
	93*	4	0.02	29.7	19.2	7.1	43.6
	25	4	0.17	79.6	57.5	38.0	75.9

*Approximate boiling point of 90% HNO_3.

glass column containing a 6-in. bed of Ottawa sand.

Attempts to detonate a 100-cc mixture of disintegrated graphite and fresh 90% nitric acid, primed by a No. 6 cap and a 5-g PETN booster, were unsuccessful.

Combustion of slightly irradiated fuel samples in a flowing stream of oxygen at 900°C volatilized significant amounts of Ru^{106}. The specimens, in porcelain boats, were burned in a furnace-heated 1-in.-dia quartz tube connected to four scrubbers in series containing 5 *N* NaOH. A $Ca(OH)_2$ bubbler at the end of the train showed that no CO_2 passed through the scrubbers. From specimens containing 3, 3, and 10.9% uranium, respectively, 60, 94, and 40% of the Ru^{106} was volatilized, most of it being condensed on the cool exit end of the reaction tube but some going as far as the fourth caustic scrubber. All the Zr^{95}, Cs^{137}, and Ce^{144} in the specimens remained with the ash. Combustion was complete in 3 to 4 hr.

Coated Fuels. – In initial experiments with unirradiated fuel of 125-μ UO_2 particles coated with 17-mil-thick Al_2O_3 and dispersed in graphite, the uranium loss to the residue after two leaches with 90% HNO_3 was 99.2%. Combustion of the fuel in oxygen at 700 to 900°C and digestion of the ash with boiling 10 *M* HNO_3 for about 8 hr recovered only 9.9% of the uranium. Uranium losses from unirradiated samples of the Pebble Bed Reactor fuel, which had been coated with Si-SiC, on burning in oxygen at 700 to 900°C and digestion of the ash with boiling 10 *M* HNO_3 for 6 to 8 hr, were 0.35 and 2%, respectively, with coatings 3 and 30 mils thick. The U/Si weight ratios in the respective samples were 4.5 and 0.33.

Uranium Carbide Fuel

Uranium carbides react with most aqueous reagents and a number of gases, and processes selected will depend on the type of cladding and bonding used in specific fuel elements, safety, and reaction rates. The advisability of using 90% HNO_3 to disintegrate uranium carbide-graphite fuel, such as that of the HTGR, is partially dependent on establishing that the carbide–nitric acid reaction does not produce potentially explosive gas mixtures or solutions. Since the chemistry of the uranium carbides is virtually unknown, the stoichiometries and rates of reactions of uranium carbides with water, nitric acid,

common aqueous decladding solutions such as aqua regia, sulfuric acid, and sodium hydroxide, and such gases as oxygen and chlorine are being studied.

High-purity uranium monocarbide reacted with water at 80°C in a helium atmosphere to produce a finely divided brown uranium(IV) compound and 93 ml (STP) of gas per gram of uranium carbide hydrolyzed.[13] The gas consisted principally of 86.7 vol % methane and 10.4 vol % hydrogen, but also contained 1.8% ethane, 0.69% propane, 0.27% butane, 0.009% isopentane, 0.050% *n*-pentane, 0.045% branched hexane isomers, 0.010% *n*-hexane, and <0.001% *n*-heptane. At least three and probably all four branched-chain hexane isomers were present. No ethylene or other unsaturated hydrocarbons were detected. Each gram of uranium carbide theoretically contained 4.00 mmoles each of carbon and uranium; experimentally 3.99 mmoles of uranium and 3.95 mmoles of carbon were found. By comparison, a total of 3.91 mmoles of carbon and 16.1 mmoles of hydrogen were found in the gas phase. At 90°C the reaction rate was higher than at 80°C, but the products were essentially the same. The off-gas results do not agree with those of Litz,[14] who reported that the hydrogen concentration increased from 12 to 22% and the methane decreased from 81 to 72% as the hydrolysis temperature was raised from 83 to 90°C.

The brown uranium precipitate was an amorphous solid readily oxidized by air. After dissolution in chlorine-free 6 *M* HCl, 99% of the uranium was in the tetravalent state. The uranous chloride solution contained <0.05 mmole of carbon per gram of uranium carbide. Reaction of high-purity uranium monocarbides with 5.6 *M* HCl at 80°C was slower than with water, but the gaseous products were essentially the same; the uranium dissolved as uranous chloride.

In preliminary water-hydrolysis experiments with uranium carbide, as the C/U mole ratio increased from 1 to 1.6, the hydrogen concentration in the off-gas increased from 10 to 23%, while the methane concentration decreased from 87 to 14% (Table 1.4). The total volume of gas evolved decreased from 93 to 32 ml/g. The samples with C/U ratios >1 also yielded an unidentified brown wax, which was insoluble in water but soluble in nonpolar organic solvents. The infrared spectrum of a CCl_4 solution of this wax indicated that it might contain aliphatic and aromatic double bonds, carbonyl (ester, aldehyde, and/or ketone), ether, and ester groups.

[13] M. J. Bradley and L. M. Ferris, *Processing of Uranium Carbide Reactor Fuels. I. Reaction with H_2O and HCl*, ORNL-3101 (in press).

[14] L. M. Litz, *Uranium Carbides: Their Preparation, Structure, and Hydrolysis*, Ph.D. Thesis, Ohio State University, NP-1453 (1948).

Table 1.4. Reaction of Uranium Carbides with Water at 80°C

(Helium atmosphere)

Analysis by gas chromatography

Carbide Composition (mmoles/g)			Total Gas Vol, STP (ml/g)	Total Volatile Carbon (mmoles/g)	Avg. Gas Composition (vol %)			
C/U Mole Ratio	U	Combined C			H_2	CH_4	C_2H_6	3 to 8 C
0.99	3.99	3.95	93.0	3.91	10.4	86.7	1.8	1.07
1.06	3.99	4.22	85.3	3.62**	12.5	81.1	5.4	**
1.20	3.93	4.71	76.6	3.40**	13.8	75.2	8.2	**
1.63*	3.81	6.22*	31.7	3.1	23	14	38	22

* Assuming that free carbon left after hydrolysis was unreacted in original specimen.

** Analytical procedure not very sensitive for higher hydrocarbons.

In scouting studies on the reaction of uranium monocarbide with 4.38 *M* HNO_3, NO and CO_2 were the principal gaseous products. A small amount of other nitrogen oxides and <0.01 mmole of CO per gram of carbide were also found. No hydrogen or hydrocarbons were evolved. The uranyl nitrate solution was dark red and contained 40 to 50% of the original carbon. Ion exchange appeared promising as a method for separating uranium from the dark red species, which is sorbed by anion- but not by cation-exchange resins.

1.5 PROCESS STUDIES ON ADVANCED MIXED OXIDE AND METAL FUELS

Process development studies were started on the more advanced fuels, e.g. BeO-UO_2 and Al_2O_3-UO_2 mixed oxide and Nb-U metallic sinters, and methods of dissolving beryllium metal and Hastelloy-X, a newly developed cladding material, were studied.

Processes for Fuels Containing Beryllium Oxide and Aluminum Oxide

Materials such as BeO and Al_2O_3 are being considered as matrix materials for gas-cooled reactor fuel elements. The BeO-containing fuels are in two main categories: (1) those containing more than 60 wt % UO_2, e.g. those planned for the GCRE and MGCR, and (2) those containing less than 10 wt % UO_2. The ceramic material generally is in the form of small pellets and is clad in metal, currently Hastelloy-X, which has the approximate composition 46.0% Ni, 22.5% Cr, 17.2% Fe, and 9.3% Mo.

In preliminary experiments the Hastelloy-X cladding of the GCRE fuel dissolved in boiling 1 to 3 *M* HNO_3–4 *M* HCl at a rate of ~25 mg cm^{-2} min^{-1} (Table 1.5). Solutions stable at room temperature which contained 50 g of alloy per liter were prepared. The reaction may be represented as 0.494 Ni + 0.25 Cr + 0.195 Fe + 0.061 Mo + HCl + 4 HNO_3 → 0.494 $Ni(NO_3)_2$ + 0.25 $Cr(NO_3)_3$ + 0.195 $Fe(NO_3)_3$ + 0.061 $Mo(NO_3)_6$ + NOCl + 2.5 H_2O + 0.156 NO + 0.156 NO_2. Standard Darex (5 *M* HNO_3–2 *M* HCl) and Sulfex (4-6 *M* H_2SO_4) dissolvents were unsatisfactory for the dissolution of Hastelloy-X, with initial dissolution rates of 0.2 and 0.1 mg cm^{-2} min^{-1}, respectively.

Virtually all the uranium was leached from prototype GCRE fuel pellets containing 70% UO_2–30% BeO, 0.44 cm dia by 0.52 cm long, in about 4 hr in a typical decladding solution containing 25 g of Hastelloy-X per liter, 4.1 *M* hydrogen ion, and 3.4 *M* chloride ion. The final solution contained about 4 g of uranium per liter. Most of the BeO matrix remained as an undissolved residue.

Table 1.5. Initial Rates of Dissolution of Hastelloy-X* in Boiling Dilute Aqua Regia Solutions

Dissolution time: 10 min

Nitric Acid Conc. (*M*)	Hydrochloric Acid Conc. (*M*)	Rate (mg cm^{-2} min^{-1})
0	3	0.05
1	3	7.7
3	3	0.6
5	3	0.4
0	4	0.05
1	4	26
3	4	26
5	4	5.9
0	5	0.05
1	5	27
3	5	28
5	5	13

*46% Ni, 22.5% Cr, 17.2% Fe, and 9.3% Mo.

Leaching, with uranium losses to the BeO residue of <0.2%, required about 6.5 hr in boiling 6 to 13 *M* HNO_3, but much longer times were necessary for complete leaching with boiling 4 *M* HNO_3. In 6 to 7 hr leaching with 8 *M* HNO_3 about 50% of the BeO from the matrix was dissolved (Table 1.6); about 50 hr was required to solubilize the last traces of BeO.

Uranium was completely leached in 6 to 15 hr from GCRE fuel pellets with nitric acid–sulfuric acid mixtures with HNO_3/H_2SO_4 mole ratios of $\frac{3}{5}$, $\frac{3}{7}$, $\frac{5}{3}$, and $\frac{7}{3}$, the rate being higher with the higher nitric acid concentrations. The pellets dissolved completely in 24 hr to yield solutions containing about 5 g of uranium per liter. The sulfuric acid had little effect on the rate of UO_2 dissolution, but almost doubled the rate of dissolution of the BeO matrix. For example, in solutions containing 3 to 7 *M* H_2SO_4, 80% of the BeO dissolved in 6 to 7 hr compared to only 50% in solutions containing no sulfuric acid.

Table 1.6. Uranium Recoveries in Leaching of GCRE Fuel Pellets (70% UO_2–30% BeO) with Boiling Nitric Acid

HNO_3 Conc. (*M*)	Leaching Time (hr)	Amount in BeO Residue (%)	
		Uranium	Beryllium
4	4.0	22.7	39.8
6	6.77	0.13	66.2
8	6.78	0.059	59.3
10	6.73	0.094	43.2
10	6.78	0.12	50.3
13	6.78	0.12	48.8

When GCRE fuel pellets were heated in air, spalling and physical disintegration occurred. The resultant powder dissolved completely in 1 hr in boiling 3 *M* HNO_3–3 *M* H_2SO_4. With MGCR fuel pellets, which contain 61% UO_2–39% BeO and are 1.05 cm dia by 1.12 cm long, about 24 hr was required to completely leach the uranium with boiling 8 *M* HNO_3.

The UO_2-BeO fuels containing less than 10% UO_2 did not dissolve rapidly in common aqueous reagents (Table 1.7). Rates were highest in acidic fluoride solutions, with sintered BeO and BeO–8% UO_2 dissolving initially at rates of about 1.7 mg cm^{-2} min^{-1} in boiling 5.8 *M* NH_4HF_2.

Ceramic UO_2-Al_2O_3 is being considered as an alternative fuel for the MGCR; the fuel pellets would be clad in stainless steel or Hastelloy-X. Two types of high-density unirradiated pellets, "homogeneous" and "heterogeneous," containing 4 to 75% Al_2O_3 were used in processing studies. The "homogeneous" pellets consisted of 10-μ grains of UO_2 dispersed in an Al_2O_3 matrix; the UO_2 particles in the "heterogeneous" matrix were about 150 μ. Uranium losses were affected by both the type of pellet and the Al_2O_3 content. In 4 hr leaching with boiling 10 *M* HNO_3 the loss from "homogeneous" pellets containing 4% Al_2O_3 was about 0.002% while that from pellets containing 61% Al_2O_3 was 88%. In general, losses from "heterogeneous" pellets were about half those from the "homogeneous," other conditions being the same. In all cases, <1% of the Al_2O_3 dissolved. Extended leaching for 72 hr or addition of hydrofluoric acid to the nitric acid did not appreciably increase uranium recovery. Boiling 5 *M* HNO_3–5 *M* HCl was also ineffective in leaching either uranium or aluminum from the pellets.

Niobium and Beryllium Dissolution

The use of niobium and niobium pentoxide as fuel cladding, cermet, or ceramic material is very probable because of favorable physical, chemical, and nuclear properties.[15] The insolubility of niobium pentoxide[16] in acids in the absence of large amounts of highly corrosive fluoride, sulfate, or chloride complexing ions[17-19] practically excludes conventional acid dissolution methods, and the precipitation of Nb_2O_5 interferes with dissolution and filtration.[17]

The reaction rates of niobium with anhydrous chlorine, hydrogen chloride, and hydrogen fluoride and with aqueous solutions of concentrated caustic and sulfuric acid and boiling hydrofluoric–nitric acid were studied. The use of anhydrous chlorine at 300°C appeared to offer the best processing method, unless a suitable material of construction can be found for hydrofluoric-nitric acid. Anhydrous fluorine also reacts readily with niobium.[20]

The average dissolution rates of niobium in 30-min tests in boiling sulfuric acid were 2 mg cm^{-2} min^{-1} at 232°C in 16 *M* H_2SO_4, 5 mg cm^{-2} min^{-1} at 290°C in 18 *M* H_2SO_4, and 7 mg cm^{-2} min^{-1} at 140°C in 19.3 *M* H_2SO_4. In tests with boiling mixed HNO_3-HF solutions, dissolution rates in 5-min tests were as high as 35 mg cm^{-2} min^{-1} with 9 *M* HF–3 *M* HNO_3; the rate in 6 *M* HF–1 *M* HNO_3 was 5 mg cm^{-2} min^{-1}. In 10 *M* KOH solution containing 5 and 10 *M* KF, the dissolution rates in 10-min tests were about 0.1

[15] J. A. DeMastry and R. F. Dickerson, *Nucleonics* 18, 87 (1960)

[16] G. L. Humphrey, *J. Am. Chem. Soc.* 76, 978 (1954).

[17] T. A. Gens and F. G. Baird, *Modified Zirflex Process for Dissolution of Zirconium- and Niobium-bearing Nuclear Fuels in Aqueous Fluoride Solutions: Laboratory Development*, ORNL-2713 (Dec. 8, 1959).

[18] Yu. A. Buslow and N. S. Nikolaev, *Russ. J. Inorg. Chem.* (English translation) 4, 210 (1959).

[19] J. H. Kanzelmeyer, J. Ryan, and H. Freund, *J. Am. Chem. Soc.* 78, 3020 (1956).

[20] L. Trevorrow, *Studies on the Behavior of Niobium Pentafluoride in the Fused Salt Processing of Zirconium-Uranium Fuel Alloys*, ANL-5789 (December 1957).

Table 1.7. Initial Rates of Dissolution of Fuels Containing < 10% BeO

Material	Reagent	Initial Dissolution Rate (mg cm^{-2} min^{-1})
BeO	4 *M* HNO_3	0.003
BeO–8% UO_2	4 *M* HNO_3	0.02
BeO	15.8 *M* HNO_3–0.2 *M* NaF	0.03
BeO	4 *M* H_2SO_4	0.05
BeO	8 *M* H_2SO_4	0.26
BeO–8% UO_2	8 *M* H_2SO_4	0.05
BeO–8% UO_2	5 *M* NH_4F	0
BeO	5.8 *M* NH_4HF_2	1.7
BeO–8% UO_2	5.8 *M* NH_4HF_2	1.5
BeO	5 *M* NH_4HF_2–2 *M* NH_4NO_3	1.9

mg cm^{-2} min^{-1}; the rate in 30 *M* KOH at 325°C was 6 mg cm^{-2} min^{-1}.

In tests with anhydrous Cl_2, HCl, and HF at elevated temperatures, reaction with Cl_2 gave the best rates. Niobium was attacked by Cl_2 at a rate of 12 mg cm^{-2} min^{-1} at 300°C and at 28 mg cm^{-2} min^{-1} at 360°C. The reaction rate with HCl was 0.1 mg cm^{-2} min^{-1} at 450°C and 3 mg cm^{-2} min^{-1} at 600°C. With HF, rates were 0.1, 1.8, and 6 mg cm^{-2} min^{-1} at 500, 600, and 650°C, respectively.

Beryllium metal, which is frequently mentioned as a cladding material for uranium oxide fuel elements for gas-cooled reactors, dissolved readily in boiling 4 *M* H_2SO_4, 6 *M* NaOH, and dilute nitric acid containing 0.05 to 0.1 *M* NaF. Initial dissolution rates varied from 2 to 63 mg cm^{-2} min^{-1} (Table 1.8).

1.6 CORROSION STUDIES[21]

The corrosion evaluation program includes work on materials of construction for the Thorex, Modified Zirflex, Sulfex, and Zircex process dissolvers and for a centrifuge to clarify various types of fuel solutions, and on possible materials for fluoride-containing solvent extraction equipment and for a mixture of fuming nitric and sulfuric acids.

[21]Work done by members of the Reactor Chemistry Division.

Table 1.8. Initial Rates of Dissolution of Sintered Beryllium Metal in Various Boiling Reagents

Reagent	Initial Dissolution Rate (mg cm^{-2} min^{-1})
6 *M* NaOH	2
4 *M* H_2SO_4	63
4 *M* HNO_3	0.02
15.8 *M* HNO_3	0.04
4 *M* HNO_3–0.05 *M* NaF	8
4 *M* HNO_3–0.01 *M* NaF	11

Thorex Process

In the Thorex process ThO_2-UO_2 pellets are dissolved in boiling 13 *M* HNO_3–0.04 *M* fluoride with or without aluminum or borate. Continuation of earlier tests[5] confirmed the suitability of titanium for batch feed adjustment boildowns, but localized attack by condensate above refluxing solutions of constant compositions, such as would be obtained in a continuous process, was severe. The presence of 0.2 *M* borate in the solution for criticality control did not affect the localized attack. The maximum overall corrosion rate at a total exposure time of 316 hr was 0.05 mil/month for 100 batch boildowns. Overall rates in continuous reflux tests were between 1.8 and 2.5 mils/month for 2016 hr exposure. The solutions used

in these tests had an initial composition of 9.5 *M* HNO_3, 0.04 *M* F^-, 0.04 *M* $Al(NO_3)_3$, 0.06 *M* $UO_2(NO_3)_2$, 0.8 *M* $Th(NO_3)_4$, 0.0025 *M* HCl, and 0.004 *M* $Fe(NO_3)_3$. The same solution containing 0.2 *M* borate showed no appreciable difference in corrosion behavior.

In 96 hr exposure of LCNA[22] to initial Thorex dissolver solution, 13 *M* HNO_3–0.04 *M* NaF–0.05 *M* $Na_2B_4O_7$, attack was uniform, with a maximum value of 11.5 mils/month in the vapor phase. When 0.1 *M* $Al(NO_3)_3$, 0.1 *M* $Th(NO_3)_4$, and both 0.1 *M* $Al(NO_3)_3$ and 0.1 *M* $Th(NO_3)_4$ were present in the dissolvent, maximum rates were 3.2, 10.0, and 2.6 mils/month, respectively. These rates are little, if any, better than those of Ni-o-nel, but localized intergranular attack, which is observed in the heat-affected zone of welded Ni-o-nel,[5,21] was not observed with LCNA.

Sulfex Process

In the Sulfex process, stainless steel cladding is removed from UO_2 or UO_2-ThO_2 fuel by dissolution in 3.5 to 6 *M* H_2SO_4. LCNA and two Haynes experimental alloys, EB4358 and EB5459, exposed to boiling 6 *M* H_2SO_4 and to 6 *M* H_2SO_4 containing 10 g of stainless steel per liter, showed maximum corrosion rates of 3.3, 2.9, and 2.4 mils/month, respectively in 120 hr exposure to 6 *M* H_2SO_4.[19] In the solution containing 10 g of stainless steel per liter, maximum 120-hr rates of the three alloys were 1.7, 0.47, and 0.52 mils/month, respectively. LCNA showed a maximum rate in the vapor phase, but both Haynes alloys were corroded more rapidly in the solution phase, and all showed some random pitting in the solution.

Modified Zirflex Process

In the modified Zirflex process studies, welded specimens of Hastelloy F, LCNA, and types 304L and 309SNb stainless steel were exposed ~500 hr to boiling 5.4 *M* NH_4F–0.33 *M* NH_4NO_3 to which hydrogen peroxide was added continuously to maintain it between 0.0028 and 0.0032 *M*. LCNA performed the most satisfactorily, with a maximum overall rate of 1.15 mils/month and some slight grain boundary attack. Hastelloy F, 304L, and 309SNb stainless steels all showed extensive weld decay with overall maximum rates of 3.1, 13.4, and 2.3 mils/month, respectively.

In a boiling solution prepared by dissolving 61 g of Zircaloy-2 in 1 liter of 5.4 *M* NH_4F–0.33 *M* NH_4NO_3–0.003 *M* H_2O_2, specimens of 304L and 309SNb stainless steel were corroded at rates which accelerated as the exposure time was increased from 24 to 48 hr. For 304L the 24- and 48-hr maximum rates were 14.3 and 23.9 mils/month, respectively, and for 309SNb, 3.7 and 4.0 mils/month. The 304L suffered edge corrosion and pitting attack.

A tentative flowsheet was developed for dissolution of the 8% U–92% ZrH alloy of the TRIGA fuel, which in one step uses a dissolvent of 90 vol % 21 *M* HNO_3–10 vol % 20 *M* H_2SO_4. The temperature would be controlled at 50°C to decrease corrosion. LCNA, type 309SNb, and INOR-8 were investigated as potential materials of construction for the dissolver. INOR-8 performed the most satisfactorily, with an overall maximum rate of 0.17 mil/month for 336 hr exposure. No localized attack was observed and the corrosion rates of the solution and vapor phase specimens were almost identical. Both LCNA and 309SNb suffered extensive weld decay and intergranular attack in the vapor phase even though overall maximum rates were only 0.9 and 2.9 mils/month, respectively. Flushing the vapor space with dry air lowered the maximum rate for Ni-o-nel to 0.3 mil/month and decreased but did not completely eliminate localized attack.

Titanium for Non-Darex Applications

Since titanium has shown[23] superior resistance to all the commonly used aqueous processing dissolvents except sulfuric acid and fluoride-containing solutions, tests were made to evaluate its resistance to the HNO_3-$Fe(NO_3)_3$ solutions used for dissolution of uranium–10% molybdenum fuel alloy. Welded specimens of Titanium-45A were exposed to 3.5 and 8 *M* HNO_3, 0.5 *M* in $Fe(NO_3)_3$ and containing 0.6 *M* $UO_2(NO_3)_2$ and 0.02 *M* MoO_3 to approximate spent dissolver solutions. The 24- to 72-hr behavior of titanium in these boiling solutions was somewhat erratic, varying, without

[22] A special low-carbon alloy differing in composition from Ni-o-nel only in its lower carbon content.

[23] W. E. Clark and T. A. Gens, *A Study of Dissolution of Reactor Fuels Containing Zirconium in a Titanium Vessel*, ORNL-3118 (in preparation).

apparent pattern, from slight weight gains to corrosion rates as high as 0.24 mil/month. At longer exposure times, rates became steady and slowly decreased. When the tests were terminated after 1000 hr exposure, the maximum rate was about 0.06 mil/month with no apparent localized attack.

Studies[24] to determine the feasibility of inhibiting titanium by chromate in processes that use fluoride for zirconium-containing fuel showed that when the F/Zr ratio was ≤ 4 (Fig. 1.11) the corrosion rate of Titanium 65A was <3 mils/month, but at F/Zr ratios >5 corrosion rates were very high. A continuous process was postulated in which a dissolvent, 16 *M* HNO_3–0.58 *M* Cr–1.9 *M* F, is continuously added to a dissolver in which the equilibrium concentrations are 16 *M* HNO_3–0.58 *M* Cr–1.9 *M* F–0.5 *M* Zr, and an equal volume of product is continuously withdrawn. With this flowsheet it was determined that the Zircaloy-2 dissolution rate would be 2 mg cm^{-2} min^{-1} (Fig. 1.12).

In tests in which titanium was exposed to boiling 0.5 *M* HBF_4–0.3 *M* $(NH_4)_2Cr_2O_7$ and in which the HNO_3 was made 3, 9, 12, and 15 *M*, the corrosion rates were 50, 150, 295, and 270 mils/month, respectively, in the absence of zirconium and 19, 140, 110, and 190 mils/month in the presence of dissolving zirconium.

Zircex Process

In the Zircex process zirconium and molybdenum fuels, and possibly certain ceramic and graphite-containing fuels, are contacted with hot Cl_2, HCl, HCl-air and CCl_4-N_2 gas to convert them partially or wholly to volatile chlorides. Specimens of Haynes 25, Inor-8, Nichrome V, and Pyroceram exposed for 48 hr to flowing 15% HCl–85% air at 400°C showed maximum corrosion rates of 0.06, 0.03, 0.06, and 0 mil/month, respectively. Specimens exposed 360 hr to flowing anhydrous HCl at 350°C showed maximum rates of 0.25, 0.03, 0.16, and <0.01, respectively.

Multipurpose Material of Construction

Several candidate materials were exposed at 35°C to spent decladding or dissolver solutions produced by the Darex, Zirflex, Sulfex, Thorex, and UO_2 core dissolution processes in order to determine whether a satisfactory common material of construction could be found and thus eliminate duplication of expensive equipment. Hastelloy F appeared to have the best general resistance to attack of the materials studied (Table 1.9). The addition of 0.05 *M* $Al(NO_3)_3$ to the UO_2 core solution decreased the corrosion rates for titanium

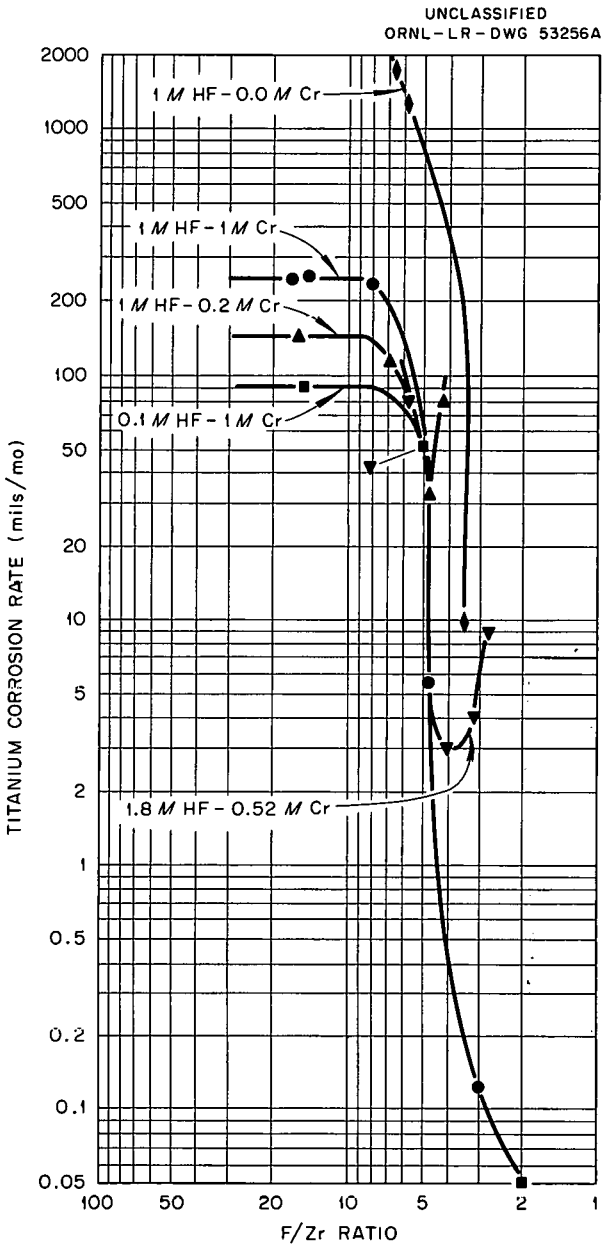

Fig. 1.11. Corrosion Rates of Titanium 65-A in Refluxing 16 *M* HNO_3-Zirconium Solution.

[24] *Construction Materials for Various Head-End Processes for the Aqueous Reprocessing of Spent Fuel Elements*, BMI-1375 (Aug. 28, 1959).

Table 1.9. Multipurpose Material-of-Construction Corrosion Tests

Alloy	Darex[a]		Zirflex[b]		Thorex[c]		UO_2[d] Dissolvent		Sulfex[e]	
	Exposure (hr)	Rate (mils/mo)	Exposure (hr)	Rate (mils/mo)	Exposure (hr)	Rate (mils/mo)	Exposure (hr)	Rate (mils/mo)	Exposure (hr)	Rate (mil/mo)
Titanium-45A	674	0.01	672	6.06	672	0.03	528-336	9-11.1	672	0.04
Hastelloy C	674	0.36	672	0.01	672	0.33	336	5.2	672	0.06
Hastelloy F	674	0.05	672	0.04	672	0.03	840	0.69	672	0.01
LCNA	506	57.3	504	0.01	672	0.03	840	0.27	672	0.08
Carpenter 20 SNb	506	6.7	504	0.03	672	0.03	840	0.48	672	0.02

[a]Darex decladding solution: 45 g of 304 stainless steel and 5 g of type 302B stainless steel disso ved in 1 liter of 2 *M* HCl–5 *M* HNO_3.

[b]Zirflex decladding solution: 25 g of zirconium dissolved in 1 liter of 6 *M* NH_4F–1.0 *M* NH_4NO_3.

[c]Thorex solution: 375 g of 96% ThO_2-4%UO_2 pellets dissolved in 1 liter of 13 *M* HNO_3–0.04 *M* $Al(NO_3)_3$–0.04 *M* NaF.

[d]UO_2 core dissolvent: 453 g of UO_2 dissolved in 1 liter of 10 *M* HNO_3 containing 0.01 *M* Zr^{4+} and 0.05 *M* NaF.

[e]Sulfex solution: 30 g of Type 304 stainless steel dissolved in 1 liter of 4 *M* H_2SO_4–0.001 *M* NaF.

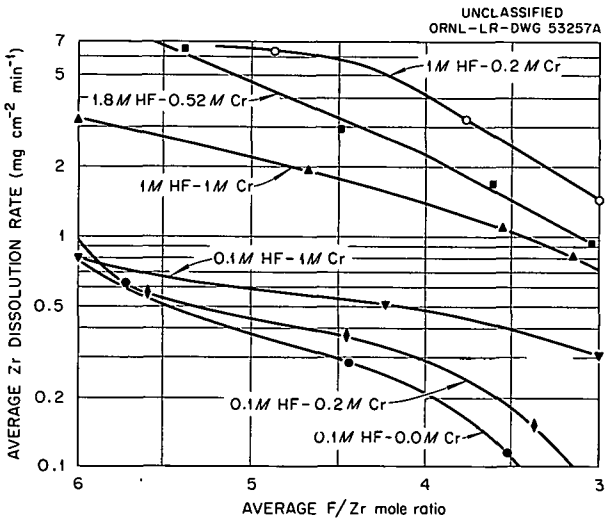

Fig. 1.12. Dissolution Rate of Zircaloy-2 in 16 *M* HNO_3–HF–$(NH_4)_2Cr_2O_7$.

and Hastelloy F to 3.42 and 0.09 mils/month, respectively, for 528 hr exposure but caused heavy pitting of the titanium.

Solvent Extraction Feed

In the Modified Zirflex Process, in which zirconium-uranium alloy fuels are dissolved in 6 *M* NH_4F–1 *M* NH_4NO_3–H_2O_2, the spent dissolver solution is prepared for solvent extraction by addition of HNO_3 and $Al(NO_3)_3$. The composition of the feed solution will be dictated partly by container corrosion. The corrosion rate of LCNA in 288 hr exposure to 1 *M* Al^{3+}–0.4 *M* Zr^{4+}–2.7 *M* F^-–1 *M* H^+–4.2 *M* NO_3^- was 0.08 mil/month.

Borosilicate Glass Rings as Nuclear Poisons

The storage of highly concentrated (> 200 g/liter) aqueous solutions of uranium and plutonium in conventional tanks is feasible if heterogeneous nuclear poisoning is used for criticality control, e.g. high-boron (5.8%) borosilicate glass Raschig rings. The results of tests on high-boron glass and titania-coated (1-μ-thick coat) high-boron glass rings, with normal (4% boron) rings as a control, indicated that normal borosilicate glass is satisfactorily chemically resistant under process conditions; the high-boron glass rings were judged unsuitable.

The uncoated rings were fire polished and annealed. All were exposed for 650 hr to 2 and 6 *M* HNO_3 at 23 and 65°C for eight combinations of variables. The normal borosilicate rings showed only +0.4 to –0.6 mg weight change per ring, but the bare high-boron rings lost weight under all conditions, with temperature having a greater effect than acid concentration. The weight loss occurred by both solubilization of boron and sodium and flaking off of silica. Crazing of the inner surface of the high-boron rings and considerable chipping and internal cracking were noted, and a fine glass powder was produced at 65°C. Solution samples indicated that both boron and sodium were leached at a steadily decreasing rate. Weight losses of the coated rings were only very slightly less than for uncoated rings, but most or all of the weight change may represent loss of coating. These rings showed no evidence of chipping or cracking of the glass at 65°C, but the titania coating had spalled and/or separated from the glass in extensive areas. Failure of the titania coating was confined to the inner surface of the rings; the coating on the outer surface was fully intact on all rings.

1.7 SOLVENT EXTRACTION STUDIES

Acid Thorex Flowsheet

In the acid Thorex process[6] nitric acid rather than aluminum nitrate is used for salting, the chief advantage being that the waste can be concentrated about 15-fold vs. 1.5-fold with aluminum nitrate present. The uranium and thorium are coextracted from acid-deficient feed with 30% TBP in Amsco, with nitric acid salting below the feed point. After being scrubbed with nitric acid and water, the loaded solvent is fed to the midpoint of the partitioning column, where thorium is stripped with 0.01 *M* HNO_3 and uranium is scrubbed from the aqueous stream with fresh solvent. Finally, uranium is stripped from the solvent with 0.01 *M* HNO_3. The flowsheet was demonstrated in three 2-in.-dia pulsed columns with 12-ft sections for extraction, scrubbing, partitioning (thorium stripping and uranium scrubbing), and uranium stripping. The total losses (Table 1.10) of both thorium and uranium were less than 0.1% with one exception where the uranium loss in the stripped solvent was 0.39% because the flow ratio was set too close to the pinch point.

Table 1.10. Uranium and Thorium Losses in Three Acid Thorex Flowsheet Runs in 2-in.-ID Pulsed Columns

Run No.	Feed Flow Rate (ml/min)	Feed U (g/l)	Feed Th (g/l)	AP Flow Rate (ml/min)	AP U (g/l)	AP Th (g/l)	AP U Loss (%)	AW Flow Rate (ml/min)	AW U (g/l)	AW Th (g/l)	AW U Loss (%)	AW Th Loss (%)
A Column (Extraction)												
ATP-3	73.7	20.3	240	539	2.38	31.4		172	< 0.001	0.010	0.012	0.01
ATP-4	78.0	20.3	240	533	3.15	29.6		174	0.0002	0.005	0.002	0.005
ATPR-2	75.7	20.6	230	577	3.11	31.5		173	0.0003	0.005	0.003	0.005
B Column (Partitioning)												
				BT				BU				
ATP-3				279	0.002	59.3	0.038	629	2.25	0.013		0.026
ATP-4				333	0.005	54.5	0.104	620	2.84	0.027		0.084
ATPR-2				279	0.003	59.0	0.054	663	10.9	0.010		0.030
C Column (Uranium Stripping)												
				CU				CW				
ATP-3				172	7.51	0.027		629	0.001	<0.002	0.040	
ATP-4				184	9.26	0.086		620	0.011	0.005	0.390	
ATPR-2				87.3	20.0	0.060		663	< 0.0005	0.015	<0.020	
				Total Losses (%)								
				U	Th							
ATP-3				0.090	0.036							
ATP-4				0.496	0.089							
ATPR-2				0.077	0.035							

Otherwise, most of the losses were due to incomplete separation of thorium and uranium in the partitioning column, where good flow control is required and additional column length would decrease the losses.[25]

Revision of the flowsheet used in the above runs so that part of the aqueous stream from the uranium stripping column was returned as a stripping agent for thorium to the partitioning column and the remainder withdrawn as uranium product built up the uranium concentration to a maximum in the upper section of the partitioning column where the thorium concentration is low. Further down the column thorium salting caused extraction of the uranium, preventing loss out the bottom. By proper choice of flow ratios, uranium was completely stripped, resulting in increased concentration at the bottom of the column. In a 12-hr demonstration run with a 24-ft sieve-plate stripping column at a feed/scrub/recycle/product flow ratio of 1.0/0.15/0.48/0.15, the uranium concentration increased to 20 g/liter, more than twice that without reflux. Uranium loss was 0.054% to the thorium product and <0.02% to the stripped solvent; thorium loss was 0.03%.

The flow capacity and efficiency of both sieve and nozzle plate columns used for extraction and stripping in the Thorex flowsheet (Table 1.11) were in general agreement with those previously reported for the standard Purex flowsheet.[6] Typically, with a 1-in. pulse and 50 cpm frequency the capacity was about 1000 gal ft^{-2} hr^{-1} and the HETS was 2 to 3 ft for extraction of thorium in either a sieve-plate column operated with a top interface or a nozzle-plate column with a bottom interface.

Laboratory experiments showed that the capacity of a plant may be increased without loss in decontamination by increasing the thorium in the feed

[25] A. D. Ryon, *McCabe-Thiele Graphical Solution of Uranium-Thorium Partitioning from 30% TBP-Amsco Solvent*, ORNL-3045 (Jan. 17, 1961).

Table 1.11. Flooding Capacity and HETS for Pulsed Columns Operating on Acid Thorex Flowsheet

Pulse amplitude: 1 in.

Column	Pulse Frequency (cpm)	Flooding Capacity, total flow (gal ft^{-2} hr^{-1})		HETS (ft)	
		Top Interface	Bottom Interface	Top Interface	Bottom Interface
		Sieve Plate, 0.125-in.-dia holes, 23% free area			
Extraction	50	1030	1690	Th 2.1	4.0
Partitioning	30	950			
	50	750			
Stripping	35	1290	1290	Th 6.1	6.1
				U 4.2	4.6
		Nozzle Plate, 0.125-in.-dia holes, 23% free area			
Extraction	30		1400		
	50		1250		Th 2.5
	70		500		
		Nozzle Plate, 0.188-in.-dia holes, 23% free area			
Extraction	50				Th 4.0
Stripping	35	2080	2280	Th 6.1	Th 6.2
				U 4.4	U 5.0

from 260 to 325 g/liter and correspondingly increasing either the concentration or volume of the solvent.

Point of Acid Addition

Changing the point of addition of the acid to different extraction stages modified the thorium and acid profiles of the column and thereby affected both the decontamination factors and thorium loss. When acid was added at the feed plate decontamination factors from ruthenium and zirconium-niobium were 1000 and 3000, respectively, and the thorium loss was 0.3%. When the acid was added to the fourth extraction stage, the corresponding values were 600 and 10,000, and 0.6%. When the acid was added at the last stage the loss was 2%. A second organic phase was formed when the acid was added at the feed plate but not when it was added to any other stage.

Effect of Equilibration Time

Equilibration of solutions under feed plate conditions at 55°C for 1 hr decreased decontamination from ruthenium and zirconium-niobium by factors of 2 and 4, respectively, compared with a standard 5-min contact. The contact time in a pulsed column is only about 8 min.

Thorium Stripping with Dibasic Aluminum Nitrate

The use of dibasic aluminum nitrate to selectively strip thorium from the 30% TBP thorium-uranium extract gave an acid-deficient thorium product solution. This could be directly concentrated by evaporation to prepare an acid-deficient feed for the second thorium cycle solvent extraction without the high-temperature feed adjustment required with dilute nitric acid stripping. The uranium product was also more concentrated due to the decrease in acid in the organic phase to the stripping column. Flowsheet conditions were:

Feed: 42.3 g/liter Th, 2.69 g/liter U, 0.05 *M* HNO_3, 30% TBP in Amsco, 7 volumes
Strip: 0.05 *M* $Al(OH)_2NO_3$, 4.2 volumes
Scrub: 30% TBP in Amsco, 1.4 volumes
Stages: 5 strip, 5 scrub

The thorium contained 0.06% of the uranium and was 0.04 *N* acid deficient. The uranium product stream contained 0.08% of the thorium and was less than 0.01 *M* in HNO_3.

Effect of Self-irradiation

The solvent extraction feed for the acid Thorex processing of CETR fuel will generate about 15 watts/liter, which amount of self-irradiation greatly decreased decontamination from fission products with the aluminum-salted Thorex flowsheet, and the bisulfite treatment was developed to counteract this effect.[26] Irradiation of synthetic CETR feed solutions to ~5 whr/liter in a Co^{60} source decreased decontamination by a factor of not more than 2, but irradiation to about 65 whr/liter increased decontamination by a factor of 4 when the bisulfite treatment was used.

Homogeneous Criticality Poisons

Laboratory experiments have demonstrated the chemical compatibility with process solutions of cadmium or boron, which have been proposed as homogeneous criticality poisons in the dissolution and feed adjustment of reactor fuel.[27] In subsequent countercurrent batch extraction experiments with the acid Thorex process, the concentrations of these neutron absorbers were decreased from 0.004 g of boron and 0.01 g of cadmium per gram of thorium in the feed to less than 7.8 ppm of boron and 0.4 ppm of cadmium in the thorium product in a single solvent extraction cycle.

Waste Concentration

Concentration of a synthetic acid Thorex first cycle aqueous waste solution to 6% of its original volume resulted in only a slight amount of precipitate. The solution, simulating aqueous waste from the processing of CETR fuel by the acid Thorex process, initially contained 0.043 *M* $Al(NO_3)_3$, 0.043 *M* H_3BO_3, 0.043 *M* $NaHSO_3$, 0.17 *M* NaF, 0.0043 *M* H_3PO_4, 0.0043 *M* $Fe(NH_2SO_3)_2$, and 2.6 *M* HNO_3 but no fission products. It was concentrated to about 1.3% of its original volume to remove most of the nitric acid and then diluted to 6% of its original volume with water. This volume of concentrated aqueous waste from the acid Thorex process is equivalent

[26] R. H. Rainey, A. B. Meservey and R. G. Mansfield, *Laboratory Development of the Thorex Process. Progress Report, Dec. 1, 1955 to Jan. 1, 1958*, ORNL-2591.

[27] J. G. Moore and R. H. Rainey, *Chemical Feasibility of Homogeneous Neutron Poisons for Criticality Controls in Consolidated Edison Fuel Processing Solutions*, ORNL-2854 (Mar. 25, 1960).

to 0.2 liter per kilogram of thorium processed, a factor of 10 less than that from the aluminum nitrate–salted scheme.

Second Cycle Uranium Flowsheet

In laboratory experiments with 15% TBP and acid rather than aluminum for the second uranium cycle, capacities were higher and decontamination factors were equivalent to those found with 2.5, 5, or 10% TBP (Table 1.12). With a feed of 6.3 g/liter U, 1 g/liter Th, and 3 *M* HNO_3, a scrub of 2 *M* HNO_3, and 4 scrub and 6 extraction stages, the percentage saturation of solvent was highest with the highest TBP concentration.[24]

Table 1.12. Effect of Varying TBP Concentration in Final Uranium Purification Cycle

4 scrub, 6 extraction stages

	2.5% TBP	5% TBP	10% TBP	15% TBP
Feed				
U (g/liter)	6.27	6.49	6.3	6.28
Th (g/liter)	1.00	0.98	0.99	0.96
H^+ (*N*)	3.35	2.98	3.0	3.03
Volume ratio	1	1	1	1
Scrub				
H^+ (*N*)	2.0	2.0	2.0	2.0
Volume ratio	0.50	0.112	0.05	0.03
Solvent vol ratio	3.3	0.86	0.35	0.21
Organic Product				
U (g/liter)	1.95	7.61	18.0	30.7
H^+ (*N*)	0.03	0.07	0.08	0.11
Aqueous Waste				
H^+ (*N*)	2.92	2.76	2.88	2.88
Vol	1.5	1.112	1.05	1.03
Column* uranium capacity (g/hr)	130	320	450	508
Gross γ D.F.	1.58×10^3	1.2×10^4	1.2×10^4	1.3×10^4
Ru γ D.F.	2.22×10^4	$>4.2 \times 10^4$	2.4×10^4	1.8×10^4
Zr-Nb γ D.F.	3.92×10^3	3.4×10^4	3.2×10^4	3.9×10^4
TRE β D.F.		$>1.2 \times 10^5$	9.1×10^4	8.5×10^4
D.F. from Th	76	25	47	140
U loss (%)	0.60	1.0	0.83	2.4
U material balance (%)	103	102	101	105
U Saturation at feed point (%)	25	38	43	47

*Assuming a column capacity of 100 liters/hr and feed of 6.3 g/liter.

The use of nitric acid instead of aluminum nitrate in the second uranium cycle extraction with 5% TBP in Amsco was studied in a 2-in.-dia pulsed column. The extraction flooding rate was >1000 gal ft^{-2} hr^{-1} and the HETS was <2 ft at a pulse frequency of 50 to 70 cpm (Table 1.13). HETS values for stripping were 2 to 3 ft at 50 cpm. Typical feed/scrub/solvent flow ratios were 6/1/7. The feed consisted of 3 *M* HNO_3 containing 10 g U/liter; the scrub was 2 *M* HNO_3.

Experiments with High-activity Feed

In a series of acid Thorex decontamination experiments in mini-mixer solvent extraction equipment with feed solutions containing 5 to 25 times the activity used in laboratory studies, decontamination factors were 10^4, 5×10^3, and 2×10^5 from ruthenium, zirconium-niobium, and rare earths, respectively. Due to the limited number of stages in the equipment the thorium loss was 5 to 20%. The limiting activity in each product was zirconium-niobium. Ruthenium and rare earths were removed to the limits of analytical detection. The activity in these tracer runs was from 1 to 5×10^8 γ c min^{-1} ml^{-1} but was only about 0.1% of the activity expected in the CETR fuel.

Solvent Extraction Chemistry of Zirconium and Niobium

Leached borosilicate glass has been shown to adsorb zirconium and niobium from low-concentration nitric acid solutions[28] and glass wool to remove Nb^{95} daughters by selective adsorption

[20] C. S. Lowe and H. W. McVey, *Rare Earth–Actinide Separation by Adsorption*, U.S.P. 2,903,333 (Sept. 8, 1959).

Table 1.13. Flooding and HETS for Second Uranium Cycle, 5% TBP Flowsheet

Pulse amplitude: 1 in.
Column dia: 2 in.

Column	Pulse Frequency (cpm)	Flooding Capacity, Total Flow (gal ft^{-2} hr^{-1})		HETS (ft)	
		Top Interface	Bottom Interface	Top Interface	Bottom Interface
Sieve Plates, 0.125-in.-dia Holes, 23% Free Area					
Extraction-Scrub	50	1480		2.2	
	70	975		1.2	
	90	550		1.0	
Stripping	30	775			
	50	475		3.1	
	70	275			
Nozzle Plates, 0.125-in.-dia Holes, 10% Free Area					
Extraction-Scrub	50		1790		1.5
	70		820		1.5
	90		380		
Stripping	30	375	950		
	50	260	550	3.2	1.9
	70	140	325		

from solutions of high nitrate concentration.[29] Zirconium solutions in which 95% of the activity was Zr^{95} were prepared by passing solutions containing 20 g/liter Zr, 10 *M* HNO_3, ~10^6 c min^{-1} ml^{-1} Zr^{95}-Nb^{95}, and 25 g of 100-mesh unfired borosilicate glass per liter through two 13-mm-long by 10-mm-dia columns containing 1 g of >100 mesh unfired Vycor. The zirconium adsorption decreased with increasing acidity, from 2 to 16 *M*, but niobium adsorption was maximum from 10 *M*. Unfired borosilicate glass had a higher capacity for adsorption of zirconium and niobium and probably a greater potential for separating the two elements. In laboratory tests the distribution coefficients for zirconium between 30% TBP in dodecane and an aqueous solution 0.01 *M* in zirconium and 2 *M* in HNO_3 indicated the presence of at least two species of zirconium, the most extractable having a distribution coefficient of about 0.12. With 4 *M* HNO_3 solutions the coefficient was 0.42 and did not vary for contact times ranging from 5 to 60 min; with 6 *M* HNO_3 it was 1.6.

In preliminary experiments on the extraction of Nb^{95} from 4 *M* HNO_3 with 30% TBP in dodecane containing 10 vol % chemically degraded TBP in Amsco, the distribution coefficient for the extractable niobium species was 0.90; ~20% of the niobium was in an unextractable form. The distribution coefficient from organic containing Nb^{95} to fresh aqueous solution ranged from 0.4 to 2.0.

1.8 MECHANICAL PROCESSING

The facility for mechanical dejacketing of stainless steel–clad NaK-bonded uranium fuel from Core 1 of the SRE was completed, tested with unirradiated fuel, and used to declad SRE Core 1 assemblies with an average burnup of 675 Mwd per ton of uranium. A 250-ton fuel shear, built by the Birdsboro Corporation to a joint ORNL-Birdsboro design, was installed in the chop-leach facility along with a rotary-screw conveyor-feeder and an inclined rotary-screw leacher. Testing of the facility with unirradiated fuel was started.

[29] V. M. Vdovensko, L. N. Lazarev, and Ya. S. Khvorosten, *Radiokhimiya* 1, 364 (1959).

Dejacketing of SRE Fuel

SRE Core 1 fuel burned to ~675 Mwd/ton and decayed ~2 years is being dejacketed at a rate of 2 to 3 kg/hr. Tests with unirradiated prototype fuel supplied by Atomics International had indicated a rate of 10 to 20 kg/hr, and the lower rate with spent fuel is attributed to embrittlement of the 10-mil-thick tubular stainless steel jackets so that they are not appreciably expanded by an internal hydraulic pressure of up to 1700 psig. The uranium fuel slugs were slightly bent and swollen 10 to 30 mils dia and could not always be hydraulically removed from the tubular jackets as expected. In processing a typical irradiated cluster (70 kg) consisting of seven fuel rods, the slugs from one rod were removed hydraulically, and one rod was cut into slug lengths (6 in.) and dejacketed separately in the auxiliary dejacketer which split the jackets by roller cutters, the jackets then being pried from the slug surfaces. Five rods required the use of a jackscrew ramrod to physically dislodge the slugs from the open-end tubular jackets.

The dejacketed slugs were steam cleaned free of NaK, canned in aluminum cans, and stored in a shielded facility to await off-site shipment to a chemical processing plant. The emptied jackets were cleaned free of NaK, rolled and flattened into a coil, and disposed of by ground burial along with the spacer wires, end caps, and the metallic spiders sawed from each end of a fuel cluster.

The fuel clusters appeared to be relatively undamaged by a temperature excursion which melted some fuel rods and stopped reactor operation. The surfaces of the stainless steel tubes were severely discolored by a black to dark brown powdery deposit, indicating carbon embrittlement by organic coolant which leaked into the reactor. The spent fuel slugs were severely pitted (orange peel appearance) in some instances but were typically gold in color and smooth textured.

The dejacketing equipment complex, consisting of a traversing-receiving table, multipurpose disassembly saw, hydraulic wire cutter, hydraulic dejacketer, slug steam cleaner, canning device, auxiliary dejacketer and NaK disposal system, performed mechanically as expected. Operational bottlenecks were: transfer of canned fuel to a storage cell, insertion of a cannister containing a spent cluster from the carrier to the segmenting cell, transfer of the NaK to a

metering pot when the NaK is in an oxidized, waxy form, and removal of jackets from highly pitted slugs after the jacket has been cut several times.

Prior to the runs with fuel rods, the adequacy of the facility and of the equipment components of the mechanical dejacketing complex was demonstrated by various tests on the automatic fire fighting equipment, the ventilation system, the shielding of the facility and shipping carrier, the decontamination system, the NaK disposal system, the auxiliary dejacketer, the multipurpose disassembly saw, emergency retrieval devices, and some materials to solve lubrication problems and related troubles. Secondary containment barriers for compliance with the ORNL policy for the containment and control of radioactive particulates and gases were completed.

The processing of NaK-bonded fuel presents a fire and explosion hazard not usually encountered in fuel processing. Therefore the SRE fuel is dejacketed and the uranium slugs are discharged under an oil (Bayol-D) blanket. The NaK bond, about 100 cc per fuel rod, is simultaneously discharged into the oil and transferred by a nitrogen-purged vacuum system to a vessel where it is safely reacted with steam. The hydroxide formed is further diluted with water and transferred to the waste drain. Operational tests demonstrated this disposal method to be satisfactory with a Bayol-D oil blanket. Bayol-D is a deodorized, highly refined kerosene consisting of highly branched saturated hydrocarbons containing a small amount of cyclic saturated hydrocarbons, with a flash point of 185°F, density of 0.77 g/cc, and 35.5 SUS viscosity at 100°F.

The auxiliary dejacketer roll cutters were redesigned and tested. Cutters of Carpenter K. W. Steel, 60-62 Rockwell C hardness, with a 15-mil-deep cutting edge at a 60° included angle, were not dulled after making 12 consecutive slits, 6 in. long, through SRE jackets containing steel slugs of 7 mils camber. The test was conducted by pushing the 6-in.-long jacketed slugs through the roll cutters by a 3-in.-dia cross section air cylinder. The cutters operated at a minimum of 20 psig air pressure (140 lb force). The maximum operating pressure available would produce ~670 lb force, if needed.

Two materials, Teflon and nylon, showed excellent resistance to NaK while submerged in NaK with a Bayol-D blanket at 100°C for two weeks. The materials were tested for use as liners in stainless steel plug valves since the Bayol-D dissolves most lubricants and allows the stainless steel valves to gall. A Teflon-lined plug valve was installed in the NaK reactor drain line.

Shear-and-Leach Process Development

Shearing of tubular fuel elements into 1-in.-long sections and leaching the UO_2 or UO_2-ThO_2 core material permits recovery of fissile and fertile material from spent power reactor fuel elements by the conventional Purex or Thorex process without dissolution of the metallic jacketing material and end adapters. These inert materials can be stored directly as a minimum-volume solid waste. A shear-and-leach facility, consisting of a shear, conveyor (feeder), a leacher (Fig. 1.13), was installed and 33 Kanigen-brazed prototype fuel elements, each consisting of 36 stainless steel tubes, were purchased. Half the assemblies were filled with UO_2 and the other half with UO_2-ThO_2 or ThO_2 alone. Each run in the cold shear-and-leach complex will require about 60 kg of fuel pellets (two assemblies).

Fabrication and assembly of the 250-ton shear by Birdsboro Corporation for shearing multitube stainless steel fuel assemblies into 1-in. lengths were completed. Wear tests on Stoody 1, 420F, and 416 stainless steel, selected from previous elimination tests without lubrication, with water as a lubricant, and with water containing MoS_2 indicated Stoody alloy to be the best alloy for gibs and liners. Despite some inconsistencies in measurement, there was ample evidence that a water suspension of MoS_2 greatly decreased the wear rate of the test liners over that of dry operation and made less critical the choice of liner materials. This lubricant ultimately cakes on non-rubbing surfaces and causes a hard crust, which may complicate servicing. Grain orientation of the wear specimens had no apparent effect on the results of the tests. Tests on the ¼ scale wooden shear model and talc to simulate UO_2 fines indicated that 23 spray nozzles with a total capacity of ~9.5 gpm at 40 psi should be adequate to wash and decontaminate the interior of the shear.

The stainless steel spiral-drum conveyor has 14 flights on a 6-in. pitch. The conveyor will receive the chopped sections of spent fuel from

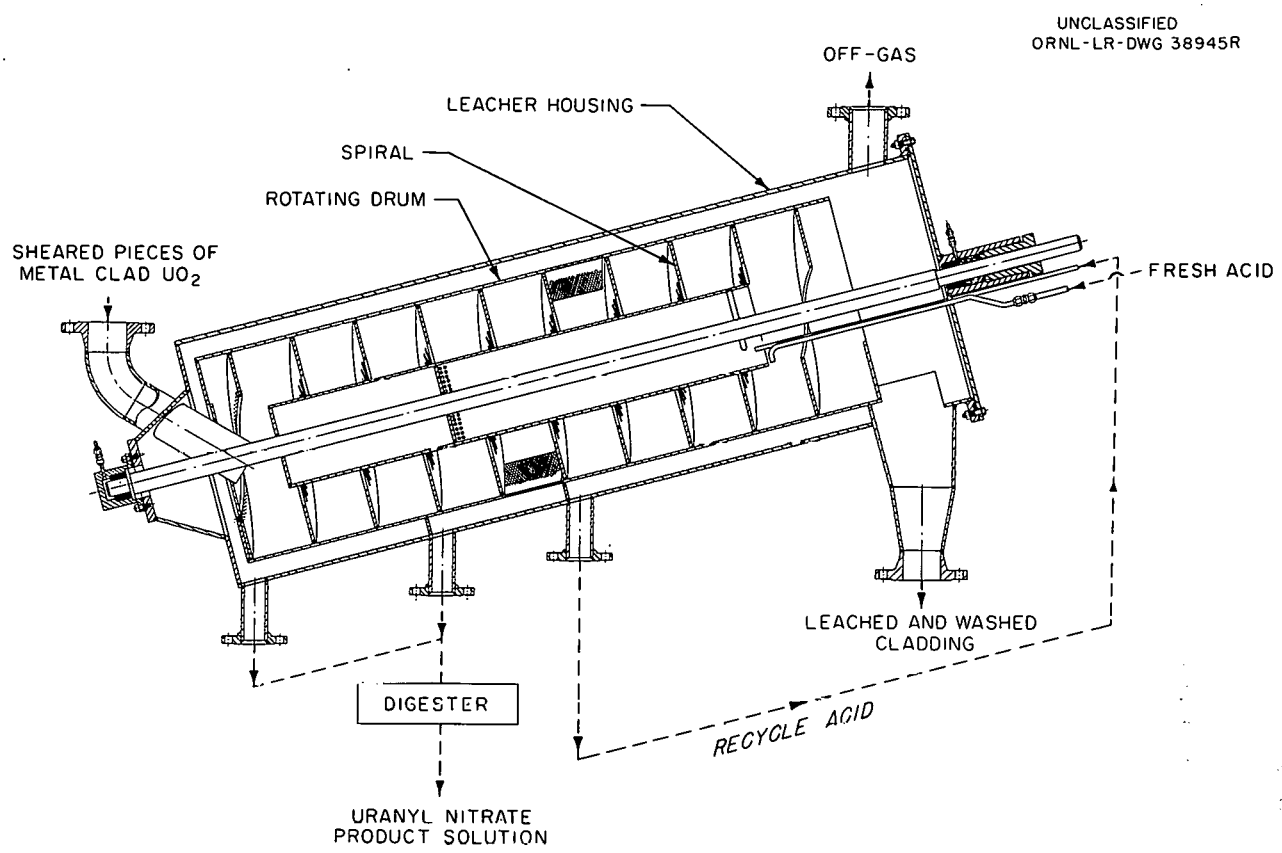

Fig. 1.13. Inclined-Drum Leacher for Countercurrent Nitric Acid Leaching of UO_2 from Sheared Pieces of Metal-Clad UO_2.

the shear, surge-store the material, and feed the leacher in discrete batches at a predetermined rate. A layer of cadmium was installed in the outer shell and the inner cylinder, and the latter was filled with straight-chain polyethylene for criticality control in processing fuels of up to 10.8% enrichment. Some of the factors still to be evaluated are: (1) disposition of fines that enter the feeder; (2) disposition of shear wash water; and (3) lubrication.

An inclined rotary-drum leacher was fabricated, and preliminary tests with chopped stainless steel rods (0.5 in. o.d. × 1 in. long) demonstrated the mechanical operability of the equipment. Chopped sections of fuel are transferred through the spiral drum countercurrently to the HNO_3 leach at a regulated rate to provide UO_2-free jacket shells at the discharge end of the leacher. The first four flights are dissolution stages, the fifth and sixth are dump flights to prevent dilution of the nitric acid with the wash liquid in the leacher, and the last four flights are water-wash flights. The leacher is operated with an oscillating motion. Preliminary testing was based on a 4-hr dissolution cycle for UO_2 (one revolution per hour).

A $\frac{1}{16}$-scale 4-stage mockup of the leacher was operated. The model consisted of nine 500-ml Pyrex flasks, each representing a dissolution stage. The dissolvent was 7 *M* HNO_3 added at a HNO_3/UO_2 mole ratio of 4.33. Each stage initially contained approximately 600 g of rejected PWR UO_2 pellets, and a stage was placed on-stream each hour. The maximum number of stages on-stream at any given time was four, to correspond to the four stages of dissolution in the inclined rotary drum leacher. The condensable overheads were returned to a mixing pot where they were mixed with the fresh feed acid for return to any one of the nine stages. The noncondensable overheads (oxides of nitrogen) were removed in a caustic scrubber. Three to four stages were required to attain steady-state operation,

when the uranium concentration varied from 500 to 300 g/liter and the acidity from 3.2 to 1.2 *M*. The composite product uranium concentration and acidity were 410 g/liter and 2.3 *M*, respectively.

The instantaneous dissolution rates of the UO_2 pellets in the glass model in boiling 2 to 8 *M* HNO_3–0 *M* uranium, and 0.5 to 2.5 *M* HNO_3–2 *M* uranium (Fig. 1.14) were correlated by the equation

$$\log R = -0.276 + 0.183\,(M\,U) + 0.184 + 0.0625\,(M\,U)^2\,(M\,H^+)$$

where R is in milligrams per square centimeter per minute, based on the superficial surface area of the cylindrical pellets. The data apply only to these specific pellets. These measurements extend the rate data into the region of high uranium–low acid concentration, a condition important for stage countercurrent dissolution such as that in the inclined rotary-drum leacher.

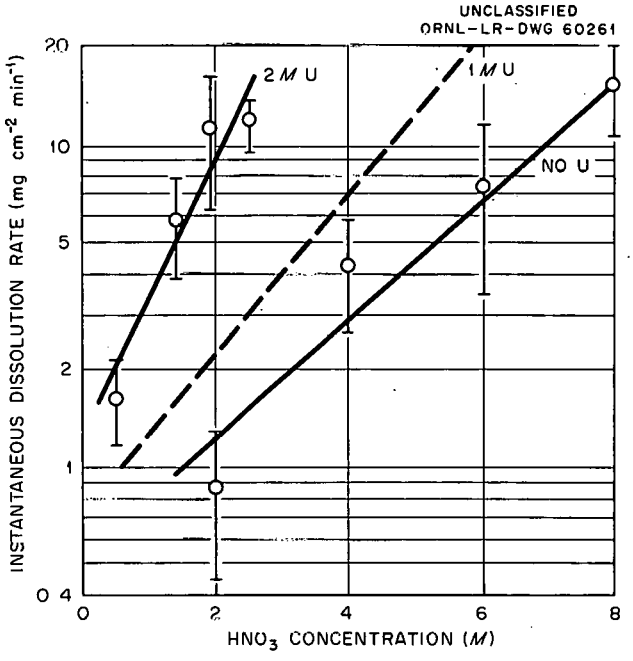

Fig. 1.14. Instantaneous Dissolution Rates of UO_2 Pellets in Boiling Aqueous Nitric Acid–Uranyl Nitrate Solutions. Pellets 0.37 in. long, 0.37 in. dia, 10.1 g/cc density. Equation of curves: $\log R = [-0.276 + 0.183\,(M\,U)] + [0.184 + 0.0625\,(M\,U)^2]\,(M\,H^+)$.

1.9 ENGINEERING STUDIES

Engineering efforts were devoted to criticality studies and to modification of the Immi Facility in cell 1 of Bldg. 4507 for anion exchange processing of plutonium-aluminum alloy fuel. Because of recent AEC decisions that future pilot planting of fuel recovery processes will be done at the ICPP under a co-operative effort between ORNL and Phillips Petroleum Company, selection of processes to be pilot-planted are being considered jointly.

Criticality Studies

Annular vessels that will use fixed poisons for nuclear safety control were approved and are being fabricated for pilot plant use. An annular container for shipping U^{233} solutions was approved, fabricated, tested, and placed in service. A tank packed with Pyrex glass Raschig rings for storage of U^{233} solution was approved and is being installed.

The annular U^{233} shipping container can be used to transport up to 125 liters of U^{233} solution at a uranium concentration up to 225 g/liter. It is shielded with 8 in. of concrete as protection from gamma radiation from the daughters of the U^{232} present. The vessel is fabricated of 1.9-in.-thick stainless steel, and the 175-liter cylindrical void is filled with paraffin. The outer surfaces are covered with a 30-mil-thick sheet of cadmium, which causes the vessel to simulate the neutron multiplication properties of a slab that is only nominally reflected and cannot sustain a nuclear reaction because of large neutron leakage. Since cadmium has a very high cross section for thermal neutrons and a low cross section for fast neutrons, it prohibits the return of fast neutrons born in the fissile solution, which escape the vessel and are moderated in either the outer concrete shield or the paraffin core. A neutron multiplication test performed while the container was being filled with 125 liters of U^{233} solution containing 225 g of U^{233} per liter showed a maximum source multiplication of no more than 5, which indicates that the effective multiplication constant was no more than ~0.8.

A glass-Raschig-ring-packed tank is being installed in cell 3 of Bldg. 3019 for storage of up to 60 kg of U^{233} as a solution of 100 to 200 g of U^{233} per liter. The storage tank is a 3-ft-dia 260-gal tank packed with 1.5-in. Pyrex Raschig

rings to a glass volume of ~20%. The problems of glass corrosion, precipitation of U^{233}, radiation damage, radiolytic hydrogen generation, breaking and settling of rings, leaks, external radiation, and mixing were considered in the design of the tank. A neutron multiplication measurement with U^{233} solution will be made in the tank before it is placed in service.

Plutonium-Aluminum Alloy Fuel Processing

The recovery of highly irradiated plutonium from plutonium-aluminum alloy for use in plutonium cross-section studies is planned in cell 1, Bldg. 4507, starting in July 1961. The dissolver and process equipment originally installed for the intermediate-scale head-end solvent extraction facility will be used. Two cycles of anion exchange with Permutit SK resin have been added for the actual separation of the plutonium in order to achieve a greater decontamination and higher product concentration than with the single solvent extraction cycle. Additional instrumentation, a product-loading glove box, sample-handling facilities, and a shielded dissolver slug chute pedestal have also been added, and a special 10-ton fuel-rod shipping cask has been fabricated.

2. FLUORIDE VOLATILITY PROCESSING

2.1 PROCESSING OF URANIUM-ZIRCONIUM ALLOY FUEL

Modifications[1] to the Volatility Pilot Plant required for processing uranium-zirconium alloy fuel elements were completed. Modifications now in progress to meet containment requirements consist of building changes to permit the required air flow and pressure controls, and installation of a KOH scrubbing system for all off-gas. The Giannini data logging system was installed for continuous monitoring of 96 electrical and 24 pneumatic process signals. Paper tape output will be processed routinely by the Oracle for conversion of the signals to "engineering units," print-up and curve plotting of the data, and storage of data on magnetic tape for subsequent calculations.

The basic fluoride volatility flowsheet (Fig. 2.1) involves dissolution of fuel elements in molten NaF-LiF-ZrF_4 (37.5-37.5-25.0 mole %) by HF, fluorination of UF_4 to UF_6 with F_2, further purification by absorption on and desorption from an NaF bed, and recovery of UF_6 in a cold trap. Processing conditions tentatively fixed as a result

[1] *Chem. Tech. Ann. Progr. Rept. Aug. 31, 1960*, ORNL-2993, p 68.

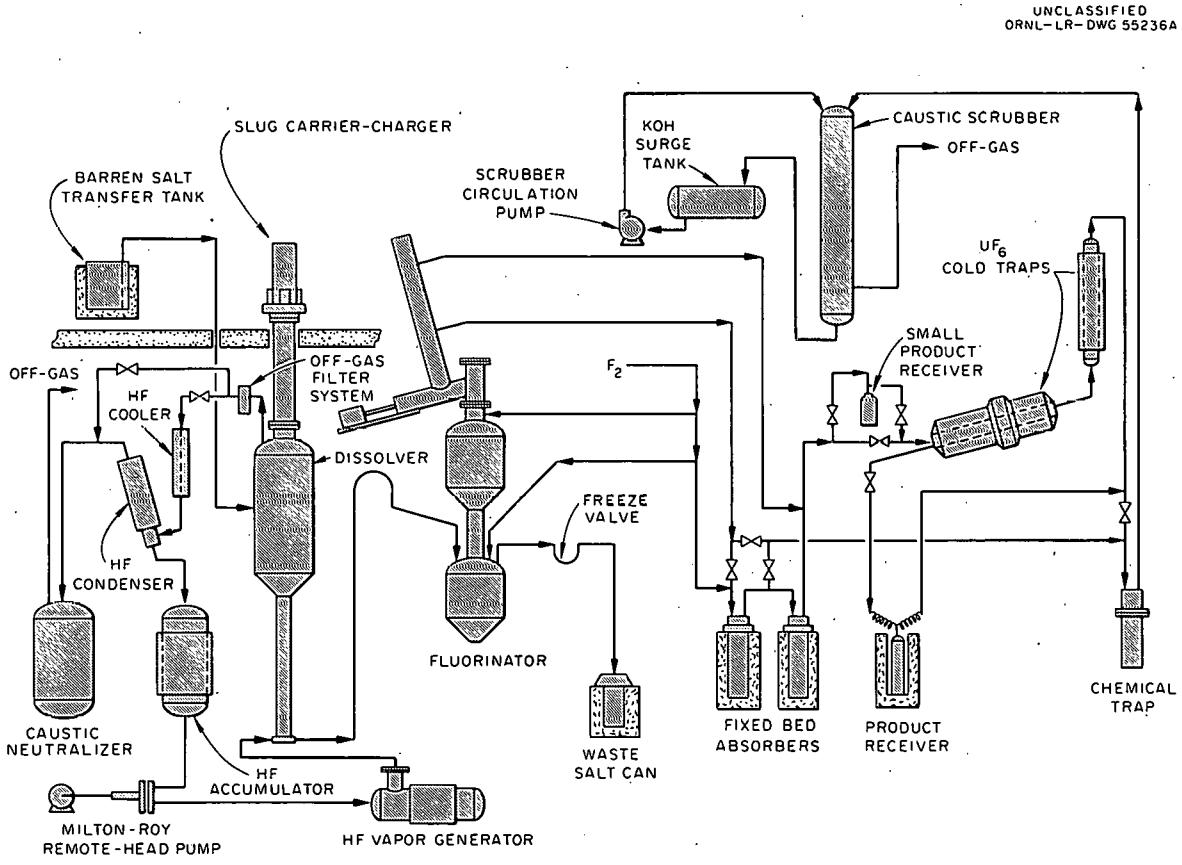

Fig. 2.1. Schematic Diagram of Volatility Pilot Plant.

of experimental runs are: (a) dissolution temperature ~50°C above the salt melting point (in most cases temperature initially 650°C and gradually decreased to 500°C as dissolution proceeds), (b) HF flow rate of 150 g/min, (c) the use of a movable-bed absorber rather than the fixed-bed absorbers, which will be available for emergency use, and (d) the use of a small product receiver to recover for sampling the UF_6 from each individual run followed by transfer of product from several runs to the larger shipping cylinder. The fluorine flow rate is still being studied.

The first seven development runs (T-1 to 7, Table 2.1) were partial flowsheet runs in which dummy Zircaloy-2 fuel elements were dissolved to determine the operability of the dissolution system. A major operating difficulty was plugging of the dissolver off-gas valves by 0.01- to 2-μ particles formed in the dissolver during dissolution. The particles appeared to be 25 to 40% salt, the remainder being metallics, principally iron, tin, chromium, nickel, and molybdenum. The average concentration in the off-gas during a dissolution was about 1 g/m^3. Filtration with copper mesh, which provided a large amount of impingement surface, was the most successful method tried for removing the particles; it was 85 to 92% efficient as the dust loading increased from 0 to 18.0 lb/ft^3. Filtration by porous metal and separation by a 2.5-in.-ID cyclone were even less satisfactory. A system for continuous washing of the off-gas line with liquid HF is being designed.

The first seven of a series of complete flowsheet demonstration runs (TU-1 to TU-7) with nonirradiated fully enriched zirconium-uranium alloy fuel elements were completed. A total of 3579 g of uranium was processed, 2849 g of which was sent to Y-12 Product Processing. Approximately 531 g of uranium was retained in recoverable form (samples, absorbed on NaF, cylinder heels). System holdup was determined to be 200 ± 100 g. Fuel dissolution rates were >3.5 kg/hr with an

Table 2.1. Summary of Dissolution Runs

Runs T-1 through T-7: dummy Zircaloy-2 fuel, ~30 kg per element
Runs TU-1 through TU-7: nonirradiated fully enriched zirconium-uranium alloy fuel, ~1% U, ~40 kg of fuel per run
Molten salt: 37.5-37.5-25.0 mole % NaF-LiF-ZrF_4

Run No.	Salt Temp. (°C)		Avg. Dissolution Rate* (kg/hr)	Time* (hr)	Avg. HF Flow Rate (g/min)	Avg. HF Utilization* (%)	Salt Recovery (%)
	Max.	Min.					
T-1	560	520	0.84	32.1	104	13.5	105.5
T-2	530	525	0.69	34.6	40	28.9	97.0
T-3	625	550	1.46	20.2	90	27.0	102.6
T-4	630	495	1.45	18.5	90	26.9	101.8
T-5	625	530	1.21	22.5	90	22.4	100.1
T-6	650	500	1.20	22.0	150	13.4	99.0
T-7**	655	523	2.77	19.0	135	34.4	100.0
TU-1**	670	490	2.46	18.2	92	44.5	100.5
TU-2**	650	500	2.82	15.5	125	37.3	102.4
TU-3**	655	495	3.22	12.3	150	35.8	98.0
TU-4**	650	555	3.34	7.6	150	33.4	100.1
TU-5	650	500	2.50	15.7	150	24.5	98.1
TU-6	650	500	1.89	18.8	121	22.8	92.8
TU-7	650	500	3.68	10.8	150	35.7	106.7

*Based on 90% completion of dissolution.
**Two-element dissolutions.

HF flow rate of 150 g/min (Table 2.1). In fluorination of the UF_4 to UF_6 with fluorine flow rates from 4 to 16 standard liters/min for 85 to 150 min, the uranium loss to the waste salt was < 10 ppm (Table 2.2). There were no serious difficulties in the absorption of UF_6 on and desorption from NaF. Nonrecoverable uranium losses averaged < 0.8 g per run, ~0.1 wt % of the fuel charged.

Total cation impurities in the UF_6 product varied from ~250 to ~1400 ppm UF_6 (Table 2.3). The only theory advanced for the trend in sodium (from 1300 to < 10 ppm) is that in TU-1, with the fixed absorber, there was considerable entrainment of the NaF fines. Starting with TU-2, the movable bed absorber was used, and there should have been negligible NaF entrainment from the bed itself. There was probably an appreciable amount of NaF in the lines, but once the lines were clear, the sodium content should have dropped off. One questionable point is that a value of < 10 ppm is lower than would be expected from this theory alone; a sodium buildup in future runs to a level of ~100 ppm would not be surprising. No explanation has been proposed for the behavior of copper and molybdenum.

Table 2.2. Summary of Fluorination Data

Feed salt: NaF-LiF-ZrF_4 (~27.5-27.5-45.0 mole %)
Fluorination temperature: 497-515°C

Run No.	Salt U Conc. (ppm)		F_2 Flow (st l/m)	Fluorination Time (min)	F_2 Utilization* (%)	Mole Ratio of F_2 Used* to Original U	Fluorination Time to Obtain 10 ppm U in Salt (min)	Total Nonrecoverable U Losses	
	Initial	Final						(g)	(wt %)
TU-1	2,830	1.2	12	150	4.9	20.6	77	0.372	0.07
TU-2	2,040	3.8	6	150	11.7	8.5	55	1.227	0.28
TU-3	3,003	9.1	9	105	8.9	11.2	75	1.935	0.31
TU-4	5,118	5.6	4, 12**	75, 60**	8.9	11.2	97	1.006	0.16
TU-5	2,205	1.0	4, 16	60, 30	6.1	16.4	63	0.236	0.05
TU-6	2,667	0.7	6, 16	60, 25	5.8	17.3	56	0.177	0.04
TU-7	2,201	4.2	6, 16	60, 40	4.1	24.2	86	0.277	0.06

*For minimum of 99.7% conversion of UF_4 to UF_6.
**4 standard liters/min for 75 min, 12 standard liters/min for 60 min.

Table 2.3. Cation Impurities in UF_6 Product of Volatility Process

Run No.	Amount (parts per 10^6 parts UF_6)									
	Cr	Cu	Fe	Li	Mo	Na	Ni	Sn	Zr	Total
TU-1	< 1	10	2	< 2	100	1300	3	2	< 1	< 1421
TU-2	< 1	17	< 1	< 2	69	600	< 1	1	< 1	< 693
TU-3	< 1	74	5	< 2	17	600	24	4	< 1	< 728
TU-4	1	210	6	< 1	21	< 10	4	4	< 1	< 253
TU-5	< 1	4	< 1	< 1	61	< 10	4	< 1	< 1	< 84
TU-6, 7	< 1	8	2	< 1	220	< 10	6	2	< 1	< 251

Engineering-scale studies on sorption of UF_6 from a flowing UF_6-N_2 stream by a deep fixed bed of granular NaF indicated that the removal rate is controlled by the diffusion of UF_6 through the solid phase and through the film, and by the rate of heat transfer between the solid and the gas stream. The importance of each process depended on flow rate, gas concentration, and initial solid temperature. Calculated film coefficients for mass transfer of UF_6 are ~0.05 cm/sec and for solid phase diffusivities, $\sim 10^{-5}$ cm^2/sec. A monitoring system for continuously determining the UF_6 concentration in the range 100 ppm to 20 mole % in a UF_6-N_2 mixture, which uses a Thermistor cell to sense effects due to the change in density of sample gas with change in UF_6 concentration, showed a response time of < 10 sec. One of the fission product fluorides that is volatilized at fluorinator temperatures is MoF_6; the reactions of MoF_6 with the NaF absorber were studied to determine its effectiveness in removing MoF_6 from the UF_6 stream. Laboratory-scale measurements of the dissociation pressure of the $MoF_6 \cdot x$NaF complex indicated that molybdenum contamination in the product UF_6 can be minimized by proper choice of UF_6 absorption temperature and fluorine flow rate. As with the $UF_6 \cdot 3$NaF complex, the classical relation between dissociation pressure and temperature exists over a wide range in the NaF/MoF_6 ratio:

$$\log p_{mm\ Hg} = 10.21 - 3630/T°K$$

The $MoF_6 \cdot x$NaF complex is colorless in contrast to the yellow UF_6-NaF complex; they are alike in being stable to O_2 and N_2 but not to H_2O, which causes hydrolysis of the molybdenum complex. Complex dissociation pressures determined by a static bomb method over approximately a 100°C temperature range were reproducible generally to ±5% (Fig. 2.2), observed variations being attributed to temperature variations and the impurities WF_6 and HF. Dissociation pressure apparently did not depend on the complex composition (Table 2.4). The only low values, obtained at a NaF/MoF_6 mole ratio of 248/1, are attributed to the use of only 0.002 mole % MoF_6 in a total volume of about 60 ml.

Corrosion rates in the Inor-8 dissolver were somewhat encouraging. During the 14 nonradioactive dissolution runs (Table 2.1) with total salt and HF exposure times of 765 and 404 hr,

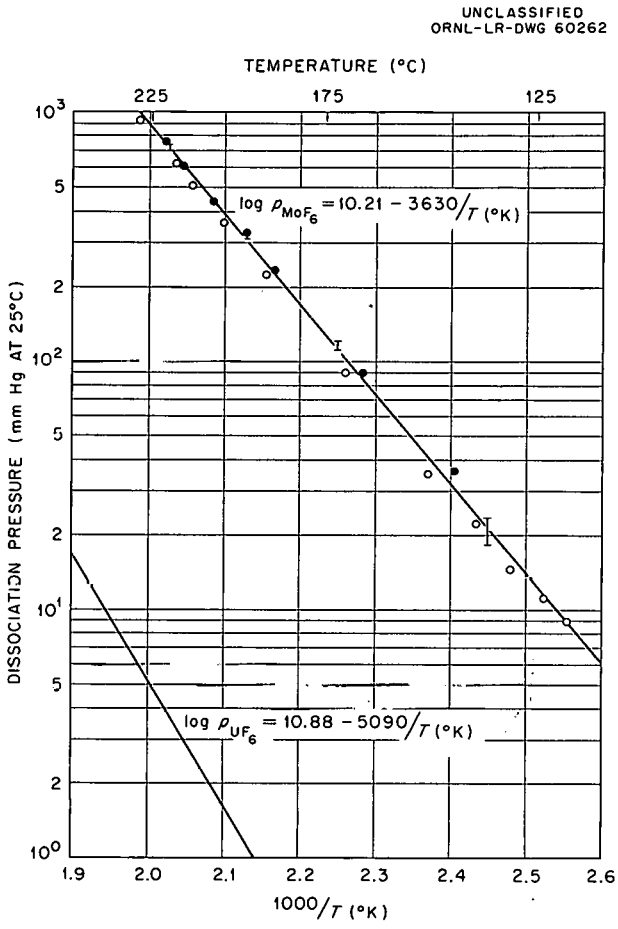

Fig. 2.2. Dependence of MoF_6-NaF Dissociation Pressure on Temperature: Comparison with Dissociation Pressure of $UF_6 \cdot 3$NaF Complex.

Table 2.4. Dissociation Pressures at Various NaF/MoF_6 Ratios

NaF/MoF_6 Mole Ratio	Pressure (mm Hg at 25°C)			
	At 135°C	At 172°C	At 197°C	At 220°C
5.40	20.2	114	317	725
5.52	-	110	-	-
8.21	23.0	111	313	717
16.3	19.6	119	325	729
31.6	18.2	115	311	691
248	12.2	73	-	-

respectively, the maximum decrease in metal thickness based on ultrasonic measurements was 25 mils, for a rate loss of 0.06 mil per hour of HF exposure or 24 mils per month of salt-HF residence time. Ultrasonic measurements showed only bulk metal losses as opposed to intergranular corrosion or small pits. However, complete gamma radiography and some replication with dental wax indicated no significant pitting.

Fluorinator corrosion rates were higher than those experienced in the dissolver. Fluorine exposure during preliminary tests and the seven runs with nonirradiated uranium in the melt (Table 2.2) was 20.3 hr with 694 hr exposure to salt. Ultrasonic thickness measurements indicated ~1 mil/hr corrosion based on F_2 exposure and 20 to 25 mils/month based on exposure to salt-F_2 conditions. However, a life of ~115 runs is predicted for both vessels since the fluorination runs require only ~1.5 hr exposure to F_2 as compared to ~18 hr of HF exposure per run in the dissolver.

Data from 20 engineering-scale dissolutions of Zircaloy-2 in HF and fused salt were correlated by

$$r = k(V/1.0)^{-1/3} \ln (W/0.40)$$

where

r = dissolution rate, lb hr^{-1} ft^{-2}

k = rate constant, lb hr^{-1} ft^{-2}

V = kinematic viscosity, ft^2/hr

$V/1.0$ = dimensionless kinematic viscosity, which includes temperature and ZrF_4 concentration dependences

W = HF flow rate, lb/hr

$W/0.40$ = dimensionless HF rate

The value of k was 0.04345 for salt with a Na/Li ratio of 43/57 and ZrF_4 concentration from 0 to 43 mole %, with temperature from 535 to 810°C and HF rates from 1 to 5.8 lb/hr. The term $W/0.40$ represents the HF rate corrected for a specific geometrical arrangement of vessel and fuel element.

2.2 APPLICATION TO STAINLESS STEEL–CONTAINING FUELS

Dissolution of stainless steel–clad fuels with HF in fused fluoride salts followed by volatilization of UF_6 is feasible as a means of processing stainless steel–clad fuels. A process flowsheet based on laboratory data has been suggested for use in the Volatility Pilot Plant with the EBR-1 Core 2 meltdown fuel, 88% U–2% Zr–10% type 347 stainless steel plus iron container material. This flowsheet uses the high dissolution rate in 37-52-11 mole % LiF-NaF-ZrF_4 with subsequent addition of ZrF_4 to bring the composition to 26-37-34-3 mole % LiF-NaF-ZrF_4-UF_4, a composition favorable for fluorination at 500°C and with an adequate solubility for the stainless steel fluorides. Small-scale tests of this flowsheet were completely successful, including good uranium recovery. The corrosion rate for Inor-8 (the material of construction currently favored for the dissolution vessel) ranged from 0.064 mil/hr for the initial composition to 0.005 mil/hr for the latter.

The dissolution rate of type 347 stainless steel coupons was ~0.5 mg cm^{-2} min^{-1} at 650°C in 60-40 mole % NaF-ZrF_4, in which the solubilities of NiF_2 and FeF_2 are high. In 26-37-37 mole % LiF-NaF-ZrF_4, a salt from which uranium can be removed by fluorination at 500°C, the rate of dissolution was 0.24 mg cm^{-2} min^{-1}. This composition of salt for many reasons is the best for process use of all compositions tested (Table 2.5). The solubilities of stainless steel fluorides in 26-37-37 mole % LiF-NaF-ZrF_4 were observed to be suitable (Table 2.6). Flinak salt (LiF-NaF-KF) has a comparable solubility for stainless steel fluorides but ZrF_4 must be added to 30 mole % to allow recovery of the uranium by fluorination.

Table 2.5. Dissolution Rates of Type 347 Stainless Steel in Fused Fluorides by Hydrofluorination

Salt Composition (mole %)	Temp. (°C)	Dissolution Rate (mg cm^{-2} min^{-1})
60 NaF–40 ZrF_4	600	0.38
	650	0.55
	700	1.1
37 LiF–52 NaF–11 ZrF_4	650	1.7-2.1
26 LiF–37 NaF–37 ZrF_4	500	0.24
	600	0.67
50 KF–50 ZrF_4	650	2.0-2.2
60 KF–40 ZrF_4	650	0.89-1.0
46 LiF-11.5 NaF-42 KF	550	9.7
	600	8.5
	650	5.5

Data for dissolution of various oxides, such as those contained in stainless steel–clad oxide fuels, in fused salt (Table 2.7) together with previously published metallic dissolution results indicate that the fused salt volatility process is generally applicable to heterogeneous fuel. The possibility of recovering uranium from oxide fuels prompted corrosion studies of fused salt–HF–oxides (and water vapor) systems. Results of one laboratory test at BMI[2] in which BeO was hydrofluorinated in 45.6-54.4 mole % ZrF_4-NaF indicated that at 570°C corrosion is no worse than during the hydrofluorination of zirconium in 43-57 mole % NaF-LiF at 700°C. Corrosion rates in the BeO case ranged from 0.1 mil/month in the liquid phase away from the HF sparge tube to 5 mils/month at the vapor-liquid interface.

[2]F. W. Fink, BMI, letter to R. P. Milford, April 19, 1961.

2.3 APPLICATION OF FUSED SALT SYSTEMS TO Pu RECOVERY

The initial plutonium work was conducted at the low level of 2 ppm plutonium to explore the effect of temperature, salt composition, and F_2 flow rate before proceeding to a higher concentration. The results indicate that PuF_6 volatilization is a first-order reaction under the conditions used

Table 2.6. Solubilities of Mixed Fluorides of FeF_2, NiF_2, and CrF_2 in 26-37-37 mole % LiF-NaF-ZrF_4

FeF_2, NiF_2, and CrF_2 added successively in the proportions found in stainless steel 347, and samples of filtered salt taken after each addition

Addition	Sampling Temp. (°C)	Concentration (wt %)					
		Fe		Ni		Cr	
		Calc.	Obs.	Calc.	Obs.	Calc.	Obs.
1	600	3.8	3.5	0.37	0.48	0.63	0.59
2	600	5.6	3.9	0.54	0.46	0.86	0.73
3	600	7.4	4.6	0.71	0.45	1.09	0.84
-	500	7.4	3.0	0.71	0.49	1.09	1.05

Table 2.7. Dissolution of Oxides by Hydrofluorination in Fused Salt

Material*	Salt (mole %)	Temp. (°C)	Dissolution Rates (mg cm^{-2} min^{-1})
ZrO_2	31 LiF–24 NaF–45 ZrF_4	650	1.1, 1.4
36% UO_2–64% ZrO_2	31 LiF–24 NaF–45 ZrF_4	650	1.0, 1.2
UO_2	31 LiF–24 NaF–45 ZrF_4	650	11.5
BeO	49 NaF–40 LiF–11 BeF_2	600	0.60, 0.56, 0.62
ThO_2	(Apparently much faster in 31 LiF–24 NaF–45 ZrF_4 than in any of above due to metathesis with ZrF_4; specific rates difficult to determine)		

*All materials high-fired.

(Fig. 2.3). Although the reaction is bimolecular, it seems probable that the activity of F_2 in the tests was fairly constant, thus making the rate of PuF_6 volatilization proportional only to the plutonium concentration in the salt. The first-order effect, however, might be partly due to the rate of removal of gas from the free space above the fused salt. The effect of salt composition and temperature was relatively insignificant, but the rate of removal was approximately proportional to the F_2 flow rate. This indicates that either the percentage saturation of the gas stream is fairly constant at different flow rates or the effect of increased agitation at the higher F_2 flow rate is neutralized by an effectively shorter residence time. All the work was conducted with 50-g batches of salt in a 1-in.-dia nickel reactor with a 0.25-in.-o.d. dip tube. The superficial F_2 mass flow rate in these tests varied from 0.43 mole ft^{-2} min^{-1} at 50 ml/min to 1.29 mole ft^{-2} min^{-1} at 150 ml/min. The average residence time varied from 5.1 to 1.7 sec.

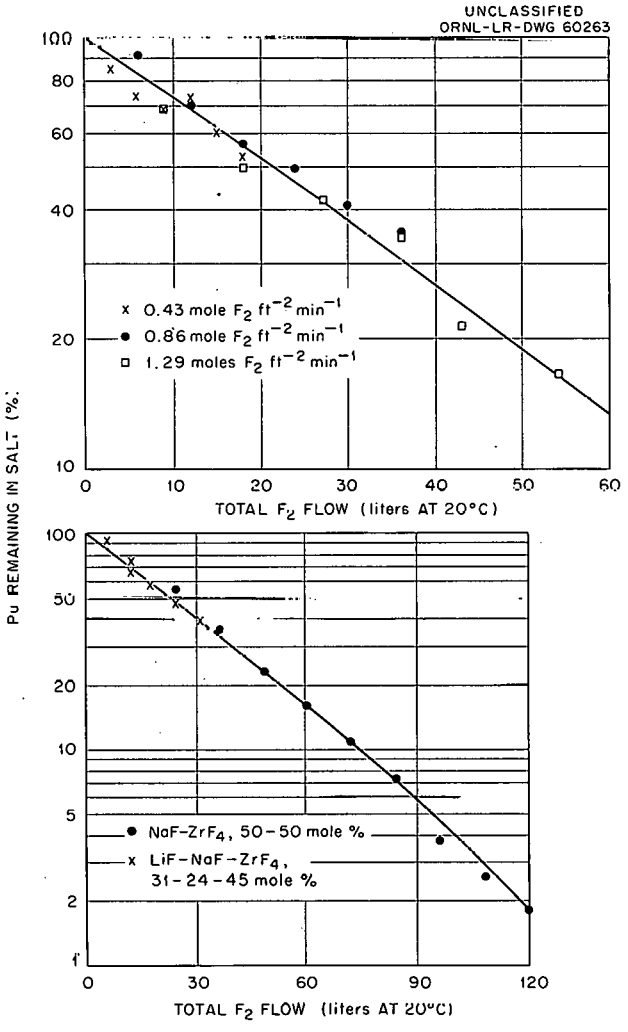

Fig. 2.3. PuF_6 Volatilization at 600°C. Effect of (*a*) fluorine flow rate, with 50 g of 31-24-45 mole % LiF-NaF-ZrF_4, and (*b*) time and salt composition with F_2 at 100 ml/min. Initial plutonium concentration 2 ppm.

3. MOLTEN SALT REACTOR FUEL PROCESSING

Uranium is recovered from the Molten Salt Reactor fuel and blanket salts by the fluoride volatility process (Chap. 2), the UF_4 being fluorinated to UF_6 which volatilizes and is collected. The fuel carrier salt, Li^7F-BeF_2, is decontaminated by dissolution in 90% HF–10% water.

3.1 FLUORINATION

In four runs in a laboratory-scale steady-state fluorinator uranium was 97 to 98% recovered from synthetic MSR fuel by 40 min fluorination at 650°C. Corrosion of the nickel container was severe. The fluorinator, which contained about 70 ml of salt, was a 1-in.-dia nickel tube; salt overflowed through a ¼-in.-dia tube into a jackleg from which samples were taken.

Two significant experimental runs were made with LiF-NaF-ZrF_4 (26-37-37 mole %) containing 1 wt % UF_4 in one case and 0.2 wt % in the other. In the first case fluorination near 700°C with excess fluorine and an average salt residence time in the fluorinator of about 40 min left 100 to 200 ppm of uranium in the spent salt, 1 to 2% of the original concentration. In the other experiment, with a temperature of 600 to 650°C, the uranium content of the overflow salt was 25 to 50 ppm, also 1 to 2% of the feed concentration. Preferred conditions would include a lower temperature, about 550°C or less, and a shorter salt residence time. Corrosion rates based on nickel concentrations were of the order of 1 mil/hr at 700°C and 0.1 to 0.2 mil/hr at 600°C.

3.2 CARRIER SALT RECOVERY

Dissolution rates of relatively large pieces of solidified 63-37 mole % LiF-BeF_2 in stirred, boiling 90% HF–10% H_2O were sufficiently rapid to eliminate the necessity of preliminary atomization of fused salt to produce solids of high surface area. In two experiments the rate was ~50 mils/hr in the first 10 min, decreasing to <10 mils/hr after 1 hr because of a layer of soft solids, probably BeF_2, left on the surface. When the salt specimen was vigorously agitated with a magnetic stirrer it dissolved very rapidly, ~200 mils/hr, as the weakly adherent surface layer was mechanically removed. The salt samples dissolved were capsule shaped, 270 to 290 mils dia by about 700 mils long, prepared by casting in a split graphite mold.

The solvent SbF_5-HF for carrier salt was investigated on the basis of data showing that rare earth fluorides are soluble in these solutions, SbF_5 being the strongest acid in the hydrogen fluoride solvent system if an acid is defined as a substance that increases the concentration of the solvated cation of the solvent (H_2F^+ in this case).[1] In initial tests HF containing about 20% SbF_5 reacted with both LiF and rare earth fluorides, as indicated by heat evolution. The compound formed with LiF was not very soluble, but that formed with rare earth fluorides was very soluble. There was no apparent interaction or solubility with ThF_4.

The solid formed by adding liquid SbF_5 to an HF solution of LiF was not stoichiometric, the Li/Sb mole ratio typically being around 1.4, but was recrystallized from anhydrous HF to yield the 1:1 LiF·SbF_5 with a chemical analysis of 50.4% Sb, 2.67% Li, and 46.5% F and a Li/Sb mole ratio of 0.93 and F/(Li + 5Sb) ratio of 0.99. The compound gave a good x-ray diffraction pattern, showing monoclinic symmetry, with the cell dimensions

$a = 5.42$ A $c = 7.50$ A
$b = 5.18$ A $\beta = 93.6°$

Systematic extinction indicated the space group Cs^3-Im. The pattern persisted as the hygroscopic solid absorbed water until it was almost completely in solution. The compound was somewhat soluble in HF, 0.23 mole (1.6 g) of lithium per

[1] A. F. Clifford and S. Kongpricha, *J. Inorg. & Nuclear Chem.* 5, 76 (1957).

liter at the boiling point and less at lower temperatures, but was quite soluble in water. Structures for the analogous Tl, NH_4, Rb, and Cs compounds[2] and for $NaSbF_6$ and $NaSb(OH)_6$ (ref 3) have been published, but some of these may have contained water. The corresponding $KF\text{-}SbF_5$ compound was prepared to complete the alkali metal series, and the $AgF\text{-}SbF_5$ compound was prepared. Crystal structures of these new compounds are being determined.

The $LiSbF_6$ compound decomposed on being heated from 400 to 650°C in an inert atmosphere in nickel or copper containers, as indicated by the appearance of a white smoke when the vapor contacted moist air. The volatile material was SbF_3, indicating a reaction of $LiSbF_6$ with the container to form SbF_3 and NiF_2 or CuF_2. Decomposition occurred at lower temperatures in copper than in nickel, that in nickel being incomplete at temperatures as high as 700°C.

Attempts to prepare the $LiF\cdot SbF_5$ compound by reaction of solid LiF with SbF_5 vapor were unsuccessful. The SbF_5 was carried by argon gas that bubbled through liquid SbF_5 at temperatures between 25 and 60°C to the LiF powder spread in an Inconel or nickel boat in a tube held at or above 100°C. The metal surfaces became coated with a viscous liquid layer.

The rare earth fluoride–SbF_5 compound could not be purified by recrystallization since it was very soluble, 200 to 300 g of rare earth per liter. The solid obtained by evaporation or cooling of the saturated solution was a very-fine-particle material associated with a quantity of the solution.

Since SbF_5-HF solutions dissolve rare earth fluorides but not ThF_4, the possibility that this reagent could decontaminate ThF_4 from MSBR blanket salt was investigated. The LiF was leached from a salt spiked with Cs, Ce, and Pm activities with 95% HF–5% water, rinsed with HF, and then leached twice with 5 vol % SbF_5 in HF. The ThF_4 was not significantly decontaminated from rare earths.

[2]N. Schrewelius, *Arkiv Kemi, Mineral. Geol.* **16B**, No. 7 (1943).

[3]N. Schrewelius, *Z. anorg. u. allgem. Chem.* **238**, 241 (1938).

4. HOMOGENEOUS REACTOR FUEL PROCESSING

The program for development of processing systems for aqueous homogeneous reactor fuel was terminated when operation of the HRT was suspended May 1. Evaluation of the performance of hydroclone systems throughout the fuel processing program[1] indicates that a multiclone unit operating at underflow rates >5% should remove circulating solid corrosion products from the HRT as rapidly as they are formed. The multiclones with several times as many parallel hydroclones needed for large reactors presumably could be operated with high efficiencies. However, an underflow stream of many gallons per minute would have to be processed, which might require individual hydroclones and underflow receivers. The disadvantages of such a complex system might outweigh the advantages. Since circulating solids, and therefore neutron poisons, remain low in any case as a result of deposition on reactor surfaces, descaling of heat exchangers on a very infrequent schedule might be more economical than continuous high-rate hydroclone processing.

4.1 MULTICLONE SYSTEM STUDIES

With a multiclone system of thirteen 0.6-in.-dia units on a 10-min cycle in the HRT, solids were removed at a rate of 1 g/hr in a 1000-hr run, but

[1]Details are reported in HRP progress reports, e.g. for May 31, 1961, ORNL-3167.

at normal corrosion rates of 0.5 mpy for stainless steel surfaces and 10 mpy for the Zircaloy core tank, solids are produced at a rate of 1.5 g/hr (ref 2). In a new system with eighteen 0.4-in.-dia units and the full head (90 ft) of the reactor circulating pump used across the system instead of only 42 ft as in the first, the solids collection rate was improved. Removal rates in the first 50 hr of individual reactor runs were about 1.5 g/hr. However, in an attempt to further improve the efficiency, the system had been installed for induced-underflow operation, and this resulted in the rates dropping after a few hundred hours to an apparent equilibrium value of 0.3 g/hr. In a total of 2100 hr operation (reactor runs 22 through 24) removal rates averaged less than 0.5 g/hr, and general performance was comparable to that with a single hydroclone. The overall efficiency of <5% for the 1-μ particles in the reactor is consistent with efficiencies measured in cold water tests with ThO_2 slurries of 1.1 to 1.6 μ mean particle size. These ranged from an expected 65% at 10% underflow, not induced, down to only 10% at 20% induced underflow. Results with other parallel units were similar. The apparent induced underflow rate for the HRT unit was 3.5%, compared with an expected value of 1.3% for a single hydroclone, and for other units the underflow rate varied from 2.5 to 5 times the value for single hydroclones of the same dimensions.

In previous work at high underflow rates, hydroclone efficiency was not impaired by operation of several in parallel on a single underflow receiver, provided the individual hydroclones were matched, and at high underflow rates, the efficiency of the larger parallel units was identical to that of a single hydroclone. However, although the 18 individual hydroclones had been fabricated with port tolerances of ±0.0005 in. to ensure proper matching, the efficiencies dropped drastically as underflow rates were decreased.

A method of monitoring the performance of a multiple hydroclone for changes in operating characteristics was devised, based on the constancy of the ratio of the difference between feed and underflow pressures to feed and overflow pressures over wide ranges of flow rates and the significant change in the ratio when one or more ports in the unit become plugged. This was necessitated by plugging of the feed ports in the original 13-unit multiclone after about 1000 hr operation, which drastically lowered the efficiency but was not detected until after removal of the unit from the cell.

4.2 FUEL PROCESSING BY URANYL PEROXIDE PRECIPITATION

The nickel concentration in reactor fuel solutions must be limited to about 500 ppm to ensure fuel chemical stability, which for a large power station, with several kilograms of uranium in the fuel, would necessitate daily processing. Of several possible methods of removing nickel, peroxide precipitation of the uranium appears most promising because no foreign materials other than peroxide are added. Uranyl peroxide is soluble to the extent of 3 g of uranium per liter at 10 to 25°C. Laboratory and full-scale tests with nonirradiated fuel solutions indicated that it should be possible to process 4 kg of uranium on a 1- or 2-day schedule with uranium losses as low as 2% and a decontamination factor from soluble components of at least 100.

In laboratory studies with simulated HRT fuel containing normal concentrations of uranium, copper, nickel, sulfate and excess acid, the optimum technique was slow addition of 4-fold excess hydrogen peroxide to the top of the solution, with agitation. Decontamination factors were >10 with little or no washing, and uranium recoveries were consistently 95% or better. The peroxide precipitate was held satisfactorily on a glass filter of 10 to 15 μ nominal pore size, but not on nominal 3-μ sintered stainless steel except when 10 g of diatomaceous earth per liter of solution was included. With a solution uranium concentration of 75 g/liter the filtration characteristics of the precipitate were considerably better than with 150 g/liter.

In three engineering-scale runs in a 6-in.-dia 20-ft-high precipitator column with 4-kg batches of simulated HRT fuel, uranium losses were 6% without rinsing the precipitate and 3% with rinsing. Recycling the initial portion of the filtrate, which always contained high uranium concentrations, would decrease the losses still further. Decontamination factors were 8 without washing and 100

[2] *Chem. Tech. Ann. Progr. Rept. Aug. 31, 1960*, ORNL-2993.

with three rinses. Reprecipitation of the decontaminated uranium from one run with two rinses of the precipitate gave a further decontamination of only 2. Losses were only 0.4%, probably because excess acid had been removed in the initial precipitation and the uranyl peroxide was therefore less soluble.

The precipitator column used in the experiments was equipped with external cooling and heating coils and two sintered stainless steel filters. A 2-in.-dia by 3-ft-long cylindrical filter extended up from the column bottom, and contained a 5-in.-dia flat filter disk, which was used for the final 10 to 20 liters.

4.3 RELATED SYSTEMS

Charcoal Off-Gas Adsorber Beds

In order to decrease the potential hazard from a leak in the off-gas system, which is located underground but uncontained except for the primary piping, the system was operated below atmospheric pressure the past year. A vacuum pump controlled the charcoal bed exit pressure at 11 psia, whereas previously it was discharged into the stack at atmospheric pressure. Because of the lower pressure, which decreased the holdup time for fission gases, three beds were operated in parallel, instead of the normal two with one in standby. No difficulties were noted. Samples of the off-gas from each bed indicated that the significant differences in holdup time for the three beds noted in early tests still existed, but with no apparent gross changes. Less than 0.5 curie/day of Kr^{85} and Xe^{133} was released.

Off-Gas Sampler

A system for sampling the reactor off-gas upstream of the charcoal beds was devised and used in the final reactor run. Approximately 100 liters of off-gas was routed to the vapor space above the chemical plant decay tanks and removed subsequently via bubbler lines on the tank level instruments. Samples were removed without difficulty after 3 days' decay.

5. WASTE TREATMENT AND DISPOSAL

The objective of this program is to develop and demonstrate an integrated process for safe treatment and permanent disposal of both low- and high-radioactivity-level wastes. For low-activity waste, e.g. very dilute salt solutions such as cooling and canal water, treatment by a scavenging–ion exchange process to remove radioactive constituents is proposed, with discharge of the effluent to the environment. The retained waste solids or slurries can be combined with high-activity wastes produced in fuel processing operations, evaporated to dryness, and calcined to oxide. The feasibility of adding fluxing materials to the wastes to fix the fission products in a low-solubility glass is an alternative to calcination. The calcined or fixed solids, contained in the stainless steel cylinder (pot) in which they were calcined, could be shipped to an ultimate storage site such as a mine in salt or limestone for permanent disposal. Ultimate disposal possibilities are being evaluated along with storage and shipping parameters as part of a general engineering, economic, and hazards evaluation of the complete waste complex.

5.1 HIGH-ACTIVITY WASTE TREATMENT

Pot calcination of synthetic Purex, Darex, and TBP-25 wastes containing millicurie amounts of ruthenium is being developed on both a laboratory and engineering scale to provide design information for the construction of a pilot plant. In the proposed process (Fig. 5.1) the waste is fed to an evaporator together with nitric acid or water to maintain the acid concentration in the evaporator below 6 *M*, which minimizes ruthenium volatilization. Evaporation may be either batch or continuous; a catch tank is used between the evaporator

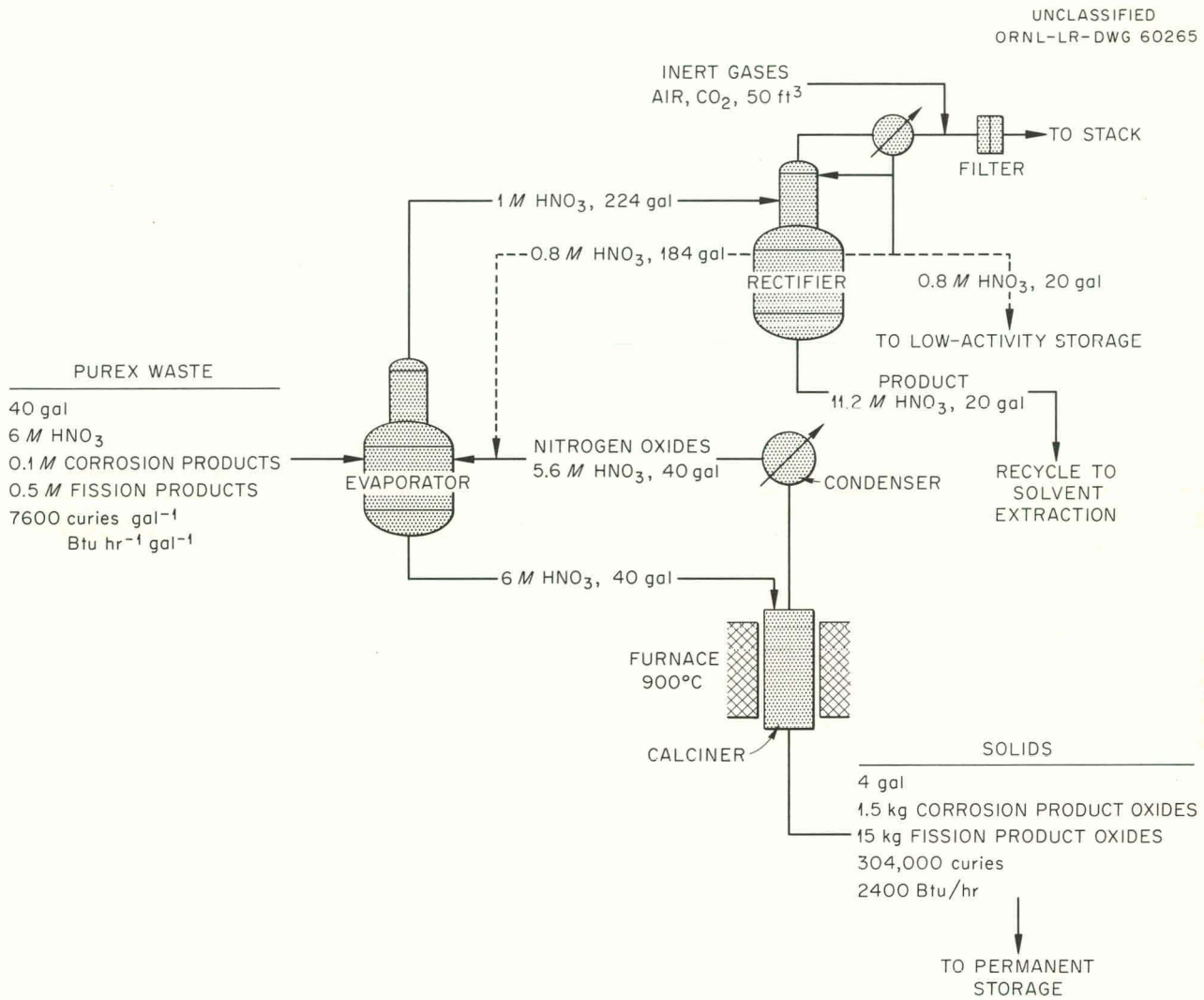

Fig. 5.1. Conversion of High-Activity Wastes to Solids by Pot Calcination. Basis: Purex process waste containing 1 ton of spent uranium, irradiated to 10,000 Mwd/ton and decayed 3 years.

and calciner in batch operations. This continuous flowsheet differs from that shown previously[1] in the recycling of calciner off-gases, containing nitrogen oxides, through the evaporator and continuous addition of dilute nitric acid to the evaporator. The evaporator concentrates go to an electrically heated pot at essentially their initial concentrations, where they are evaporated to dryness and calcined to 900°C. Chemical additives, such as calcium or magnesium salts, and phosphorus acids may be added prior to calcination to decrease sulfate and fission product volatility or to produce a melt in the pot after calcination. After being filled with calcined solids, the stainless steel pot will be sealed and used as both the shipping and permanent storage vessel. About 90% of the nitrogen oxides in the calciner off-gas can be absorbed during condensation of water vapor in the evaporator condenser and the remainder in the rectifier reflux condenser. About 1 ft^3 of noncondensable gas per gallon of feed is anticipated in relatively leaktight process equipment; only a small final absolute filter and gas cleanup system will be required. Calcination and heat dissipation rates in final storage media are satisfactory.[1,2]

[1] *Chem. Tech. Ann. Progr. Rept. Aug. 31, 1960*, ORNL-2993, pp 93–95.

[2] J. J. Perona and M. E. Whatley, *Calculation of Temperature Rise in Deeply Buried Radioactive Cylinders*, ORNL-2812 (Feb. 3, 1960).

Evaporation-Calcination

In laboratory experiments, synthetic Purex waste (Table 5.1), 40 gal per ton of uranium processed, was evaporated and calcined to a volume of 5.7 gal/ton. The product had a bulk density of 1.32 g/ml, with a calculated porosity of 58%. The addition of 10% stoichiometric excess sodium and magnesium (1.2 moles of NaOH and 0.2 mole of MgO per liter) decreased the sulfate volatility during evaporation to 0.28–0.7%, as compared with 70% in the absence of additives. The use of calcium instead of magnesium was unsatisfactory because of precipitation of calcium sulfate in the feed. Nitric oxide gas was introduced into the pot during calcination at a rate sufficient to keep the system at atmospheric pressure. The experiments were performed in an 18- × 4-in.-dia stainless steel pot in a 9-kw furnace equipped with a downdraft condenser, packed absorber column, polyethylene expansion bag (to measure net noncondensable gas volume), and gas recirculation pump.[3] The initial boil-off rate in evaporation was 100 ml/min and calcination was to a temperature of 900°C. In three similar experiments with initial boil-off rates of 125 ml/min, the volume was decreased to 4.0, 4.5, and 4.2 gal per ton of uranium, respectively, the lower final volumes being attributed to the higher boil-off rate. The NO consumption was 0.39, 0.36, and 0.43 mole per liter of waste. As in previous experiments with NO added to the system during evaporation-calcination, the net off-gas production was nil. Stable ruthenium in the condensate was 31.8 to 45.8% of that in the feed in the first two runs and 19.5 and 17.6% in the last two, the higher values being obtained when NO was introduced into the vapor space of the calciner, and the lower when it was introduced into the liquid feed line to the calciner. Sulfate in the condensate varied from 0.28 to 0.70% of the original in the feed and appeared to be caused mainly by entrainment.

The results of eight engineering-scale evaporation-calcination runs (Table 5.2), in 8-in.-dia pots, showed that Purex (with calcium additive), Darex, and TBP-25 wastes can be calcined successfully at acceptable rates to produce a product suitable for ultimate storage. Sulfate

[3] *Ibid.*, Fig. 6.2.

Table 5.1. Laboratory-Scale Continuous Evaporation and Pot Calcination of Synthetic Purex Waste to 900°C

Initial waste composition (equivalent to 40 gal per ton of uranium processed): 6.1 *M* NO_3^-, 5.6 *M* H^+, 1.0 *M* SO_4^{--}, 0.6 *M* Na^+, 0.5 *M* Fe^{2+}, 0.1 *M* Al^{3+}, 0.01 *M* Cr^{++}, 0.01 Ni^{++}, 0.002 *M* Ru

Additives: 1.2 moles of NaOH and 0.2 mole of MgO per liter

Calciner pot: 4 in. dia 18 in. high

Expt. No.	Initial Boiloff Rate (ml/min)	NO Sweep Rate (moles/liter)	Final Vol (gal/ton U)	Residue Density (g/cc)	Residue	Amount (% of original)		
						NO_3^- in Residue	In Condensate	
							SO_4^{--}	Ru
1	100	0.40	5.7	1.32	Hard brown solid, calcd. porosity 58%	0.18	0.28	31.8*
2	125	0.39	4.0	1.86	Hard, brown solid, calcd. porosity 41%	0.18	0.51	45.8*
3	125	0.36	4.5	1.66	Hard, brown solid, calcd. porosity 47%	0.21	0.70	19.5**
4	125	0.43	4.2	1.78	Hard, brown solid, calcd. porosity 43%	0.25	0.56	17.6**

*NO introduced into vapor space of calciner pot.

**NO introduced into liquid feed entering calciner pot.

Table 5.2. Engineering-Scale Evaporation and Pot Calcination of Waste to 900°C

Initial waste composition (equivalent to 40 gal per ton of uranium processed): 6.1 *M* NO_3^-, 5.6 *M* H^+, 1.0 *M* SO_4^{--}, 0.6 *M* Na^+, 0.5 *M* Fe^{++}, 0.1 *M* Al^{3+}, 0.01 *M* Cr^{++}, 0.01 Ni^{++}

Run No.	Waste Type	Avg. Feed Rate (l/hr)	Calciner Size, in.		Solid Bulk Density (g/cc)	Additive	Feed Stoichiometric Ratio $SO_4^{--}/Na^+ + Ca^{++}$	Sulfate in Condensate (% of feed)	Nitrate in Cake (ppm)
			Dia	Height					
30	Purex	16	6	84	1.5	0.6 *M* NaOH 0.6 *M* CaO	1.15*	5.0 (0.05 *M*)	300
31	Purex	22	8	84	1.2	0.6 *M* NaOH 0.62 *M* CaO	1.15**	12.0 (0.12 *M*)	60
32	Purex	24	8	84	2.5	1.0 *M* Na_2SO_4 0.5 *M* NaOH	1.29	3.0 (0.03 *M*)	5000
33	Purex	21	8	84	2.5	1.0 *M* Na_2SO_4 0.5 *M* NaOH	1.29	3.0 (0.03 *M*)	500
37	Purex	20	8	90	1.3	1.2 *M* NaOH 0.2 *M* MgO	0.91	0.2 (0.002 *M*)	Not analyzed
36	Purex	20	8	90	1.2	None	3.34	Not analyzed	Not analyzed
34	Darex	24	8	90	1.1	None			300
35	TBP-25	30	8	90	0.83	None			60

*1.1 *M* SO_4^{--} in feed.
**1.5 *M* SO_4^{--} in feed.

volatility was only 0.2% when the stoichiometric ratio of SO_4^{--} to Ca + Na was less than 1, but was 3 to 12% with higher ratios. The cake nitrate content was acceptably low, 60 to 5000 ppm, and bulk densities ranged from 1.1 to 1.3 g/cc. In two runs (32 and 33) 1.0 *M* Na_2SO_4 was added to the feed to give a denser, more uniform, and more thermally conductive cake. The calcined product melted at 850 to 900°C, producing a solid with a high thermal conductivity, 0.6 Btu hr^{-1} ft^{-1} $°F^{-1}$ compared to the usual 0.2 Btu hr^{-1} ft^{-1} $°F^{-1}$, and a density of 3.0 g/cc. However, sodium sulfate addition is not recommended because in one run a large amount of gas was suddenly evolved during the late stages of the test, causing the molten contents of the pot to splash up into the off-gas system. This may have been caused by $NaHSO_4$ decomposition or by partly calcined solids with large residual contents of nitrate and water falling into the melt and releasing their volatile constituents suddenly. In runs 36 and 37 the calciner contents partially melted, producing a dense cake at the bottom separated by a void space from the sintered upper layer. In run 37, containing sodium and magnesium additives, the cake melted and corrosion in the calciner was severe. This result with sodium and magnesium additives is contrary to the results in laboratory runs (Table 5.1) where melting did not occur and corrosion was negligible. A thermocouple failure followed by excessively high temperatures makes interpretation difficult, however. The dense cake at the bottom of the pot was found to have a melting point near 700°C. The appearance of this low-melting mixture was not expected from laboratory studies and may be due to segregation in the long pots. Further studies of magnesium additive are indicated.

In runs 36 and 37, a continuous 25-liter evaporator directly coupled to the calciner pot (Fig. 5.2) was successfully used to supply ~440 liters of synthetic Purex waste to the pot. Except for a

rise in acidity to 6.5 *M* during a pressure upset, the desired control was achieved:

Evaporator liquid volume	22 ± 1 liter
Evaporator contents density	1.32 ± 0.05 g/cc
Evaporator contents boiling point	111 ± 3°C
Evaporator pressure	1.0 ± 0.25 psi below atmospheric
Calciner liquid volume	48 ± 0.5 liters

The ratio of water addition to feed was about 3 to 1 to hold the evaporator acidity below 6 *M*. The calciner feed rate averaged 20 liters/hr, but varied from 60 to 4 liters/hr as the calciner demand changed.

The continuous evaporator was set up as an analog control system and tested on the ORNL Analog Computer with three variables: liquid level control by steam to coil, liquid density control by feed addition, and liquid acid concentration control by water addition for steam stripping. Generally, the analog system operated satisfactorily, but since some assumptions did not apply to the real system, liquid level control was affected somewhat.

Thermal Conductivity. – The thermal conductivity, *k*, of a calcined Purex waste, measured in the

UNCLASSIFIED
ORNL-LR-DWG 60266

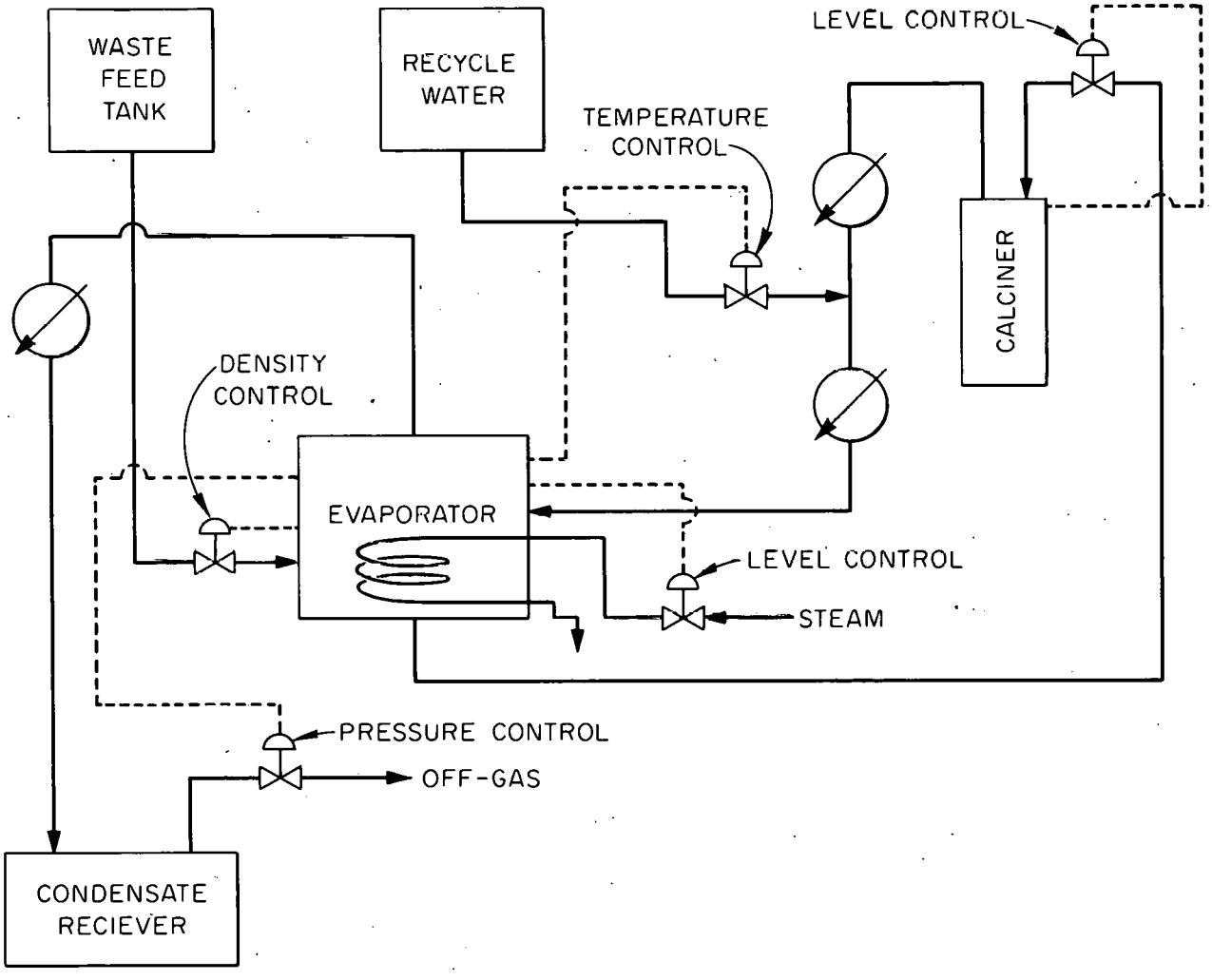

Fig. 5.2. Close-Coupled Continuous Calciner-Evaporator Control System.

original 18-in.-high × 4-in.-dia stainless steel pot, varied almost linearly from 0.19 at 400°C to 0.66 Btu hr^{-1} ft^{-1} $°F^{-1}$ at 1600°F (Fig. 5.3). Sodium and magnesium had been added to the waste to prevent sulfate volatility (Table 5.1, Expt. 1). The linearity with temperature for the calcined solids is typical of a granular, gas phase continuous, rather than a cellular, solid phase continuous, material although the pot-calcined solid had the physical appearance of a cellular material. The variation of k with temperature for a true granular material, sand, is shown in Fig. 5.3 for comparison.

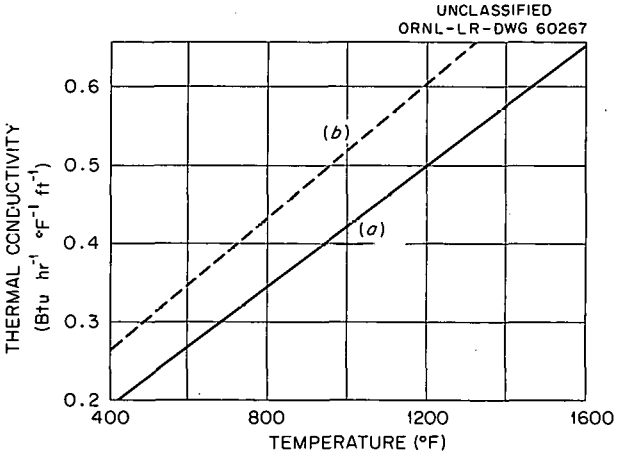

Fig. 5.3. Variation of Thermal Conductivity with Temperature. (*a*) Calcined synthetic Purex waste containing sodium and magnesium, ρ = 1.32 g/ml; (*b*) Ottawa sand, 20 to 30 mesh, ρ = 1.72 g/ml. Theoretical composition of Purex cake, wt %: 21.0 Fe_2O_3, 0.4 NiO, 0.4 Cr_2O_3, 2.7 Al_2O_3, 67.1 Na_2SO_4, 6.3 $MgSO_4$, 2.1 MgO.

Ruthenium Volatility. – The addition of 1.5 *M* phosphite to Purex waste prior to evaporation-calcination decreased the ruthenium in the condensate to 0.03% of the total present (Table 5.3, Fig. 5.4); with 0.5 *M* phosphite the amount volatilized was greater by a factor of >10. Ruthenium volatility was not increased by increasing the ruthenium concentration from 0.002 to 0.2 *M*. The ruthenium is probably volatilized after the phosphite has been oxidized by the nitrate. A disadvantage of phosphite addition is the increased production of noncondensable gases, e.g. N_2 and N_2O, although the magnitude of this problem remains to be established.

Fixation in Glasses

An ideal end product of high-activity waste treatment is a solid refractory material, representing maximum volume reduction, which is mechanically strong and has a high thermal conductivity and low solubility in natural environmental water. Fixation of the activity in an insoluble glass is not essential since wastes are to be stored in a dry environment, but the above advantages plus the additional safety in shipping to the ultimate disposal site may warrant the extra cost.

To eliminate void spaces, which weaken a glass, decrease its thermal conductivity, and increase its leachability by increasing the available leaching surface, fluxing agents are added to the melt. With borate and phosphate as fluxing agents, plus sodium and magnesium or calcium to retain the sulfate, solids were produced which fulfill the criteria to a reasonable degree (Table 5.4). Densities were in the range 2.6 to 2.8 g/cc, and 1 gal of final solid represented between 5.2 and 6.9 tons of processed uranium. Solid leach

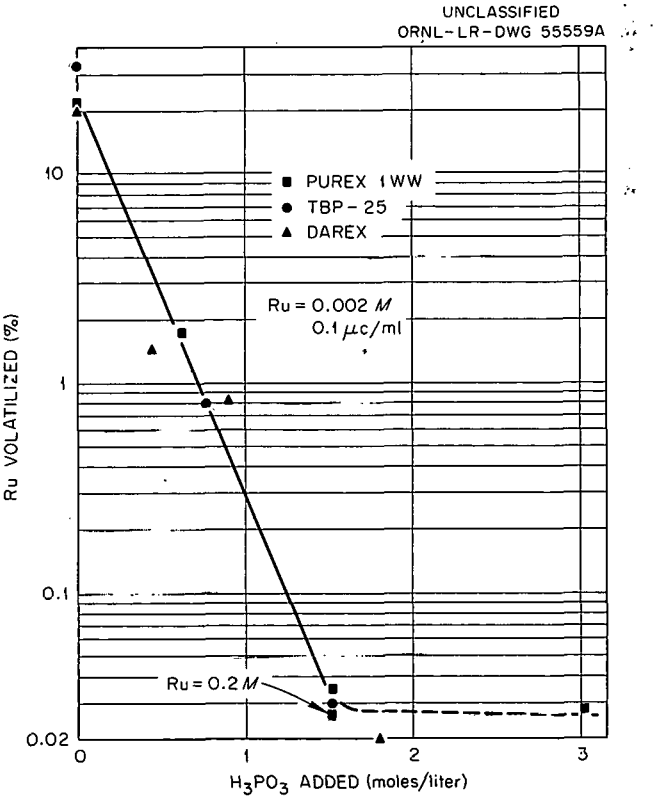

Fig. 5.4. Effect of Phosphite on Ruthenium Volatility in Pot Calcination of Purex Waste.

Table 5.3. Ruthenium Volatility in Batch Evaporation-Calcination of Synthetic Wastes

Purex (moles/liter): 6.1 NO_3^-, 5.6 H^+, 1.0 SO_4^{--}, 0.6 Na^+, 0.5 Fe^{3+}, 0.1 Al^{3+}, 0.01 Cr^{++}, 0.01 Ni^{++}, 0.01 μc Ru^{106}

Darex (moles/liter): 7.19 NO_3^-, 2.00 H^+, 1.21 Fe^{3+}, 0.38 Cr^{++}, 0.17 Ni^{++}, 0.04 Mn^{++}, 0.001 Cl^-, 0.1 μc Ru^{106}

TBP-25 (moles/liter): 5.35 NO_3^-, 0.5 H^+, 0.026 SO_4^{--}, 0.002 Fe^{3+}, 1.6 Al^{3+}, 0.01 Hg^{++}, 0.07 NH_4^+, 0.1 μc Ru^{106}

Expt. No.	Additives (moles/liter waste)	Ru^{106} (% of total)				Material Balance (%)
		In Residue	In Equipment Wash	In Condensate	In Bubblers	
			Purex			
1	0.60 H_3PO_3 0.80 $Ca(OH)_2$	94.98	2.51	1.79	0.10	99.38
2	1.52 H_3PO_3 0.80 $Ca(OH)_2$	100.24	0.47	0.04	0.00	100.75
3*	1.52 H_3PO_3 0.80 $Ca(OH)_2$	98.83	0.58	0.03	0.00	99.44
			Darex			
4	0.46 H_3PO_3	98.57	0.65	1.47	0.00	100.69
5	0.91 H_3PO_3	99.02	0.66	0.18	0.02	99.98
6	1.52 H_3PO_3	99.10	0.55	0.22	0.00	99.87
7	1.82 H_3PO_3	100.00	0.16	0.02	0.00	100.18
			TBP-25			
8	None	64.58	3.20	32.90	0.22	100.90
9	0.38 H_3PO_3	97.50	0.35	0.30	0.00	98.15
10	0.75 H_3PO_3	100.20	0.82	0.80	0.00	101.82

*Stable Ru concentration increased 100-fold to 0.2 *M*.

(dissolution) rates in a 14-day period in distilled water, as shown by cesium tracer, were 10^{-3} g/cm^2 the first day, but dropped rapidly to the limit of detectability, 10^{-5} g cm^{-2} day^{-1} by the seventh day. One of the more satisfactory solid products contained 22.2, 30.0, 5.0, and 8.9 wt %, respectively, of SO_3, P_2O_5, B_2O_3, and MgO (Fig. 5.5).

Corrosion Studies

Corrosion by high-activity wastes occurs in the waste tanks during interim storage in the permanent equipment in the calciner plant (evaporators, condensers, tanks) and in the calciner pot both during the evaporation-calcination and storage.

Both 304L and 347 stainless steels in Darex-Purex and in Darex-Thorex wastes showed grain boundary attack after several hundred hours' exposure at temperatures above 50°C. The onset of visible grain boundary corrosion was delayed by decreasing the free nitric acid concentration from 5 to 2 *M* and the temperature from 80 to 50°C, and by the presence of polyethylene in the system.

Table 5.4. Results of Precipitation-Clarification-Ion Exchange Treatment of Low-Activity Waste*

Fission Product	Amount of FP's Removed in Precipitation-Filtration (% of original)	FP's Removed by Ion Exchange (% of remaining)	Typical Overall Process D.F.
Cs	1–10	>99.9	1000
Sr	~50	>99.9	1000
Ce and other R.E.'s	90–99	10	100
Co	70–95	10	10–40
Ru	70–90	10	10
Zr-Nb	50	Not determined	Not determined

*Volume reduction from original waste to resin is at least 1500.

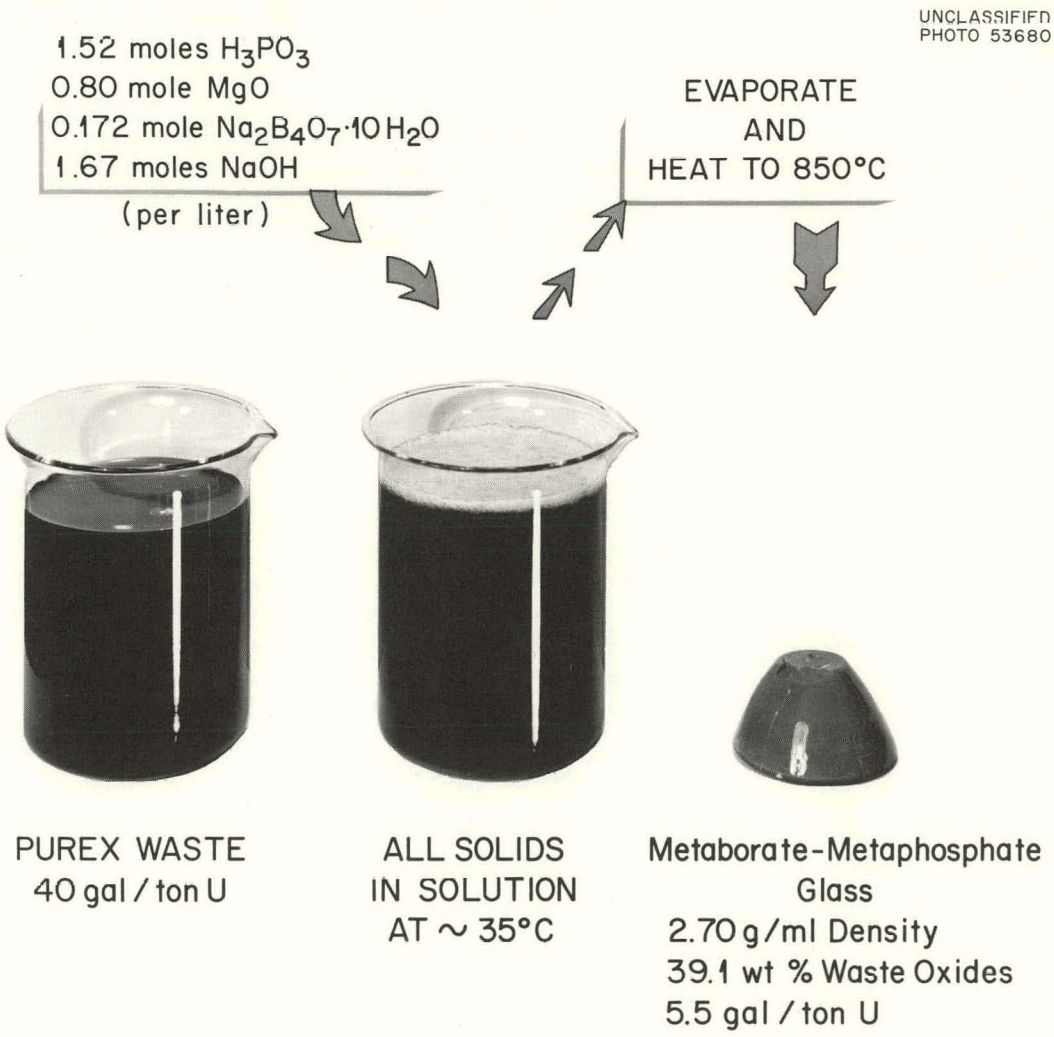

Fig. 5.5. Metaborate-Metaphosphate Glass Formed from Synthetic Purex Waste.

Overall rates varied from a few hundredths to 0.1–0.2 mil/mo when the temperature was varied from 50 to 80°C. Tests with and without chloride indicated that the grain boundary attack is due to the effects of high concentrations of iron (~67 g/liter) and possibly chromium (~19 g/liter) rather than to the presence of up to 100 ppm of chloride.

Under the conditions in the evaporator condenser, Hastelloy F, LCNA, type 347 stainless steel, and Titanium-45A were corroded at rates of 3.2, 0.82, 3.6, and 1.4 mils/mo, respectively, in boiling 6 *M* HNO_3–0.05 *M* H_2SO_4, the average composition of Purex condensate. Exposure times varied from 300 to 1000 hr. All materials except titanium suffered aggressive grain boundary attack, particularly in the vapor phase. LCNA and Hastelloy F were subject to this type of attack in the absence of sulfate. Ni-o-nel containing 0.2% Pt was corroded at a rate 6 to 7 times as rapidly as LCNA.

In the calcination step the nitric acid concentration is about 15 *M* but the sulfuric acid varies from essentially zero in 4-in.-dia pot tests to an average of 1.0 *M* in 8-in.-dia pot tests. Titanium was corroded at a maximum rate of 2.01 mils/mo in 1145 hr exposure to boiling 15 *M* HNO_3–1.0 *M* H_2SO_4 (final condensate composition) with only slight localized attack in the heat-affected zone near welds.

Pot corrosion by a sulfate-bearing synthetic Purex waste solution, 5.6 *M* H^+, 6.1 *M* NO_3^-, 1.0 *M* SO_4^{--}, 0.6 *M* Na^+, 0.5 *M* Fe^{3+}, 0.1 *M* Al^{3+}, 0.01 *M* Cr^{3+}, 0.01 *M* Ni^{++}, and 0.002 *M* $RuCl_3$, was investigated under evaporator and calciner conditions. Evaporation of the solution to solid followed by heating to 900°C for 24 hr to simulate a calcination cycle resulted in a total penetration of 0.22 mil (~7.4 mils/mo) in 304L stainless steel. About 1.4 mils/mo can be expected from air oxidation on the outer surface of the pot at 900°C. When a specimen was held at 900°C for 168 hr, the internal total corrosion rate, including that during evaporation and calcination, was 3.6 mils/mo.

Long-term internal and external corrosion tests have not yet been run on the pot storage vessel.

Design of Pot Calcination Pilot Plant

A preliminary design study, which resulted in a proposal for the construction of a waste calcination pilot plant at ORNL or ICPP, was prepared.[4] Included were a design summary and cost estimate for a pilot plant building at ORNL and the subsequent installation of an ORNL pot calcination unit and a BNL rotary calciner along with the necessary common feed, off-gas treatment, and mechanical equipment in this building or in three of the five cells in the ICPP hot pilot plant. The cost of the new building at ORNL was estimated to be $1,500,000, and the cost of procurement and installation of the equipment at either site was estimated at an additional $1,000,000. The facility will permit storage of the calcination pots or rotary calciner powder receivers for one year to permit observation of temperature, pressure, and vessel integrity prior to final disposal.

The pilot plant is designed to demonstrate calcination of Purex, Thorex, Darex, or TBP-25 wastes at average batch rates of 5 gal/hr, to a final calcination temperature of 900°C. Evaporation could be either batch or continuous if certain safety considerations are satisfied. The equipment could ultimately be used to demonstrate the fixation of wastes in phosphate glasses with either the pot or rotary calciners.

The BNL rotary calciner contains a 10-in.-dia by 4-ft-high Inconel rotating vessel heated to 700°C, 20% filled with ¾-in.-dia stainless steel balls. Waste solution is fed to the calciner through a central feed tube and drips out the rotating bed of balls. Vapor from the solution leaves the calciner through a vapor line while the solids formed are pulverized and flow by gravity to a powder receiver. Since the pot and rotary calciners can be operated with common auxiliary process and mechanical handling equipment, both will be tested at a large saving in both time and cost over that which would be required for separate installations. Preliminary design of the pilot plant is scheduled to start January 1962 and equipment installation at the ICPP by January 1963.

Engineering, Economic, and Hazards Evaluation

A comprehensive study has been undertaken on the economics and hazards associated with methods for ultimate disposal of highly radioactive liquid and solid wastes. A 6-ton/day plant is assumed, processing 1500 tons per year of uranium-converter

[4] J. M. Holmes, *Waste Calciner Pilot Plant Proposal*, ORNL CF-60-12-121 (Dec. 14, 1960).

fuel at a burnup of 10,000 Mwd/ton and 270 tons/year of thorium converter fuel at a burnup of 20,000 Mwd/ton. This hypothetical plant could process all the fuel from a 15,000-Mw_e nuclear economy, which may be in existence by 1970.

Preliminary operations to be evaluated are: interim liquid storage, conversion to solids by pot calcination, interim storage of solid waste in pots, and shipment as liquids or calcined solids. Ultimate disposal methods to be evaluated are: pot-calcined solids in salt deposits, in vaults, and in vertical shafts and liquids in salt deposits, in deep wells, by hydrofracture, and in tanks. A cost estimate of each preliminary step as a function of time since reactor discharge and of each ultimate disposal method as a function of decay time prior to storage will be made for acid and neutralized Purex and Thorex wastes. From the graphs obtained, the disposal cost of any of the four types by any of the disposal methods can be calculated for any solid and liquid interim storage period. The hazards evaluation will be made separately from the economic since it will be more qualitative.

The economic evaluation of interim liquid storage was completed. A conceptual design of a tank farm was made in which water flowing through tank cooling coils passes through heat exchangers served by a secondary cooling loop, including a cooling tower. Heat exchangers, pumps, and cooling towers were sized and cost estimated for storage times of 0.5 to 30 years. Tanks of Savannah River design were used, with stainless steel construction for acid wastes. Cells and a steel building were included for shielding and secondary containment. An interest rate of 4% was assumed and used with the present value method of financing future capital outlays. With interim storage defined as filling time plus full time, tank costs were minimum when full time was roughly three-quarters of the interim storage time. For waste storage times of 0.5 to 30 years, costs ranged from 2.0×10^{-3} to 9.3×10^{-3} mill/kwh_e for acidic wastes and from 1.5×10^{-3} to 4.7×10^{-3} mill/kwh_e for neutralized wastes (Fig. 5.6).

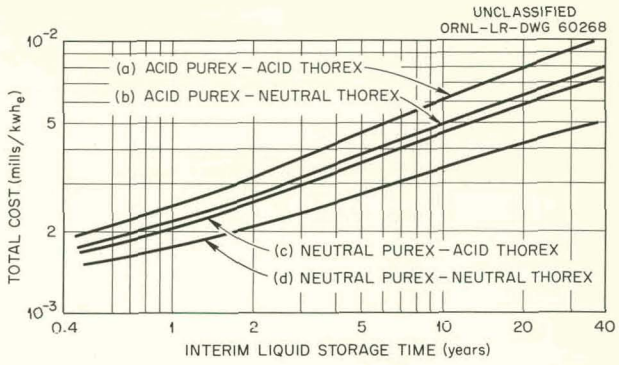

Fig. 5.6. Cost of Interim Liquid Waste Storage as a Function of Storage Time.

5.2 LOW-ACTIVITY WASTE TREATMENT

A scavenging-ion exchange process[5] (Fig. 5.7) is being developed, on both a laboratory and pilot plant scale, for decontaminating the large volumes of slightly contaminated water produced in nuclear installations. The process uses phenolic resins, which are much more selective for cesium in the presence of sodium than the polystyrene resins used in earlier technology. The Cs/Na separation factor is 160 for CS-100 resin vs 1.5 for Dowex 50; other cations, e.g. strontium and rare earths, are sorbed. The solution must be clarified prior to ion exchange since ion exchange media do not remove colloidal materials efficiently.

Development Program

In the scavenging ion exchange process, the water is made 0.01 *M* in NaOH (pH ~ 12) and 5 ppm in iron to form a floc, which settles and removes all suspended material, carrying 50 to 99% of the rare earths, cobalt, ruthenium, and zirconium for which the ion exchange step is less effective (Table 5.4). After settling and filtration the water is passed through a CS-100 ion exchange resin column where >99.9% of the cesium and strontium are sorbed during the passage of 2000 resin bed volumes of water. At pH 12, a large fraction of the phenolic groups on the CS-100 resin (phenolic-carboxylic type) are ionized and free to sorb cations. As a result of the two steps, the radioactivity content of ORNL low-activity waste would be approximately the maximum permissible concentration for discharge to the uncontrolled environment. The activity is eluted from the resin with dilute nitric acid and the acid recovered by evaporation. The combined dry volume of evaporator

[5] J. T. Roberts and R. R. Holcomb, *A Phenolic Resin Ion-Exchange Process for Decontaminating Low-Radioactivity-Level Process Water Wastes*, presented at the American Chemical Society Meeting, New York, Sept. 11–16, 1960 (ORNL CF-60-8-103); also presented in ORNL-3036 (Mar. 17, 1961).

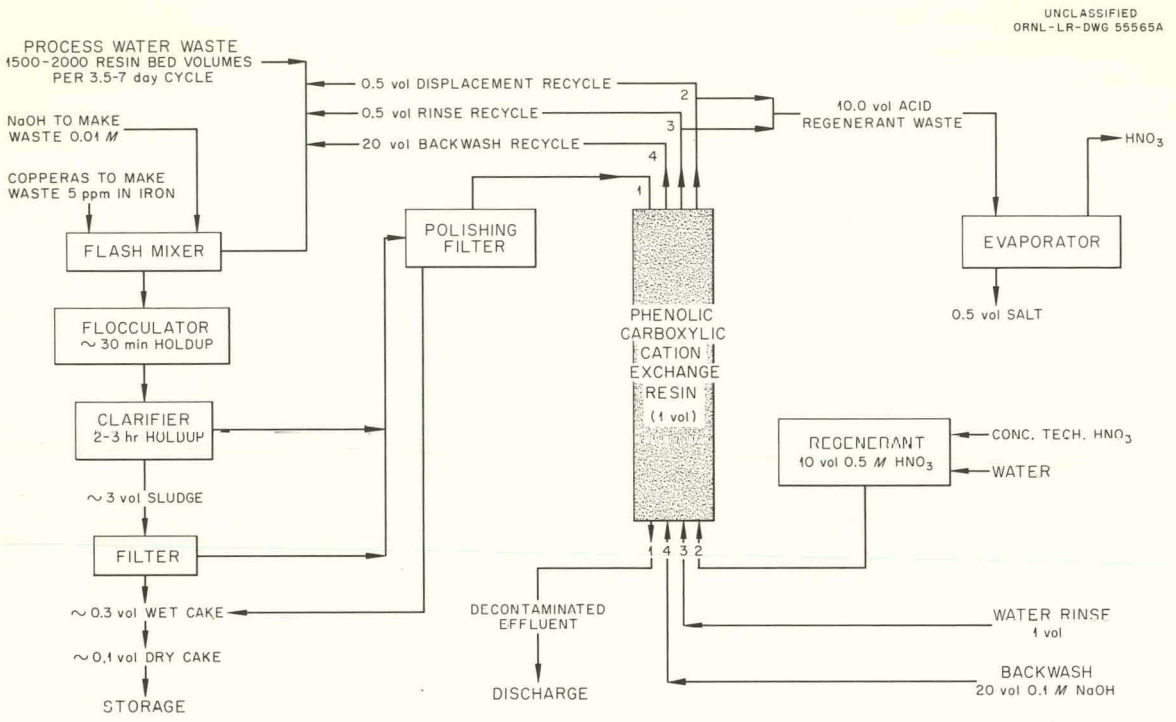

Fig. 5.7. Process Water Decontamination with Carboxylic-Phenolic Ion-Exchange Resin.

salt residue and flocculation cake is about 0.6 vol, i.e., about 0.03 vol % of the treated water. The flowsheet in Fig. 5.7 represents an improvement over earlier ones in that with CS-100 resin nitric acid rather than hydrochloric is the regenerant, and only 0.1 as many equivalents of acid are required for elution (Fig. 5.8).

The scavenging precipitation step (flash mixing, flocculation, settling, and filtration) was studied extensively in 15-liter/hr equipment with tap water. Slow mixing with large blades was important in floc formation, the inlet stream to the settler had to be at the bottom to take advantage of the settling action of the floc blanket, and a screen was needed on the outlet to retain small amounts of suspended flocs. The step is now being studied on actual ORNL low-activity waste on a 60-liter/hr basis (Fig. 5.9). In initial runs the gross beta activity of the water was decreased from 28 to 1.1 c min^{-1} ml^{-1}, a decontamination factor of 25.

In studies with other exchange media >99.9% (DF = 1000) of the cesium and strontium were removed from 6900 bed volumes of ORNL low-activity waste with 19.2 ml of clinoptilolite, a naturally occurring zeolite mineral. The column

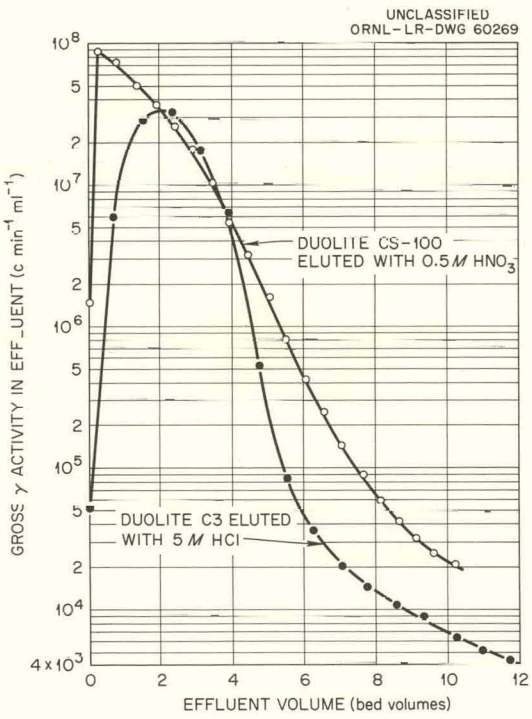

Fig. 5.8. Elution Characteristics of Phenolic Ion-Exchange Resins.

diameter was 0.5 in. and the flow rate 20 gal hr^{-1} ft^{-2}. This represented a breakthrough level of 1% of the feed activity concentration; 8700 vol had passed through at the 50% breakthrough level. The breakthrough was attributed entirely to cesium since strontium could not be detected in any of the effluent samples.

Design of Low-Activity Waste Treatment Pilot Plant

A pilot plant for treatment of ORNL low-activity waste was designed at an estimated total cost of $65,000. Startup is scheduled for August 1961. The design capacity is 10 gal/min with water from the ORNL settling basin. Objectives are to determine the type of equipment required to achieve results comparable to laboratory data, i.e., removal of 99.9% of the cesium and strontium from 1500 ion-exchange bed volumes. A further objective may be the demonstration of processes using natural mineral zeolites, such as clinoptilolite, as the ion-exchange medium. This information will be used in the design of a full-scale plant to treat 750,000 gal/day.

The major equipment pieces include (in flow sequence) a flash mixer, flocculator, clarifier, polishing filter, and ion-exchange columns. Acid regeneration equipment and chemical feeders for the required reagents are provided. The process is designed for dilute nitric acid regeneration. If an HCl flowsheet is used for regeneration of the ion exchanger resins, space will be provided for the evaporation equipment. However, the acid tanks, ion exchange columns, and piping will be compatible for either HCl or HNO_3 solutions.

The flash mixer, flocculator, and clarifier combination are designed to remove at least 90% of the initial feed turbidity plus the solids precipitated

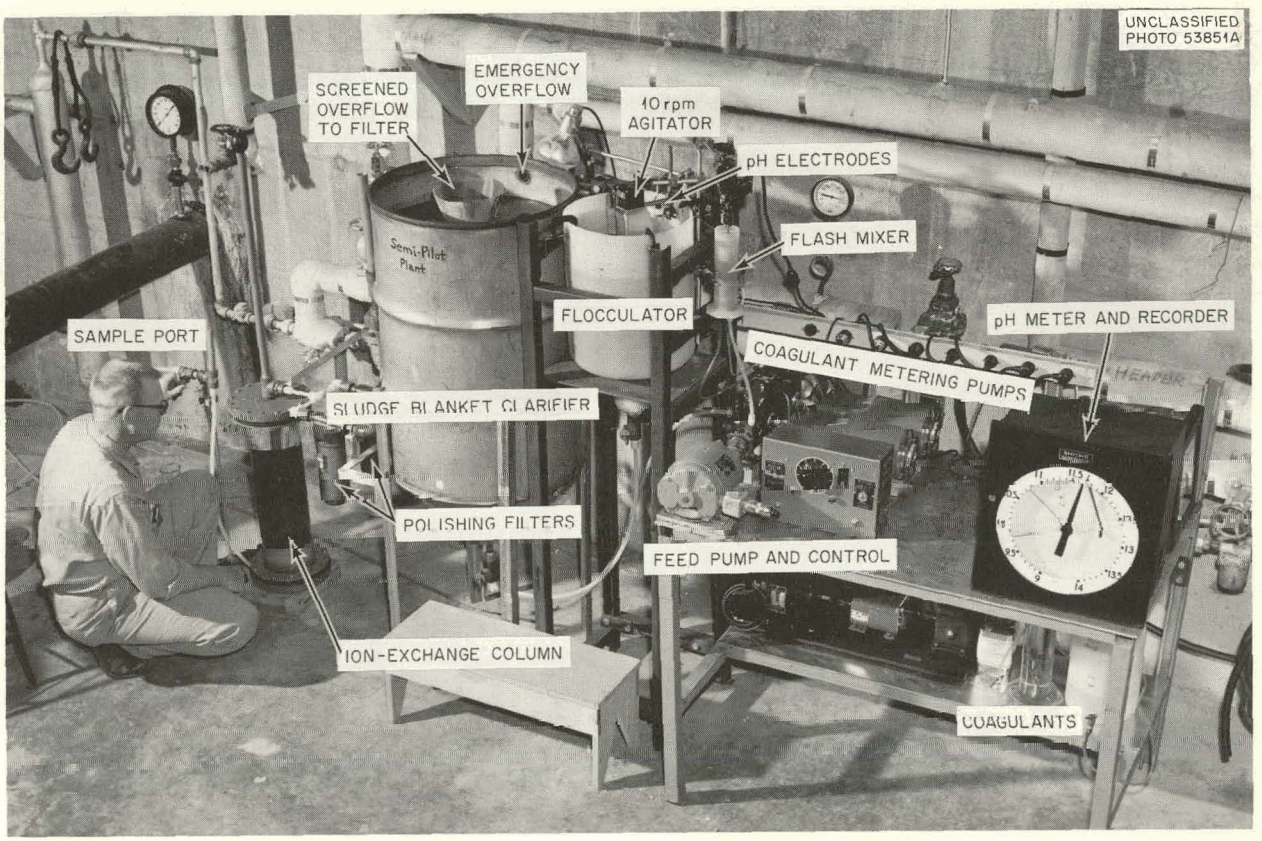

Fig. 5.9. Semi-Pilot Plant for Demonstration of Ion-Exchange Treatment of Low-Activity Process Waste Water.

by the addition of NaOH and coagulant to the feed (pH 11.7). The polishing filter will decrease the level of undissolved solids to less than 0.2 ppm and will demonstrate filtration of the clarifier sludge during shutdown. Two ion exchange beds ($\frac{1}{50}$ of plant scale volume) will be tested separately. The 10-in.-dia × 8-ft-high bed is scaled down at constant liquid velocity from the proposed plant bed. The 18-in.-dia by 32-in.-high bed has the same height to diameter ratio as that in the proposed plant and will determine if the data obtained from the 8-ft bed must be corrected for a lower ratio when scaling up to plant size. About 72 hr should be required to exhaust one of the beds. The ion exchangers will be regenerated by feeding acid upflow to the beds followed by a water and caustic wash to convert the resin to the sodium form. Activity removed by the beds will be returned to the settling basin or sent to the concrete waste tanks.

6. PILOT PLANT DECONTAMINATION

Since Nov. 20, 1959 a full-scale decontamination program[1] has been in progress in the Radiochemical Processing Pilot Plant following an evaporator explosion caused by deflagration of nitrated organic compounds. The area beneath the sampling gallery was enclosed to serve as a containment wall and an air flow plenum chamber which routed all the air from the penthouse area through the cells.[2] Since this time, 521,000 liters of various decontaminants has been used to decrease the alpha activity level by a factor of 1000 from an original 10^8 d/m/100 cm^2. Transferable activity, in a few spots, of the order of 10^5 d/m/100 cm^2 that could not be cleaned by exhaustive flushing and hand scrubbing (Table 6.1) was sealed to the wall and ceiling surfaces with three or more coats of color-coded paint (red, gray, and white). After being painted, surfaces that had probed $> 10^5$ d/m/100 cm^2 were outlined with a magneta stripe and a standard warning sign was affixed. Process vessels in some areas (cells 6 and 7) were painted with water-soluble polyvinyl acetate paint to permit possible future decontamination. Stainless steel floors are still being cleaned with small rotary buffing machines followed by total immersion in 1 *M* HNO_3 and 0.1 *M* NaF at 90–100°C.

The initial phase of the cleanup program consisted in flushing residual plutonium from process vessels with a solution of 2 *M* HNO_3–0.02 *M* fluoride–0.04 *M* boron. A total of 1.5 kg of plutonium was flushed from process equipment[3] but only 3% of this was found in equipment that was not a part of the ruptured evaporator (Table 6.2).

The cell walls, ceilings, and cubicles, which were contaminated to a transferable α activity level of 10^8 d/m/100 cm^2, were flushed with various decontaminating solutions. From a temporary cubicle, fabricated from Lucite and plywood and placed at the entrance to cell 6 (Fig. 6.1), a total of 21,900 liters of laundry compound detergent was sprayed onto walls and debris, removing 57 g of plutonium.

Concrete shielding blocks and debris were then removed to decrease the radiation background in

[1] *Chem. Tech. Div. Ann. Prog. Rep. Aug. 31, 1960*, ORNL-2993.

[2] J. R. Parrott, *Decontamination of Cells 6 and 7, Building 3019, Following Plutonium Release Incident*, ORNL-3100 (in press).

[3] L. J. King, W. T. McCarley, *Plutonium Release Incident of November 20, 1959*, ORNL-2989, Feb. 1, 1961.

Table 6.1. Activity Level of Processing Cells Prior to Painting

Cell No.	No. of Smears	Transferable Activity (d/m/100 cm^2)		Fixed α Activity (d/m/100 cm^2)			β, γ Activity (mr/hr)	
		Avg.	Max.	No. of Probes	Avg.	Max.	Background	Max.
3	73	79	488	91	<8830*	4.5×10^4	<2	10
4	132	273	1276	142	5465	8.0×10^4	15	10,000**
5	150	216	2584	85	9974	1.8×10^5	30	5,000
6, 7	211	1.8×10^4	5.0×10^5	212	2.5×10^5	$>7.0 \times 10^5$	20	3,000

*38 probe readings were <5000 d/m/100 cm^2.

**Inaccessible area.

Table 6.2. Plutonium Removal from Cell Equipment

Equipment	Flushes		Plutonium Removed	
	Total No.	Volume (liters)	(g)	(% of total)
Feed preparation	1	1,510	2.03	0.1
Solvent extraction	17	12,250	45.77	3.0
Evaporators				
P-65	7	3,865	21.54	1.4
P-15*				
Body	40	15,879	804.26	51.9
Catch tank	7	2,105	492.58	31.7
Exterior	91	252,610	184.90	11.9
Total	163	288,200	1,551.08	100.00

*Ruptured evaporator.

the cell and eliminate the source of sand and grit, which were detrimental to the steam jets used for solution transfer. The blocks were first packaged in mild steel drums with clamp-on lids, and debris was enclosed in plastic bags within drums and the drums encased in another plastic bag to prevent leakage of α-contaminated particles into noncontaminated areas. The ruptured evaporator and associated components were also removed, the largest component being the steam stripper which was packaged in a plywood box wrapped with plastic. A portable telescoping elevator was used in the cells for handling the material at higher elevations.

With the radiation cell background decreased from 1000 to 2000 to 50 mr/hr, cell flushing was resumed. A total of 430,600 liters was sprayed in the cell by Chempumps supplying a hand-operated spray wand or a Sellers high-pressure jet cleaner. Turco 4501 solution was recirculated through a heat exchanger to increase the temperature. Of the total of 141 g of plutonium removed from the surfaces, 50% was found in the first 32,000 liters and 99% in the first 240,000 liters (Fig. 6.2).

The hazard associated with the long-lived α air activity necessitated close surveillance of

Fig. 6.1. View of Temporary Cubicle from Plenum Chamber.

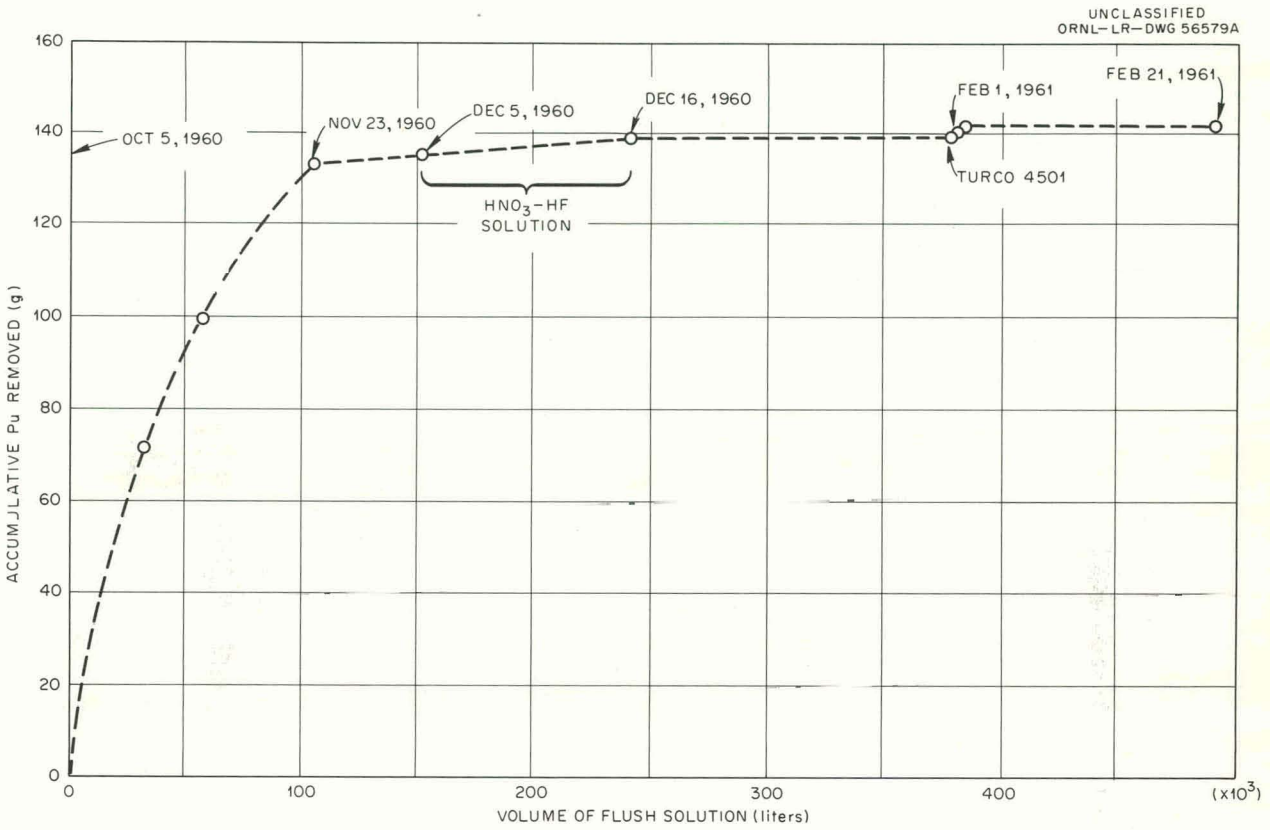

Fig. 6.2. Plutonium Removal vs Volume of Flush Solution.

working areas. From air-contamination data (Fig. 6.3) and the results of thorough surface contamination surveys "resuspension factors" were calculated and used to estimate the air-borne contamination when the plutonium surface contamination is known (Table 6.3). These factors overlap a resuspension factor obtained from the literature[4] of 4×10^{-8} (μc/cc air $\div$ μc/cm^2 surface) by a factor of 5 to 10.

[4]E. J. Leahy and A. I. Smith, *Contamination Control Procedures for Special Weapons Accidents*, USNRDL-TR-283, Dec. 22, 1958.

[5]L. J. King, *Processing of Air Monitoring Data in the Radiochemical Processing Pilot Plant* (in preparation).

The long-lived α activity data accumulated daily from 20 air sampling stations were reduced to final results in a variety of forms by three programs written for the IBM 7090, labeled AIRCØUNT, DAILY TAPE, AND AIRPLØT.[5] These programs may be applied, without modification, to processing of air-sampling data collected elsewhere.

Of the total 1.5 $\pm$ 0.2 kg of plutonium flushed from process equipment, 1.1 kg was in solution in concentration sufficient to justify processing. These solutions were evaporated, and the plutonium recovered was by anion exchange (Sect. 19.4).

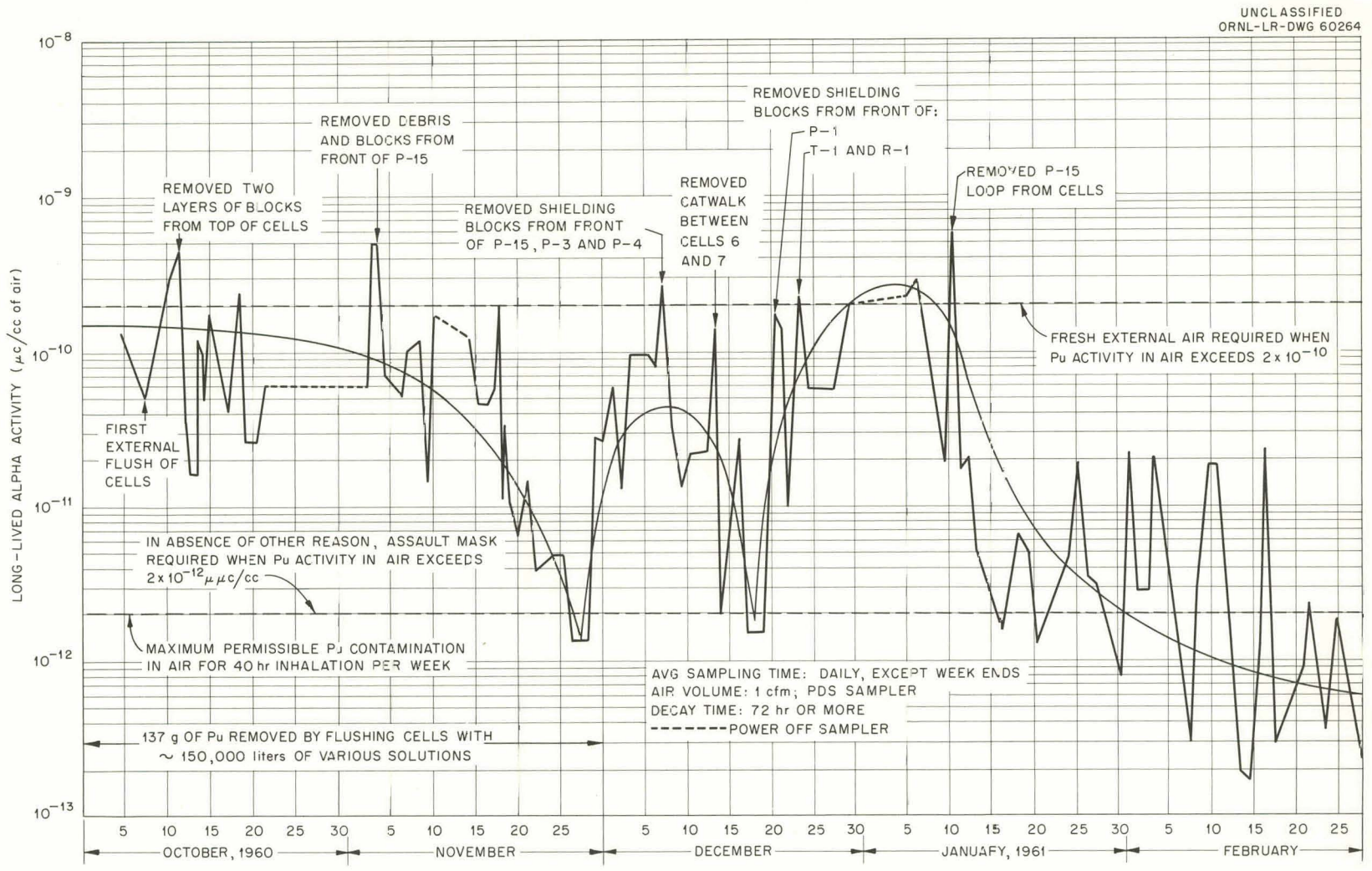

Fig. 6.3. Long-Lived Alpha Activity During Decontamination of Cells 6 cnd 7.

Table 6.3. Plutonium Resuspension Factors

Date	Cell No.	Operation in Cell	Weighted Average of Transferable Surface Activity ($\mu c\ cm^{-2}$)	Air Activity in Cell (μc/cc air)	Resuspension Factor μc/cc air ÷ $\mu c/cm^2$ surface
1/11/61	6, 7	Removal of damaged equipment	8.33×10^{-2}	1.1×10^{-10}	1.32×10^{-7}
2/13/61	6, 7	Cleanup in progress	5.28×10^{-3}	1.54×10^{-12}	1.89×10^{-8}
2/21/61	6, 7	Cleanup in progress	8.25×10^{-3}	3.38×10^{-13}	7.88×10^{-9}
3/30/61	6, 7	Floor being cleaned	4.82×10^{-4}	1.18×10^{-12}	2.45×10^{-7}
4/3/61	5	Cleaned, unpainted	4.49×10^{-5}	7.65×10^{-13}	1.70×10^{-8}
4/14/61	5	Cleaned, unpainted	9.73×10^{-5}	4.39×10^{-14}	4.51×10^{-8}
2/2/61	3	Contaminated with U^{233}	3.24×10^{-5}	1.50×10^{-13}	4.62×10^{-7}

7. GCR COOLANT PURIFICATION STUDIES

The anticipated nonradioactive gaseous contaminants that will have to be removed from helium coolants of gas-cooled reactors are H_2, CO, CO_2, H_2O, and trace amounts of hydrocarbons. These contaminants may be maintained at low levels in the coolant by continuous purification of a small portion of the total coolant stream. The method proposed for removing the contaminants is oxidation of all oxidizable contaminants (H_2, CO, and hydrocarbons) to H_2O and CO_2 followed by cosorption of H_2O and CO_2.

7.1 OXIDATION BY O_2

Kinetic tests were made with oxidation of the individual contaminants (Table 7.1) and with simultaneous oxidation of H_2 and CO, H_2 and CH_4, and H_2, CO, and CH_4. The tests with simultaneous oxidation of two or more contaminants

Table 7.1. Conditions of Catalytic Oxidation of Individual Contaminants

No. of Tests	Catalyzed Reaction	Gas Flow Rates (g moles $cm^{-2}\ min^{-1}$)	Initial Contaminant Conc. (vol %)
24	$H_2 + 0.5\ O_2 = H_2O$	~0.067 0.219	H_2 = 0.35-2.08
15	$CO + 0.5\ O_2 = CO_2$	0.067 0.115 0.216	CO = 0.425-1.94
17	$CH_4 + 2\ O_2 = CO_2 + 2\ H_2O$	0.067 0.114 0.218	CH_4 = 0.22-0.63

showed that the preference of oxidation was hydrogen first, carbon monoxide second, and methane last. Although these effects were not quantitative, for a conservative reactor design it should be assumed that the first portion of the oxidizer will oxidize hydrogen, the next portion CO, and finally, CH_4. Thus, the necessary reactor volumes are additive for each contaminant and the oxygen mole fraction to be used in each zone is the total unused oxygen in the gas stream. A typical design for the EGCR purification system was a catalytic oxidizer with 3.77 ft^3 of catalyst.

Gases in a flowing stream of helium were passed through a fixed bed of $\frac{1}{4}$-in. Girdler G-43 platinum[1] in a 2-in.-dia oxidizing vessel (Fig. 7.1) at 300 psia, 500 ± 25°C. The contaminated helium stream and the oxidizer off-gas were analyzed for H_2, CO, CH_4, and O_2 by a gas-adsorption chromatograph with lower limit of detection ~10 ppm for H_2 and 5 ppm for O_2, CO, and CH_4.

Empirical correlation of the data gave the following[1] reactor design equations for use in design of catalytic oxidizers for gas-cooled-reactor helium purification systems:

For hydrogen,

$$V_H = \frac{248\,F}{\pi G^{0.65}} \ln \frac{\left[\sqrt{2y_{O_0}\,y_{H_0}} + y_{H_0} + (2y_{O_0} - y_{H_0})/2\right]}{\left[\sqrt{(2y_{O_0} - y_{H_0})y_{H_f} + y_{H_f}^2} + y_{H_f} + (2y_{O_0} - y_{H_0})/2\right]}$$

For carbon monoxide, where oxygen is less than stoichiometric,

$$V_C = \frac{1.052\,F}{(\pi^{1.5}G^{0.982})\sqrt{y_{C_0} - 2y_{O_0}}} \times \ln \frac{\left(\sqrt{y_{C_0}} - \sqrt{y_{C_0} - 2y_{O_0}}\right)\left(\sqrt{y_{C_f}} + \sqrt{y_{C_0} - 2y_{O_0}}\right)}{\left(\sqrt{y_{C_0}} + \sqrt{y_{C_0} - 2y_{O_0}}\right)\left(\sqrt{y_{C_f}} - \sqrt{y_{C_0} - 2y_{O_0}}\right)}$$

For carbon monoxide when oxygen is greater than stoichiometric,

$$V_C = \frac{2.10\,F}{(\pi^{1.5}G^{0.982})\sqrt{2y_{O_0} - y_{C_0}}} \left(\tan^{-1}\sqrt{y_{C_0}/(2y_{O_0} - y_{C_0})} - \tan^{-1}\sqrt{y_{C_f}/(2y_{O_0} - y_{C_0})}\right)$$

For methane,

$$V_{CH} = \frac{2.2\,F}{\pi^2 G^{0.859}(2y_{CH_0} - y_{O_0})} \ln \frac{y_{CH_f}\,y_{O_0}}{y_{CH_0}\,y_{O_f}}$$

[1] C. D. Scott, *Kinetics of the Catalyzed Oxidation of Hydrogen, Carbon Monoxide, and Methane by Oxygen in a Flowing Stream of Helium*, ORNL-3043 (Feb. 7, 1961).

where

V_H, V_C, V_{CH} = volume of platinum catalyst necessary for the oxidation, cc

F = gas feed rate, g moles/min

π = total pressure, atm

G = mass flow rate, g moles cm^{-2} min^{-1}

y_{H_0}, y_{C_0}, y_{CH_0}, y_{O_0} = initial mole fraction of H_2, CO, CH_4, and O_2

y_{H_f}, y_{C_f}, y_{CH_f}, y_{O_f} = final mole fraction of H_2, CO, CH_4, and O_2

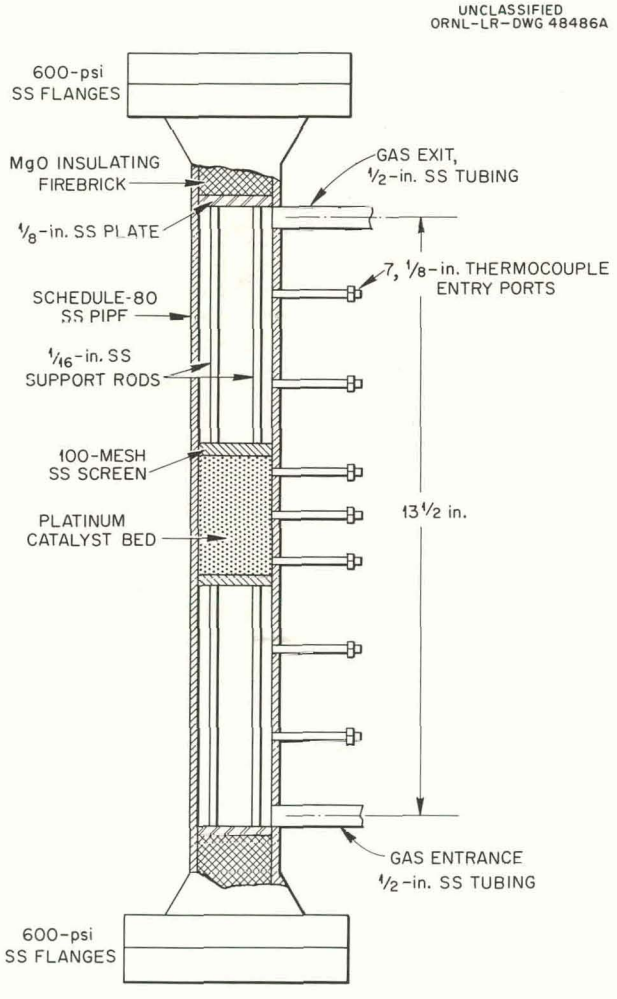

Fig. 7.1. 2-In.-dia Oxidizer in Helium Purification Test Facility.

7.2 OXIDATION BY CuO

Initial results of a kinetic study on the oxidation of H_2, CO, and CH_4 from a flowing stream of helium by a fixed bed of 1/8-in.-dia CuO pellets indicated that mass transfer of the H_2 and CO from the bulk gas stream to the CuO reaction site is the rate-controlling mechanism. The rate-controlling mechanism for CH_4 oxidation is not yet known.

Such an oxidation would operate in a cycle in which the CuO would be reduced to copper metal and regenerated to CuO by air. Operating conditions tested were 400 to 600°C, 10 to 30 atm pressure, gas flow rates of 0.086 to 0.257 g mole cm^{-2} min^{-1}, and contaminant levels of 0.01 to 1.0 vol %. The 2-in.-dia oxidizer (Fig. 7.1) was used.

A theoretical model has been postulated for the heterogeneous reaction $H_2 + CuO \rightarrow Cu + H_2O$ in which external diffusion (gas film diffusion) and internal diffusion (molecular diffusion in the pores of the porous solid) of H_2 are the rate-controlling steps (Fig. 7.2). This model appears to describe

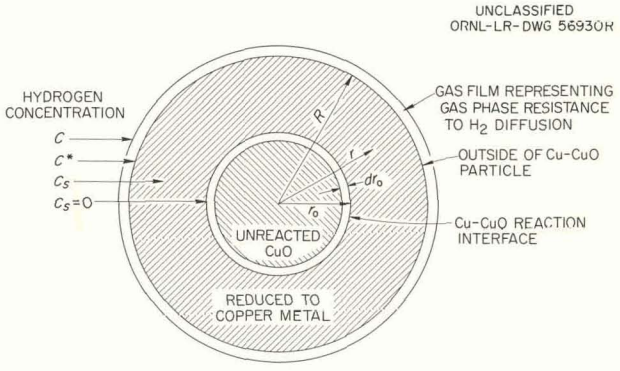

Fig. 7.2. Section of Spherical Model Used to Describe Rapid, Irreversible Reaction of H_2 and CuO with Reaction Rate Controlled by External and Internal Diffusion of H_2.

the experimental results of both differential beds of CuO and deep beds of CuO in a flowing stream of helium contaminated with hydrogen. Based on this model, two differential equations describing the hydrogen concentration in the bulk gas stream

as a function of time and position in the CuO bed can be derived:

$$\left(\frac{\partial C}{t}\right)_z + V\left(\frac{\partial C}{\partial z}\right)_t$$

$$= \frac{k_{ga}C}{\beta}\left[1 - \frac{k_{ga}}{\tau}\left(\frac{R - r_0}{4\pi\alpha r_0 R + k_{ga}(R - r_0)}\right)\right]$$

$$\frac{r_0}{R}\left[4\pi D R\, r_0 + \frac{k_{ga}}{\tau}(R - r_0)\right] = -\frac{\alpha D k_{ga} C}{h}\, dt$$

where C = hydrogen concentration in bulk gas phase, g moles/cc

t = time of reaction, sec

V = linear velocity of the gas through the interstices between CuO pellets, cm/sec

z = height in CuO bed measured from the bottom of the bed, cm

k_g = mass transfer coefficient through the external gas film, cm/sec

a = specific external surface area of CuO pellets, cm^2/cm^3

β = external porosity of CuO bed

τ = number of CuO pellets per unit volume of bed, pellets/cc

R = radius of hypothetical CuO sphere with volume equal to volume of average CuO pellet, cm

r_0 = radius of reaction interface (Cu–CuO) within the sphere, cm

α = effective internal porosity of the CuO pellet

b = CuO molar density within CuO pellet, g moles/cc

These two differential equations can be solved by a finite difference method on a high-speed digital computer and then used as design equations for a fixed-bed CuO oxidizer for H_2 in a flowing stream of helium. The CO and CH_4 oxidations will be treated similarly.

7.3 DESIGN OF HELIUM PURIFICATION SYSTEMS

A helium coolant side-stream purification system consisting of parallel sections for radioactive and nonradioactive decontamination was designed for the pebble bed reactor experiment. Primary equipment components are two gas coolers, gas heater, charcoal trap, CuO oxidizer, Molecular Sieve adsorber, and full flow filters. The charcoal trap is sized to provide a holdup of 30 min for krypton isotopes, 6 hr holdup for xenon isotopes, and 99.9% retention of iodine isotopes, resulting in "decontamination factors" varying from 1 for Kr^{85} to 556 for I^{131}. Nonradioactive decontamination will result in a steady-state concentration of CO_2 in the coolant of 20.8 ppm or less. The total estimated cost of the system, excluding auxiliary equipment and containment, is estimated to be $26,690.

A helium coolant purification system for the proposed 800-Mwt Pebble Bed Reactor was designed to operate on a coolant side stream of 1% of the total coolant flow. There are provisions for radioactive and nonradioactive contamination removal. Primary equipment components are dual oxidizers, an economizer heat exchanger, a gas cooler, dual adsorbers, a fission product gas trap, and dual filters. The fission product trap is sized to provide a holdup of 30 min for krypton and 6 hr for xenon and for 99.9% retention of iodine. Nonradioactive decontamination is sufficient to maintain oxygen-bearing contamination at <30 ppm in the coolant. The total cost of the system, excluding auxiliary equipment and containment, was estimated to be $176,360.

8. EQUIPMENT DECONTAMINATION

A solution of 0.3 *M* sodium oxalate–1.0 *M* hydrogen peroxide–0.056 *M* oxalic acid at pH 5 and 95° was recommended for spray decontamination of the mild steel EGCR charge and service machines, but the pH had to be adjusted frequently because of peroxide instability, accelerated by a rise in pH. The solution was improved by replacing the sodium salt with the more soluble ammonium oxalate, which is a better decontaminant, is easily decomposed and volutilized from waste solutions without residues, and increases solution stability by its improved buffering effect. Solution stability was increased to 6 hr at 95°C without pH adjustment, even in the presence of 100 ppm Fe^{3+} and large surfaces of iron, by lowering the H_2O_2 concentration to 0.3 *M* and the pH to 4.0 and adding 0.1 *M* ammonium citrate to complex iron and as extra buffer.[1] Several peroxide stabilization reagents normally used in industry had little effect. The solution is very corrosive to copper, and is rapidly decomposed by it. Without peroxide, the solution is too corrosive for use on carbon steels.

Peroxide acted as a corrosion inhibitor for both carbon and stainless steels. Corrosion rates at 95°C and pH 4.0 were > 1.6 vs 0.010 mil/hr for high-carbon ball bearings and 0.32 vs 0.001 mil/hr for type 440C stainless ball bearings, without vs with 0.3 *M* H_2O_2. Aluminum corroded at 0.12 to 0.24 mil/hr in oxalate-peroxide solutions at 95°C. Several commercial corrosion inhibitors were without effect on mild steel in peroxide mixtures.

Liquid spray decontamination in the EGCR charge and service machines was simulated by the use of a modified household dishwasher.[1] Fifty-four coupons of carbon steel, type 347 stainless steel, and aluminum were contaminated with eight pure fission products and with mixed fission products by a drying and baking technique, washed with hot water, gamma-counted, and then exposed for 90 min in the washer at 75 to 90°C with 0.3 *M* $(NH_4)_2C_2O_4$ + 0.28 to 0.36 *M* H_2O_2, and to the same solution with 0.1 *M* citrate, at pH 4.1 to 4.4. Nearly all test coupons were decontaminated by factors of 10^3 to 10^5.

Steam sprays containing oxalic or nitric acid with added H_2O_2 decontaminated samples of stainless steel gas loop piping exposed to UO_2 in the LITR and contaminated with I^{131}, Ru^{103}, and Ce^{141}. Decontamination factors were; gross, 65; ruthenium, 100 to 180; iodine, 75 to 130; and cerium, 120 to 140.[2]

Homogeneous reactor scale was dissolved from a rupture disk of the HRT by Deoxidine 170, a proprietary inhibited phosphoric acid metal cleaner. Ruthenium and niobium were then removed by alkaline $KMnO_4$ and oxalic acid–H_2O_2 solutions. The total decontamination factor was 330, from an initial activity level of 200 r/hr at 1 ft. The remaining activity, as judged from a gamma-spectrometer scan, was due to Co^{60} from neutron activation of the steel.

A mixture of 1% (0.3 *N*) H_2SO_4 and 1% (0.3 *M*) H_2O_2 was a good decontaminant for 347 stainless steel, and the addition of 0.1 *M* NaF greatly enhanced the effect.[2] The peroxide essentially prevented corrosion in either case (0.001 and 0.002 mil/hr). Comparisons between these and many other decontaminating solutions showed mixtures of oxalates and oxalic acid to be generally superior. Fluoride (0.2 *M*) in the oxalate-peroxide mixture at pH 4.0 was extremely corrosive to mild steel, however (136 mils/hr at 95°C).[1]

A literature review on equipment decontamination was completed.[3]

---

[1] *GCR Quart. Progr. Rept. Mar. 31, 1961* (in press).

[2] A. B. Meservey, *Decontamination of EGCR Components*, ORNL CF-60-12-37 (Dec. 9, 1960).

[3] A. B. Meservey, *Procedures and Practices for the Decontamination of Plant and Equipment*, ORNL CF-60-12-71 (Jan. 17, 1961) (to be chapter in *Progress in Nuclear Energy Series IV*, Pergamon).

9. HRP THORIA BLANKET DEVELOPMENT[1]

9.1 PREPARATION OF ThO_2 PELLETS

Study of methods for preparing thoria pellets for use as a stationary water-cooled blanket for an aqueous homogeneous reactor was continued. Rounded pellets of good integrity could not be consistently prepared by pressing and sintering, primarily because of strains produced by the pressing operation. Efforts to coat pellets with attrition-resistant materials were only moderately successful. Most of the effort was expended on adapting the sol-gel process (Chap. 10) to produce dense, rounded, attrition-resistant pellets for aqueous homogeneous reactor use.

Preparation of Pellets by Pressing and Sintering

In preliminary tests the tendency of ThO_2 to crack was considerably lessened by increasing the pour density of the original powder by either precalcination or prepressing and regranulation (Table 9.1). In some cases annealing the pellets at 1200 to 1300°C before the final sintering at 1750°C decreased cracks in the final pellets. A considerable improvement was also made by minimizing the curvature of the punch faces to provide a more even pressing pressure across the pellet.

Preparation of Pellets by Sol-Gel Process[2]

Since the thoria-urania gel fragments prepared in the Fuel Cycle studies (Chap. 10) were of nearly theoretical density and appeared to be very hard and strong, 10 fragments, containing nominally 5 wt % uranium and having approximately the shape and size desired were subjected to six successive 1-hr spouted-bed attrition tests. Losses for successive hours were 2.13, 0.88, 0.68, 0.96, 1.13, and 0.28 wt %. Microscopic examination showed no degradation by cracking; weight losses were due to grinding off of edges and sharp points. The surface area determined by nitrogen adsorption was lower than the limit of detection for a 10-g sample.

Ten samples of ThO_2 fragments containing 5 wt % uranium and four pure ThO_2 gel fragments representing four size fractions, +4, −4 +10, −10 +12, and −12 U.S. sieve mesh, and five variations in sol preparations were submitted to the Reactor Chemistry Division for evaluation, mainly for resistance to attrition. Since there had been no effort to round these fragments in the sol stage of preparation, some of the fragments were very irregular, and many had cracks, sharp edges, and points. The initial unsized preparations were ground in a violently agitated spouted bed to round them and to break cracked particles down to an ultimate uncracked size.

Several attempts to prepare rounded, fired thoria gel particles by forming in a thickened sol stage were unsuccessful because of the strains induced by the large (3 to 8) shrinkage factor sustained from the forming to the final calcination step. In one approach sols were evaporated to a thixotropic paste and cast into a graphite mold or extruded. The formed gels were evaporated in air at 70°C, in vacuum at 25 and at 40°C, and in steam. All specimens cracked into at least four pieces.

Loading of sols with ThO_2 derived from oxalate precipitation and calcination at various temperatures or with nitrate-dispersed and evaporated ThO_2 gels in order to decrease shrinkage on evaporation and firing also failed to produce a large percentage of integral particles. Most of these preparations cracked in the evaporation step.

Firing of thoria gels in hydrogen unexpectedly produced a consistent small increase in density over firing in air in the temperature range 825 to 1255°C. Firing of thoria or thoria-urania gels in hydrogen or air at 1150 to 1200°C gave a consistent small increase in density over firing at 1200 to 1250°C.

[1] Details are reported in HRP progress reports, e.g. for May 31, 1961, ORNL-3167.

[2] S. D. Clinton *et al.*, *Preparation of High-Density Oxides and Vibratory Compaction in Fuel Tubes*, ORNL-2965 (Jan. 27, 1961).

Table 9.1. Effects of Variations in Fabrication Procedure on Density, Cracking, and Attrition Resistance of ThO_2 Pellets

Final calcination temperature: 1750°C for 4 hr

Pour Density of Powder Grains (g/cc)	Pellets Heated 1.5 to 2 hr at 1200 to 1300°C	Avg Fired Density of Pellets (g/cc)	Samples with Visual Cracks (%)	Attrition Rate (%/hr)
2.14	No	8.84	67	1.02
	Yes	8.74	33	0.86
2.42	No	8.50	67	1.12
	Yes	8.89	0	0.91
2.48	No	8.82	67	1.41
	Yes	8.80	0	0.90
2.50	No	8.73	67	0.34
	Yes	8.74	0	0.30
2.65	No	9.03	67	0.46
	Yes	9.15	0	0.36
2.77	No	9.29	0	0.27
	Yes	9.34	16	0.55

Coating of ThO_2 Pellets with Metals and Oxides

The feasibility of coating ThO_2 pellets with nickel, chromium, Al_2O_3, Ta_2O_5, ZrO_2, or TiO_2 by the plasma jet apparatus was studied. Powders of –325 mesh, fluidized by argon or argon-hydrogen mixtures, were passed through the arc and deposited on the pellets held in the jet stream 3 to 5 in. from the hot exit. The arc was struck in argon or argon-hydrogen at 25 volts and 325 or 700 amp. At the higher power settings, pellets were successfully coated.

Only the nickel-coated pellets, which had been post-annealed at 1200°C in hydrogen, showed greater resistance to attrition in the spouting bed test than did the original thoria pellet. In the first two of six successive 1-hr tests the nickel-coated pellets showed weight losses of 0.07 and 0.04% per hour. After the third hour, the coat came off the pellet, evidently sheared at sharp edges.

9.2 DEVELOPMENT OF GAS RECOMBINATION CATALYST

Work on the development of a catalyst for use in aqueous oxide slurries to recombine radiolytic gas continued with a re-evaluation and recalibration of the gas-injection apparatus and further studies with slurries containing the sol-prepared palladium catalyst.

Gas-Injection Apparatus

Experiments in the gas-injection apparatus indicate that sol-prepared palladium catalyst in thorium-urania slurries is an acceptable recombination catalyst for radiolytic gas produced in a 10-kw/liter power density blanket for a thermal breeder.

Recalibration of the gas-injection equipment showed a significant holdup of gas in the capillary tubing connecting the gas-charging system to the reaction autoclave, which led to several erroneous conclusions as to the activity and properties of the palladium catalyst being used in the gas recombination work. The holdup volume between the pressurizable gas burette and the reaction autoclave had been estimated at 0.92 ml, 0.36 ml in the capillary tubing between the gas burette and the charging valves, and 0.56 ml in the capillary between the charging valve and the reaction autoclave. The data suggest that the holdup volume is probably closer to 1.1 ml. Re-evaluation of the gas

recombination data as a result of the recalibration indicates that there is little or no deactivation of the catalyst under excess oxygen, reaction is obtained even at very low hydrogen partial pressures, combination of the oxygen and hydrogen in the reaction vessel is complete, and the solubilities of both oxygen and hydrogen in the slurry catalyst system are consistent with those predicted from the Henry law constants obtained at both BMI[3] and ORNL.[4] The enhanced catalytic activity in the presence of excess hydrogen may indicate a different kinetic process than that which applies on the oxygen-rich side.

Palladium Catalysis

Further work on the sol-prepared palladium catalyst indicated a catalytic activity more than sufficient to recombine the radiolytic gas (at 100 psi D_2 partial pressure) produced in a blanket slurry at the 10-kw/liter power level expected in a breeder blanket. The rate dependence on the deuterium (hydrogen) partial pressure was first order and on the oxygen partial pressure was 0.5 order in systems containing excess oxygen. The work, which was done in support of the in-pile slurry corrosion studies being made by the Reactor Chemistry Division, was carried out on samples of pumped Th–0.4% U^{235} oxide slurry from preoperational testing of the in-pile slurry loop (L2-26S-6-4)[5] and of slurries containing the Th–12.4% U^{235} oxide projected for the next in-pile autoclave slurry-corrosion experiment.

Th–0.4% U^{235} Oxide Slurry.—The slurry from the in-pile loop contained 483 g Th/kg D_2O, 0.4% uranium oxide, and 640 ppm Pd/Th of the palladium catalyst. It had been pumped several hundred hours under oxygen and subjected to deuterium-oxygen reaction tests at 280°C during the loop operations. In two series of experiments with this slurry in which the initial oxygen partial pressure was held constant at 215 and 353 psi, an excess of oxygen, the initial reaction rate showed first-order dependence on the deuterium partial pressures up to D_2/O_2 ratios of about 1 (Fig. 9.1). In a third series of experiments at 280°C the initial deuterium partial pressure was held within a narrow range, 35 to 100 psi, and the initial reaction rate showed a probable 0.5-order dependence on the oxygen partial pressure between 113 and 765 psi (Fig. 9.2). The rate data plotted as initial reaction rate divided by the initial hydrogen partial pressure vs the 0.5 power of the oxygen pressure was a fairly good linear fit. These experiments were carried out prior to the calibration experiments and corrections were made for the calculated amounts of the gases held up in the tubing. The apparent decrease in rate with increasing oxygen pressure (Fig. 9.1) and the fact that the rate data obtained at a constant oxygen partial pressure of 215 psi do not extrapolate to zero at zero deuterium partial pressure probably result from inaccuracies introduced by the calculated corrections.

Th–12.4% U^{235} Oxide Slurry.—Data obtained with the slurry to be used for in-pile corrosion studies in autoclaves indicate that the catalyst will maintain the partial pressure of D_2 at $\leq$100 psi at 280°C. The slurry contains 782 g Th/kg D_2O of the Th–12.4% U^{235} oxide and 1460 ppm Pd/Th of the sol-prepared palladium catalyst. The power density in the LITR will be about 26 watts/ml. In two series of experiments with this slurry the initial reaction rates were correlated by a kinetic expression involving a first-power dependence of rate on the deuterium partial pressure and a 0.5-power dependence on oxygen partial pressure. In one series the slurry contained 68 g Th/kg D_2O of the Th–12.4% U^{235} oxide and 154 ppm Pd/Th, and in the other, 86.3 g Th/kg D_2O of the oxide plus 1460 ppm Pd/Th catalyst. Prior to use in the recombination studies, the first slurry was heated in O_2 (600 psi above steam) at ~280°C for 68 hr and the second for 3 weeks.

A limited number of experiments were made with the first slurry at 700 psi O_2 and 62 to 108 psi D_2 initial pressure. The reaction rate constant was obtained from the slope of the plot of $(dP/dt)/p_{O_2}^{0.5}$ vs p_{D_2} (Fig. 9.3). The average CPI (catalyst performance index) at 280°C of 1.2 watts/ml for the dilute slurry indicates a CPI >100 watts/ml for the in-pile slurry, assuming linear dependence of catalytic activity on catalyst concentration. The CPI is the specific power generation rate, in watts per milliliter, that will produce

[3] H. A. Pray, C. E. Schweickert, and B. A. Minnich, *Ind. Eng. Chem.* 44, 1146 (1952); also BMI-T-25, May 15, 1960.

[4] H. F. Soard, *Solubility of Oxygen and Hydrogen in Thorium Oxide Slurries*, ORNL CF-60-3-153 (Mar. 25, 1960).

[5] E. L. Compere *et al.*, *HRP Quart. Progr. Rept. Apr. 30, 1960*, ORNL-2947, p 107.

a steady-state D_2 partial pressure of 100 psi at the stated temperature and O_2 partial pressure. It is obtained by dividing the combination rate produced by the catalyst at 100 psi of D_2 by the rate of D_2 formation at a power density of 1 watt/ml.

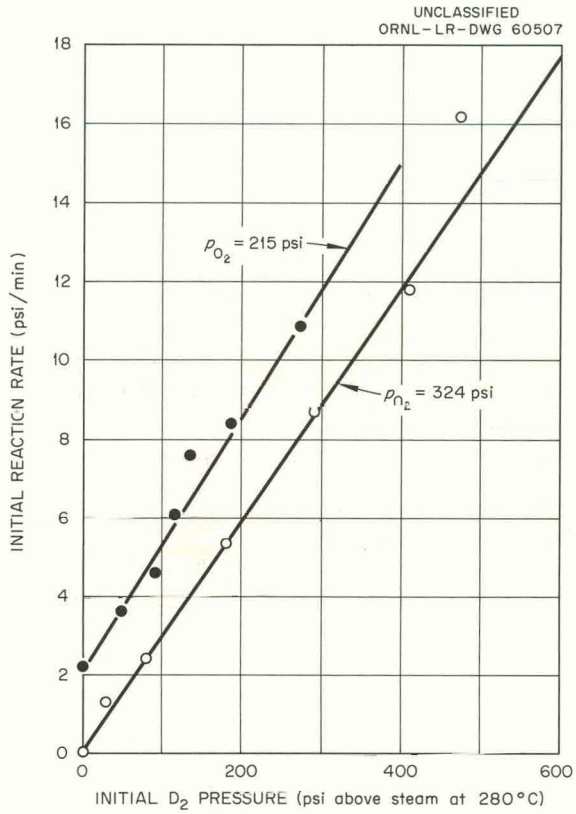

Fig. 9.1. Initial Reaction Rates of D_2-O_2 Mixtures in Aqueous ThO_2–0.5% U Oxide Slurries for Constant Initial Oxygen Pressures at 280°C.

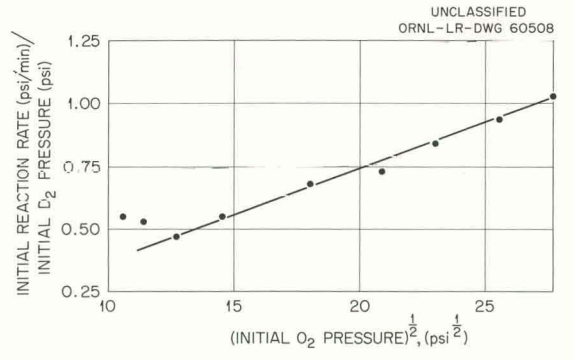

Fig. 9.2. Reaction Rates of D_2-O_2 Mixtures in Aqueous ThO_2–0.5% U Slurry Containing Palladium Catalyst at 280°C. P_{O_2} = 161 to 765 psi above steam; P_{D_2} = 35–100 psi above steam.

For the second slurry the initial reaction rate at 280°C was studied as a function of the initial O_2 partial pressure from 200 to 800 psi and a constant D_2 partial pressure of about 110 psi. The plot of $(dP/dt)/p_{D_2}$ vs $p_{O_2}^{0.5}$ (Fig. 9.4) was linear and the CPI at 280°C and 700 psi O_2 was 6.8 watts/ml, indicating a CPI >60 watts/ml for the in-pile experiment. When the reaction rate was measured at only 200 psi O_2 and 280°C, the first reaction proceeded at a measurable rate, but in the next two

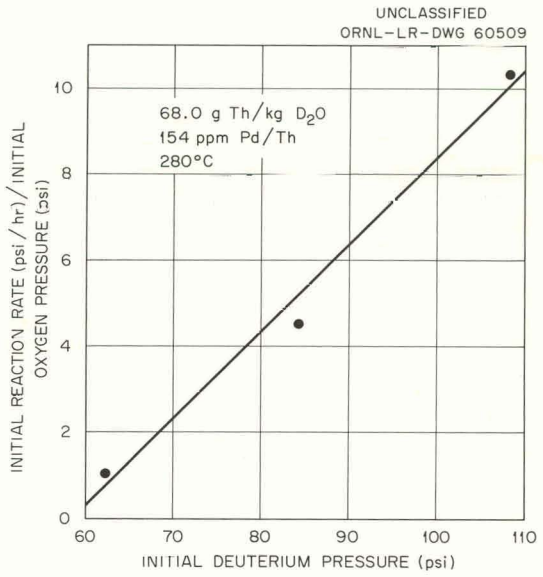

Fig. 9.3. Effect of Deuterium Partial Pressure on Recombination Rates in Thorium–12.4% Uranium Oxide Slurry.

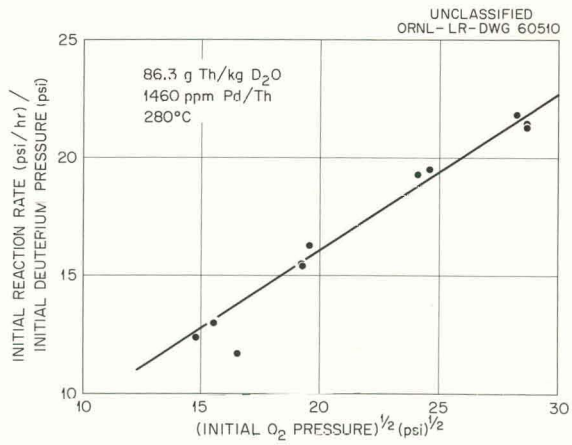

Fig. 9.4. Effect of Oxygen Partial Pressure on Recombination Rate in Thorium–12.4% Uranium Oxide Slurry.

experiments the D_2 reacted as rapidly as it was charged. The series was repeated with the same results. This may indicate that the catalytic activity is enhanced at low O_2 partial pressures or low O_2/D_2 ratios. This enhancement of catalytic activity at low O_2 partial pressures is also seen in the data of Fig. 9.2.

9.3 THORIUM OXIDE IRRADIATIONS

Thoria Pellet Irradiation

A 2900-hr irradiation in the LITR at 250°C and a thermal flux of $\sim 2 \times 10^{13}$ n cm^{-2} sec^{-1} of a settled bed of 50 thoria pellets in D_2O (Exp. C-43-2) was completed. The pellets were prepared by treating 1400°C-fired Davison Chemical Company pellets with dibasic aluminum nitrate and refiring at 1750°C. When the irradiation autoclave was opened, 20 of the pellets were found[6] to have broken into fragments and fines. The remainder had essentially the same bulk and pycnometric densities as the original material (Table 9.2) but showed damage from surface chipping and breaking off of spherical segments (Fig. 9.5a). All surfaces were porous. A carbonaceous, black, apparently vitreous, substance, about 1 wt % of the recovered solids, was found in the upper half of the irradiation autoclave (Fig. 9.5b). Pellets removed from a parallel laboratory control experiment showed no apparent damage and no evidence of the black vitreous material. These pellets are inferior to those now being manufactured, and the radiation effect, while real, may not necessarily be so severe for the best thoria pellets now available.

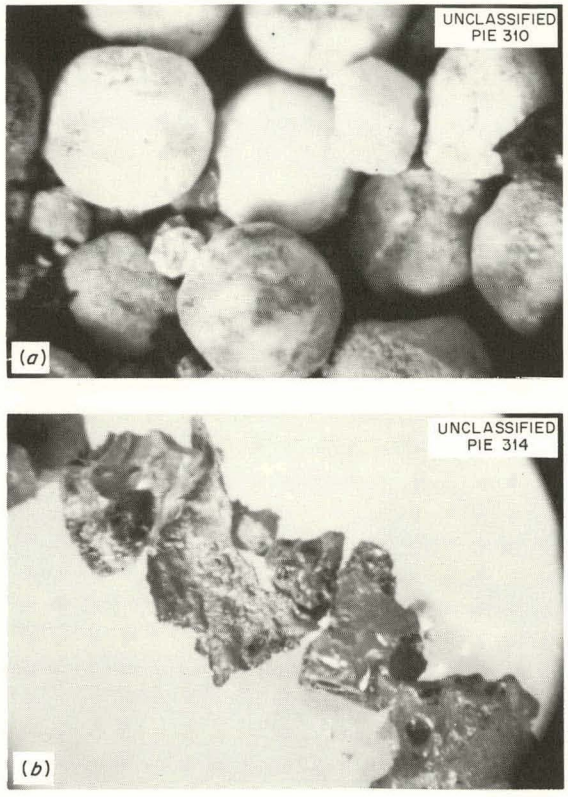

Fig. 9.5. (*a*) Irradiated Thoria Pellets and (*b*) Carbonaceous Material Found in Thoria Pellets Irradiated Wet.

[6] R. E. McDonald, Post-Irradiation Examination Group, Metallurgy Division, ORNL.

Table 9.2. Thoria Pellet Irradiation Data

Pellets irradiated 2900 hr in D_2O at 250°C and 2×10^{13} $n/cm^2 \cdot sec$

Pellets	Avg wt (g)	Avg Vol (cc)	Thorium Content (%)	Aluminum Content (%)	Bulk Density (g/cc)	Pycnometric Density (g/cc)	Surface Area (m^2/g)
Unirradiated	0.43	0.060	86.4	0.54	7.2		<0.1
Control	0.43	0.059	87.1	0.54	7.3	9.2[a]	<0.1
Irradiated	0.38	0.056			6.8	8.5[b]	

[a] Measured pycnometrically in water after drying at 110°C. A pycnometric density measurement on the control pellets before drying showed a density of 9.7 g/cc, indicating that heating at 250°C had resulted in filling with water pores not ordinarily filled during the usual density measurements made at room temperature.

[b] By weighing in air and then in water to constant weight.

Analysis of the black vitreous deposit indicated >76% volatile matter; it was identified spectrographically as carbonaceous and had a density of 1.18 g/cc. It contained 0.23% thorium, 0.07% iron, 0.07% uranium, and some fission product activity. The source of the material was probably a carbon residue from the polyvinyl alcohol binder used in the pellet fabrication and not removed by the 1750°C firing, but repeated analyses of the unirradiated pellets did not show sufficient carbon to account for the amount of material found in the irradiation autoclave.

Slurry Irradiations

A D_2O slurry of classified thorium–0.4% U^{235} oxide (DT-22) was irradiated 5 weeks at 280°C in the LITR to a total nvt of 5×10^{19} n/cm^2 to determine the effect of reactor irradiation on particle integrity. Twelve percent of the irradiated material (initially 2.1 μ in average size and 0.5% <1 μ) was recovered as a dispersed suspension with an average particle size of 2500 A (Fig. 9.6). A portion of the material (≧6%) that had settled to the bottom of the autoclave and been resuspended by stirring had an average size of 1.6 μ but a very steep size distribution curve. The bulk of the irradiated material settled on the bottom of the autoclave and was not readily resuspended by stirring. A laboratory control experiment in which part of the same slurry batch was subjected to identical temperature, pressure, and agitation yielded a slurry of an average particle size of 1.8 μ, with 10% <1 μ (Fig. 9.7). Apparently the control slurry was also degraded by high-temperature water, possibly releasing fines held on the classified solids which were not dislodged by the dispersing

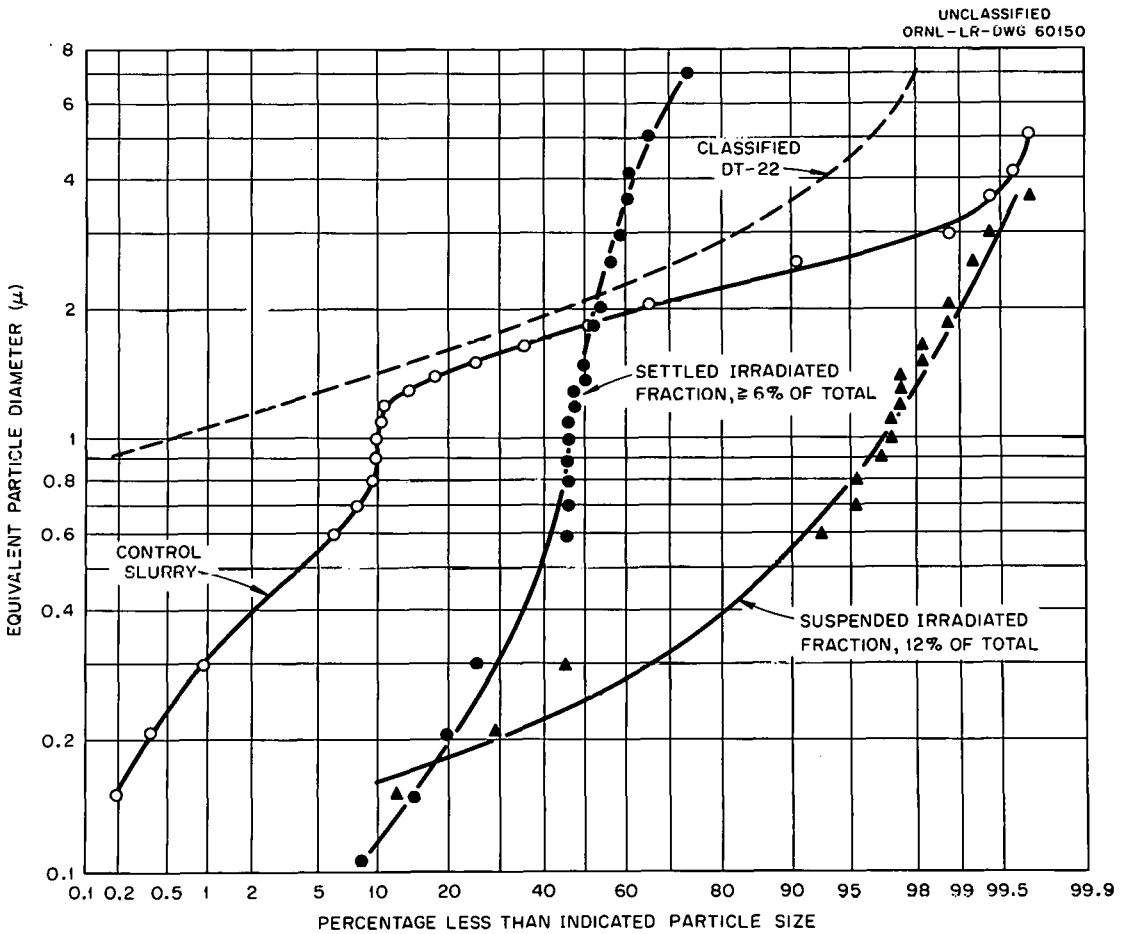

Fig. 9.6. Particle Size Data on Irradiated Thoria-Urania Slurry. Th–0.4% U^{235} Oxide (DT-22); total nvt = 5×10^{19} n/cm^2.

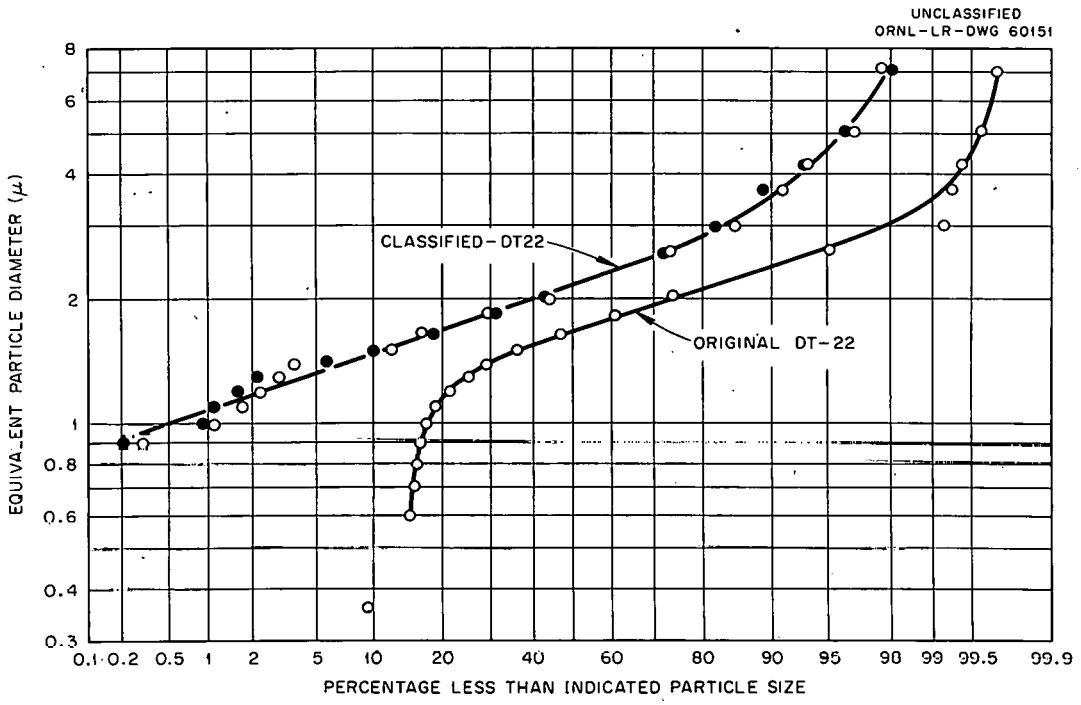

Fig. 9.7. Classification of Thoria-Urania Powder for Reactor Irradiation Damage Experiments.

agent (0.001 *M* $Na_4P_2O_7$) used in the particle size analysis.

The irradiation was carried out in a stainless steel autoclave with the slurry (1 g of solid per 7 ml of D_2O) in a settled condition. An overpressure of 100 psi of O_2 and 700 psi of helium was added at room temperature. No radiolytic gas pressure was observed during the experiment.

The mixed oxide used in the experiments was a portion of the oxide used in the in-pile slurry loop experiment.[7] It had been carefully classified to remove particles less than 1 μ by elutriation with oxalic acid at pH 2.6 and then with ammonium hydroxide at pH 10.5, the solid being washed with water in between and on completion of the classification. The classified oxide was fired at 650°C to remove adsorbed materials. The classified solids contained 87.0% thorium and had a U/Th ratio of 0.0044 and a specific surface area, measured by nitrogen adsorption, of 2.1 m^2/g. Before classification the surface area was 2.5 m^2/g.

[7] E. L. Compere, H. C. Savage, *et al.*, *HRP Progr. Rept. Aug. 1 to Nov. 30, 1960*, ORNL-3061, p 89.

[8] *Fluid Fuel Reactors*, ed. by J. A. Lane, H. G. MacPherson, and F. Maslan, Addison-Wesley, Reading, Mass., 1958, p 180.

Particle Damage by Reactor Irradiation

Data obtained in 55 slurry irradiations and a few dry thoria powder irradiations in the LITR over the last several years are being assembled in preparation of a progress report on these studies. A review of the particle size information (Table 9.3) suggests not only pronounced particle damage in some cases but also greater resistance of some oxide preparations to radiation damage than others. The damage observed in the wet irradiations as opposed to the apparent stability demonstrated by the dry oxide in tests carried out here and elsewhere suggests a radiation-water-solid interaction, but definitive comparisons between wet and dry tests have not yet been made.

The slurry irradiations were carried out primarily to determine whether or not there was gross deterioration of slurry behavior under reactor irradiation rather than to assess particle damage as such. The particular slurry investigated in each case was selected as the best available at the time of the irradiation experiment. All slurry irradiations were made in a dash-pot stirred stainless steel autoclave at 280°C;[8] the principal information obtained was whether or not the slurry could be stirred while under irradiation. Although the stirrer degraded

Table 9.3. Particle Size Effects in Reactor-Irradiated Slurries

Temperature: 280°C

Flux: $\sim 2 \times 10^{13}$ n/cm^2·sec

Exp. No.	Slurry Solids	Slurry Conc. (g Th/kg H_2O)	Irradiation Time (hr)	Stirring[a] Time (hr)	Solids[b] Recovered (%)	Average Particle Size, Microns		% Less Than 0.7 Micron		Fractional Increase In Percent Less Than 0.7 Micron, Irradiated/Unirradiated	Refs.[d]
						Unirradiated[c] Solids	Irradiated Solids	Unirradiated[c] Solids	Irradiated Solids		
3	650°C-fired ThO_2	500	258	120	(67)	2.0	<0.7	11	64	6.1	4, 5
5	900°C-fired ThO_2	500	175	12	(79)	(1.1)	0.9	(32)	37	1.2	5
8	650°C-fired ThO_2	500	165	165		2.0	1.7	11	31	2.9	5, 6
9	1600°C-fired pumped ThO_2	500	200	200	(73)	0.8	0.6	43	53	1.3	5, 6
17	900°C-fired Th–0.5% U-235 Oxide	1000	92	9	28	2.0	1.0	11	34	3.1	7, 8
21	900°C-fired Th–0.4% U-235 oxide	750	168	168	52	(0.9)	1.9	(17)	31	1.8	8, 10
26	900°C-fired ThO_2	750	198	198	33	0.8	0.8	40	47	1.2	9, 10
27	800°C-fired ThO_2	750	344	344	21	(2.0)	3.4	(15)	24	1.6	9, 10
33	1600°C-fired pumped ThO_2	500	336	320	(21)	(1.3)	1.3	(16)	16	1.0	11
38	1000°C-fired Th–0.4% Nat U Oxide	750	332	62	(50)	(0.8)	0.6	(44)	60	1.4	12, 13
40	1300°C-fired Th–0.4% U-235 Oxide	500	322	322	55	(1.7)	1.5	(32)	23	<1.0	13
44	1000°C-fired Th–4% Nat U Oxide	750	49	49	76	1.1	0.8	10	40	4.0	13, 14
46	1000°C-fired Th–4% Nat U Oxide	500	361	361	97	1.1	1.0	10	34	3.4	13, 14
47	1000°C-fired Th–4% Nat U Oxide	250	354	354	65	1.1	1.1	10	32	3.2	13, 14
48	1000°C-fired Th–4% Nat U Oxide	250	310	310	(14)	1.1	0.4	9	73	8.1	14, 15
49	1000°C-fired Th–4% Nat U Oxide	250	350	350		1.1	3.0	9	34	3.8	14, 15
54	1050°C-fired Th–8% Nat U Oxide	250	335	335	74	1.3	2.0	4	18	4.5	16, 17
55	1050°C-fired Th–9% Nat U Oxide	500	370	370	28	1.3	0.6	4	56	14	17

[a]Under Irradiation

[b]Values in parentheses estimated from settled volumes of recovered solids assuming constant settled density for all irradiated solids; others are based on Th analyses.

[c]Values in parentheses are those obtained on the solids from a control experiment; others are from the original solids.

[d]References: 4. ORNL-1943, 5. ORNL-2004, 6. ORNL-2057, 7. ORNL-2096, 8. ORNL-2148, 9. ORNL-2222, 10. ORNL-2272, 11. ORNL-2432, 12. ORNL-2493, 13. ORNL-2561, 14. ORNL-2654, 15. ORNL-2696, 16. ORNL-2743, 17. ORNL-2879

particles, particularly those larger than 1 μ, making particle size data difficult to interpret quantitatively, some experiments in which material recovery was good and particle size analyses of the irradiated material reasonably self-consistent can be qualitatively interpreted. They indicate that thorium oxide fired at 650 to 800°C is less resistant to particle damage by reactor irradiation than that fired at 900 to 1600°C, and that 200 and 330 hr irradiation of 1600°C-fired oxide causes little damage. Mixed thorium-uranium oxides containing 0.5% U^{235} did not appear to be degraded much more than those containing 0.5% natural uranium, and a 1300°C-fired Th–0.5% U^{235} oxide suffered little or no particle damage in 320 hr irradiation. Mixed thorium-uranium oxides containing 5 to 8% natural uranium showed pronounced damage, but comparison with that occurring in thorium oxide or thorium–0.5% U^{235} oxide slurries indicates that the damage may be an effect of the preparation method.

Apparent discrepancies in which large increases in the fractions of material less than 0.7 μ are accompanied by little or no change, and sometimes by an increase in average sizes, resulted from agglomeration of some of the solids when particle damage was pronounced.

10. FUEL CYCLE DEVELOPMENT[1]

Because of the radioactivity associated with thorium and U^{233} recycled from power reactors, it is highly desirable to develop fuel fabrication procedures that are simple and easily adaptable to remote operation behind shielding for reasons of economy. Vibratory compaction of thorium oxide fuel into preassembled tube bundles appears to be such a technic. This method requires oxide particles of high density and controlled particle size. The sol-gel process for making oxide particles and vibratory compaction into fuel tubes are being investigated as a joint program of the Chemical Technology and Metallurgy Divisions. The sol-gel process, which is based on the fact that drying and calcination of a thoria hydrosol produces large, near theoretical density, particles of ThO_2, consists of four major steps: preparation of ThO_2 from thorium nitrate, dispersion of the oxide to a hydrosol, drying of the sol to produce a gel, and calcination of the gel to the oxide.

10.1 SOL-GEL PROCESS FOR ThO_2-UO_2 AND ThO_2

Of various methods considered for preparing the precursor oxide – calcination of thorium oxalate, precipitation of hydrous thoria, peroxide precipitation of thorium peroxide-nitrate, or thermal denitration of thorium nitrate – flowsheet development was concentrated on hydrothermal denitration of thorium nitrate which appeared to offer the best compromise of process simplicity, low cost, and desirable product properties. In this method (Fig. 10.1) thorium nitrate is hydrolyzed in flowing steam at about 390°C and 1 atm pressure to give a thoria powder containing 4 to 5% residual volatile matter and a N/Th mole ratio of 0.13 to 0.15. The powder is dispersed in water to form a stable sol 2 *M* in thorium. The sol is aged at least 14 hr under reflux boiling, and uranium is then added as ammonium diuranate, hydrated uranium trioxide, or uranyl nitrate. The sol formed is evaporated to dryness at 70°C, yielding gel fragments of millimeter size which are precalcined on a 100°C per hour rising temperature schedule to 500°C. Final calcination is in air at 1200°C for 4 hr, and in hydrogen also at 1200°C for 4 hr if the oxide contains uranium.

Two kilograms of thoria-urania particles (Fig. 10.2*a*) containing 4.4 wt % enriched uranium prepared by this process had a particle density of

[1] Details reported in Fuel Cycle Development progress reports, e.g. ORNL CF-60-11-56 for Sept. 30, 1960; ORNL-3992 for March 31, 1961.

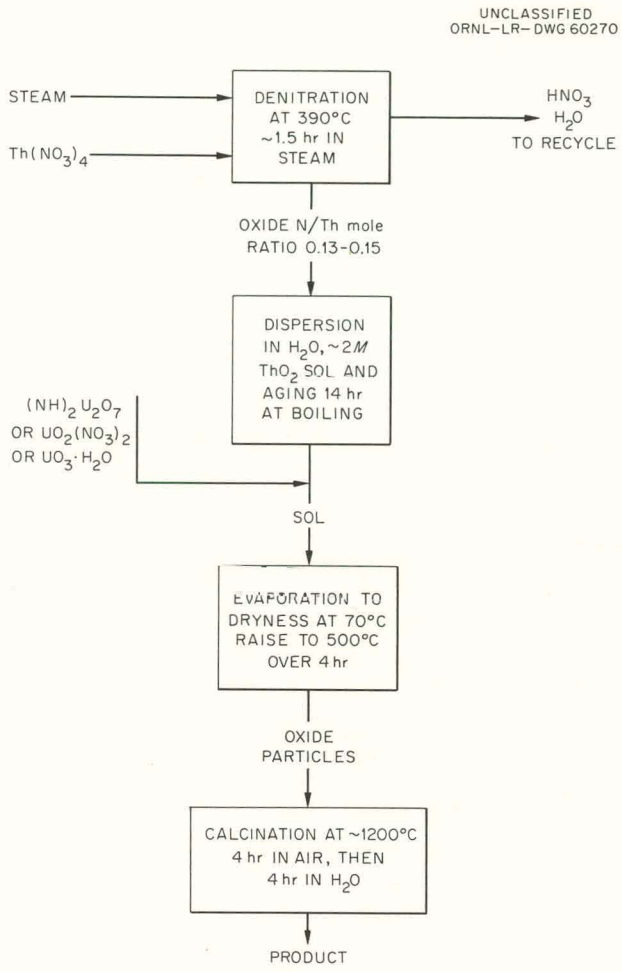

Fig. 10.1. Schematic Flowsheet for Mixed Oxide Preparation by the Sol-Gel Process.

9.93 g/cc compared to the maximum theoretical of 10.035 g/cc. It was vibratorily compacted by the Metallurgy Division to beds of 8.7 g/cc bulk density in eight $\frac{1}{4}$-in.-dia by 11-in.-long tubes and placed in the NRX reactor in March. They are scheduled for removal in August. The maximum particle density attained with similar arc-fused oxides is 8.9 g/cc.

Thoria particles (Fig. 10.2*b*) were prepared similarly.

On an engineering scale the compositions of products prepared by steam stripping of $Th(NO_3)_4$ in an agitated trough were the same as those of laboratory products when steam rates were high, steam pressures were slightly above atmospheric to avoid air inleakage, and the temperature was carefully controlled. About 9 kg of this product was easily dispersed as a sol and a sample was dried, calcined, and vibrated to 8.4 g/cc in a tube. Products that had been overstripped were dispersed as sols by addition of nitric acid. More than 99% of the nitrate released from the $Th(NO_3)_4$ was collected in the spray condenser water. About one-third of the thorium was entrained in the off-gas as incompletely stripped material, and a scaled-up rotary calciner is being designed to minimize this and other operating problems.

Six runs under identical conditions were made in the agitated trough denitrator to prepare product of N/Th mole ratio of 0.05 to 0.10 for sol dispersion-drying-clacining studies. The N/Th ratio alone does not consistently determine whether dispersion into a sol will occur or what the sol properties will be, but the density of the final product particles seemed to increase as the sol N/Th mole ratio decreased. Products of 9.72 to 9.88 g/cc as measured by toluene immersion were compacted to 8.4 or 8.5 g/cc in $\frac{5}{16}$-in.-dia tubes in tests conducted by the Metallurgy Division.

Properties of Calcined Fragments. – The gel property having the most effect on oxide particle size and density is the residual nitrogen content. Increasing the nitrogen content decreased the final oxide particle size, and decreasing it below a critical level, characteristic of the kind of thoria being dispersed, resulted in particle inhomogeneity and a decrease in particle density. Secondary influences, in approximate order of importance, were sol aging, initial thoria crystallite size, uranium content if below 10%, sol drying rate, and drying dish geometry.

Particle size and density depended markedly on the calcination procedure. It is preferable, however, to exercise size and density control in earlier steps because the effects of calcination are inherently irreversible. The precalcination procedure removes volatile matter that would shatter a gel placed directly in the 1200°C furnace. If the gel is placed on a continuous schedule to 1200°C instead of being abruptly shifted from 600 to 1200°C, particle density is lowered, typically about 5%. The removal of excess oxygen above $UO_{2.000}$ in mixed thoria-urania samples appears to be consistent with the assumption of oxygen diffusion being the rate-limiting step with about 27 kcal/mole activation

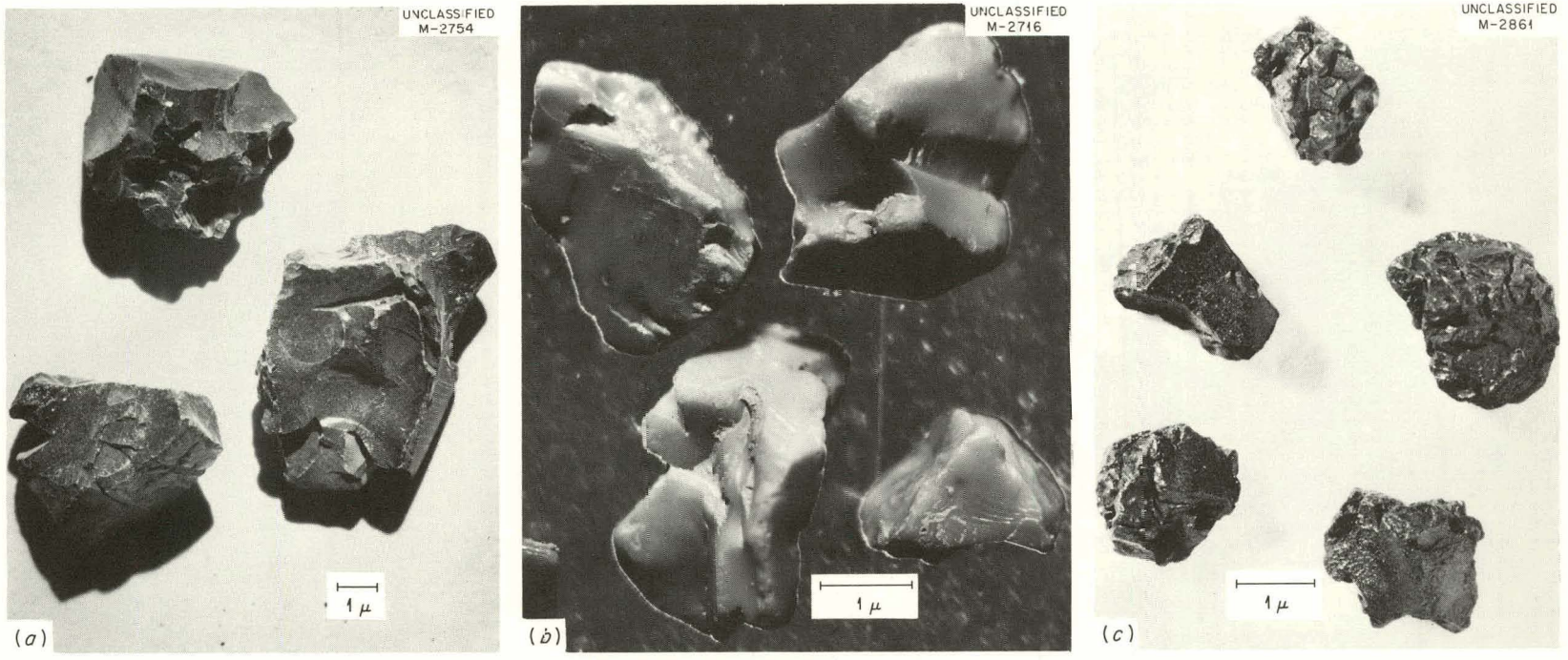

Fig. 10.2. Oxide Particles Produced by Calcination of Gels Formed from Nitrate Sols. (*a*) Thorium–5 mole % uranium oxide and (*b*) thorium oxide produced from gels formed from nitrate sols; (*c*) UO_2 procuced from hydrous urania prec pitated from uranous formate.

energy, which agrees with the value of the activation energy for diffusion of oxygen in urania.[2]

Particle size distribution with respect to weight was measured by sieving. The largest modal size reported is 4 mm (Table 10.1), but fragments of the order of 1 cm dia were made in > 25% yield. Particles smaller than 0.2 mm average size were made but not examined in detail. Densities measured pycnometrically in toluene, agitated to remove superficial air but not vacuum outgassed, give a reasonable estimate of effective particle density for packing purposes. X-ray data showed that the oxide fragments are polycrystalline rather than true amorphous glasses despite their vitreous appearance and conchoidal fracture. It is thought that the wide scatter of x-ray crystal size data is related to strain-broadening of the diffraction pattern since fine-grinding of samples caused apparent increases in x-ray crystal size.

10.2 MODIFIED SOL-GEL PROCESS FOR UO_2

A few small samples of urania (Fig. 10.2*c*) made by a modification of the sol-gel process for thoria and thoria-urania had particle densities of 10.6 g/cc compared to 10.97 g/cc theoretical maximum and an average particle size of 0.8 mm compared to 1.2-2.0 mm required for the coarse-fraction particles in vibratory compaction. The modification consisted in precipitating hydrous urania from uranous formate with a 50-50 volume mixture of concentrated aqueous ammonia and 85% aqueous hydrazine. The precipitate was centrifuged, washed with deoxygenated water, and dried at 25 to 45°C under 20 to 25 in. vacuum. The dried gel was fired in a hydrogen atmosphere on a uniformly rising temperature schedule to 450°C in 5 hr, and then placed in an argon-flushed furnace preheated to 1100°C and calcined for 2 hr in a current of hydrogen. The dried gel and the prefired oxide were intensely black and had a high vitreous sheen, but the 1100°C fired fragments had a graphite-like sheen and were dark brown. Coarse, closed voids appear to have been blown into the fragments by the vacuum drying step, resulting in toluene densities of 10.5 g/cc without outgassing and 10.6 g/cc with vacuum outgassing compared to the theoretical maximum density of 10.97 g/cc. The modal particle size of the sample was 1.2 mm, the average particle size was 0.8 mm, and 85 wt % exceeded 0.25 mm.

[2] J. Belle and B. Lustman, *Properties of UO_2*, WAPD-184, 1957, p 51.

Table 10.1. Properties of Thoria and Thorium-Uranium Oxides from Gels

Th Source	Oxide Composition		Final Calcination Conditions			Crystal Size (A)	Modal Particle Size (mm)	Density* (g/cc)
	U (mole %)	O/U Mole Ratio	Temp (°C)	Time (hr)	Pres (atm)			
Hydrous thoria	0		1200	1	Air	500	0.2	9.8
Thermally denitrated $Th(NO_3)_4$	0		1240	1.5	Air	1400	0.5	9.9
Calcined $Th(C_2O_4)_2$	0		1200	4	Air	1300	>1.2	9.9
Hydrothermally denitrated $Th(NO_3)_4$	4.6	2.008	1260	4	H_2	1300	>1.2	9.9
Hydrothermally denitrated $Th(NO_3)_4$	4.6	2.375	1300	5	Air	1300	>1.2	9.8
Hydrothermally denitrated $Th(NO_3)_4$	5.2		1250	4	Air		4.0	10.0
Calcined $Th(C_2O_4)_2$	10.3	2.039	1250	4	H_2	1400	1.0	9.7

*Toluene not outgassed.

The uranium trioxide–uranyl nitrate system does not form gels analogous to those of the thorium oxide-nitrate system,[3] and uranous nitrate solution[4] requires a holding reductant and cannot be heated. The uranous ion in general, and hydrous urania in particular, is very subject to air oxidation. Practical limitations of the available equipment with respect to exclusion of air led to the investigation of chemical precipitation of the gels in preference to formation by sol evaporation. In initial experiments chloride ion dispersion of UO_2 made by low-temperature calcination of uranous oxalate[5] and distillation of formic acid from uranous formate did not produce suitable fragments, probably because of excessive carbon present in the first case and air oxidation in both cases.

[3] S. D. Clinton *et al.*, *Preparation of High-Density Oxides and Vibratory Compaction in Fuel Tubes*, ORNL-2965 (Jan. 27, 1961).

[4] A. L. Slade, *Oxidation of Uranium(IV) by Oxygen and Nitrous Acid*, DP-554 (February 1961).

[5] C. C. Furnas, *The Relations Between Specific Volume, Voids, and Size Compositions of Broken Solids of Mixed Sizes*, U.S. Bur. Mines Rept. of Investigations No. 2894 (October 1929).

11. TRANSURANIUM ELEMENT STUDIES

Gram quantities of heavy-element isotopes up to Cf^{252} and smaller quantities of elements above californium are to be produced by a series of neutron irradiations starting with Pu^{239} (Fig. 11.1). Because of the large amount of heat released by fission of Pu^{239} during the early stages of this irradiation, the initial irradiation is best accomplished at a moderate flux until most of the fissionable plutonium (Pu^{239} and Pu^{241}) is consumed. The Pu^{242}, Am^{243}, and Cm^{244} formed in the initial irradiation in a large reactor will be separated from fission products and refabricated into targets for irradiation in the ORNL High Flux Isotope Reactor (HFIR) at $\sim 3 \times 10^{15}$ n cm^{-2} sec^{-1}. After irradiation the targets will be processed for recovery of curium, berkelium, californium, and small quantities of einsteinium and fermium. The curium will be recycled to the reactor for further irradiation.

The Chemical Technology Division, together with the Metallurgy Division in the work on HFIR target fabrication, is responsible for the separation process development, equipment design and specifications, facility design, construction, and operation of the following portions of the Transuranium Program:

(1) Isolation of Am^{243} and Cm^{244} from a rough rare earth–actinide cut made on the raffinate from the separation of Pu^{242} produced in the irradiation of the first batch of Pu^{239}. (The initial irradiation of Pu^{239} and the subsequent separation of Pu^{242} from the aluminum and fission products, as well as the rough separation of a concentrated americium–curium–rare earth fraction, will be done in a large reactor and chemical plant.)

(2) Dissolution, Pu^{242} separation and recovery, and Am^{243} and Cm^{244} recovery from possible subsequent batches of irradiated Pu^{239}.

(3) Fabrication of HFIR targets from the Pu^{242} and Am^{243}-Cm^{244}.

(4) Processing of HFIR-irradiated Pu^{242} and Am^{243}-Cm^{244} targets for the recovery of curium, berkelium, and californium and the refabrication of curium isotopes into target rods for re-irradiation in the HFIR.

(5) Processing of recycle targets from the HFIR to recover californium, berkelium, and heavier elements and to recycle residual curium to the HFIR.

(6) Separation, purification, and isolation of elements higher than californium from recycled curium irradiations. Significant

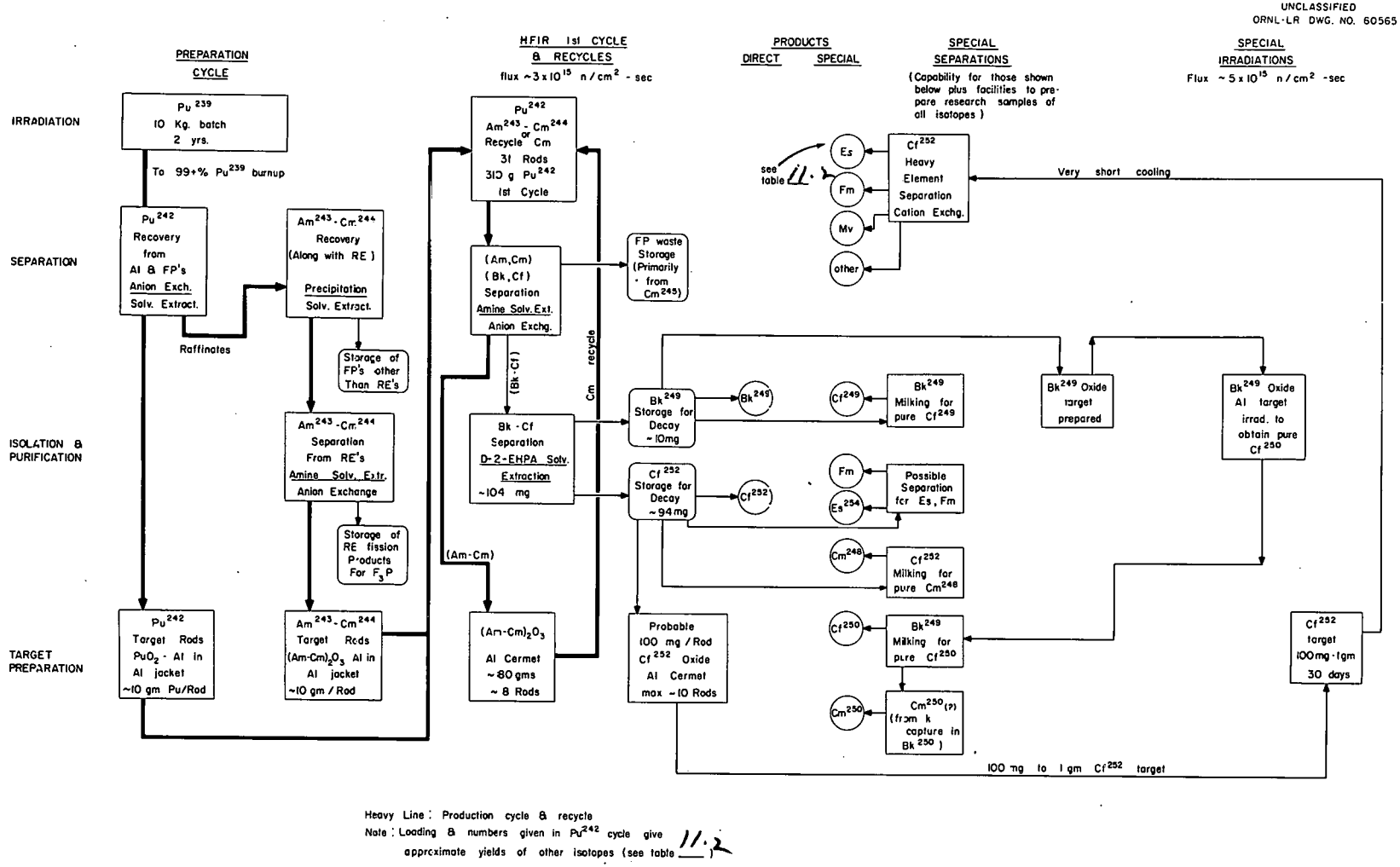

Heavy Line: Production cycle & recycle
Note: Loading & numbers given in Pu^{242} cycle give approximate yields of other isotopes (see table 11.2)

Fig. 11.1. Schematic of Transuranium Program.

quantities of elements heavier than californium will be produced. Attempts will be made to routinely recover Es^{254} (480 days).

(7) Preparation of 100-mg to 1-g californium targets for re-irradiation in the HFIR.

(8) Processing (for recovery of heavier, short-lived elements) of californium irradiated at 5×10^{15} n cm^{-2} sec^{-1} for ~30 days and decayed a very short time.

(9) Preparation, for research use, of individual isotopes of californium, curium, and berkelium by specific milking and irradiation procedures.

(10) Preparation of small quantities of other heavy-element isotopes for research use.

(11) Preparation of purified isotopes in quantities that require heavy shielding.

Work directed toward meeting these objectives has included development of chemical processes, HFIR target fabrication techniques, process equipment, and facility concepts. The Transuranium Processing Facility (TRU) that will house these operations is being designed. The overall schedule for the transuranium program is set by the schedule for design and construction of the HFIR. The current schedule for the HFIR-Transuranium complex is:

	TRU Facility	HFIR
Design completion	June 1963	Sept. 1961
Start construction	Nov. 1962	July 1961
Complete construction	Nov. 1964 (without equipment)	June 1963
Start routine operation	Nov. 1965	Jan. 1964

The Transuranium Facility will be operated with irradiated targets prior to July 1965 to test the chemical separations and target fabrication methods with the actual materials to be recovered, which can be processed only in the completed TRU Facility. To start the HFIR, ~350 g of Pu^{242} will be required by January 1963 as target rods; an additional 300 g will be required in July 1963. The HFIR will operate with these targets until July 1965, at which time Am^{243}-Cm^{244} targets will be produced in the TRU Facility and the HFIR recycle initiated. From initial HFIR target processing, it is hoped that the first milligram quantities of californium can be isolated by December 1965.

A glove box line will be installed in an existing alpha laboratory in Bldg. 3508 to produce the Pu^{242} targets for at least the first two loadings for the HFIR.

11.1 ISOTOPE PRODUCTION CALCULATIONS FOR THE HFIR

The overall production of heavy elements by the HFIR-Transuranium Facility has been optimized for maximum production of Cf^{252}. The CRUNCH code for heavy element production was used in making the calculations. The isotopes studied and their physical properties are summarized in Fig. 11.2 and Table 11.1. The cross sections given for the transuranium buildup chain are a self-consistent set of cross sections for pile neutrons. In many cases the values for individual isotopes have not been measured.

For design use cross-sections that gave a conservative estimate of shielding and heating problems were used. This is particularly important for the capture cross section of Cf^{253}, for which the best previous estimate, obtained at ~10^{13} n cm^{-2} sec^{-1}, was 15 ± 15 barns. The cross section of 60 barns used as a design basis gives a safe upper limit for the yield of Cf^{254}, whose spontaneous fission rate (55-d half-life) and neutron yield (3.9 n/fission) are controlling in shielding, heating, activation of cell components, and radiation damage. Very recent measurements at Argonne and Berkeley gave a preliminary value of 2 barns for the capture cross section of Cf^{253}. Recalculation of radiation levels are now in progress, and a special measurement of the thermal and epithermal capture and fission cross sections of Cf^{253} will be made in the ORR at ~5×10^{14} n cm^{-2} sec^{-1}; data should be available in October 1961. The final design will be based on these results.

The CRUNCH code was used to optimize the production rate of Cf^{252}, starting with a 310-g loading of Pu^{242}. Optimum irradiation times were found to be about 1, 0.6, 0.4, 0.4, 0.36 year for the first to fifth cycles, respectively. The isotopic composition at the ends of these cycles is given in Table 11.2. These values were obtained with

UNCLASSIFIED
ORNL-LR-DWG. 55564-R1

								Mv-255 ~30 m K (α 7.34) S.F. 2 d	Mv-256 1 h K			
				Fm-250 30 m α 7.43 K	Fm-251 7.5 h α 6.9(~1) K (~99)	Fm-252 36 h α 7.04 S.F. >8 y	Fm-253 5 d K (90) α 6.94 (10)	Fm-254 3.38 h α 7.22 (85) 7.18 (~15) Others σ_f ~0 σ_c ~100 S.F. 0.6 y	Fm-255 21.5 h α 7.08 Others $\sigma_f \leq 50$ $\sigma_c < 100$ S.F. >60 y	Fm-256 3.1 h S.F. 3.1 h	Fm-257 ~days S. F. ~days
		Es-246 7.3 m (K) α 7.35	Es-247	Es-248 25 m K (99+) α 6.87 (~0.2)	Es-249 2 h K (99+) α 6.76 (~0.2)	Es-250 8 h K (α)	Es-251	Es-252 ~140 d α 6.64 (K)	Es-253 20 d α 6.63 (91) γ 0.39 Others σ_f ~0/~0 σ_c 200/7 S.F. 7×10^5 y	Es-254 37 h | 480 d β 1.04 | α 6.44 K (~.1) γ .66 σ_f <100 | σ_f ~2000 σ_c <10 | σ_c ~40 S.F. 1.5×10^5 y	Es-255 30 d β σ_f ~0 σ_c ~40	Es-256 Short (β)
	Cf-244 25 m K α 7.17	Cf-245 44 m K (66) α 7.11 (34)	Cf-246 35.7 h α 6.753 (78) α 6.711 (22) γ .044 Others S.F. 2100 y	Cf-247 2.4 h K γ .285 .49	Cf-248 250 d α 6.26 S.F. 7000 y	Cf-249 360 y α 5.82 (90) 5.91 (7) γ .4 Others σ_f 630 σ_c 270 S.F. 1.5×10^9 y	Cf-250 10 y α 6.02 (83) 5.98 (17) γ .0428 σ_f 0 σ_c 1500 S.F. 1.5×10^4 y	Cf-251 ~700 y α σ_f 3000 σ_c 3000	Cf-252 2.2 y α 6.112 (84) 6.07 (16) γ .043, .10 σ_f ~0 σ_c 30 S.F. 66 y	Cf-253 18 d β σ_f 300 σ_c 60*	Cf-254 55 d σ_f ~0 σ_c 2 S.F. 55 d	
	Bk-243 4.5 h K (99+) α 6.72 (~.15) γ .15 Others	Bk-244 4.4 h K (99+) α 6.66 (6×10^{-5}) γ .90 Others	Bk-245 5 d K (99+) α 6.37 (~.1) γ .165 Others	Bk-246 1.9 d K γ .145 Others	Bk-247 7000 y α 5.67 (30) 5.50 (60) 5.30 (10) γ .085 Others	Bk-248 18 h K (25) β .67 (75)	Bk-249 290 d β .10 (99+) α 5.40 (10^{-3}) Others σ_f ~0 σ_c 1100 + 300 S.F. ~10^9 y	Bk-250 3.22 hr K (~0.1) β .73 (89) γ .99 Others σ_f 150 σ_c 500				
Cm-241 35 d K (99+) α 5.90 (.96) γ .472	Cm-242 162.5 d α 6.110 (74) 6.066 (26) γ .044 Others σ_f <5 σ_c 20 S.F. 7.2×10^6 y	Cm-243 ~35 y α 5.777 (79) 5.732 (12) γ .278 Others σ_f 490 σ_c ~250	Cm-244 18.4 y α 5.798 (77) 5.755 (23) γ .043 Others σ_f 0 σ_c 25 S.F. 1.4×10^7 y	Cm-245 8000 y α 5.36 γ .10 Others σ_f 1500 σ_c 200	Cm-246 6600 y α 5.373 σ_f 0 σ_c 15 S.F. <1.2×10^7	Cm-247 >10^7 y σ_f 200 σ_c 200	Cm-248 4.7×10^5 y α 5.054 σ_f ~0 σ_c 2-6 S.F. 4.6×10^6 y	Cm-249 64 m β .86	Cm-250 >130 y (β) S.F. ~2×10^4 y		
Am-239 12 h K (~100) γ .049 Others α 5.75 (.003)	Am-240 50 h K γ 1.02 Others	Am-241 462 y α 5.476 (84) 5.433 (14) γ .0596 Others σ_f 3 σ_c <60/700 S.F. > 1.4×10^{13} y	Am-242 152 y | 16 h K | β .625 (81) γ .049 | K (19) σ_f 6400 | γ .0422 Others σ_f 2500 σ_c 5500	Am-243 8×10^3 y α 5.267 (87) 5.224 (11) γ .075 Others σ_f 0 σ_c 138	Am-244 26 m β 1.5 (~100) K (~.04) σ_f 0 σ_c 0	Am-245 2 h β .90 γ .036 Others	Am-246 25 m β 1.2 γ .019 Others					
Pu-238 89.6 y α 5.495 (72) 5.452 (28) γ .044 Others σ_f 17 σ_c 450 S.F. 4.9×10^{10} y	Pu-239 2.44×10^4 y α 5.150 (69) 5.137 (20) γ .053 Others σ_f 729 σ_c 303 S.F. 5.5×10^{15} y	Pu-240 6.6×10^3 y α 5.162 (76) 5.118 (24) γ .050 σ_f <0.1 σ_c 250 S.F. 1.3×10^{11} y	Pu-241 13.2 y β .020 α 4.91 (4×10^{-3}) γ .100 Others σ_f 1000 σ_c 390	Pu-242 3.8×10^5 y α 4.898 σ_f <3 σ_c 52 S.F. 7.2×10^{10} y	Pu-243 4.98 h β .57 (53) γ .085 Others σ_f 0 σ_c 170	Pu-244 7×10^7 y α 4.8 σ_c 1.5 S.F. 2.5×10^{10} y	Pu-245 11 h β γ σ_c 260	Pu-246 11 d β γ .043 Others			
Np-237 2.20×10^6 y α 4.78 γ .087 Others σ_f .019 σ_c 171 S.F. ≥ 4×10^{16} y	Np-238 2.10 d β 1.26(55) 0.26(45) γ 0.044 Others σ_f 1.6×10^3	Np-239 2.33 d β .329(52) .44(31) γ .105 Others σ_f <3 σ_c 35/25 S.F. > 5×10^{12} y	Np-240 7.3 m | 1 h β 2.16(52) | β .9 γ .04 | γ .97 Others | Others	Np-241 16 m β 1.36 No γ							
U-235 26.3 m | 7.15×10^8 y IT | α 4.40 γ ≤ 0.002 | γ .18 Others σ_f 577 σ_c 106 S.F. 1.8×10^{17} y	U-236 2.39×10^7 y α 4.499 γ.050 σ_f 9 S.F. 2×10^{16} y	U-237 6.75 d β .248 γ .208 (89) .059 (81) Others	U-238 4.51×10^9 y α 4.18 β .045 σ_f <10^{-3} σ_c 2.76 S.F. 8.3×10^{15} y	U-239 23.5 m β 1.21 γ .075 σ_f 15 σ_c 22	U-240 14.1 h β .36 (75) .32 (25) γ .044						

U Uranium
Np Neptunium
Pu Plutonium
Am Americium
Cm Curium
Bk Berkelium
Cf Californium
Es Einsteinium
Fm Fermium
Mv Mendelevium

Symbols same as on G. E. chart
Numbers in parentheses after decay are percentages
Decay schemes in parentheses are uncertain

The cross section data given for the transuranium buildup chain in this chart are a self consistent set of pile neutron cross-sections chosen for the TRU design basis. Many of the individual cross sections have not been measured. Other physical constants are from the "Trilinear Chart of Nuclides" and "Reviews of Modern Physics."

*Recent measurements at Argonne and Berkeley indicate the σ_c for Cf-253 is about 2 barns for pile neutrons (MTR).

CHART OF THE TRANSURANIUM ELEMENTS
OAK RIDGE NATIONAL LABORATORY

Fig. 11.2. Chart of the Transuranium Elements.

Table 11.1. Properties of Transuranium Isotopes

Isotope	Alpha or Beta Radiation				SF Half Life, yr	neuts/sec-g		Body Burdens/g $\times 10^{-6}$	Specific Heat, watts/g
	Type	Half Life	mev/dis	curies/g		Al α-n	SF		
Pu-238	α	89.6 y	5.49	16.8	4.9×10^{10}	3.36×10^{5}	2850	420	0.546
239	α	2.44×10^{4} y	5.15	0.0613	5.5×10^{15}	1.22×10^{3}	0.0294	1.53	0.00188
240	α	6.6×10^{3} y	5.16	0.226	1.3×10^{11}	4.51×10^{3}	935	5.65	0.00693
241	β	13.2 y	0.020	113	-	-	-	126	0.00446
242	α	3.8×10^{5} y	4.90	0.00389	7.2×10^{10}	77.8	1670	0.078	1.13×10^{-4}
243	β	4.98 hr	0.57	2.59×10^{6}	-	-	-	2.6×10^{6}	2910
244	α	7×10^{7}y	4.8	2.09×10^{-5}	2.5×10^{10}	0.418	5.2×10^{3}	5.23×10^{-4}	5.95×10^{-7}
Am-241	α	462 y	5.48	3.21	1.4×10^{13}	6.42×10^{4}	9.42	32.1	0.105
242	β	16 hr	0.625	8.1×10^{5}	-	-	-	8.1×10^{5}	1000
	K	152 y	0.049	14.8				14.8	0.0014
243	α	8×10^{3} y	5.27	0.184	-	3.68×10^{3}	-	3.68	0.0058
244	β	26 m	1.5	3.3×10^{7}	-	-	-	3.3×10^{7}	0.98×10^{5}
Cm-242	α	162.5 d	6.11	3320	7.2×10^{6}	6.65×10^{7}	1.98×10^{7}	66,500	120
243	α	35 y	5.78	42.1	-	8.41×10^{5}	-	46.7	1.45
244	α	18.4 y	5.80	79.6	1.4×10^{7}	1.59×10^{6}	1.09×10^{7}	796	2.74
245	α	8×10^{3} y	5.36	0.182	-	3.65×10^{3}	-	4.55	0.0058
246	α	6.6×10^{3} y	5.37	0.22	1.2×10^{7}	4.4×10^{3}	1.39×10^{7}	4.4	0.0070
247	α	10^{7}	5.37	0.000145	-	2.9	-	0.0029	4.6×10^{-6}
248	α	4.2×10^{5} y	5.05	0.00343	4.2×10^{6}	68.5	4.32×10^{7}	0.069	1.03×10^{-4}
249	β	64 m	0.86	1.175×10^{7}	-	-	-	1.175×10^{7}	60,000
Bk-249	β	290 d	0.10	1810	6×10^{8}	-	3.1×10^{5}	2590	0.356
250	β	3.22 h	0.73	3.89×10^{6}	-	-	-	3.89×10^{6}	16,800
Cf-249	α	360 y	5.82	3.98	1.5×10^{9}	8.0×10^{4}	1.28×10^{5}	99.5	0.138
250	α	10 y	6.02	143	1.5×10^{4}	2.86×10^{6}	1.31×10^{10}	3580	5.21
251	α	700 y	6.02(?)	2.04	-	4.08×10^{4}	-	51	0.073
252	α	2.2 y	6.11	645	66	1.29×10^{7}	3.03×10^{12}	39,900	49.0
253	β	18 d	1.0(?)	28,700	1.5×10^{5}	-	1.31×10^{9}	50,500	56.6
254	α	100 y	6.1(?)	14.1	55 d	2.82×10^{5}	1.35×10^{15}	9.3×10^{6}	11,200
En-253	α	20 d	6.63	25,800	7×10^{5}	5.15×10^{8}	2.91×10^{8}	6.5×10^{5}	1014
254	β	37 h	1.04	333,000	1.5×10^{5}	-	1.35×10^{9}	4.7×10^{5}	683
	α	470 d	6.44	1092	1.5×10^{5}	2.2×10^{7}	1.35×10^{9}	2.73×10^{4}	41.7
255	β	30 d	1.0(?)	17,100	-	-	-	2.44×10^{4}	33.6
Fm-254	α	3.38 h	7.22	3.65×10^{6}	0.60	7.3×10^{10}	3.52×10^{14}	8.9×10^{7}	159,000
255	α	21.5 h	7.08	572,000	60	1.14×10^{10}	3.50×10^{12}	1.43×10^{7}	24,000
256	α	10 d(?)	7.1(?)	51,000	3.1 hr	1.03×10^{9}	5.91×10^{17}	4.0×10^{9}	4,710,000

Table 11.2. Isotopes Produced from One HFIR Loading of 310 g of Pu^{242}

Isotope	Cycle 1 1 year	Cycle 2 0.6 year	Cycle 3 0.4 year	Cycle 5 0.36 year
Pu^{242}, g	2.28			
Am^{243}, g	1.36			
Cm^{244}, g	59.0	13.4	5.27	0.92
Cm^{245}, g	0.8	0.2	0.07	0.01
Cm^{246}, g	13.9	8.9	5.8	2.30
Cm^{247}, g	0.5	0.3	0.22	0.09
Cm^{248}, g	5.6	9.9	11.2	11.7
Total Cm, g	80	33	23	15
Bk^{249}, mg	9.6	17.2	19.3	20.2
Cf^{250}, mg	6.8	12.4	14.0	14.7
Cf^{251}, mg	1.7	3.1	3.5	3.7
Cf^{252}, mg	87	208	211	220
Cf^{253}, mg	4.8	12.0	12.1	12.5
Cf^{254}, mg	3.4	10.2	8.2	8.2
Total Cf, mg	104	245	250	260

the design cross sections and with 2 barns for the capture cross section of Cm^{248}.

The HFIR target irradiation schedule can be programmed to vary isotope production rates as desired. For instance, a maximum quantity of Cf^{252} can be produced during an irradiation by loading a large number of recycle curium rods at one time. However, if the objective is to produce the maximum amount of californium per year, the reactor will always be loaded with both fresh feed material, Pu^{242} or Am^{243}-Cm^{244}, and with curium isotopes available from previous irradiations. If this is done commensurate with the heat removal capability of the target region, the target loading approaches that given in Table 11.3. The amount of actinides loaded per rod is determined by the residual fissionable isotopes, primarily Cm^{245}. For the first cycle the permissible amount of Pu^{242} per rod, 10 g, is determined by the heat production rate of Cm^{245} which reaches a maximum of 24.2 kw per rod at about 140 days. In subsequent cycles the curium isotopes can be contained in a decreasing number of rods, as shown in the table. Extrapolation of this table to an infinite number of recycles gives a Cf^{252} production rate of about 1.3 g/year, corresponding to an inventory of about 4 g of Cf^{252}.

Production of Isotopes by Irradiation of 1 g of Californium

When sufficient californium has been produced (i.e., fourth-cycle HFIR target, Table 11.2), a target loading of californium will be prepared for a special HFIR irradiation to produce large quantities of einsteinium, fermium, and possibly heavier elements. The target rods will contain 100 to 200 mg of californium as the oxide, will be irradiated in the flux trap at 5×10^{15} n cm^{-2} sec^{-1} for 30 days, and processed as soon after discharge as possible.

The isotopes available from such an irradiation of 1 g of californium are given in Table 11.4. This material will be processed within 1 or 2 days after discharge to isolate fractions of the very short half-lived isotopes of einsteinium, fermium, and possibly mendelevium.

Table 11.3. Idealized Equilibrium Operation of HFIR for Maximum Cf^{252} Production

Assumptions: Maximum heat dissipation in flux trap: 24.2 kw/rod
Total number of target rods/charge: 31
Flux: 3×10^{15} n cm^{-2} sec^{-1}
Cm^{248} capture cross section: 2 barns (conservative)*
Cf^{253} capture cross section: 60 barns (probably 2 to 6)
Cf^{253} fission cross section: 300 barns

	Cycle 1	Cycle 2	Cycle 3	Cycle 4	Cycle 5
Time in reactor, yr	1.0	0.6	0.4	0.4	0.36
Average inventory, rods in HFIR	23.1	6.02	1.11	0.505	0.23
Initial wt actinides, g/rod	10.4	6.3	9.6	14.7	25.4
Final wt actinides, g/rod	2.72	2.67	6.70	11.48	21.8
Cf^{252} at discharge, mg/rod	3.0	16.9	64.5	150	305
Rods/yr	23.1	10.1	2.78	1.26	0.64
Cf^{252}, mg/yr	69	169	179	189	195
Estimated Cf^{254}, % of Cf^{252}	3.9	4.9	3.9	3.8	3.7
Total average yearly Cf^{252} production rate for first 5 cycles**			801 mg/yr		

*The Cm^{248} σ_c may be as high as 6 barns, depending on resonance contributions.

**The re-irradiation of the curium isotopes remaining after five cycles will raise the total yearly Cf^{252} production rate to about 1.3 g, and an inventory of about 4 g of Cf^{252} will result.

Very significant amounts of Es^{254} (480 days) will be made in this special irradiation, 1.3×10^{17} atoms or 55 μg. The same amount of Es^{254} will be produced during the irradiations which produced the californium initially. It is therefore important to attempt to isolate einsteinium during routine processing of recycled HFIR targets.

Fission Product Fractions

Fission products resulting from the complete burnup of Pu^{239} in the preparation cycle for Pu^{242} will be isolated and stored for possible research or other use. Many kilograms of rare earth fission products will be available with concentrations of the heavier rare earths enriched by several successive neutron captures during the extended irradiation. The fission yields and capture cross sections of the fission products of Pu^{239} and Pu^{241} can be studied if pure Pu^{241} can be isolated and irradiated to obtain fission yield data. An important area of interest is in power reactor cycles, where at 20,000 Mwd/ton irradiation of fuel, initially 2% enriched with U^{235}, about half the total fissions are from plutonium and 10 to 20% are produced by the fissioning of Pu^{241}.

From the irradiation of first- and second-cycle HFIR targets, large quantities of the fission products of Cm^{245} can be obtained. Again, information on fission product yields and cross sections can be developed.

There appears to be some justification for a shielded calutron for separation of heavy elements and fission product isotopes. Many fission products and heavy elements will be available in quantities sufficient to perform cross section measurements with controlled-energy neutron sources.

Table 11.4. Isotopes Produced by Irradiation of 1-g Californium Samples

(Original material taken as fourth-cycle product after 55 days' decay)

ϕ	Time (days)	Amount (no. of atoms)											
		Cf^{250}	Cf^{251}	Cf^{252}	Cf^{253}	Cf^{254}	Es^{253}	Es^{254}-S	Es^{254}-L	Es^{255}	Fm^{254}	Fm^{255}	Fm^{256}
5×10^{15}	7	1.720×10^{18}	5.734×10^{17}	2.262×10^{21}	1.201×10^{20}	5.517×10^{19}	1.582×10^{19}	1.864×10^{18}	4.373×10^{16}	2.752×10^{17}	1.609×10^{17}	1.123×10^{16}	9.559×10^{14}
	15	9.627×10^{15}	3.209×10^{15}	2.026×10^{21}	1.367×10^{20}	7.560×10^{19}	3.195×10^{19}	4.977×10^{18}	1.036×10^{17}	7.065×10^{17}	4.454×10^{17}	3.360×10^{16}	2.496×10^{15}
	30	5.766×10^{11}	1.922×10^{11}	1.647×10^{21}	1.179×10^{20}	1.069×10^{20}	3.791×10^{19}	6.610×10^{18}	1.303×10^{17}	1.627×10^{18}	5.988×10^{17}	6.849×10^{16}	5.675×10^{15}
	45	3.454×10^{7}	1.151×10^{7}	1.338×10^{21}	9.622×10^{19}	1.249×10^{20}	3.305×10^{19}	5.880×10^{18}	1.147×10^{17}	2.361×10^{18}	5.337×10^{17}	6.943×10^{16}	8.141×10^{15}
	60	2.069×10^{3}	6.897×10^{2}	1.088×10^{21}	7.822×10^{19}	1.325×10^{20}	2.732×10^{19}	4.863×10^{18}	9.471×10^{16}	2.829×10^{18}	4.416×10^{17}	7.514×10^{16}	9.702×10^{15}
3×10^{15}	7	1.056×10^{15}	3.519×10^{18}	2.339×10^{21}	9.102×10^{19}	4.741×10^{19}	1.273×10^{19}	9.057×10^{17}	2.977×10^{16}	1.538×10^{17}	7.820×10^{16}	4.840×10^{15}	3.117×10^{14}
	15	4.699×10^{17}	1.567×10^{17}	2.189×10^{21}	1.183×10^{20}	5.545×10^{19}	3.043×10^{19}	2.833×10^{18}	9.094×10^{16}	3.442×10^{17}	2.534×10^{17}	1.398×10^{16}	7.224×10^{14}
	30	1.374×10^{15}	4.581×10^{14}	1.924×10^{21}	1.187×10^{20}	7.116×10^{19}	4.676×10^{19}	4.936×10^{18}	1.563×10^{17}	7.448×10^{17}	4.474×10^{17}	2.733×10^{16}	1.561×10^{15}
	45	4.017×10^{12}	1.339×10^{12}	1.690×10^{21}	1.063×10^{20}	8.227×10^{19}	4.807×10^{19}	5.236×10^{18}	1.652×10^{17}	1.104×10^{18}	4.761×10^{17}	3.455×10^{16}	2.292×10^{15}
	60	1.174×10^{10}	3.916×10^{9}	1.484×10^{21}	9.366×10^{19}	8.869×10^{19}	4.432×10^{19}	4.874×10^{18}	1.536×10^{17}	1.369×10^{18}	4.435×10^{17}	3.852×10^{16}	2.831×10^{15}
	80	4.911×10^{6}	1.637×10^{6}	1.249×10^{21}	7.884×10^{19}	9.168×10^{19}	3.793×10^{19}	4.185×10^{18}	1.319×10^{17}	1.579×10^{18}	3.810×10^{17}	4.112×10^{16}	3.247×10^{15}
	100	2.053×10^{3}	6.845×10^{2}	1.051×10^{21}	6.633×10^{19}	9.026×10^{19}	3.203×10^{19}	3.536×10^{18}	1.114×10^{17}	1.660×10^{18}	3.219×10^{17}	4.169×10^{16}	3.409×10^{15}

11.2 BASIS FOR SHIELDING DESIGN

Shielding design for the Transuranium Facility involves new problems for chemical and metallurgical cells because of the high fast-neutron flux, the large quantities of alpha emitters which must be totally contained, and the penetrating gammas from fission products and spontaneous fission. The controlling penetration radiation in determination of shield thickness is the fast-neutron contribution from the spontaneous fission of Cf^{252} and Cf^{254}. The latter isotope, with a 55-day spontaneous-fission half-life, has been assumed to be controlling. The most intense fast-neutron source will be 1 g of californium irradiated 30 days at 5×10^{15} n cm^{-2} sec^{-1}. Shielding for this source will exceed the requirements for californium in recycled HFIR targets, gamma-emitting fission products from the complete burnup of Pu^{239} and in recycle rods, and spontaneous fission gammas.

The fast-neutron source strength assumed for handling of 1 g of californium that has been irradiated 30 days at 5×10^{15} n cm^{-2} sec^{-1} and decayed 1 day, 2.4×10^{14} n g^{-1} sec^{-1}, is probably a very high estimate inasmuch as it is based on a Cf^{254} concentration of 20%. This value contains a safety factor of ~4 over the value based on the most probable neutron capture cross section value.

The maximum californium content for a fifth-recycle HFIR target rod is ~30 mg (Table 11.3). This rod will have been irradiated at $\sim 3 \times 10^{15}$ n cm^{-2} sec^{-1} for 0.36 year and will contain 3.7% Cf^{254}, based on the maximum probable values. Applying a safety factor of 4 to this value, the fast-neutron source strength for design is 6×10^{13} n/sec per rod, less than the maximum design source strength.

There are two sources of gamma rays: fission products and spontaneous fission. For design purposes the maximum quantity of fission products was assumed to be provided by rare earth fission products from the fission of 10 kg of Pu^{239} (90% burnup for the peak rare earth quantity). These fission products will report with the Am^{243}-Cm^{244}. The distribution of these fission products, by gamma photon energies, after 90 days' decay is

500,000 curies	1.0-Mev γ
80,000 curies	1.7-Mev γ
2,500 curies	2.6-Mev γ (from Pr^{143} and Pm^{147})

The 2.6-Mev maximum fraction controls the required gamma shield. These assumed values are high because Pu^{239} will be irradiated to >99.9% burnup rather than the fission product peak producing 90%.

The spontaneous fission gammas from 1 g of californium with a fission rate of 6.25×10^{13} fissions/sec give the following controlling photons in the energy range 4.75 to 6.5 Mev (90% of total spontaneous fission gamma dose), assuming fission yields similar to U^{235}:

Mev	Number of photons
4.75	2.7×10^{12}
5.5	1.1×10^{12}
6.0	4.4×10^{11}
6.5	2.5×10^{11}

The required shielding thicknesses, assuming a concrete shield with magnetite ore aggregate containing 1.67 g of iron and 0.196 g of water per cubic centimeter, are shown in Table 11.5.

The bulk shield will be 6 ft of magnetite concrete with a 0.196 g/cc minimum water retention. This thickness will reduce the radiation intensity of neutrons at the outer surface of the bulk shield to 0.15 mr/hr, where heavy occupancy is anticipated. For surfaces facing the limited-access areas, the outer surface of this shield will provide a radiation field of no more than 2.5 mr/hr. Careful attention to water retention is necessary, but there is a safety factor of at least 2 in the source strength calculations, which should be sufficient for a very low water content.

Special shielding-window design is required, using layers of glass interspersed with hydrogeneous (perhaps borated) material. The window design, not yet established pending experimental work in the Bulk Shielding Facility, will be ~6 ft thick, with non-browning cell-side lamination. The surface of the window exposed to alpha contamination will be removable from inside the sealed cell.

Table 11.5. Magnetite Concrete Shielding Requirements for TRU Facility for 0.25 mr/hr at Outer Cell Face

Source	Strength (n/sec)	Shield Thickness (in.)
Neutrons, 1 g* of Cf, 20% Cf^{254}	2.4×10^{14}	72
5% Cf^{254}	6.2×10^{13}	68
1% Cf^{254}	1.5×10^{13}	62
305 mg Cf (maximum rod)	6.0×10^{13}	68
Gammas, rare earth fission products from Pu^{239} fission	(see text)	50
Spontaneous* fission of 1 g of Cf^{252}, 20% Cf^{254}	(see text)	56

*Controlling.

Gamma heating in the shield has been calculated, that from the rare earth fission products resulting from Pu^{239} burnup being controlling. Calculations based on a source strength of 500,000 curies (conservative) of 1-Mev gammas as a 75-cm disk, 30 cm from the shield, indicate a possible 13°C temperature rise in the shield, which is not sufficient to create damaging stresses in the shield.

11.3 CHEMICAL PROCESS DEVELOPMENT

Various chemical separations have been explored in the laboratory with trace quantities of the transuranic elements. Test fabrication of target elements, with equipment similar to that for the Transuranium Facility, is planned by the Metallurgy Division; and test specimens of target pellets were made by the oxide-aluminum cermet technique.

Quantities of rare earth fission products and of americium-curium for transuranium process testing were isolated by TBP solvent extraction in Building 3019 from highly irradiated plutonium-aluminum MTR elements. Separation of berkelium and californium at a tracer level by solvent extraction was excellent. In a single test on the solvent extraction separation of californium and einsteinium, made with the assistance of a research group at UCRL, there was essentially no difference in distribution coefficients for the Cf and Es; only cation exchange separation may be feasible.

Problems of radiation damage to ion exchange resins and to organic solvents were studied sufficiently to give confidence that these materials, with appropriately diluted feed, can be used for the required separations; work will continue on radiation damage to organics under actual flowsheet conditions.

Corrosion studies for the necessary nitrate-chloride systems were started, and sufficient data were obtained that the materials of construction can be tentatively specified, although the very necessary detailed corrosion information is being collected.

Many separate chemical separation steps, as well as target and research sample preparations, are required in the Transuranium Program; to summarize the best available process information, the current processes of choice and alternatives are listed in Table 11.6.

Americium–Curium–Rare Earth Recovery from Pu Extraction Raffinates

Recovery of americium, curium, and rare earths by TBP extraction from neutral nitrate solutions was investigated, but work was discontinued because present plans no longer call for processing the irradiated Pu^{239} in the Bldg. 3019 pilot plant. In mini-mixer-settlers with 9 extraction stages and 7 scrub stages, extraction of cerium and europium was essentially complete in 5 stages with 2 *M* $Al(NO_3)_3$ feeds containing either 0.05 or 0.4 *M* HNO_3. Solvent/feed/scrub flow ratios were 3/2/1. The scrub was 1 *M* $Al(NO_3)_3$, and the solvent was 30% TBP in Amsco. At both acid concentrations 12% of the zirconium and 30% of the ruthenium were extracted.

Table 11.6. Development of Chemical Processes for Metallurgical Targets for Transuranium Program

Separation	Method of Choice	Status of Tests	Alternative Method	Status of Tests	Responsibility
1. Pu^{242} from Al, FP's Am, and Cm (from large preparation cycle targets)	Anion exchange, Dowex 1-10X	Checked at full activity level on engineering scale	Solvent extraction, dilute TBP	Checked at full activity level, pilot plant scale, Bldg. 3019	Large plant other than ORNL; Pu-Al alloy will be processed (~2 kg initial Pu^{239}) in Bldg. 4507 in FY 1962 as part of development
2. Am^{243}, Cm^{244} and RE from other FP's and Al	Precipitation of RE sulfates, conversion of sulfates to hydroxides, shipment of slurries	Lab scale, tracer level experiments	*Solvent extraction, TBP from neutral nitrate solution; *anion exchange	Checked at full activity level on pilot plant scale, Bldg. 3019	Large plant other than ORNL; raffinates from above Pu separation will be processed for Am-Cm recovery by anion exchange in Bldg. 4507 during FY 1962
3. Separation of Am^{243}–Cm^{244} from RE FP's	Solvent extraction;* tertiary amine from chloride system	Laboratory scale with tracer activity	*Anion exchange, Dowex 1-10X, from $LiNO_3$-$Al(NO_3)_3$; product in LiCl solutions	Laboratory scale with tracer activity	Transuranium Facility (C cells, Fig. 11.8)
4. Dissolution of targets and separation of Pu^{242} from Al, Am, Cm, FP's (from small preparation cycle targets)	Same as Items 1, 2, 3	Laboratory scale with tracer activity	Same as 1, 2, 3 above	Laboratory scale with tracer activity	Large plant other than ORNL, or, if necessary, Transuranium Facility (C cells, Fig. 11.8)
5. Dissolution and HFIR targets of Pu^{242}, Am-Cm recycles	Dissolve in HCl;* separation by solvent extraction tertiary amine	Laboratory scale, cold for dissolution, lab scale trace for separation	*Anion exchange (see Item 3)	See Item 3	Transuranium Facility (C cell, Fig. 11.8)
6. Separation of Am-Cm isotopes from Bk-Cf-Es, isotopes (routine recycle)	Solvent extraction* mono-2-ethyl hexylphenyl phosphonic acid	Laboratory scale, tracer level	Anion exchange, Dowex-1	See Item 3	
7. Separation of Bk and Cf + Es (routine recycle)	Solvent extraction,* di-2-ethylhexyl phosphoric acid	Laboratory, tracer levels	Anion exchange, Dowex-1	See Item 3	
8. Separation Cf and Es (cnd Fm?) (routine recycle)	Cation exchange, Dowex 50-12X	Based on work at UCRL; some laboratory tracer at ORNL	None		
9. Separation of Es, Fm, Mo, others from Cf (special 1 gm irradiation)	Cation exchange, Dowex 50-12X	Based on work at UCRL; some laboratory tracer at ORNL	None		

Table 11.6 (continued)

Separation	Method of Choice	Status of Tests	Alternative Method	Status of Test	Responsibility
10. Milking of Bk^{249} for Cf^{249}	Solvent extraction,* D-2EHPA	See Item 7	See Item 7	See Item 7	Transuranium Facility (S cells, Fig. 11.8)
11. Milking of Bk^{249} (after short irradiation for Cf^{250}, Cm^{250} (?)	Solvent extraction,* D-2EHPA	See Item 7	See Item 7	See Item 7	Transuranium Facility (S cells, Fig. 11.8)
12. Separation of Es, Fm, Mv, others from each other after special irradiation	Cation exchange, Dowex 50-12X	Based on work at UCRL	None		Transuranium Facility (C and S cells, Fig. 11.8)
13. Target fabrication, all classes a. Pu^{242} b. Am-Cm, Cf	*Al-actinide oxide cermet in Al can	Cold tests only with stand-in cerium oxide	None		Bldg. 3508, 1st two HFIR loadings, Transuranium Facility (TF and 1 cells, Fig. 11.8)
14. Special source preparations for research					Transuranium Facility (S cells, Fig. 11.8), and proposed Heavy Element Research Lab

*Process development reviewed in this report.

Distribution coefficients for cerium and europium between 30% TBP-Amsco and aqueous phases increased with increasing $Al(NO_3)_3$ concentration and decreased with increasing HNO_3 concentration. Distribution coefficients for rutherium increased as the $Al(NO_3)_3$ concentration increased but were independent of acid concentration over the range 0 to 0.6 *M* HNO_3. Zirconium distribution coefficients increased with both increasing HNO_3 and $Al(NO_3)_3$ concentrations.

It is possible that the americium–curium–rare earth fraction will be removed from the aluminum nitrate plutonium extraction raffinates by precipitation of the sulfates. The sulfates will be recovered and converted to hydroxides by metathesis with sodium hydroxide solution or by re-solution in HNO_3 followed by precipitation of the hydroxides to form acceptable feed for the separation of americium-curium from rare earths.

Separation of Americium-Curium from Rare Earths by Solvent Extraction Flowsheets

A solvent extraction process (Fig. 11.3a) for separating americium and curium from rare earths was developed in which the americium and curium are extracted into a tertiary amine organic phase from a concentrated LiCl solution. Americium and curium are readily extracted into 30% Alamine 336-DEB from feeds containing as much as 10 g/liter of americium-curium and 50 g/liter rare earths while the rare earths remain in the aqueous raffinate. The scrub is 11 *N* LiCl, and the scrub/feed/solvent flow ratios are 1/1/3. A minimum of 5 extraction and 5 scrub stages is necessary. The americium and curium are stripped from the solvent with 1 *M* HCl, with a minimum of 5 stages and a strip/solvent flow ratio of 0.5/3. In laboratory countercurrent demonstrations with 7 scrub and 7 extraction stages, americium recoveries were >99.99% with a decontamination factor from rare earths of $>10^4$.

Since the presence of nitrate greatly increases lanthanide extraction, nitrate is removed from the feed by evaporating the feed and then adding HCl to 5 *M* and extracting the nitrate with a tertiary amine. In 10 stages, the nitrate concentration is reduced to trace levels by extraction into 30% Alamine 336–diethylbenzene (DEB) with a feed/solvent flow ratio of 1/2. The nitrate-free product in 5 *M* HCl is converted to a concentrated LiCl solution containing <0.05 *M* free acid by adding LiCl, evaporating to 13 *N* LiCl, and then diluting to 11 *N* LiCl.

In an alternative flowsheet (Fig. 11.3b) the actinides are extracted into a tertiary amine from an 8 *N* LiCl–2 *N* $AlCl_3$ feed solution and stripped with dilute hydrochloric acid. In batch countercurrent experiments with five stages, with feed/scrub/organic volume ratios of 1/1/1, >98% of the Am^{241} was extracted and separated from >99.7% of the Eu^{152}. The solvent was 1 *M* triisooctylamine in diisopropyl benzene, and the aqueous phase was 8 *N* LiCl–2 *N* $AlCl_3$. The feed is prepared by extracting the actinides and lanthanides from neutral nitrate solutions with TBP, scrubbing nitrate from the TBP with 12 *N* LiCl, and stripping the actinides and lanthanides with slightly acidified 8 *N* LiCl. To this, 12 *N* LiCl and 8 *N* $AlCl_3$ are added to adjust the salt solution to feed conditions.

Variables. – The extraction of actinides and lanthanides by tertiary amine chlorides varied with amine composition and concentration, diluent composition, acidity, and the aqueous phase chloride concentration. Extraction was increased by decreasing the carbon chain lengths and thus the molecular weight of the amines (Table 11.7). Extraction also varied with the nature of the diluent. With aliphatic hydrocarbons a modifier, such as tridecyl alcohol (TDA), was added to prevent formation of a second organic phase. However, as the TDA concentration increased from 5 to 10%, the extraction coefficients decreased by a factor of 4.

Actinide and lanthanide distribution coefficients were strongly dependent on LiCl concentration, the dependence being approximately the 17th power of the LiCl concentration. In 11 *N* LiCl, the lanthanide extractability increased from cerium to europium and then decreased to lutecium (Fig. 11.4). The actinide extractability was Cf $\geq$ Fm $\geq$ En > Bk > Am $\geq$ Cm. The minimum group separation, limited by curium and europium, was ~100.

Distribution coefficients (O/A) were inversely proportional to the square of the hydrogen ion concentration and directly proportional to the square of the amine concentration. The amines formed salts with acids, the strength of salt formation being $ClO_4^- > NO_3^- > Cl^- > HSO_4^- > F^-$

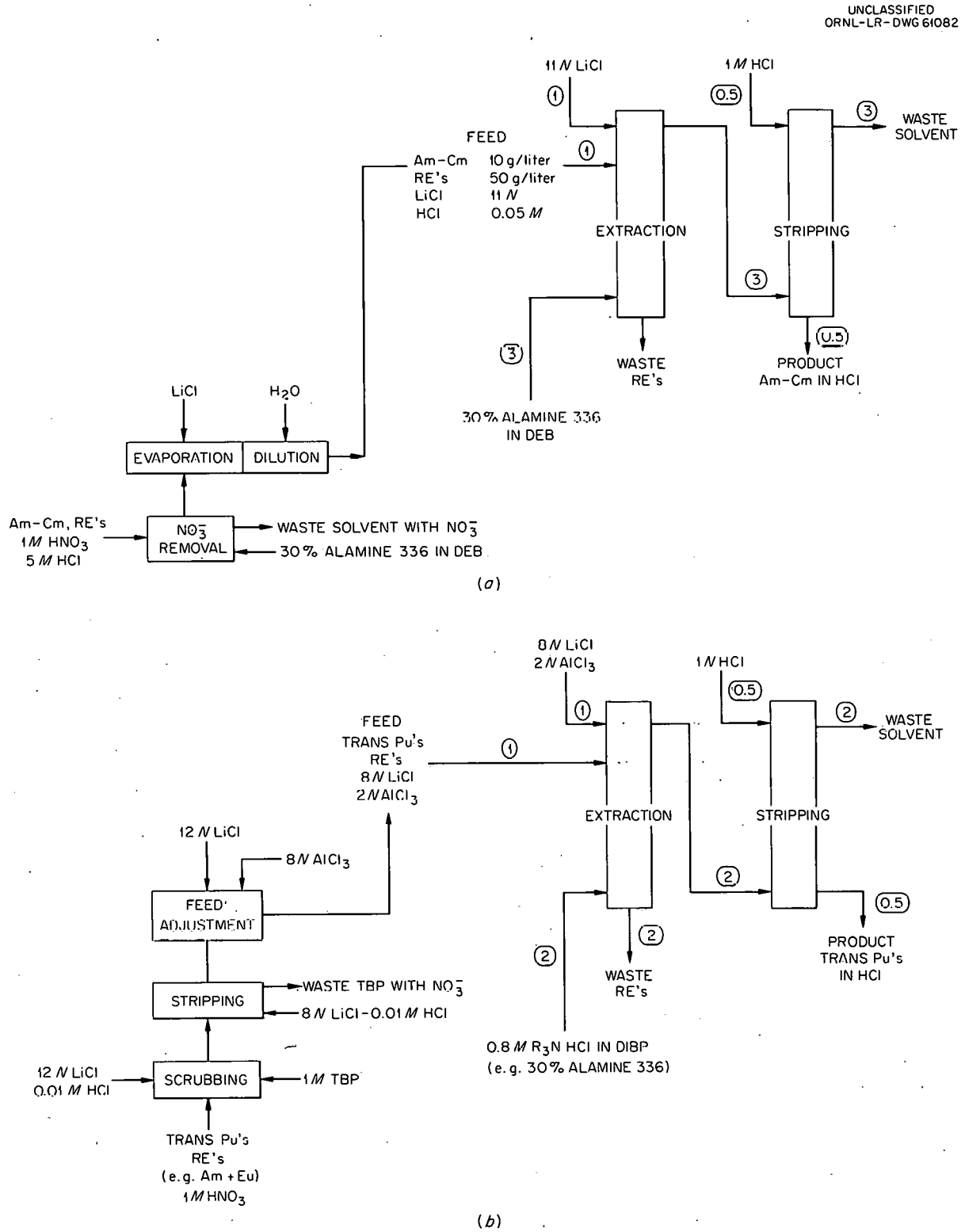

Fig. 11.3. Flowsheets of Tertiary Amine Extraction Processes for Separating Americium and Curium from Rare Earths. Circled numbers are flow ratios.

Table 11.7. Extraction Dependence on Amine and Diluent Type

Extraction by 0.5 *M* amine in diluent from 8 *M* LiCl–2 *N* $AlCl_3$

Amine	Diluent	Extraction Coefficient		Separation Factor
		Am	Eu	
Trilauryl	Solvesso-100	0.50	0.004	
Alamine 336 (octyl and decyl)	Solvesso-100	0.64	0.007	
Triisooctyl	Solvesso-100	1.02	0.008	130
Triisoheptyl	Solvesso-100	1.35		
n-Butyldilauryl	Solvesso-100	1.0		
n-Butyldidodecenyl	Solvesso-100	1.0		
Triisooctylamine	Benzene	0.27	0.0022	130
	Toluene	0.45	0.0040	110
	Xylene	0.65	0.0052	125
	sec-Butylbenzene	0.83		
	sec-Butylbenzene + 5% TDA*	0.19	0.0020	95
	Diethylbenzene	1.35	0.011	120
	Diisopropylbenzene	1.8	0.015	120
	Triethylbenzene	1.2		
	Cyclohexane	1.8	0.025	70
	Tetralin	0.07		
	Decalin	3.5	0.029	120
	Nonane + 5% TDA*	0.79		
	Hexadecane + 10% TDA*	0.74		
	Amsco G	0.13		
	Amsco 123-15 + 5% TDA*	0.49		
	Amsco 125-82 + 5% TDA*	2.5	0.03	80
	Amsco 125-82 + 10% TDA*	0.6		
	Amsco 125-82 + 5% nonylphenol	1.0		
	Varsol + 10% TDA*	0.45		
	Shell E-2342 + 5% TDA*	5.7	0.29	20
	Dibutyl carbitol	0.06		
	Acetophenone	0.2		
	Osophorone	0.3		
	Pentachloroethane	<0.001		
	Diisobutylcarbinol	$\leq$0.002		

*TDA = tridecyl alcohol.

(ref 1). With a solution containing HCl and HNO_3 the nitric acid amine salt was formed in preference to the hydrochloric acid amine salt, and actinides and lanthanides were not extracted. When extracting from neutral salts the presence of 0.2 *M* nitrate greatly increased the lanthanide extraction and thus decreased the actinide/lanthanide separation factor from 100 to about 10.

Difficulties in obtaining reproducible results were encountered when extracting from neutral LiCl into the tertiary amines. This could be overcome by addition of $AlCl_3$ to the aqueous

[1] F. L. Moore, "Liquid-Liquid Extraction with High Molecular Weight Amines," ORNL CF-61-1-77.

phase to prevent hydrolysis or by careful conditioning of the organic phase prior to use. The amine was converted to the HCl salt with 6 *M* HCl followed by two passes of 2 *N* LiCl. After this treatment, extractions were satisfactory from 11 *N* LiCl solution containing 0.01 to 0.05 *M* HCl.

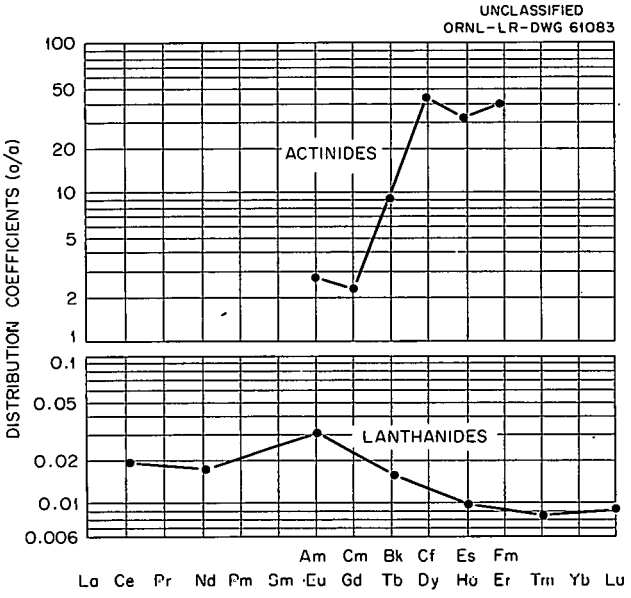

Fig. 11.4. Extractability of Actinides and Lanthanides Into 30% Alamine-336 In Xylene from 11 *M* LiCl–0.02 *M* HCl.

In further tests with TBP as the extractant for americium from concentrated chloride solutions, a single-stage separation factor of about 4 was measured between americium and europium, with smaller separations between americium and the heavier lanthanides produced by long irradiation of the primary fission products. Recent batch countercurrent tests of extraction by 1 *M* TBP in Amsco 125-82 from 8 *N* LiCl–2 *N* $AlCl_3$ solutions confirmed the americium-europium separation. A 13-stage test gave the expected overall separation factor of $\sim 10^4$.

Separation of Am and Cm from Rare Earths by Anion Exchange

In the anion exchange process being considered for separating americium and curium from rare earths (Fig. 11.5), the rare earths, americium, and curium are sorbed from 6 *M* $LiNO_3$–0.8 *M* $Al(NO_3)_3$ on a column of Dowex 1-10X (100 to 150 mesh) resin at 85°C. To load the column with 7.5 g of rare earths per liter of resin, 3 column displacement volumes are pumped through at a flow rate of 4 ml cm^{-2} min^{-1}. Washing at 85°C with 2 column volumes of 6 *M* $LiNO_3$–0.8 *M* $Al(NO_3)_3$ and 4 column volumes of 8 *M* $LiNO_3$ at 4 ml cm^{-2} min^{-1} removes iron, nickel, and chromium. The rare earths are eluted at 85°C in 10 column volumes of 10 *M* LiCl at a flow rate of 1.5 ml cm^{-2} min^{-1}, and the americium and curium are completely eluted at 85°C in 2 column volumes of 1 *M* LiCl at a flow rate of 1.5 ml cm^{-2} min^{-1}.

In laboratory demonstration in a glass column 2.5 cm dia by 60 cm high with feed containing 0.5 g iron and 5 g of mixed rare earths per liter and tracer americium, the rare earths were completely removed in 9 column volumes of 10 *M* LiCl with no detectable americium in the first 11 column volumes. More than 99% of the iron was eluted in the wash. Americium recovery was >99.99%, and the decontamination factor from rare earths was $>10^6$.

Process conditions were designed to minimize physical handling problems associated with column operation while still obtaining good decontamination from rare earths, iron, and other impurities. The presence of aluminum nitrate in the feed and in the wash is necessary to prevent iron precipitation. With no aluminum in the feed, up to 70% of of the iron precipitated in the column, causing excessive pressure drop and poor iron decontamination. After iron removal from the column is complete, aluminum nitrate is washed from the column with 8 *M* $LiNO_3$ to prevent the excessive gas formation which occurs when 10 *M* LiCl solution immediately follows $Al(NO_3)_3$ solution. Increasing the resin particle size to decrease the pressure drop spread the rare earth elution peak and gave poor rare earth decontamination factors.

HFIR Target Processing

A flowsheet for processing irradiated HFIR targets was partially developed (Fig. 11.6). Targets are dissolved in 4 *M* HCl, and americium, curium, berkelium, californium, einsteinium, and fermium are extracted from concentrated LiCl-$AlCl_3$ solution into 30% Alamine 336-DEB and stripped into HCl, which serves as feed for a mono-2-ethylhexyl phenylphosphonic acid (2-EH (ϕP)A) extraction of the berkelium-californium

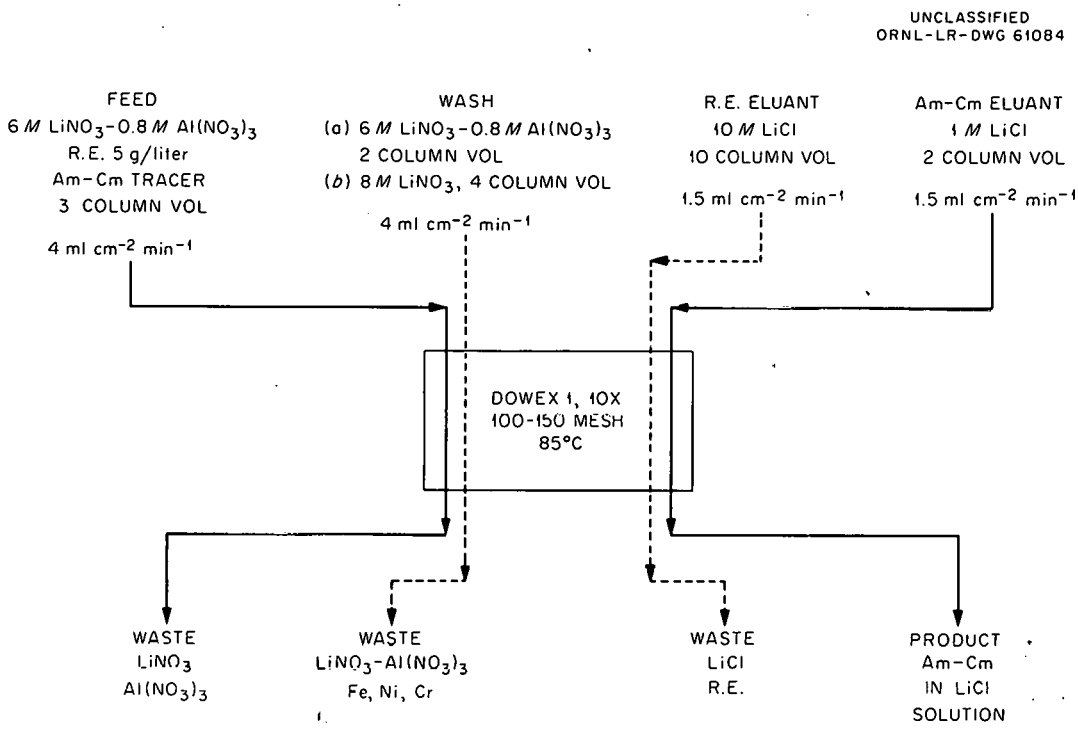

Fig. 11.5. Flowsheet of the Anion Exchange Process for Separating Americium and Curium from Rare Earths.

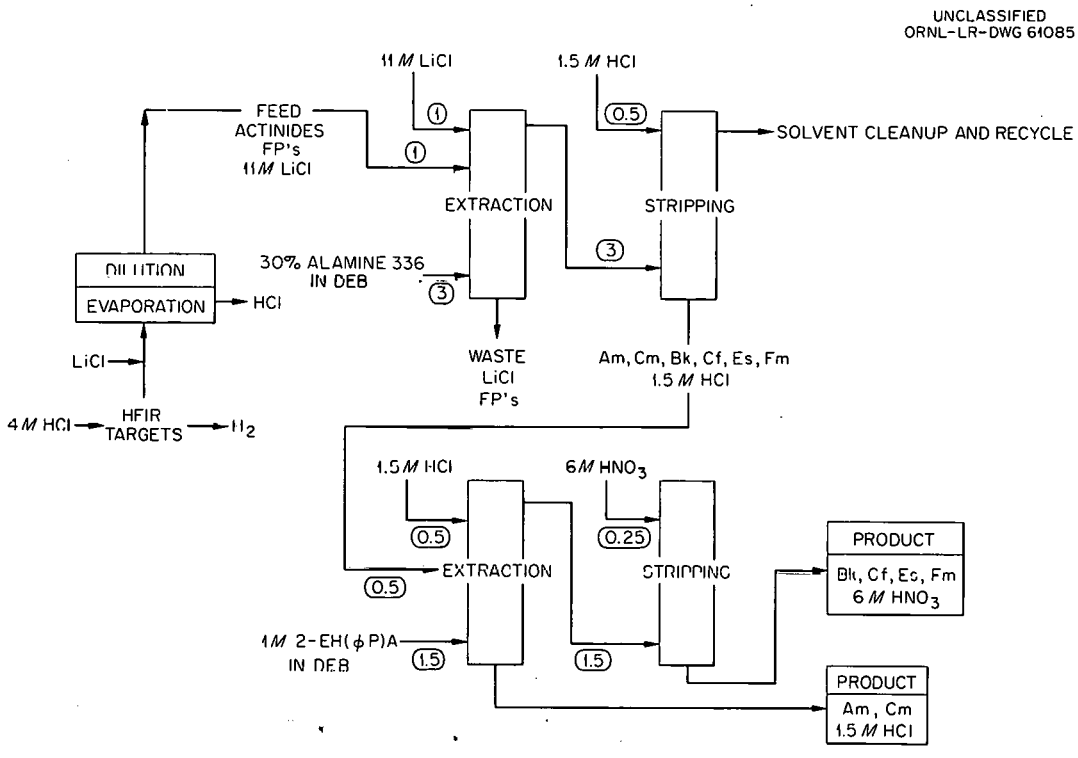

Fig. 11.6. Flowsheet for Processing HFIR Targets. Circled numbers are flow ratios.

product. If einsteinium and fermium are present they will also be extracted. The americium-curium remaining in the aqueous raffinate will be recycled for target fabrication and further irradiation.

After the aluminum-actinide oxide targets are dissolved in dilute HCl, the solution can be adjusted to 11 *M* LiCl-0.05 *M* HCl and extracted under the same conditions as those given for separating americium-curium from rare earths (Fig. 11.3). All the trivalent actinides are extracted into the tertiary amine and stripped from it with 1.5 *M* HCl. The berkelium, californium, einsteinium, and fermium are extracted from the 1.5 HCl solution by 1 *M* mono-2-ethylhexyl phenylphosphonic acid in diethyl benzene with feed/scrub/solvent flow ratios of 1/1/3. The americium-curium fraction is recovered from the raffinate; the berkelium, californium, einsteinium, and fermium are stripped from the solvent with 6 *M* HNO_3 in a minimum of 5 stages and a/o flow ratio of 0.5/3.

Laboratory-scale demonstration of the phosphonic acid extraction has been limited by berkelium-californium availability, but feasibility of the system was demonstrated with a countercurrent extraction of feed containing 1×10^3 d/m Cf^{252} and 1×10^8 d/m Cm^{242} in 1.7 *M* HCl. The scrub was 1.7 *M* HCl and the solvent 1.0 *M* mono-2-ethylhexyl phenylphosphonic acid in xylene with 3 scrub and 3 extraction stages and scrub/feed/solvent flow ratios of 1/1/3. Californium recovery was 99 ± 1% and the decontamination factor from curium was 10^3.

Distribution coefficients between 1.0 *M* 2-EH(ϕP)A in xylene and 2.0 *M* HCl show a separation factor between curium and californium of about 100 and a berkelium-curium separation factor of the order of 25 (Fig. 11.7). In 2 *M* HCl vs. 1 *M* 2-EH(ϕP)A, the americium, curium, berkelium, californium, einsteinium, and fermium distribution coefficients were 0.008, 0.01, 0.25, 1, 1.3, 3.2, respectively. Distribution coefficients were inversely third power dependent on the hydrogen ion concentration and directly dependent on the third power of the organic concentration. Under the above conditions, zirconium will be extracted quantitatively, but ruthenium distribution coefficients are less than 0.01.

A solvent extraction process to separate transcalifornium elements is not available, as is evidenced by the distribution coefficients of californium, einsteinium, and fermium in the amine-LiCl system and the 2-EH(ϕP)A-HCl system (Figs. 11.4 and 11.7). If a satisfactory solvent system cannot be found, chromatographic elution with ammonium alpha hydroxy-iso-butyrate from cation exchange resin can be used to separate Cf, Es, and Fm (refs 2,3).

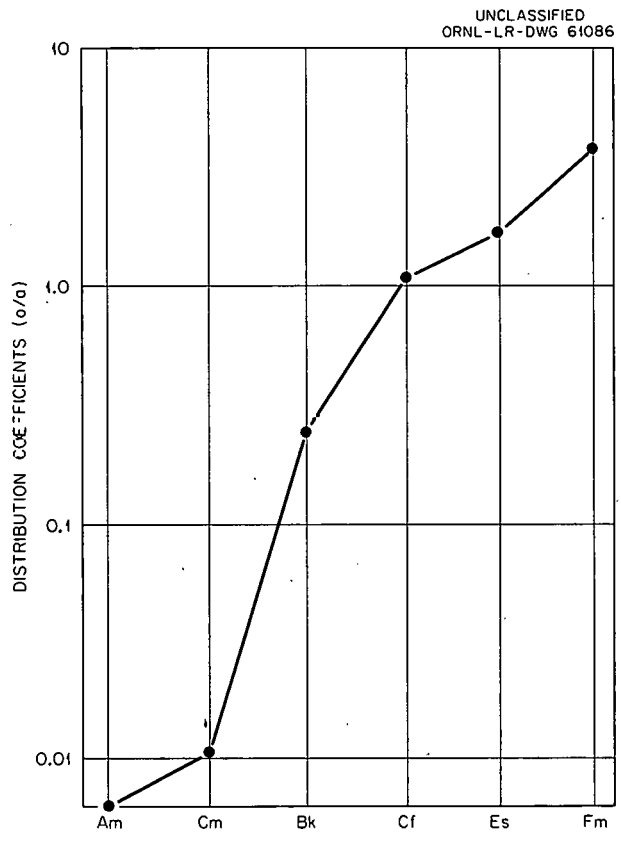

Fig. 11.7. Extractability of Actinides Into 1 *M* 2-EH(ϕP)A in Xylene from 2.0 M HCl.

Berkelium and californium were separated by solvent extraction after oxidizing the berkelium to Bk(IV) with 0.1 *M* $KBrO_3$ in 10 *M* HNO_3 and extracting with di-2-ethylhexyl phosphoric acid (D-2-EHPA). Distribution coefficients for Bk(IV) and Cf(III) in the system 10 *M* HNO_3–0.1 *M* $KBrO_3$ vs 1.0 *M* D-2-EHPA in *n*-heptane were 100 and 0.001, respectively. A single stage separation factor of $\sim 10^5$ was obtained.

[2] G. R. Chappin, B. G. Harvey, and S. G. Thompson, *J. Inorg. Nucl. Chem.*, 2 66 (1956).

[3] H. Louise Smith and Darleane C. Hoffman, *J. Inorg. Nucl. Chem.*, 3 243 (1956).

11.4 HFIR TARGET FABRICATION DEVELOPMENT

The purpose of the target array is to introduce heavy isotopes of plutonium, americium, and curium into the flux-trap region of the HFIR in such a way that fission heat is dissipated and fission products are retained in the targets. The array will be a cluster of 31 rods, each measuring $\frac{3}{8}$ in. o.d., with an actinide oxide–aluminum cermet core 20 in. long. Calculations of the target heat-transfer requirements showed that a metallurgical bond will not be required between the core and the aluminum cladding. Therefore the target fabrication sequence may be as follows: blending actinide oxides and aluminum powder, pressing pellets about $\frac{1}{4}$ in. dia by $\frac{1}{2}$ in. long, loading the pellets into an aluminum tube, seal welding an aluminum end plug, and collapsing the jacket onto the pellets to improve heat transfer. Development of HFIR target fabrication methods is the joint responsibility of the Chemical Technology and Metallurgy Divisions.[4]

Scouting experiments showed that actinide oxides can be prepared by either hydroxide precipitation with urea followed by calcination at 400°C or oxalate precipitation followed by calcination at 600 to 700°C. The dimensional stability of aluminum-cermet pellets was demonstrated with cerium oxide, and the dimensional stability of Al-PuO_2 pellets containing 10 vol % PuO_2 was confirmed by holding at temperatures as high as 600°C for 100 hr.

The quantity of the heavy-element isotopes in each target will vary with the composition (Tables 11.2 and 11.4), as limited by a total heat generation rate (due to fission of Pu^{239}, Pu^{241}, Cm^{245}, Cf^{252}, and Cf^{254}) of 24.2 kw per rod, and by a maximum spontaneous fission rate of the californium isotopes to produce no more than 300 watts per rod if stored in air or 600 watts per rod if stored in water.

11.5 DESIGN FEATURES OF THE TRU FACILITY

At the present time the Transuranium Facility design includes twelve shielded cells, a shielded transfer area, and a space for off-gas equipment and filters (Fig. 11.8a and b). Each cell will contain, at viewing window level, an alpha-tight box or cubicle sized to utilize the maximum reach of Model 8 manipulators. Behind this cubicle and separated by a light inner shielding wall, there will be a deeper cell space (Fig. 11.8c) for the tanks and process vessels that are not expected to require excessive maintenance; all valves, pumps, samplers, operating equipment, and process line disconnects will be enclosed in the cubicles. Maintenance within the cubicles will be done with Model 8 master-slaves; large pieces of equipment will be removed from inside the cubicle via a sealed, shielded caisson in such a way that the inside of the cubicle will not be opened to any space other than the inside of the caisson. Small pieces of equipment, samples, supplies, etc. can be introduced through either of two conveyor systems, which will move material in and out of the cubicles without breaking the alpha seals, via a sealed can, to be opened only after a second seal is made to the bottom of the cubicle.

Process tanks, storage vessels, and other equipment for which little maintenance is anticipated will be located in a pit behind the cubicle but still within the main shield. The process equipment in the cubicle will be connected with special gasketless remote disconnects to the tanks; all connections, both process and service lines, will be made by remote disconnects. The tank pit will be partially shielded from the cubicle by a removable 2-ft-thick wall of magnetite concrete to make it possible to do maintenance on either the cubicle (with the caisson) or the tanks. The tank pit will be flooded with water for underwater maintenance, and direct manipulation will be through the cell roof plugs. In the space behind the cubicle and over the tank pits, a General Mills manipulator can be inserted through a roof plug if needed. This manipulator will be removable and will be moved from cell to cell by the building crane in a sealed caisson.

The cell block is divided into 12 cells, each separated from the others by 2 ft of shielding to reduce the penetrating radiation contribution from one operation cell to the next, so that maintenance can be accomplished without decontamination of all cells. The sealed cubicles within each cell prevent the spread of contamination.

[4] E. S. Bomar and T. D. Watts, "Fabrication of HFIR Targets," *Met. Div. Ann. Progr. Rept. May 31, 1961*, ORNL-3160.

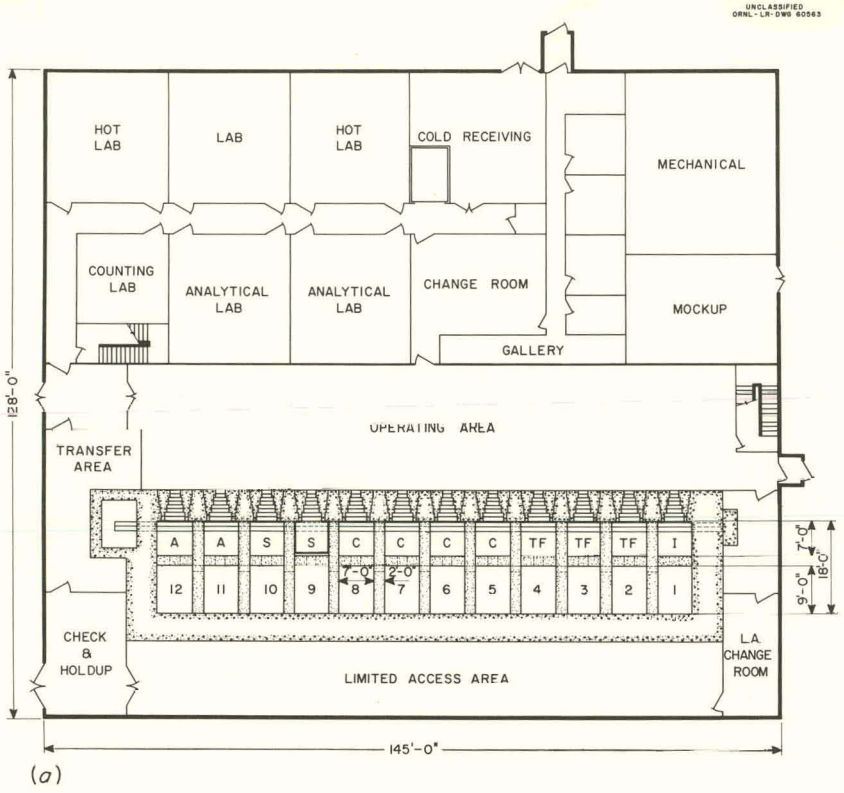

(a)

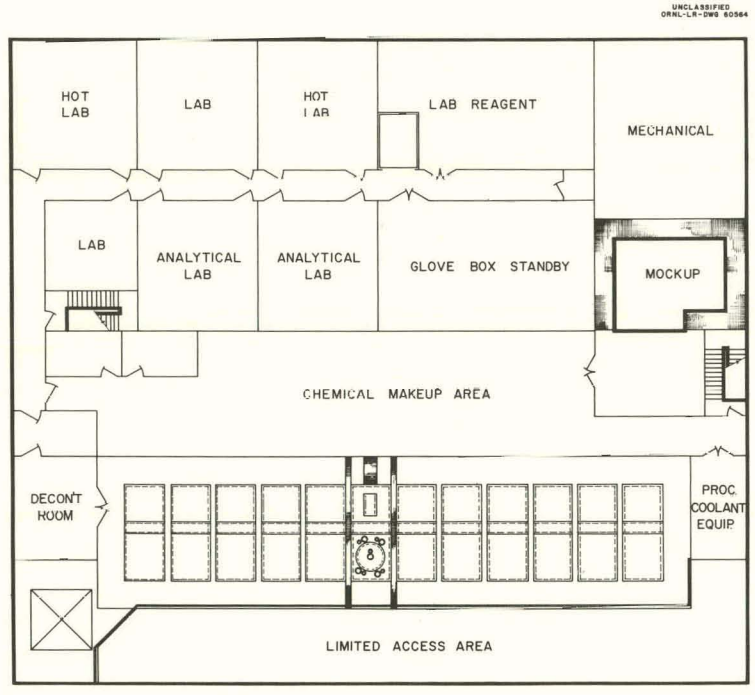

(b)

Fig. 11.8. TRU Facility Plan. (*a*) First floor, (*b*) second floor,

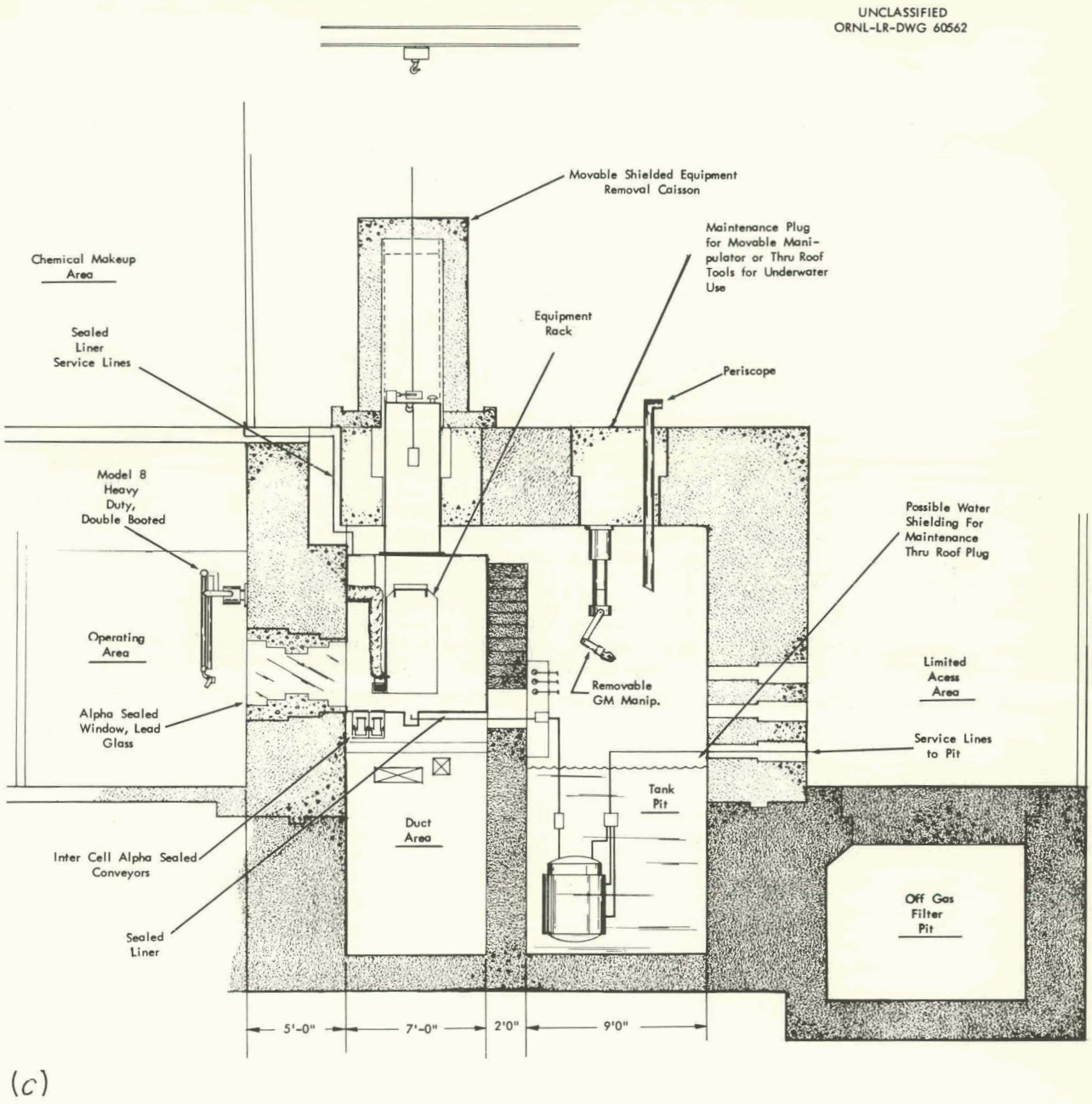

(c)

Fig. 11.8 (continued). (c) cell for vessels not requiring excessive maintenance.

Because of the extreme radiation intensity of the isotopes handled and the very low probable maximum permissible concentrations in air, three separate air systems for the in-cell area are provided: (1) a vessel vent system complete with scrubber, rough filter, absolute filter and discharged to another double-filter system; at highest vacuum; (2) a cubicle ventilation system, recirculated, with rough filters, absolute filters, chilling coils and small bleed-off to double-filter system; at higher vacuum than cell ventilation system; (3) cell ventilation system, once through air moving outside cubicles, all air inlets with absolute filters and having blowback preventers;

at lowest vacuum. The limited access area has a separate ventilation system, operated at a lower than atmospheric pressure. The building is sealed and meets the requirements for secondary containment established at ORNL. Two cells, labeled A in Fig. 11.8a, are for analytical use. Two cells, labeled S, are for special separations. Four cells, labeled C, are provided for chemical process use. Target fabrication will be performed in three cells, labeled TF; targets, free of external contamination, will be inspected and nondestructively tested in one cell, labeled I. Five nonshielded analytical laboratories are provided, plus a counting room; two cold labs, supporting four alpha labs for lower activity chemical work, and possibly for Pu^{242} target rod fabrication, are included.

12. PRODUCTION OF URANIUM-232

Two pure samples of U^{232} are to be prepared for nuclear cross-section measurements as part of a joint program of the USAEC and the UKAEA. Approximately 50 g of Pa^{231} will be irradiated in the ORR to provide the U^{232}; one sample will contain approximately 20 mg of U^{232} with < 100 ppm of U^{233}, and the other will contain approximately 1 g of U^{232} with < 1% U^{233}. The UKAEA has loaned 50 g of Pa^{231}, which will be decontaminated and converted to oxide upon completion of the U^{232} program.

The protactinium irradiation targets will be prepared as Pa_2O_5-Al cermet clad in aluminum, and the five capsules will be irradiated at 1×10^{14} n cm^{-2} sec^{-1}. Chemical processing by ion exchange to recover and purify both the protactinium and uranium will be carried out in a sealed, heavily shielded cell in Bldg. 4507. Uranium-232 cross-section targets will be prepared as UO_2-Al cermets.

12.1 CALCULATIONS OF Pa^{231} IRRADIATION

Major reactions occurring during neutron irradiation of Pa^{231} are:

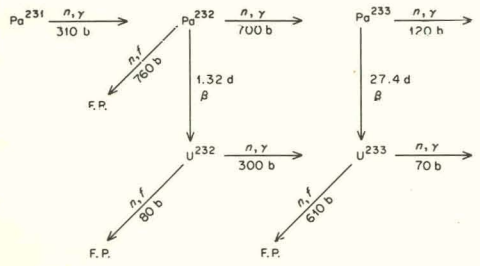

Both U^{232} production and the U^{233}/U^{232} ratio are functions of flux, irradiation time, and decay time. Calculations for irradiation at a flux of 1×10^{14} n cm^{-2} sec^{-1} are shown in Fig. 12.1. An irradiation time of 7 hr at 1×10^{14} n cm^{-2} sec^{-1} and a decay time of 20 to 50 hr can be used to produce 20 mg of U^{232} containing < 100 ppm of U^{233}. An irradiation time of 200 hr at 1×10^{14} n cm^{-2} sec^{-1} and a decay time of 65 to > 140 hr can be used to produce 1 g of U^{232} containing < 1% U^{233}.

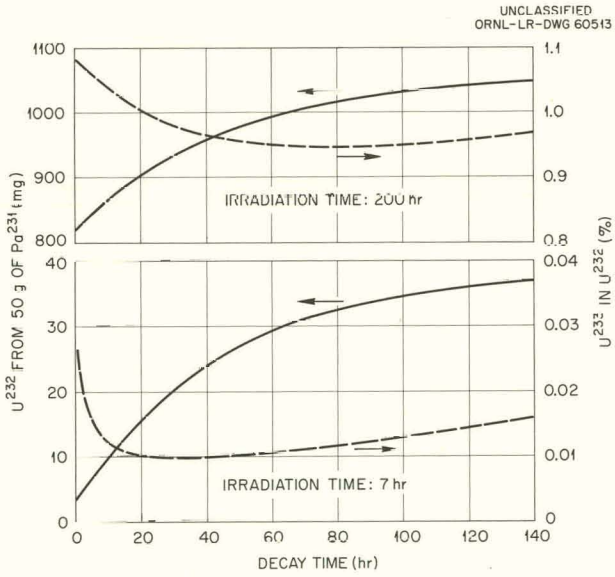

Fig. 12.1. Uranium-232 Production and U^{233} Contamination Resulting from Irradiation of 50 g of Pa^{231} at a Flux of 1×10^{14} n cm^{-2} sec^{-1}.

12.2 PROCESS DEVELOPMENT

Uranium and protactinium will be recovered and separated from fission products by anion exchange (Fig. 12.2). The aluminum jackets and matrix will be selectively dissolved in hydrochloric acid, leaving most of the Pa_2O_5, uranium, and fission products undissolved. Trace amounts of protactinium and uranium that are dissolved will be loaded on the anion exchange resin. Both protactinium and uranium form anion complexes with excess chloride ions, which are strongly sorbed on Dowex-1 resin. The protactinium can be preferentially eluted from Dowex-1 resin by 8 *M* HCl containing 0.4 *M* HF. The fluoride greatly decreases the sorption of protactinium without eluting the uranium.

The Pa_2O_5, along with the remaining uranium and fission products, will be dissolved in hydrochloric acid containing hydrofluoric acid. This solution will be passed through the same Dowex-1 resin bed and the effluent saved for protactinium recovery. The uranium will be sorbed on the column and eluted with dilute nitric acid. The basis of this procedure was developed by Kraus and Moore.[1]

The flowsheet has been checked in the laboratory through this stage. An unirradiated target, containing 100 mg of Pa_2O_5 and 8 mg of $U_3^{233}O_8$ mixed with aluminum powder, was dissolved, loaded onto a Dowex-1 column, and eluted. The waste solution, the uranium product solution, and the protactinium product solution were analyzed by alpha pulse analysis. The uranium product contained 0.04% of the protactinium, the protactinium product contained < 10% of the uranium (limit of detection), and the waste solution contained < 0.3% of the protactinium and < 3% of the uranium (limits of detection).

The effluent from the resin column, containing the protactinium and some fission products, will be purified by a second ion exchange step. Sufficient aluminum ions will be added to the solution to break the fluoride-protactinium complex, and

[1] K. A. Kraus and G. E. Moore, *J. Am. Chem. Soc.* 73, 2900 (1951).

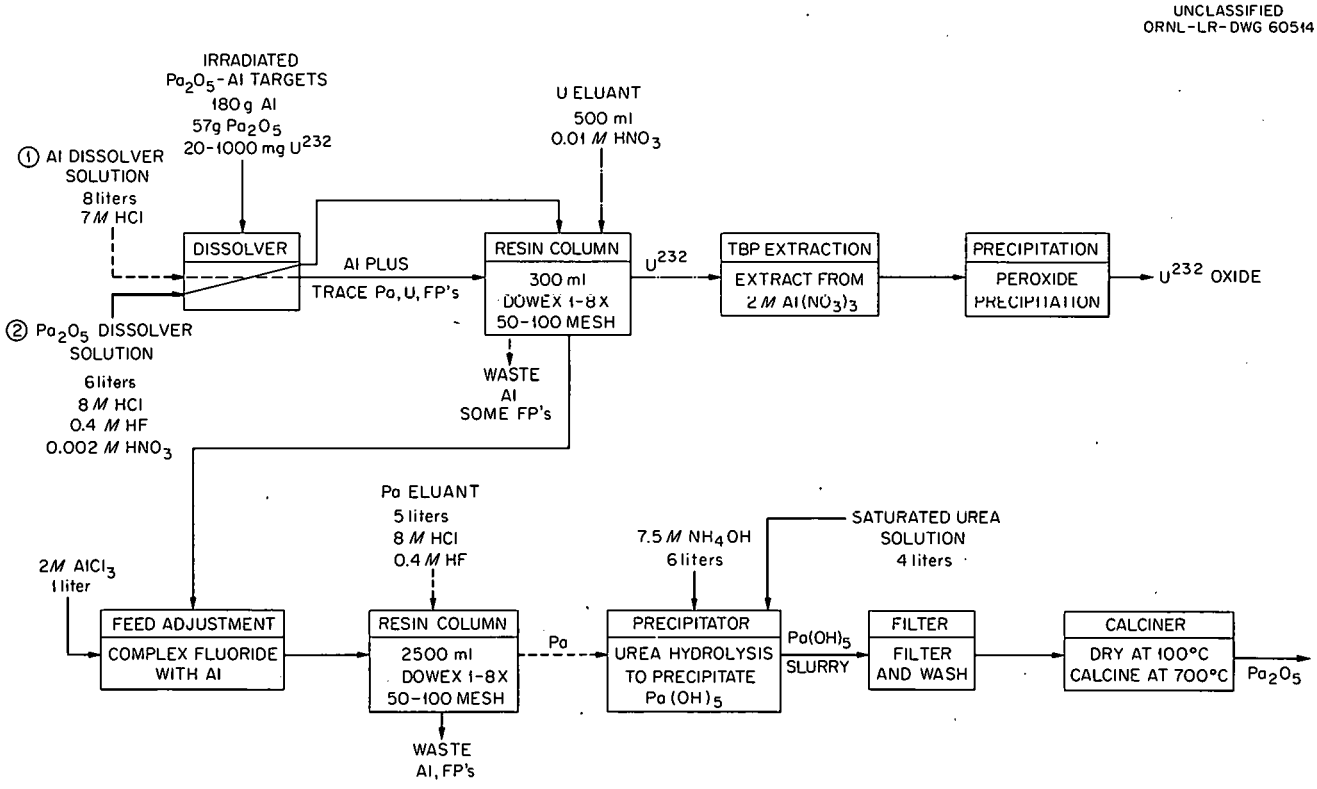

Fig. 12.2. Recovery of Protactinium and U^{232} from Irradiated Pa_2O_5.

the protactinium will be loaded onto another Dowex-1 resin column. Most of the fission products and other impurities will pass into the effluent. After elution of the protactinium with a hydrochloric acid–hydrofluoric acid mixture, the protactinium will be precipitated as $Pa(OH)_5$, filtered, washed, dried, and calcined, by the procedure used to prepare the original Pa_2O_5.[2]

[2]N. Jackson, F. J. G. Rogers, and J. F. Short, *Purification of Pa^{231}*, AERE-R-3311 (April 1960).

The uranium product solution will be purified and concentrated by a TBP solvent extraction cycle, with aluminum nitrate as a salting agent. After being stripped, the uranium will be precipitated as the peroxide and ignited to the oxide.

Laboratory studies indicate that the primary separation of the uranium and protactinium could be accomplished by TBP extraction from a chloride system if the protactinium is complexed with fluoride ions. However, the solvent extraction procedure requires large volumes of solutions (Fig. 12.3) compared with the anion exchange procedure described above.

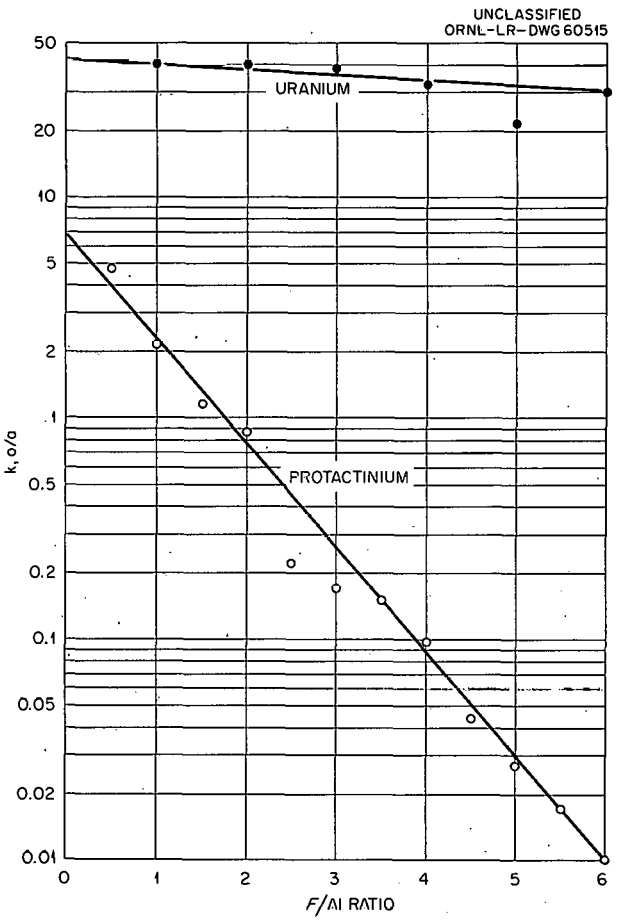

Fig. 12.3. Extraction Coefficients of Uranium and Protactinium Into 30% TBP from 8.0 *M* HCl–0.5 *M* $AlCl_3$ as a Function of Fluoride Concentration.

13. URANIUM PROCESSING

A solvent extraction process (Fig. 13.1) for purifying uranium concentrates, alternative to the tributyl phosphate (TBP) extraction process, showed promise in preliminary mixer-settler tests. Uranium was extracted with a phosphonate (diamylamyl or dibutylbutyl) and was precipitated from the solvent as ammonium uranyl tricarbonate (AUT) by contact with NH_4NO_3-$(NH_4)_2CO_3$ solution saturated with uranium. The AUT product settled and filtered rapidly and was readily converted to UO_3 by calcination at 400°C. The higher extraction power of the phosphonate compared to TBP

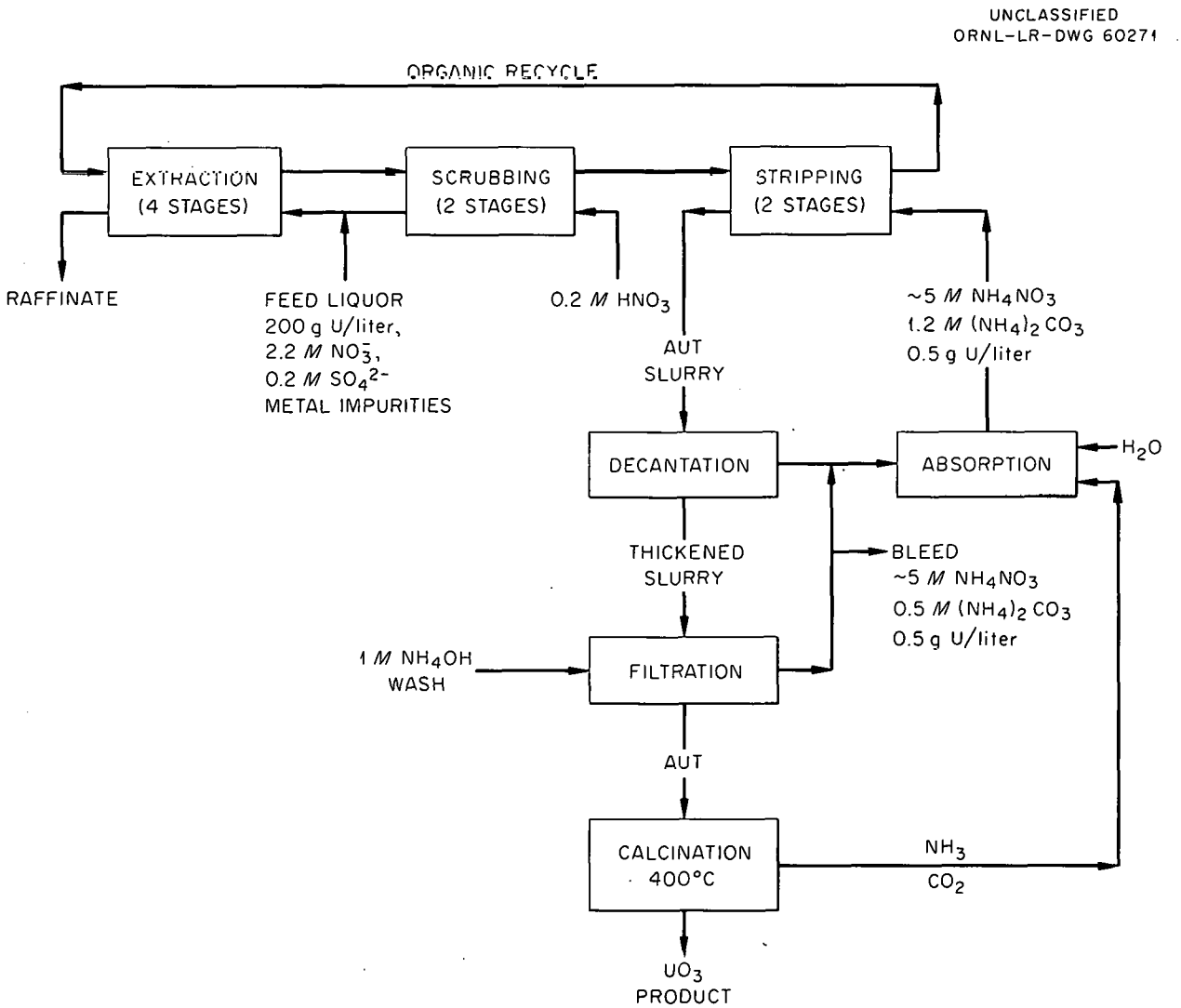

Fig. 13.1. Flowsheet for Purification of Uranium Concentrates. Organic: 1 M diamylamyl phosphonate in Amsco 123-15 diluent. Flow ratios: organic/feed liquor/scrub/recycle solution/bleed = 1/0.55/0.2/2/0.17.

permits extraction at relatively low nitrate salting (~0.5 *M* excess nitrate), and handling of the product appears simpler than evaporation and calcination of uranyl nitrate solution, which is the present product of TBP processes. A possible disadvantage of the process is the low tap density (~1.7 g/cc) of the calcined AUT.

A solvent extraction method was developed for recovering nitrate (as nitric acid) from waste streams. Such a process is applicable to uranium refineries and other plants, offering, as a secondary objective, a means of decreasing nitrate pollution of rivers. The process (Fig. 13.2) involves extraction of nitrate with a secondary amine, stripping with a lime slurry to produce calcium nitrate, and reaction of the latter with sulfuric acid to form nitric acid and waste calcium sulfate.

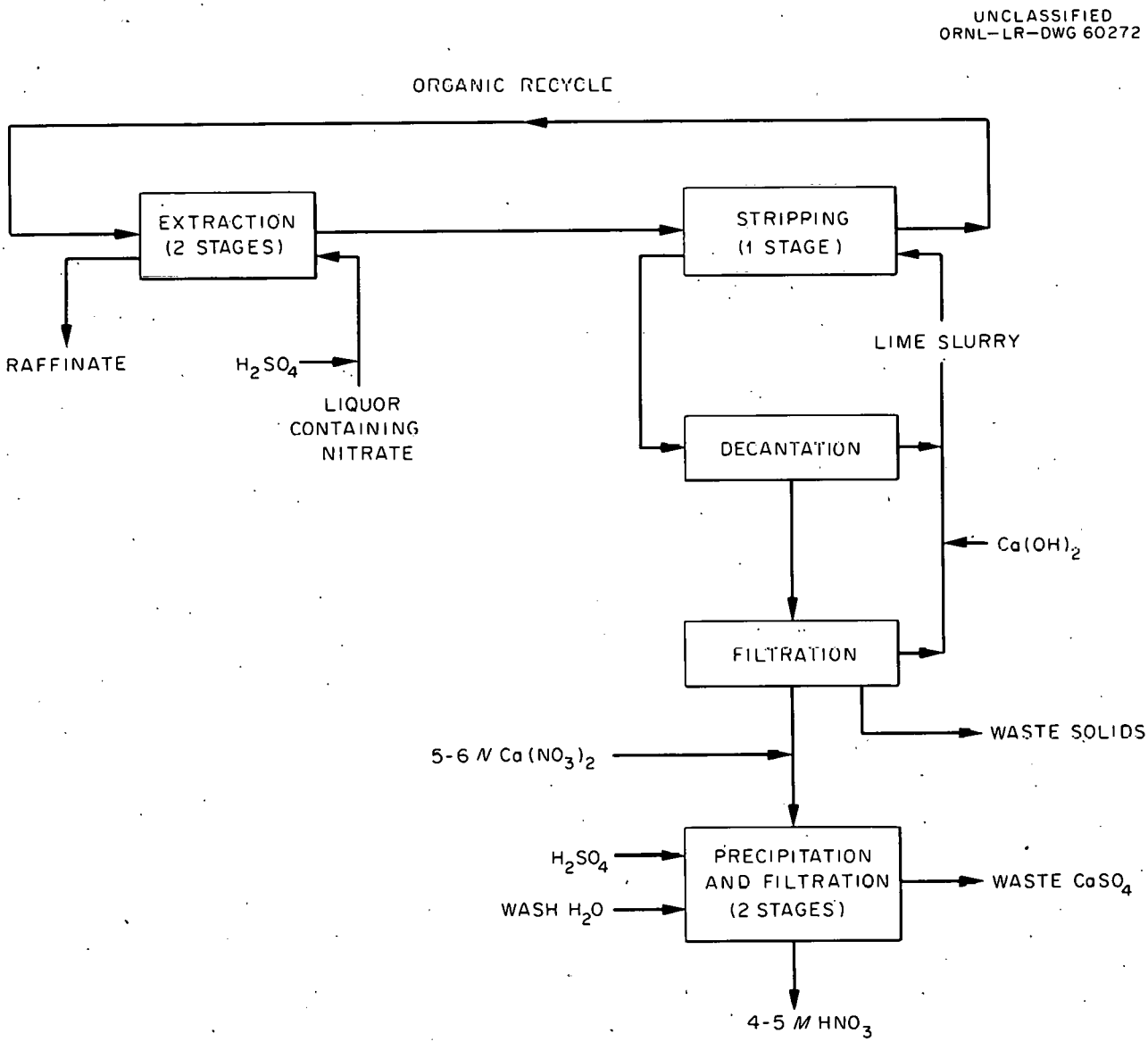

Fig. 13.2. Recovery of Nitric Acid from Waste Liquors. Organic: 0.3 *M* Amberlite LA-1 in Amsco 123-15–tridecanol diluent.

14. FISSION PRODUCT RECOVERY

The objective of this program is the development of processes for recovering megacurie quantities of fission products from reactor-fuel processing wastes. There is evidence that large quantities of these elements will be required for various industrial applications. Relatively small amounts have been recovered in the past, principally by batch precipitation techniques, and the newer technologies, such as solvent extraction and ion exchange, may offer better methods for commercial applications. Since solvent extraction shows promise of greater versatility, initial emphasis is being placed on this technique. Priority has been placed on Sr^{90}, for which there is already a large demand, and secondary attention is being given to rare earths, cesium, and zirconium-niobium.

14.1 SOLVENT EXTRACTION

Strontium and Rare Earths

As a result of further studies the four-cycle flowsheet[1] for recovering strontium and rare earths from adjusted Purex wastes by extraction with di-(2-ethylhexyl) phosphoric acid (D2EHPA) was revised to a three-cycle flowsheet (Fig. 14.1). In batch tests and in one continuous run with nonradioactive solutions in miniature mixer-settler equipment, the chemical and physical operability of the new flowsheet was excellent, with no emulsions or precipitates being formed in any cycle.

In the first cycle of the continuous run the strontium and rare earths were extracted and separated from iron. After 17 hr operation, 4.8% of the iron in the feed was being extracted but only 0.02% was being stripped into the first-cycle product, giving an iron separation factor of 4.4×10^3. This is better than the factor of 1.4×10^3 predicted from batch tests. The iron in the solvent was easily removed with sodium carbonate–sodium tartrate solution.

In the rare earth–strontium partitioning and the rare earth–stripping steps, which comprise the second cycle, 98.2% of the rare earths was recovered as product, 1.8% being lost to the used organic stream. Separation factors were: rare earths from sodium, 9×10^3; rare earths from iron, 1.3×10^2. Strontium in the rare earth product was below the level of analytical detection. The rare earths were concentrated by a factor of 30.

In the third cycle essentially 100% of the strontium was recovered and concentrated by a factor of 30. The strontium-iron separation factor was 100 and the strontium-sodium, 130.

The miniature mixer-settler equipment was installed in a hot cell in Bldg. 4507. Runs on actual Purex waste are scheduled as soon as containment changes in the building have been completed.

Cesium

Cesium can be extracted from adjusted Purex waste solutions by a solvent comprised of sodium tetraphenyl boron in hexone.[2] The cesium is stripped from the organic phase with dilute acid, but contact with acid converts the $Na(C_6H_5)_4B$ to a form that does not extract cesium, and the solvent therefore cannot be recycled.

Without extractant recycle, a satisfactory process might be devised if the organic phase could be loaded to about 1 g of cesium per liter of 0.3 *M* $Na(C_6H_5)_4B$ in hexone and if the $Na(C_6H_5)_4B$ could be obtained commercially at about $5 per pound. In studies thus far the organic solubility of the cesium has been limited to 0.3 g per liter of 0.3 *M* $Na(C_6H_5)_4B$ in hexone and tentative price quotations for $Na(C_6H_5)_4B$, currently a speciality chemical, range from $50 to $180 per pound. Other vendors are being contacted for $Na(C_6H_5)_4B$, and other diluents and diluent additives are being studied for the possibility of increasing the solubility of the cesium complex in the organic phase. Search is also continuing for a

[1] *Chem. Tech. Ann. Progr. Rept. Aug. 31, 1960*, ORNL-2993, Fig. 14.1.

[2] *Ibid.*, p 146.

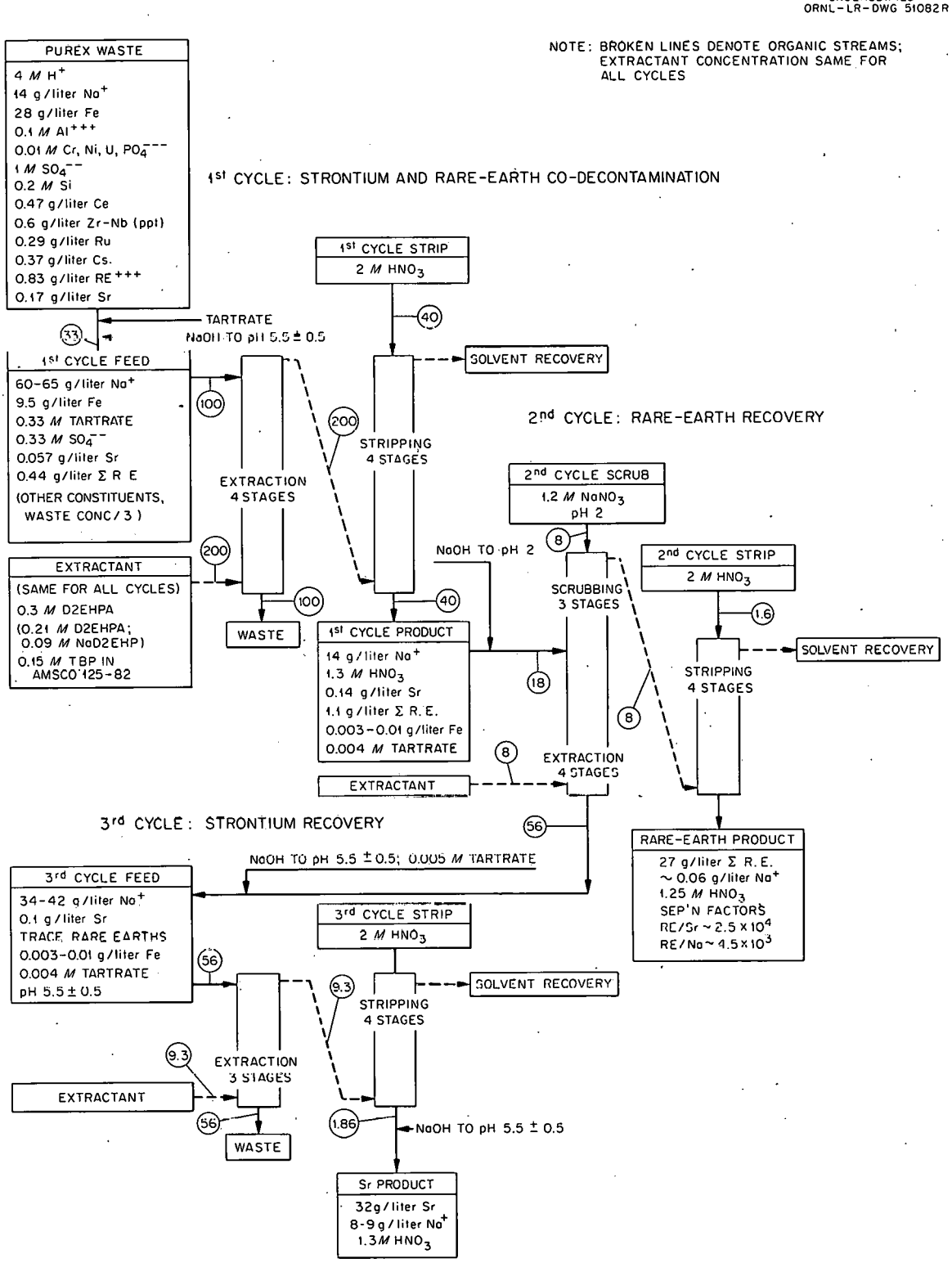

Fig. 14.1. Recovery of Strontium and Rare Earths from Purex Wastes by Extraction with D2EHPA. (Circled numbers are volume flow ratios.)

stripping method that will not destroy the cesium extraction ability of the $Na(C_6H_5)_4B$.

Zirconium-Niobium

In preliminary tests zirconium and niobium were extracted from acidic (4 *M* H^+) simulated Purex waste by 0.3 *M* D2EHPA in Amsco 125-82, a hydrocarbon diluent. Since the extraction was slow (65 to 75% extraction in 1 to 2 hr contact with an equal volume of solvent), a batch process is suggested. The extracted zirconium was stripped from the solvent with 1 *M* oxalic acid solution.

14.2 PRECIPITATION

Strontium

In the fission product production program at Hanford, strontium is recovered from Purex waste by a series of precipitation-redissolution steps, which ultimately yield a solution containing strontium along with appreciable amounts of calcium, iron, and lead. Since the presence of lead is somewhat troublesome, the possibility of further purification of strontium by additional precipitations was briefly examined.

The lead was separated by a single precipitation with ammonia, and 80% of the strontium was recovered by sequential precipitation with NH_3, Na_2CO_3, NaOH, and Na_2CO_3 (Fig. 14.2). Over-all separation factors were: Sr from Ca ~225, Sr from Fe $\sim 8 \times 10^3$, and Sr from Pb ~360 to yield a product in which the iron, lead, and calcium impurities were <3 wt % of the strontium.

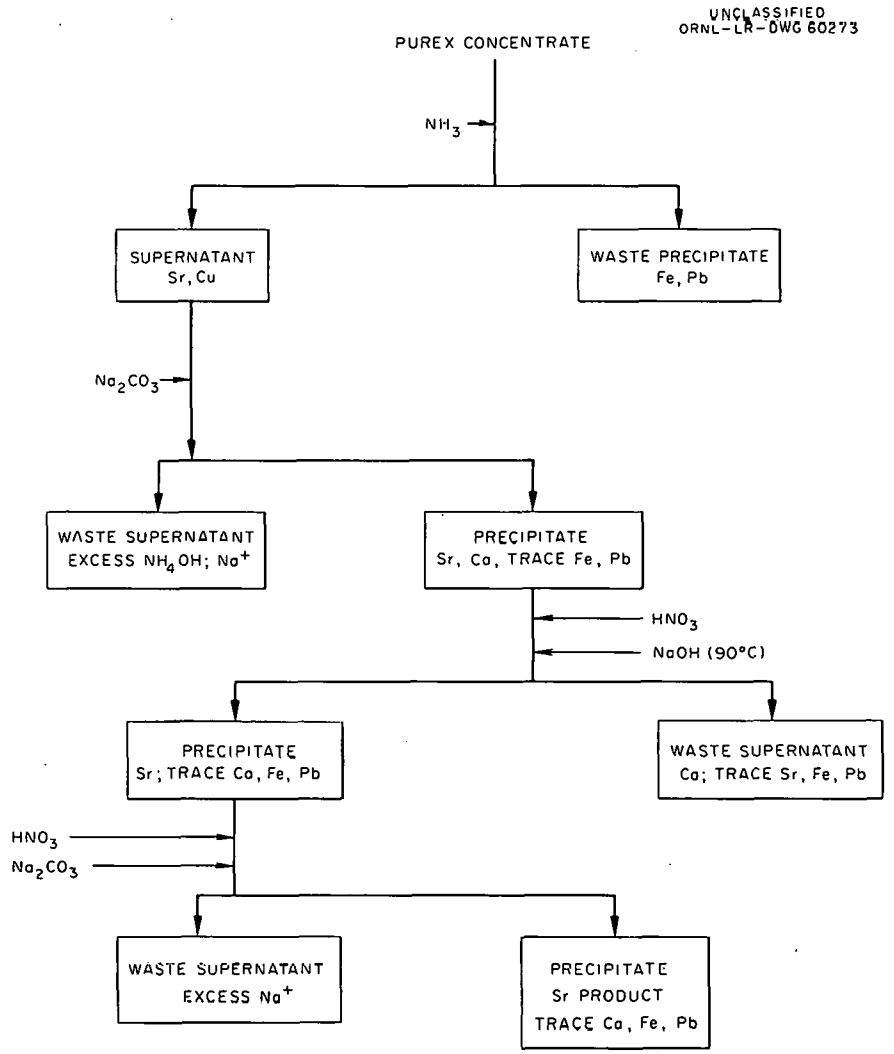

Fig. 14.2. Recovery of Sr^{90} from Purex Waste Concentrate by Sequential Precipitation.

14.3 ION EXCHANGE

A previously reported cation exchange scheme[3] for recovering strontium from Purex waste[4] did not appear competitive because the resin capacity for strontium was at least 100-fold less than for other cations in the waste. Direct precipitation of strontium followed by redissolution, prior to ion exchange, is interfered with by the 1 *M* sulfate ion in Purex waste.

In laboratory studies, >85% of the sulfate in Purex waste was precipitated by adding excess ferric ion and then sufficient fuming nitric acid to give a final nitric acid concentration of 50 to 55%.

Data[2] on the solubilities (Fig. 14.3) of the nitrates of strontium and of the chief cationic impurities in Purex waste, Al^{3+} and Fe^{3+}, indicated that >90% of the strontium could be precipitated in 80% HNO_3 with <20% of the aluminum and <1% of the iron, but this step has not yet been investigated. The strontium precipitate thus formed would be dissolved in nitric acid and the strontium recovered from the solution by ion exchange.

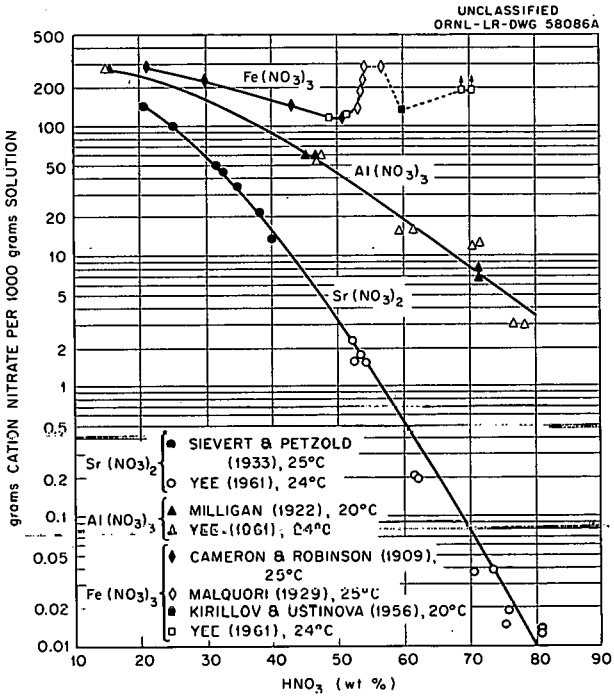

Fig. 14.3. Solubility of $Sr(NO_3)_3$, $Al(NO_3)_3$, and $Fe(NO_3)_3$ as a Function of Nitric Acid Concentration. Conditions: 100 ml of solution with excess salt equilibrated 24 and 48 hr; samples of solution analyzed at each time interval. (See references 5–9.)

[3] *Ibid.*, Sec 14.2.

[4] Synthetic Purex waste composition: 6.1 *M* NO_3^-, 1.0 *M* SO_4^{--}, 4.6 *M* H^+, 0.6 *M* Na^+, 0.5 *M* Fe^{3+}, 0.1 *M* Al^{3+}, 0.01 *M* Cr^{3+}, 0.01 *M* Ni^{++}, 0.01 *M* UO_2^{++} plus stable elements equivalent to 3.75 g of gross fission products per liter.

[5] A. Sieverts and W. Petzold, *Z. anorg. u. allgem. Chem.* 214, 27–32 (1933).

[6] L. H. Milligan, *J. Am. Chem. Soc.* 44, 567 (1922).

[7] F. K. Cameron and W. O. Robinson, *J. Phys. Chem.* 13, 251 (1909).

[8] G. Malquori, *Atti accad. Lincei* (6) 9, 324 (1929).

[9] I. P. Kirillov and Z. A. Ustinova, *Trudy Ivanovsk. Khim.-Techol. Inst.* 1956, No. 5, 59.

15. THORIUM RECOVERY FROM GRANITE

In the long-range future, nuclear fuel supplies for power production will inevitably depend on low-grade sources, since high-grade reserves of uranium and thorium are extremely limited. Information on the extent and probable treatment costs of low-grade thorium sources is being obtained, with the initial effort centered on granite. Preliminary studies on granite rock were reported by Brown and Silver.[1]

15.1 SAMPLE COLLECTION

Approximately 200 granite samples, for determination of thorium and uranium content and for

[1] H. Brown and L. T. Silver, *The Possibilities of Securing Long-Range Supplies of Uranium, Thorium, and Other Substances from Igneous Rocks*, P/850, Proc. Intern. Conf. on Peaceful Uses of Atomic Energy, Geneva (1955), Vol. 8, p 129.

process studies, were collected[2] from major granitic bodies in the western United States and New England. Many of the samples already analyzed contain thorium at a concentration 2 to 7 times the 12 ppm value cited for "average grade" granite. Although sampling is sparse, the Conway granite of New Hampshire may represent an important reserve of thorium (and uranium). Fifteen samples of this granite ranged from 13 to 76 ppm thorium (average 47) and 2 to 16 ppm uranium (average 10). A more extensive survey of the Conway formation is planned with a portable transistorized gamma-ray spectrometer. Granite samples from other areas, some representing extremely large batholiths, e.g., Pikes Peak, were well above "average" in thorium content. Lateritic soils and extrusive (volcanic) rocks are also being examined as potential low-grade sources of thorium, although relatively few samples have been collected. A sample of Arkansas bauxite analyzed 70 ppm thorium, and several volcanic rock samples from Nevada and New Mexico contained 18 to 40 ppm.

[2]By Rice University under subcontract to ORNL.

15.2 ACID LEACH–SOLVENT EXTRACTION METHODS

Because of large variations in mineralization, granite from different sites responded very differently to treatment. Initial laboratory studies were concentrated on an acid leach–solvent extraction flowsheet. Thorium recoveries (Table 15.1) in sulfuric acid leaching ranged from 30 to 85% for 16 samples, poor recoveries in some cases being attributed to the presence of part of the thorium in minerals (zircon, monazite) that are impervious to a dilute acid leach. Usually a relatively high acidity (pH <0.7) was needed for

Table 15.1. Estimated Total Costs for Recovering Thorium and Uranium from Granite

Granite Sample	Head Conc'n. (ppm)		Recovery in Leaching* (%)		Acid Consumption (lb H_2SO_4 per ton ore)	Estimated Recovery Cost** per lb Th + U
	Th	U	Th	U		
Silver Plume, Colo.	95	3.5	31	26	91	75
	92	3.5	37	29	104	70
Conway, N.H.	72	14	85	65	78	31
	71	16	85	73	91	32
Boulder Creek, Colo.	71	5	55	62	75	50
Colorado	40	4.5	29	16	97	190
Boulder batholith, Colo.	33	6	50	25	52	110
	20	4.5	49	31	82	200
	8	1.5	61	24	101	450
Pikes Peak, Colo.	24	4	71	33	113	135
Cathedral Peak, Calif.	23	10	46	50	99	150
Dillon Tunnel, Colo.	22	8	41	50	97	180
Enchanted Rock, Tex.	21	4	66	13	120	180
Washington	16	3.5	60	45	89	210
Phillipsburg batholith	12	3	32	43	94	450
Minnesota	12	4.5	35	20	131	510

*6–24 hr leaching with 2.0 *N* H_2SO_4 at 60% pulp density.

**Assume $0.68 direct mining costs per ton of granite in each case.

rapid and efficient dissolution of the soluble thorium fraction, and acid consumption was high. Recoveries were similar with sulfuric, nitric, and hydrochloric acids and were not improved by grinding smaller than −48 mesh.

A double leach with sodium carbonate–sodium bicarbonate solutions at 95°C dissolved ~70% of the thorium from Conway granite. Under the same conditions, recoveries from Pikes Peak and Boulder samples were < 15%.

Both sulfuric acid and sodium carbonate–sodium bicarbonate solutions were completely ineffective in dissolving thorium from a pumice sample (50 ppm thorium) from Lipari, Italy. Two samples of bauxite showed better response to acid leaching, although recoveries were still poor (20–45%) and acid consumption was extremely high. Recoveries by carbonate leaching of bauxites were < 10%.

Thorium was extracted ($E_a^\circ > 1000$) from granite sulfate leach liquors with primary amines; phase separation was rapid.

15.3 COST STUDIES

A preliminary cost estimate[3] (Table 15.2) for treating granite by an acid leach–solvent extraction flowsheet showed costs ranging from $3.61 to $5.30 per ton of granite, variation within this range depending primarily on differences in acid consumption and assumed ore/waste ratios for different granite formations. Costs for recovery of thorium from the 16 granite samples studied thus far were estimated at $31 to $510 per pound of thorium plus uranium recovered (Table 15.1). The lowest cost was for a sample of Conway granite and the highest for a granite of approximately "average grade."

Table 15.2. Estimated Costs for Treating Granite

Assumptions: Treatment of 100,000 tons of granite per day
10 years' amortization
14% annual return on investment

	Processing Costs per ton granite
Mining	$0.45–0.90
Milling	
Crushing to pregnant recovery	0.57
Pregnant treatment to product	0.11
Sulfuric acid plus lime	0.64–1.88
Other chemicals	0.10
Total direct operating costs	$1.87–3.56
Overhead	0.24
Contingency	0.27
Amortization*	0.51
Return on investment*	0.72
Total	$3.61–5.30

*Based on capital costs of $40,000,000 for mining and $145,000,000 for milling.

[3]Made in cooperation with A. H. Ross and Associates of Toronto, Canada.

16. SOLVENT EXTRACTION TECHNOLOGY

Solvent extraction is a unit operation of considerable importance and utility, particularly in remote-control operations, but only a few solvents, applicable to a narrow range of aqueous compositions, have so far found extensive use. In the former ORNL raw materials program a number of new solvents were developed that are now used commercially for extracting uranium and other metals from acid ore leach liquors. Some of these solvents extract by cation or anion exchange, offering a separations technology that uses the principles of ion exchange on a liquid-liquid basis with the inherent engineering advantages of liquid-liquid systems.

16.1 FINAL CYCLE PLUTONIUM RECOVERY BY AMINE EXTRACTION

To compete with tributyl phosphate extraction–anion exchange cycles already designed, amine extraction of plutonium after typical Purex extraction and partitioning from uranium must provide high decontamination and reasonably high concentration in a single cycle as well as being simpler and consuming less nitric acid. Work[1–4] at higher concentrations than those so far investigated at ORNL was used as a guide. The currently visualized flowsheet (Fig. 16.1) will take as feed a Purex partitioning-cycle plutonium-product stream in the range 1 to 2 *M* HNO_3, carrying some sulfate from the ferrous sulfamate plutonium reductant. The expected nitric acid concentrations are about those most favorable for plutonium extraction with tertiary amines,[5,6] and the only feed adjustment expected is reoxidation of the reduced plutonium to Pu(IV) with nitrite. An organic scrub to decrease TBP carryover may be desirable.

With expected feed plutonium concentrations of 0.5 to 2 g/liter (~0.002 to 0.01 *M* plutonium), the desired product concentrations of 20 to 60 g/liter should be obtainable with an amine concentration of 0.3 *M*. The required plutonium concentration in

[1] R. S. Winchester, "Aqueous Decontamination of Plutonium from Fission Product Elements," LA-2170 (May 15, 1958).

[2] J. C. Sheppard, "The Extraction of Neptunium (IV) and Plutonium (IV) from Nitric Acid Solution with Tri-*n*-octylamine," HW-51958 (Aug. 22, 1957); A. S. Wilson, "Tertiary Amine Extraction of Plutonium from Nitric Acid Solutions," *Proc. Int. Conf. Peaceful Uses of Atomic Energy*, Geneva, 1958, P/544, vol 17, p 348, U.N., New York; W. E. Keder, J. C. Sheppard, and A. S. Wilson, "The Extraction of Actinide Elements from Nitric Acid Solutions by Tri-*n*-octylamine," *J. Inorg. Nucl. Chem.*, 12, 237 (1960).

[3] A. S. Wilson, Hanford Atomic Products Operation, personal communication, Oct. 5, 1960.

[4] A. Chesne, P. Faugeras, C.E.A., Fontenay-aux-Roses, and A. C. Zanetto, Centre de Marcoule, France, personal communication, Sept. 20, 1960.

[5] B. Weaver and D. E. Horner, "Distribution Behavior of Neptunium and Plutonium Between Acid Solutions and Some Organic Extractants," *J. Chem. Eng. Data*, 5, 260 (1960).

[6] D. E. Horner and C. F. Coleman, "Plutonium Extraction from Nitrate and Sulfate Solutions by Amines and Organophosphorus Compounds," ORNL-3051 (Feb. 23, 1961).

UNCLASSIFIED
ORNL-LR-DWG 60798

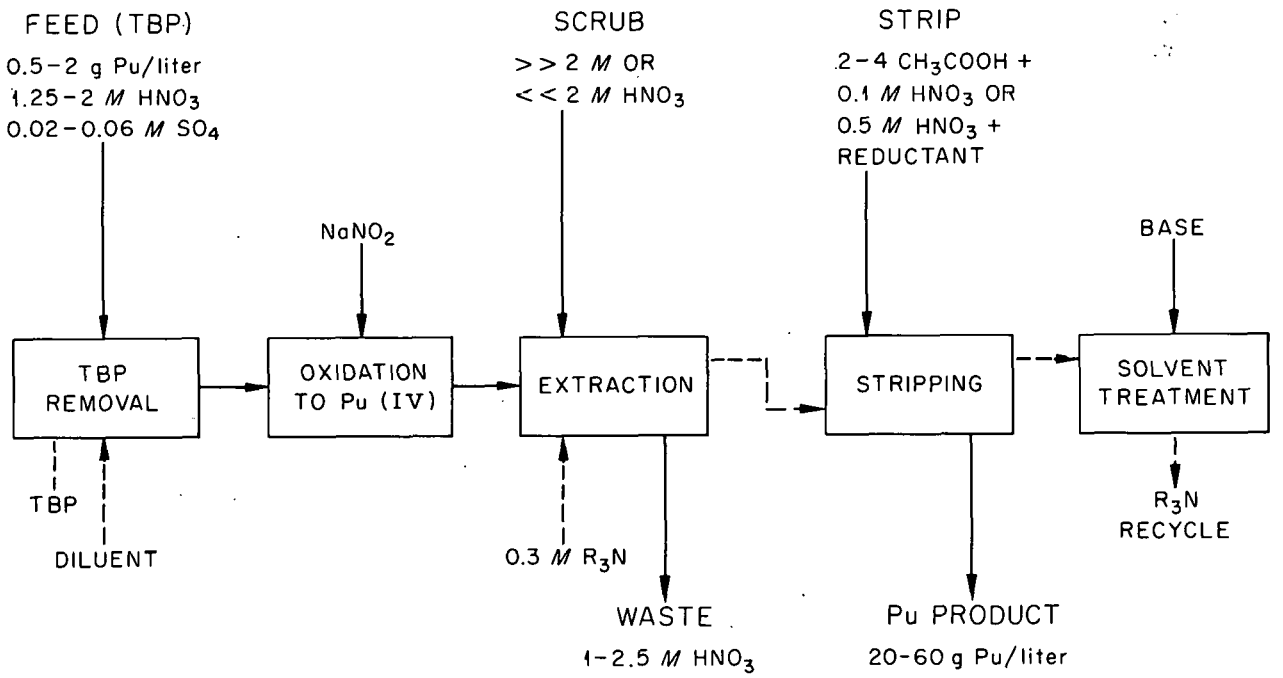

Fig. 16.1. Amine Extraction Cycle for Final Plutonium Recovery.

the organic, 15 g/liter, was obtained in stable solutions with 0.3 *M* trilaurylamine in Solvesso 100 or in diethylbenzene and with 0.3 *M* Alamine 336 in the same diluents modified with 10% tridecanol. Extraction at A/O flow ratios of 4/1 should thus be feasible with up to 0.015 *M* plutonium in the feed and of 10/1 at lower plutonium concentrations.

The extraction isotherms up to 15 g/liter were usefully well fitted by the empirical expression

$$E_a^\circ(\mathrm{Pu}) \approx E_1(M_{\mathrm{amine}} - 3\,M_{\mathrm{Pu}})^2 .$$

E_1 was ~3300 in extraction from 1.5 *M* HNO_3 with both trilaurylamine and Alamine 336. This was decreased moderately by addition of sulfuric acid in the expected concentration range, and severely by higher concentrations (Table 16.1).

Table 16.1. Pu(IV) Extraction Isotherms by ~0.3 *M* trilaurylamine or Alamine 336

$$E_a^\circ(\mathrm{Pu}) \approx E_1(M_{\mathrm{amine}} - 3\,M_{\mathrm{Pu}})^2$$

HNO_3 (*M*)	$NaNO_3$ (*M*)	H_2SO_4 (*M*)	E_1
2	1	0	5000
1.5	0	0	3300
1.5	0	0.032	1200
1.5	0	0.113	400
1.5	0	0.334	120

The Pu(IV) extraction coefficients with tertiary amine remained high enough over a wide nitric acid concentration range to permit scrubbing at acidities either considerably higher or considerably lower than the feed acidity, e.g., >>2 *M* HNO_3 for emphasis on eliminating ruthenium or <<2 *M* HNO_3 for emphasis on eliminating zirconium. The most useful scrub will be defined by runs with actual feed solutions.

Although plutonium extraction coefficients decrease rapidly with decrease of nitric acid concentration below 1 *M*, they are not low enough for water stripping unless the tertiary amine concentration is considerably less than 0.1 *M*. The most promising methods for stripping without causing product contamination are those using organic-soluble reductants, e.g., di-*tert*-butylhydroquinone (Fig. 16.2), and complexing and displacement with acetic acid (Fig. 16.3). Ferrous sulfamate[6] and several other water-soluble organic reductants were

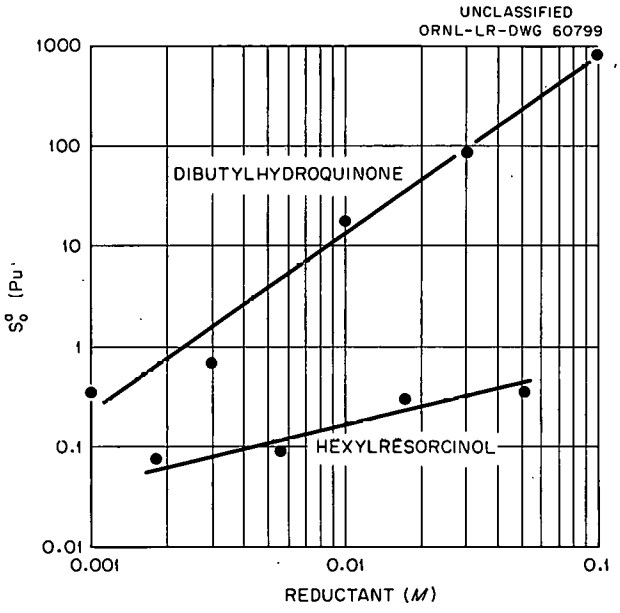

Fig. 16.2. Plutonium Stripping from 0.3 *M* Alamine 336 with Oil-Soluble Reductants. Solid reductant added in amount to give indicated molarity in organic phase, and plutonium then stripped with 0.5 *M* HNO_3 (stripping coefficient in second of two equal-volume contacts).

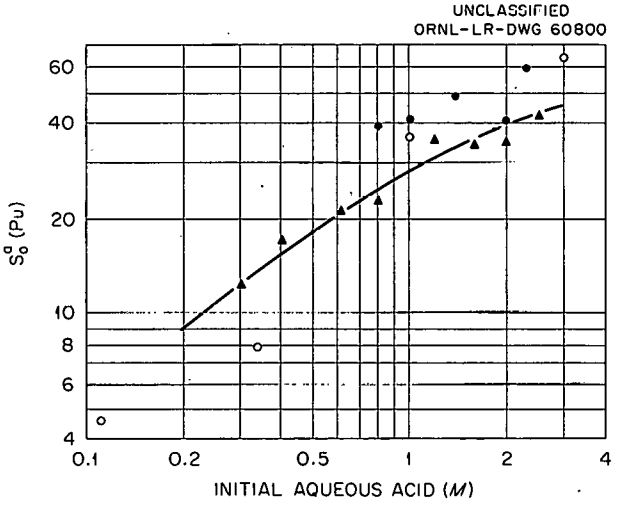

Fig. 16.3. Plutonium Stripping by (●,○) Acetic and (▲) Sulfuric Acids from 0.3 *M* Alamine 336. Geometric mean of stripping coefficients in two equal-volume contacts.

also effective – hydroquinone, resorcinol, and ascorbic acid – as well as sulfate[4] complexing, but these leave residues in the product solution.

Solvent degradation, as shown by formation of detectable amounts of an as yet unidentified compound or compounds that are strong zirconium extractants resulted from long contact of amine with moderate to high concentrations of nitric acid. Scrubbing with basic chromate decreased the extraction of zirconium in a subsequent contact (see also Sec. 16.4).

16.2 METAL NITRATE EXTRACTION BY AMINES[7]

Study of the amine extraction characteristics of fission- and corrosion-product metals of interest in nitrate solutions included work on extraction of zirconium, cerium, and stainless steel metals by a straight-chain quaternary (Aliquat 336), a straight-chain tertiary (trilauryl), a highly branched secondary [Amine S-24, *bis* (1-isobutyl-3,5-dimethylhexyl)], a slightly branched secondary (ditridecyl), and a highly branched primary amine (Primene JM-T).

In preliminary tests zirconium extraction was fairly well fitted by the empirical equation

$$E_a^o(\mathrm{Zr}) \approx K(M_{\mathrm{amine}})^a (M_{\mathrm{HNO_3}})^b (M_{\mathrm{NO_3}})^c$$

with $a = b = c = 2$ ($M_{\mathrm{NO_3}}$ includes $M_{\mathrm{HNO_3}}$ here).[8] More detailed analyses showed best fit with non-integral values of the exponents, and with noticeable differences between amines, especially in the response to acidity (Table 16.2).[9] Extraction coefficients were highest with the quaternary ammonium compound at the highest acidities, but were still low, e.g., 0.005 with 0.24 *M* Aliquat 336 in 8 *M* HNO_3.

Extraction coefficients for Ce(III) from nitric acid solutions with up to 0.4 *M* trilaurylamine were all <0.02.[9] With Amsco–decanol as diluent they were 0.01, and with toluene as diluent, 0.005. They increased at low acidity in the presence of sodium nitrate, 0.025 in 1.3 *M* HNO_3–6 *M* $NaNO_3$, but passed through maximums between 2 and 4 *M* HNO_3 without salt. Cerium(IV) was extracted strongly, $E_a^o \approx 10$, from 2 *M* HNO_3 – 6 *M* $NaNO_3$ with 0.3 *M* trilaurylamine in toulene, but it is not stable in the amine solution and is not expected to be encountered in process solutions.

Extraction coefficients for the stainless steel metals chromium, iron, nickel, and cobalt were

[7] Work done by the Department of Nuclear Engineering, MIT, under subcontract.

[8] *Chem. Tech. Ann. Progr. Rept. Aug. 31, 1960*, ORNL-2993, p 157.

[9] V. C. A. Vaughen and E. A. Mason, MIT, "Equilibrium Extraction Characteristics of Alkyl Amines and Nuclear Fuel Metals in Nitrate Systems," *Summary Report, July 1, 1958 to July 1, 1960, Subcontract 1327.*

Table 16.2. Zirconium Extraction by Amines from Acid Nitrate Solutions at Room Temperature

Amine (in toluene)	$E_a^o(\mathrm{Zr})$*
Quaternary	
Aliquat 336	$(2.5 \times 10^{-5}) (M_{\mathrm{amine}})^{1.5} (M_{\mathrm{HNO_3}})^{0.8} (M_{\mathrm{NO_3}})^{2.6}$
Tertiary	
Trilaurylamine	$(8 \times 10^{-7}) (M_{\mathrm{amine}})^{1.5} (M_{\mathrm{HNO_3}})^{1.8} (M_{\mathrm{NO_3}})^{3}$
Secondary	
Ditridecylamine or Amine S-24	$(6 \times 10^{-8}) (M_{\mathrm{amine}})^{1.5} (M_{\mathrm{HNO_3}})^{2} (M_{\mathrm{NO_3}})^{2}$
Primary	
Primene JM-T	$(5 \times 10^{-6}) (M_{\mathrm{amine}})^{1.5} (M_{\mathrm{HNO_3}}) (M_{\mathrm{NO_3}})^{2.7}$

*$M_{\mathrm{NO_3}}$ includes $M_{\mathrm{HNO_3}}$.

Table 16.3. Extraction of Stainless Steel Metals by Amines from 6 *M* HNO_3 at Room Temperature

Amine (0.3 *M*, in toluene)	E_a°			
	Cr(III)	Fe(III)	Co(II)	Ni(II)
Trilaurylamine	8×10^{-7}	2×10^{-5}	1×10^{-5}	$<10^{-5}$
Ditridecylamine	5×10^{-7}	1×10^{-5}	8×10^{-6}	$<10^{-5}$
Amine S-24	4×10^{-7}	1×10^{-5}	1×10^{-5}	$<10^{-5}$
Primene JM-T	2×10^{-5}	7×10^{-6}	2×10^{-4}	1×10^{-4}

all below 10^{-3} with 0.3 *M* amines in toluene.[10] Extractions were highest, with a few exceptions, from 6 *M* HNO_3 (Table 16.3).

Equilibrations at higher temperatures showed zirconium extraction coefficients with trilaurylamine and Amine S-24 in toluene and in Amscodecanol about 20% lower at 55 than at 25°C. Extraction coefficients for excess nitric acid were less affected, dropping <15% over the same range.[11] The amines were noticeably discolored at 55°C, but still gave close to the previous results when used again at 25°C.

Table 16.4. Uranium, Neptunium, and Technetium Products from Continuous Countercurrent Test with Plant Feed[12]

Product	% Recovery	Decontamination Factor from —		
		Tc	Np	U
U	~100	60	20	
Np	93	125		160
Tc	97		200	$>10^5$

16.3 TECHNETIUM-NEPTUNIUM-URANIUM RECOVERY

Laboratory development was completed of the tertiary amine single-cycle process for coextraction of uranium, neptunium, and technetium from fluorination plant residues and separation by consecutive stripping. In a continuous countercurrent demonstration of the chemical flowsheet in laboratory-scale equipment (without the close control described below), with a commercial amine and actual plant feed solution, recoveries were good and mutual separation of the products was high (Table 16.4).[12] An unusual feature of this flowsheet is that the technetium-nitrate separation can be included in the single cycle (Fig. 16.4). This is possible because the separation factor for pertechnetate from nitrate is so high (>200) that the pregnant organic stream can enter the same stage from which the discard aqueous nitrate stream is removed. To approach complete elimination of nitrate from the technetium requires nearly complete hydrolysis of the amine salt with close control, e.g., 98 ± 1%. A control test with pH indicator solution[13] was developed to distinguish between <97, 97–99, and >99% hydrolysis. With this, estimates indicate that a nitrate-removal section of perhaps only 12 ideal stages would produce an ammonium pertechnetate concentrate essentially free from nitrate.

[10] E. A. Mason and R. E. Skavdahl, *ibid., Jan. 1 to Sept. 30, 1960*, TID-11196.

[11] K. Tamai (Atomic Fuel Corporation, Tokyo, Japan), "Effect of Temperature on the Extraction of Zirconium from Nitrate Solutions by Alkyl Amines," report to E. A. Mason, MIT, Sept. 1, 1960.

[12] C. F. Coleman, F. A. Kappelmann, and B. Weaver, "Solvent Extraction Recovery of Technetium, Neptunium, and Uranium from Fluorination Plant Residues," *Nucl. Sci. Eng.*, 8, 507 (1960).

[13] Equilibrate a 5-ml sample of the amine solution with first 1 ml and then 2 ml more of 0.015 *N* standard base containing thymol blue, bromcresol green, and bromthymol blue at ~5 ml of standard 0.04% aqueous solution of each per liter; colorless at <97%, colorless and then blue at 97–99%, immediately blue at >99% hydrolysis.

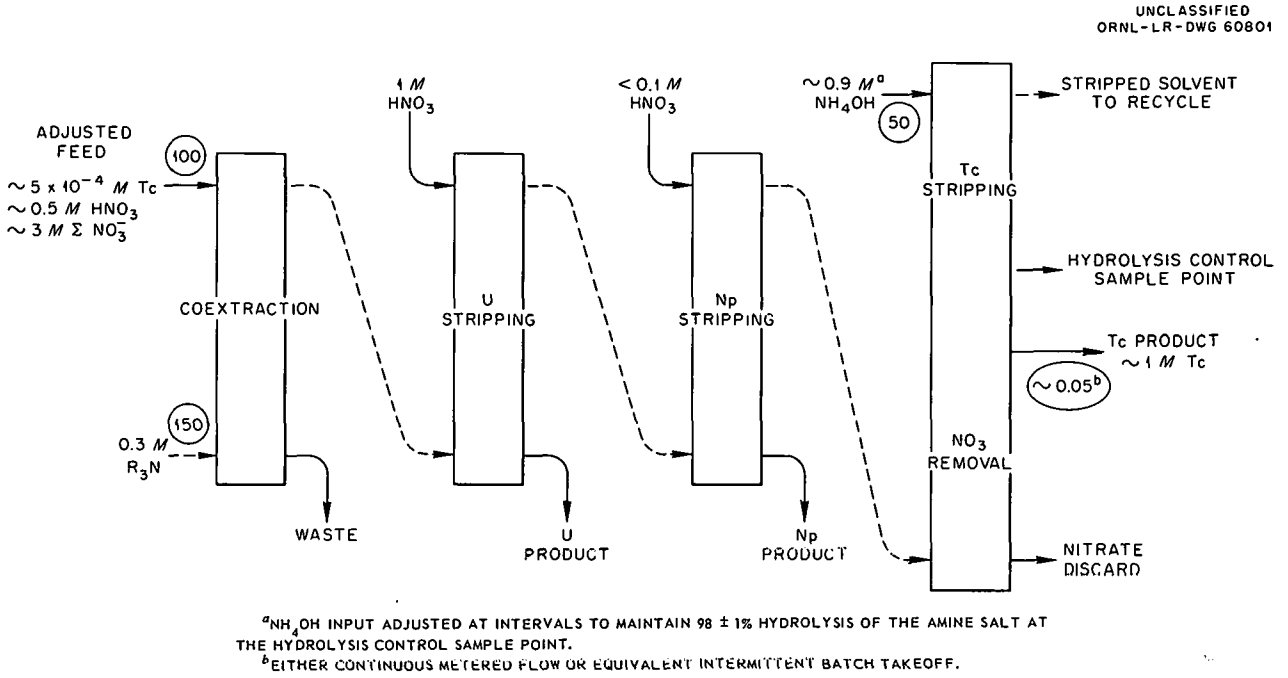

[a]NH_4OH INPUT ADJUSTED AT INTERVALS TO MAINTAIN 98 ± 1% HYDROLYSIS OF THE AMINE SALT AT THE HYDROLYSIS CONTROL SAMPLE POINT.
[b]EITHER CONTINUOUS METERED FLOW OR EQUIVALENT INTERMITTENT BATCH TAKEOFF.

Fig. 16.4. Chemical Flowsheet of Tc-Np-U Recovery Process. Circled numbers represent relative flows.

16.4 EXTRACTION PERFORMANCE AND CLEANUP OF DEGRADED EXTRACTANTS

Many of the difficulties encountered in cleaning up used TBP-Amsco 125-82 solvent stem from degradation products of the Amsco 125-82 diluent,[14] which have been shown[15] to be nitrogen-containing compounds, in addition to the acid degradation products of TBP. In recent studies nitro-paraffins (RNO_2) gave the same infrared spectrum as and performed in extraction tests similarly to a nitrogen-bearing component that had been separated from degraded diluent and to nitric acid-degraded diluent. Tests were devised to measure both solvent degradation and cleanup, and new diluents have been investigated.

Tests of Solvent Degradation

The test for measuring the degree to which TBP-Amsco solvent has been degraded, by measuring its extraction power for Zr^{95}-Nb^{95}, was modified to take advantage of the tautometry of the degradation products of the diluent:

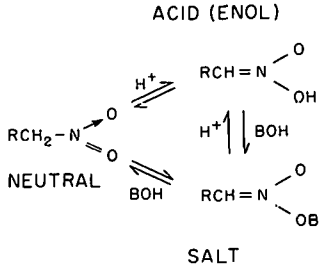

The tautomeric shift from the neutral to the acid or enol form is slow, but from the neutral to the salt form, in the presence of certain alkaline compounds, can be more rapid. For example, a large portion of the neutral nitro-paraffins in a degraded solvent can be converted fairly rapidly to the salt form by contacting with solid calcium hydroxide. The salt form in turn is converted immediately to the acid form upon contact with acid such as is experienced in extraction tests with acidic liquors. Both the neutral and acid forms of the nitro-paraffins in themselves are weak extractants for Zr-Nb. However the combination of the acid form with TBP provides a relatively strong extractant.

[14] *Chem. Tech. Ann. Progr. Rept. Aug. 31, 1960*, ORNL-2993.

[15] G. L. Richardson, "Purex Solvent Washing with Basic Potassium Permanganate," HW-50379 (May 29, 1957).

In view of these properties of the diluent degradation products, the modified extraction test has been established as follows:

(1) Make the degraded solvent 1 *M* in TBP and scrub twice with an equal volume of 0.2 *M* aqueous Na_2CO_3 to remove low-molecular-weight acids, primarily DBP and MBP (10 min each contact).
(2) Contact 30 min with solid calcium hydroxide, ~200 g solid/liter of organic phase, and separate from solid.
(3) Contact with Zr^{95}-Nb^{95} tracer solution in nitric acid and measure the extraction. An equal volume of tracer solution containing 10^4 c sec^{-1} ml^{-1} in 2 *M* HNO_3 is customarily used.

Figure 16.5 shows the results of such testing on a 1 *M* TBP solution in Amsco 125-82 which had been irradiated with Co^{60} γ rays while being intimately mixed with 2 *M* nitric acid. Extraction of Zr-Nb by the degraded solvent decreased markedly with carbonate scrubbing (curve 2 in Fig. 16.5) and subsequent acid scrubbing did not alter this low level. Subsequent contacting with solid calcium hydroxide increased the extraction so that at 50 whr/liter it was equal to that of the irradiated sample prior to carbonate scrubbing. At 90 whr/liter the extraction by carbonate plus calcium hydroxide scrubbed material was nearly 4 times that of the material scrubbed only with sodium carbonate. The test method described above has also been used to determine that many of the degradation products originate in the higher boiling fractions of the Amsco 125-82, where there are more complex molecules with more sites active toward nitration.

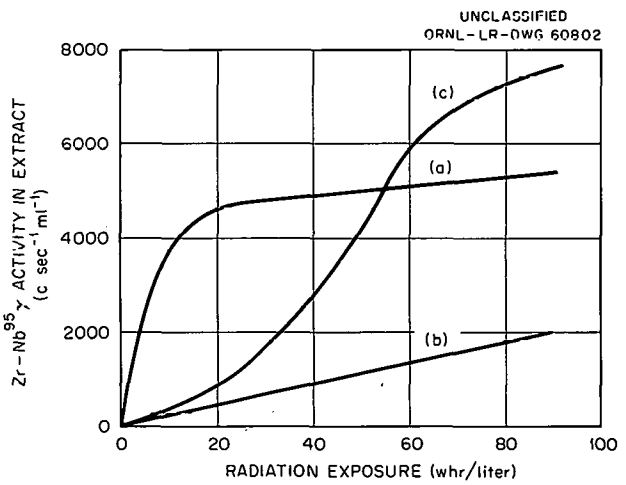

Fig. 16.5. Extraction Performance of TBP. (*a*) 1 *M* TBP in Amsco 125-82 degraded by irradiation while in contact with aqueous nitric acid; (*b*) degraded solvent scrubbed with aqueous sodium carbonate; (*c*) degraded and scrubbed solvent treated with solid calcium hydroxide. Extraction from 2 *M* HNO3, containing initially Zr^{95}-Nb^{95} at 10^4 c sec^{-1} ml^{-1}.

Tests of Solvent Cleanup

Current practice in TBP extraction plants for removing degradation products from used solvents is treatment with alkaline permanganate solution[15] to form solid MnO_2 which sorbs the degradation products. Efforts to develop liquid scrubbing methods, which would be more convenient than a solids-handling method, have been unsuccessful. The best method investigated was a combination of alkaline scrubbing with sorption of the degradation products on Al_2O_3, but for performance equivalent to that of the alkaline permanganate method, 20 times more Al_2O_3 than MnO_2 was needed. With both the permanganate and alumina treatment impurities causing 50 to 60% of the Zr-Nb extraction were easily sorbed. Removal of another fraction causing 20 to 25% of the Zr-Nb extraction required further relatively large additions of solid, but even at the highest solids levels used the solvent retained 20 to 25% of its Zr-Nb extraction power. No practical way has yet been found to remove the last traces of complexed Zr-Nb from used degraded solvent.

In obtaining the above results the two methods were compared on a 1 *M* TBP–Amsco 125-82 solution that had been exposed in the presence of nitric acid to 45 whr/liter in a Co^{60} source. For the alkaline scrubbing-Al_2O_3 tests, degraded solvent was treated with an equal volume of 0.2 *M* Na_2CO_3 at room temperature and 0 to 200 g of solid Al_2O_3 was added per liter of organic phase. Samples of the centrifuged, treated solvents were analyzed for their ability to extract Zr-Nb. The particle size of the alumina and predrying of it had no effect on the results. The alkaline permanganate treatment was similar, varying concentrations of Na_2CO_3 and $KMnO_4$ being tried, and treatment was at room temperature and 50°C.

New Diluents

Since no very effective liquid scrubbing method has been found for removing diluent degradation products from the aliphatic diluents now used, investigations were started to find less easily degraded diluents. Aromatic diluents impart greater radiation stability to extracting reagents such as TBP and also permit higher organic solubility of the extractant metal salts.[14] An advantage of the use of the aromatic Solvesso-100 as diluent for TBP was shown to be the higher decontamination factors for Purex-type feeds:

TBP (*M*)	Diluent	Separation Factors, U D.C./F.P. D.C.	
		Gross α	Gross γ
0.7	Solvesso 100	7670	7750
0.7	Amsco 125-82	1560	1715
1.4	Solvesso 100	1740	1770
1.4	Amsco 125-82	775	735

However, Solvesso has highly branched side chains and the Solvesso-diluted extractant was severely degraded chemically. A 1 *M* TBP solution in this diluent degraded by 4 hr treatment with 2 *M* HNO_3 at 107°C completely extracted tracer Zr-Nb from a synthetic feed, as shown by calcium hydroxide tests (Table 16.5).

Compounds with but one side chain of the simplest configuration on the benzene rings gave encouraging results as diluents in the calcium hydroxide treatment test. The best ones tested, the butylbenzene series, have flash points of about 130°F (closed cup) which should be suitable for some plants. Longer chain substituents are yet to be tested. The higher extraction by diisopropyl than by the isopropyl derivative can be a consequence of enhanced susceptibility of the di-substituted compound toward oxidation of its side chains. Nitration of the benzene ring itself was shown not to increase Zr-Nb extraction ability, which is consistent with the inability of tertiary nitroparaffins to enolize as shown above.

Table 16.5. Performance of Degraded Diluents

Extraction by 1 *M* TBP in diluent after chemical degradation with 2 *M* HNO_3 for 4 hr at 107°C (total reflux) and removal of low-molecular-weight acids by carbonate scrubbing
Tracer solution initially 1×10^4 c sec^{-1} ml^{-1} Zr^{95}-Nb^{95} γ in 2 *M* HNO_3
Extraction at equal phase ratios

Diluent	Flash Point (°F)		Zr^{95}-Nb^{95} Extracted in Calcium Hydroxide Test (c sec^{-1} ml^{-1})
	Closed Cup	Open Cup	
Amsco 125-82	128		4,000
Solvesso 100	118		10,000 (100%)
Shell E-2342	>140		5,000
Diethylbenzene		138	9,500
Isopropylbenzene	102		5,000
Diisopropylbenzene		170	8,500
n-Butylbenzene		160	40
tert-Butylbenzene		140	80
Isobutylbenzene			400
sec-Butylbenzene	126	145	3,000

*Tested by modified calcium hydroxide test described in this section.

16.5 SUPPRESSION OF Zr-Nb AND Ru EXTRACTION BY TBP–AMSCO FROM FEEDS PRETREATED WITH KETO-OXIMES

Improved decontamination of uranium from zirconium-niobium and ruthenium was noted previously[16] when aqueous nitrate feed solutions were treated with nitrous acid and acetone before solvent extraction with phosphates or phosphonates. Further tests showed the importance of both acetone and nitrous acid in the suppression of Zr-Nb and Ru extraction by TBP. A plausible explanation for these effects is the reaction of the ketone with nitrous acid to form a keto-oxime, a potential complexing agent for metal ions:

$$R-\overset{O}{\overset{\|}{C}}-CH_3 + HONO \longrightarrow R-\overset{O}{\overset{\|}{C}}-CH{=}NOH + H_2O$$

Tests on a number of compounds of this general structure in TBP extraction systems indicated that the addition of a keto-oxime compound will improve decontamination factors from ruthenium and zirconium-niobium in Purex and Thorex type processes by an order of magnitude.

Diacetyl monoxime, $CH_3COCNOHCH_3$, decreased the Zr-Nb and Ru extraction by fresh and degraded TBP-Amsco extractants, while not altering significantly the extraction of uranium and thorium. The TBP-diluent phases were degraded by nitric acid treatment with and without Co^{60} γ irradiation. The degraded solvents are strong Zr-Nb and Ru extractants, stronger than the fresh materials; therefore the decrease in extraction indicates the formation of very strong aqueous-phase complexes.

Nearly all the extractions were made after treatment of the aqueous phase with diacetylmonoxime at 80°C, since preliminary testing showed enhancement of aqueous phase complex formation at elevated temperatures. Assuming a tendency toward slow equilibrium in these systems similar to that in the reaction of nitroparaffins, the temperature dependence seems reasonable.

In a typical experiment (Fig. 16.6) extraction of Zr-Nb by 1 *M* TBP–Amsco 125-82, irradiated to 44 whr/liter (Co^{60} γ) in the presence of nitric acid, decreased rapidly with the first small additions of diacetyl monoxime to the nitric acid tracer solution. At 0.05 and 0.1 *M* oxime the Zr-Nb extraction coefficient was decreased by factors of 10 and 25, respectively. Diacetyl monoxime (0.1 *M*) decreased the ruthenium extraction coefficient of fresh TBP–Amsco by a factor of 17 when the solution was warmed during the treatment but did not change the extraction when the solution was treated at room temperature. Changes in the uranium and thorium extraction coefficients with oxime-treated aqueous solution by TBP–Amsco, both fresh and degraded, were small and temperature had no effect.

In batch countercurrent tests of both the acid and acid-deficient Thorex process solutions, Zr-Nb and Ru extraction coefficients were decreased and Pa extraction increased by the addition of 0.02 *M* diacetyl monoxime to 1 *M* TBP in Amsco 125-82. There was no change in rare

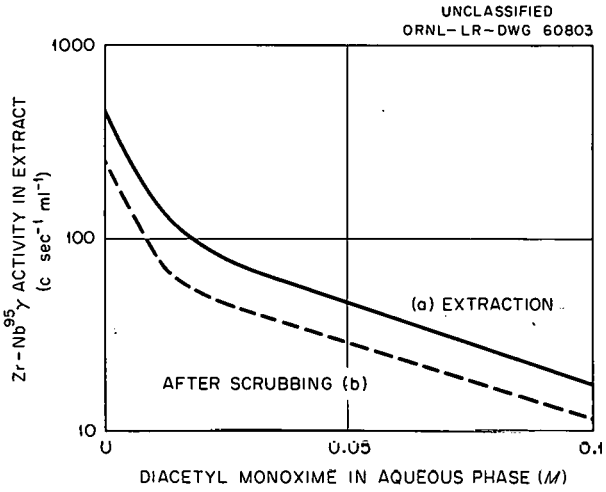

Fig. 16.6. Suppression of Zr^{95}-Zb^{95} Extraction by TBP–Amsco 125-82 Solutions from Aqueous Feed Treated with Diacetyl Monoxime. The dashed line represents the activity remaining in the organic extract after three successive scrub stages with 2 *M* HNO_3. Organic: 1 *M* TBP–0.25 *M* HNO_3–Amsco 125-82, irradiated (Co^{60}) to 44 whr/liter; aqueous: 2 *M* HNO_3, initially 1×10^4 c sec^{-1} ml^{-1} Zr^{95}-Nb^{95} γ. Extraction equal-volume aqueous vs organic phases, room temperature; 10-min contact after pretreatment of aqueous with diacetyl monoxime for 2 hr at 80°C (steam bath). Scrubbing: activity remaining in organic extract after three successive scrubs with equal volumes of 2 *M* HNO_3 for 10 min each.

[16] *Chem. Tech. Ann. Progr. Rept. Aug. 31, 1960*, ORNL-2993.

Table 16.6. Pa, TRE, Zr-Nb and Ru Extraction in Thorex Process: Effect of Aqueous Complexing by Diacetyl Monoxime

Acidic feed: 242 g Th/liter, 13.5 g U/liter, 1.88 *M* HNO_3, 1.26×10^5 Pa c/m/ml, 1.22×10^7 TRE c/m/ml, 2.75×10^6 Zr-Nb c/m/ml, 7.7×10^5 Ru c/m/ml

Acid deficient feed: 261 g Th/liter, 14.8 g U/liter, 0.1 *N* HNO_3-deficient, 1.35×10^5 Pa c/m/ml, 1.33×10^7 TRE c/m/ml, 2.86×10^6 Zr-Nb c/m/ml, 8.09×10^5 Ru c/m/ml

Aqueous scrub: 2 *M* HNO_3

Organic extractant: 1.1 *M* TBP in Amsco 125-82

F/S/O ratio: 1/1/7

Feed adjusted to 0.02 *M* diacetyl monoxime and then heated 2 hr at about 90°C

	Acidic Feed			Acid-Deficient Feed		
	E_a° Control	E_a° Treated	$\frac{E \text{ Control}}{E \text{ Treated}}$	E_a° Treated	E_a° Treated	$\frac{E \text{ Control}}{E \text{ Treated}}$
Pa	0.007	0.015	0.5			
TRE	0.012	0.012	1	0.012	0.011	1
Zr-Nb	0.007	0.005	1.4	0.005	0.0016	3.1
Ru	0.093	0.014	6.6	0.055	0.0045	12.2

earth extraction (Table 16.6) and no important change in thorium extraction.

A keto-dioxime, 5-methyl-1,2,3-cyclohexanetrione-1,3-dioxime, also suppressed zirconium-niobium extraction. Similar reagents having the oxime groups but not the keto groups were not effective.

16.6 ALKALINE EARTH EXTRACTION BY DI(2-ETHYLHEXYL) PHOSPHATES

In a detailed study of strontium extraction from sodium nitrate solutions by mixtures of sodium di(2-ethylhexyl) phosphate (NaD2EHP) plus di(2-ethylhexyl) phosphoric acid (D2EHPA) in benzene, sodium-hydrogen and strontium distribution data were established over the acidity range $10^{-1} \geq (H^+)_{aq} \geq 10^{-13}$. Strontium extraction coefficients varied directly with the organophosphate concentration, and inversely with the square of the hydrogen ion concentration in some cases but with continuously varying power dependences in others.

The solubility of NaD2EHP in benzene decreased sharply with decreasing ionic strength of equilibrium aqueous phase. Consequently, 4 *M* $NaNO_3$ aqueous phases have been used in studying alkaline earth extraction into this organic system. Accurate relations between pH meter readings and hydrogen ion molarity were established in large volumes of 4 *M* $NaNO_3$ under inert atmospheres and pure benzene layers. Similarly, pH readings were made on such aqueous phases equilibrated with benzene solutions of various mixtures of D2EHPA and NaD2EHP. From the two sets of data the fraction of the D2EHPA-NaD2EHP mixture in the sodium form was obtained as a function of $(H^+)_{aq}$, at a given total extractant concentration in the benzene. At $\Sigma(R)_{org} = 0.1$, for example, 1% NaD2EHP corresponds to $(H^+)_{aq} = 1.0 \times 10^{-4}$, and 99% NaD2EHP to $(H^+)_{aq} = 2.0 \times 10^{-8}$. Within this range, which is precisely the concentration range of greatest interest for the alkaline earth extraction studies, the organic phase is an excellent buffer, since a given D2EHPA-NaD2EHP mixture equilibrated with pure 4 *M* $NaNO_3$ will establish of its own accord the exact aqueous acidity required with only negligible change in its own sodium-hydrogen content.

In curves of tracer strontium extraction as a function of the aqueous hydrogen ion concentration (Fig. 16.7), a large number of the data obtained at 0.5 *M* total extractant showed the expected inverse square dependence of the extraction coefficient on $(H^+)_{aq}$. The slope of the curve at $\Sigma(R)_{org} = 0.1$ shows a continuous change from ~ -1 to ~ -4 as the $(H^+)_{aq}$ decreases. In both cases the maximum is at the point where the extractant is about one-quarter sodium salt; similarly, both curves level off at about 99% NaD2EHP and remain level from then on.

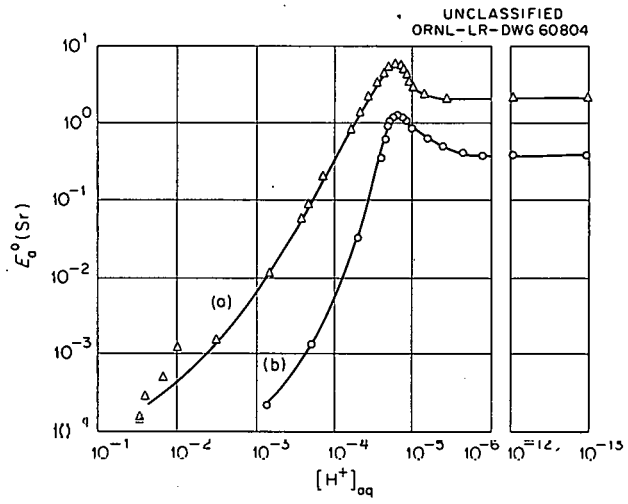

Fig. 16.7. Coefficient of Strontium Extraction by D2EHPA-NaD2EHP in Benzene Diluent as a Function of Aqueous Hydrogen Ion Concentration. (*a*) Reagent concentration 0.49 *M*, total strontium 5×10^{-8} *M*. (*b*) Reagent concentration 0.1 *M*, total strontium 1×10^{-5} *M*.

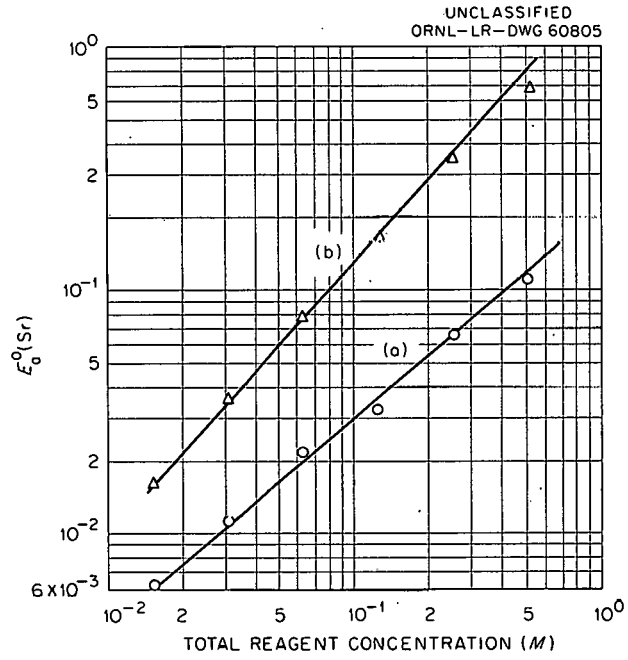

Fig. 16.8. Coefficient of Strontium Extraction by D2EHPA-NaD2EHP in Benzene Diluent as a Function of Total Reagent Concentration. (*a*) 2% of reagent in sodium form. (*b*) 40% of reagent in sodium form.

The strontium extraction coefficient is dependent on the extractant concentration (Fig. 16.8). With 2% of the extractant in the sodium form the coefficient increases somewhat more rapidly than with 40% in the sodium form. While it is conceivable that these dependences are due to the extraction of $SrOH^+$ by a monomeric reagent, it seems more likely that Sr^{++} is being extracted by the usual dimeric form of the D2EHPA.

16.7 URANYL SULFATE DIFFUSION IN SOLVENT EXTRACTION

Studies of the kinetics of the solvent extraction of uranyl sulfate from aqueous phases of varying sulfate ion concentration have indicated that the uranyl ion is about six times as effective as either the mono- or the disulfate complex in transferring uranium to the organic phase.[17] These results also suggest that the rate-controlling process occurs entirely on the aqueous side of the interface. Accordingly, diffusion of uranyl sulfate in the aqueous phases alone was studied.

Average diffusion rate constants determined as a function of sulfate ion concentration (Fig. 16.9) were close to those computed from formation constants for the uranyl sulfate complexes,[18] assuming that the uranyl ion is transporting 10 times as much uranium as either the mono- or the disulfate complex.

[17] K. A. Allen, "The Relative Effects of the Uranyl Sulfate Complexes on the Rate of Extraction of Uranium from Acidic Sulfate Aqueous Solutions," *J. Phys. Chem.*, 64 667 (1960).

[18] K. A. Allen, "The Uranyl Sulfate Complexes from Tri-*n*-octylamine Sulfate Extraction Equilibria," *J. Am. Chem. Soc.*, 80 4133 (1958).

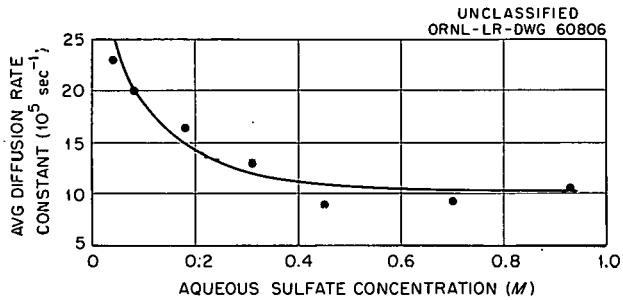

Fig. 16.9. Diffusion Rate Constants as a Function of Aqueous Sulfate Molarity. Points are experimental data; the solid line was computed with the assumption that UO_2^{++} transports 10 times as much uranium per unit time as either UO_2SO_4 or $UO_2(SO_4)_2^{--}$.

The apparatus consisted of two glass cells separated by a vertical fritted glass disk and connected at the bottom by a long capillary U tube. An aqueous solution of a given sulfate ion concentration was introduced into both cells, and to one side sufficient uranyl sulfate solution, of the same total sulfate ion molarity, was added to produce an initial concentration of 0.01 *M* UO_2SO_4. Both were sampled at timed intervals.

16.8 SOLVENT EXTRACTION SYSTEM ACTIVITY COEFFICIENTS

Measurements of vapor pressures, for use in determining activity coefficients, for the system tri-*n*-octylamine–benzene vs benzene (both H_2O saturated) agreed within a few microns with values computed from Raoult's law up to an amine molarity greater than 0.2 *M* (Table 16.7). The ideal behavior of this amine-solvent system in this concentration range confirms the hypothesis used[19] in deriving equilibrium constants for the system TOA-C_6H_6:H_2SO_4-H_2O. The apparatus and technique used were described previously.[20]

[19]K. A. Allen, "The Equilibria Between Tri-*n*-octylamine and Sulfuric Acid," *J. Phys. Chem.*, 60 239 (1960).

[20]A. L. Myers, "Summer Work on Vapor Pressure Apparatus and Technique Development," ORNL CF-60-1-18 (Jan. 12, 1960).

Table 16.7. Vapor Pressure Results: TOA in C_6H_6 (H_2O sat.)*

n_2/n_1	[TOA]	Δp Observed (mm Hg)	Δp Calculated** (mm Hg)
0.00729	0.082	0.543	0.539
0.01214	0.136	0.873	0.894
0.01487	0.167	1.080	1.091
0.02055	0.230	1.498	1.501
0.02737	0.307	2.057	1.984
0.03504	0.394	2.287	2.522

*The calculated values in the last column were computed from the Raoult's law expression: $\Delta p = p_0 \frac{x_1^2}{x_1 + n_1/n_2}$, where p_0 is the vapor pressure of the pure solvent, x_1 is the mole fraction of the benzene in the solvent flask (from the solubility of water in benzene) and n_1 and n_2 are the numbers of moles of benzene and amine in the solution flask, respectively.

**Based on $p_0(C_6H_6, 20^\circ C) = 74.84$ mm Hg.

17. MECHANISMS OF SEPARATIONS PROCESSES

17.1 DISTRIBUTION OF NITRIC ACID BETWEEN AQUEOUS AND TBP-AMSCO 125-82

An empirical equation for calculating the distribution of 0 to 4 *M* HNO_3 between an aqueous phase and 5 to 100 vol % TBP in Amsco 125-82 was formulated from data obtained in single-stage equilibrations. For the equilibrium relation

$$H^+_{aq} + NO^-_{3\ aq} + TBP_{org} \rightleftharpoons TBP \cdot HNO_{3\ org}$$

the equilibrium constant K^c_1, in molar units, is defined by

$$K^c_1 = \frac{[TBP \cdot HNO_3]_{org}}{[H^+]_{aq}\,[NO^-_3]_{aq}\,[TBP]_{org}} = \frac{(TBP \cdot HNO_3)_{org}}{y_s^2 c_s^2\,(TBP)_{org}} \frac{y_{TBP \cdot HNO_3\ org}}{y_{TBP\ org}} \qquad (1)$$

where brackets refer to activities; parentheses to concentrations; y_i to the activity coefficient of any species i; y_s and c_s to the stoichiometric activity coefficient[1] and concentration of nitric acid in the aqueous phase, respectively; and the subscripts aq and org to the aqueous and organic phases. Following McKay *et al.*,[2] $(TBP \cdot HNO_3)_{org}$ is equated to the analytically determined concentration of HNO_3 in the organic phase and (TBP) to the quantity $(\text{Total TBP})_{org} - (HNO_3)_{org}$, where $(\text{Total TBP})_{org}$ is defined as $(TBP_s)_{org}$.

The acidities of organic and aqueous phases that had been equilibrated (0.01 to 8 *M* HNO_3) vs 5 to 100 vol % TBP in Amsco 125-82 and then separated, the water contents of the organic phases, and nitrate contents of some of the organic phases were measured and substituted in the equation

$$\frac{K^c_1 y_{TBP\ org}}{y_{TBP \cdot HNO_3\ org}} = \frac{(HNO_3)_{org}}{y_s^2 c_s^2 \left\{(TBP_s)_{org} - (HNO_3)_{org}\right\}} = \frac{(TBP \cdot HNO_3)_{org}}{[H^+]_{aq}\,[NO^-_3]_{aq}\,[TBP]_{org}} \qquad (2)$$

The logarithm of the values of the first term vs the ratio $(HNO_3)_{org}/(TBP_s)_{org}$ were straight lines in all cases (Fig. 17.1):

$$\log \frac{K^c_1 y_{TBP}}{\left\{y_{TBP \cdot HNO_3}\right\}} = A + B \frac{(HNO_3)_{org}}{(TBP_s)_{org}}$$

$$= \log \frac{(HNO_3)_{org}}{y_s^2 c_s^2 \left\{(TBP_s)_{org} - (HNO_3)_{org}\right\}} \qquad (3)$$

From Eq. (3) and the experimentally determined values of constants A and B (Table 17.1), the distribution of 0 to 4 *M* HNO_3 can be calculated.

Table 17.1. Equation (3) Correlation Constants for Distribution of HNO_3 Between Aqueous and TBP–Amsco 125-82 Phases at 25 ±2°C

TBP Conc. in Diluent		Correlation Constants	
Nominal vol %	*M*[a]	*A*	*B* (moles TBP/mole HNO_3)
5	0.172_0	−0.5747	−0.3974
10	0.351_8	−0.4442	−0.5084
15	0.521_0	−0.2617	−0.6723
30	1.095	−0.1486	−1.0389
65	2.334	+0.0223	−1.3466
100	3.651_5	+0.1758	−1.6344

[a] The molarity of TBP in the diluent is based on the dry acid-free solution.

[1] The activity coefficients of F. Hartmann and P. Rosenfeld, *Z. physik. Chem.* 164, 377 (1933), were used in this work.

[2] H. A. C. McKay *et al.*, *Trans. Faraday Soc.* 52 and 54, 1956 and 1958.

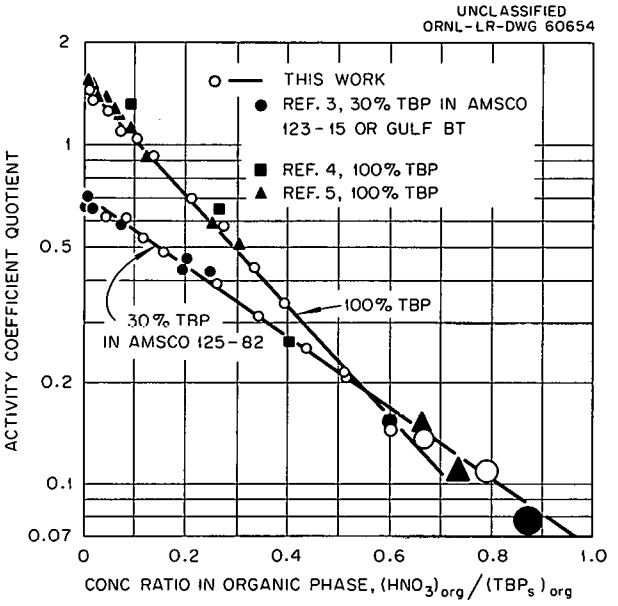

Fig. 17.1. Correlation of Data in Extraction of Nitric Acid by 30 and 100% TBP. Activity coefficient quotient =

$$\frac{K_1^c \gamma_{TBP\ org}}{\gamma_{TBP \cdot HNO_3\ org}} = \frac{(HNO_3)_{org}}{y_s^2 c_s^2 \{(TBP_s)_{org} - (HNO_3)_{org}\}} .$$

Final mathematical analyses of the distribution data have not been completed, but preliminary analyses show that both the constants A and B are nearly linear functions of the quantity

$$\left[Y_{dil} / \left(Y_{dil} + Y_{TBP_s} \right) \right]^2_{org} ,$$

where Y_{dil} and Y_{TBP_s} are mole fractions of Amsco 125-82 and TBP, respectively, in the organic phase.

In the correlations shown in Fig. 17.1 the organic phase nitric acid concentration is the independent variable. This leads to simpler functions, which can be interpreted in terms of standard solution theories, than the aqueous phase concentrations used in earlier[1] work. Plots (Fig. 17.1) of some of the literature data[5-8] from Eq. (3), after the value of $(TBP_s)_{org}$ had been corrected for an increase in volume due to the transfer of HNO_3 in the organic phase (1 liter of TBP_{org} is 1.04 liters of TBP containing 1 mole of HNO_3), were in all cases straight lines very close to the straight lines obtained in this work.

17.2 RADIATION DAMAGE TO TRIBUTYL PHOSPHATE-AMSCO 125-82 SYSTEMS[9]

Data on the radiolytic decomposition of nitric acid and TBP are significant in radioactive fuel processing since they can be used to calculate the extent of gas formation, the possibility of precipitate formation when solubilities of dibutyl and monobutyl phosphates are known, and, eventually, the extent of changes in distribution coefficients of uranium and plutonium. Such effects are additive with those due to thermal reaction of TBP and nitric acid. A radiation density of 1 whr/liter corresponds to 3.7×10^{-4} mole/liter. Thus, for Thorex processing of short-decayed fuel[10] with energy densities of 0.1 whr liter^{-1} pass^{-1} and for two nitrogen atoms per gas molecule[11] (N_2, N_2O), the calculated radiolytic gas generation rate due to nitric acid decomposition is in the range 10 cc of gas per pass per liter of solution, and dibutyl phosphoric acid production from TBP decomposition is in the range 4×10^{-5} to 10×10^{-5} mole per pass per liter of solution. The latter could cause precipitation of uranyl or zirconium dibutyl phosphates in the aqueous phase[12] or their retention in the organic phase in a single pass at such high radiation levels and would cause similar difficulties at lower radiation levels if these

[3] J. W. Codding, W. O. Haas, Jr., and F. K. Heumann, *Ind. Eng. Chem.* 50, 145 (1958).

[4] T. V. Healy and P. E. Brown, AERE C/R 1970 (June 6, 1956).

[5] D. R. Olander, L. Donadieu, and M. Benedict, *A.I.Ch.E. J.* 7, 152 (1961).

[6] T. V. Healy and P. E. Brown, AERE C/R 1970 (June 6, 1956).

[7] N. R. Geary, UKAEA-8142 (August 1955).

[8] A. T. Gresky *et al.*, ORNL-1367 (Dec. 17, 1952).

[9] Work performed partly at ORNL and partly at Stanford Research Institute.

[10] W. Davis, Jr., *Radiation Densities and TBP Radiolysis During Thorex Short Decay Runs*, ORNL-2764 (Aug. 6, 1959).

[11] A. H. Samuel, R. S. Farrand, and W. E. Wilson, *Radiation Stability of Organic Liquids*, Stanford Research Institute Semiannual Rep. No. 1, Project Agreement No. 25, Contract AT(04-3)-115, January 31, 1961; *ibid.*, No. 2, June 1961.

[12] W. Davis, Jr., *Solubilities of Uranyl and Iron(III) Dibutyl and Monobutyl Phosphates in TBP Solvent Extraction Solutions*, ORNL-3084 (Apr. 19, 1961).

degradation products were not removed continuously.

In previous studies of the radiolysis of TBP–Amsco 125-82 solutions[13] containing dissolved nitric acid and water, yields for nitric acid decomposition, $G(-HNO_3)$, were unexpectedly large, 3 to 5 molecules/100 ev, but somewhat uncertain because of the marked decrease in nitric acid concentration during the experiments. In further studies[11] made under conditions such that the amount of nitric acid decomposed was negligible compared with the total amount present, $G(-HNO_3)$ values were even higher. With 1-Mev electron irradiation, $G(-HNO_3)$ increased from 4 to 11 molecules/100 ev at a dose of 45 whr/liter as the acidity of the organic phase increased from 0.1 to 0.7 *M* (Table 17.2); at the higher acidity, $G(-HNO_3)$ decreased from 11 to 8 as the dose increased from 45 to 405 whr/liter. Yields of dibutyl phosphoric acid formation, G(HDBP), showed similar trends, an increase from 1.2 to 3 at 45 whr/liter as the organic acidity increased from 0.1 to 0.7 *M* and a decrease from 3 to 0.8 at the higher acidity as the dose increased from 45 to 405 whr/liter. There were no apparent trends in the yield of monobutyl phosphoric acid (Table 17.2), and in all experiments,[11] the yield of orthophosphoric acid was close to or below the limits of analytical detection, i.e., $G(H_2MBP) \leq 0.6$ molecule/100 ev.

[13] L. H. Towle and R. S. Farrand, *Radiation Stability of Organic Liquids*, Stanford Research Institute Semiannual Rept. No. 7 on Subcontract 1081, June 15, 1960; *Chem. Tech. Ann. Progr. Rept. Aug. 31, 1960*, ORNL-2993.

Table 17.2. Yields in the Radiolysis of HNO_3-H_2O Solutions of 1 *M* TBP in Amsco 125-82

HNO_3 Concentration		Dose Rate	Dose	Yield (molecules/100 ev)		
Aq	Org	(w/liter)	(w hr/liter)	$G(-HNO_3)$	G(HDBP)	$G(H_2MBP)$
			Irradiation by 1-Mev Electrons			
0.772	0.116	220.2	45	4.82	1.16	0.12
0.776	0.116	220.2	45	4.00	1.21	0.10
0.865	0.0640	165.5	135	3.74	0.761	0.048
0.867	0.0645	165.5	135	3.73	0.806	0.038
0.874	0.0629	165.5	135	3.70	0.593	0.026
0.674	0.177	220.2	135	3.55	0.98	
2.42	0.452	178.3	45	5.86	2.31	0.07
2.44	0.447	178.3	45	5.25	2.52	0.07
4.21	0.706	178.3	11.9	6.86	6.33	
4.15	0.679	220.2	45	12.22	3.15	0.24
4.22	0.654	220.2	45	10.91	2.97	0.06
4.13	0.691	347.1	45	10.93	2.87	0.39
4.13	0.709	347.1	45	7.85	2.95	0.12
4.46	0.734	178.3	135	9.98	1.76	0.11
3.84	0.618	220.2	135	8.00	2.13	0.25
3.85	0.632	220.2	135	7.89	1.86	0.13
4.38	0.718	178.3	221	7.23	1.42	0.07
4.28	0.431	165.5	405	7.59	0.801	0.047
			Irradiation by Co^{60} Gamma			
1.95	0.401	2.24	0			
1.85	0.335	2.09	46.2	10.5		
1.84	0.323	2.04	57.2	14.0		
1.73	0.290	1.99	90.0	10.4		

The results of a few experiments made at ORNL with Co^{60} gamma irradiation agreed closely with those at Stanford. The value $G(-HNO_3)$ was between 10 and 14 molecules/100 ev at dose rates of 2 w/liter, a dose rate lower by a factor of about 100 than that used at Stanford.

17.3 FOAM SEPARATION

As a method for separating radioactive elements, foam separation has been seriously studied only during the last few years.[14] Separation occurs because surface active solutes exist in higher concentrations at a gas-liquid interface than in the bulk solution. In practice, the surface is generated in the form of bubbles, or foam.

Separation Model

Separation of cationic fission products from an aqueous solution requires that the cation become part of a surface active molecule. With strontium, for example, the sodium form of a surfactant, such as an alkyl or aryl sodium sulfonate, is added to the solution and strontium becomes part of the surfactant:

$$2\,RSO_3^- + Sr^{++} \rightleftharpoons (RSO_3)_2Sr\,.$$

The model that best describes the excess concentration of a surfactant at a gas-liquid interface of a solution containing several surfactants is based on the Langmuir equation, which defines conditions for monolayer adsorption:

$$\frac{\Gamma_i'}{\Gamma_{mi}} = \frac{\alpha_i a_i}{1 + \alpha_1 a_1 + \alpha_2 a_2 + \ldots + \alpha_n a_n}$$

$$= \frac{\Gamma_i + c_i\tau}{\Gamma_{mi}} \approx \frac{\Gamma_i}{\Gamma_{mi}} \qquad (4)$$

where

α_i is a constant for surfactant species i, cm^3/mole

a_i is the bulk phase activity of species i, mole/cm^3

c_i is the bulk phase concentration of species i, mole/cm^3

τ is the thickness of the surface phase, cm

Γ_i' is the concentration of surfactant species i in the surface phase, moles/cm^2

Γ_{mi}, or Γ_m if only one surfactant is present, is the concentration of surfactant species i in a (saturated) monolayer of species i, moles/cm^2

$c_i\tau$ is the concentration of species i that would be expected at the surface if it were not surface active, moles/cm^2

Γ_i is, by Eq. (4), the increase in concentration of species i at the surface due to its surface activity over the concentration it would show if it were not surface active, moles/cm^2

$\Gamma_i + c_i\tau \approx \Gamma_i$ since Γ_i is several orders of magnitude greater than $c_i\tau$ for surfactants of interest in foam separation

Combining of Eq. (4) with the Gibbs equation,

$$-\frac{d\gamma}{RT} = \Gamma_1 d\ln a_1 + \Gamma_2 d\ln a_2 + \ldots + \Gamma_n d\ln a_n \qquad (5)$$

and assuming that values of Γ_{mi} are essentially constant gives a Gibbs-Langmuir equation

$$\gamma_0 - \gamma = \Gamma_m RT \ln (1 + \alpha_1 a_1 + \alpha_2 a_2 + \ldots + \alpha_n a_n)\,. \qquad (6)$$

Thus, if values of a_i for a solution are known, the degree to which surfactants can be separated from solution or from each other can be calculated from surface tension measurements, γ and γ_0 of solution and pure water, respectively.

The Gibbs-Langmuir model was verified by comparing measured surface tensions of solutions of several surfactants with values calculated from α_i's of the pure individual surfactants, and by comparing the separations calculated from surface tension and surface radioactivity with experimental values obtained in a total recycle foam column with the same chemical systems (Table 17.3). Agreement of values of Γ_m or Γ/c obtained from the different experimental methods is very good. Similarly, agreement was good between measured and calculated surface tensions, in the range 35 to 70 dynes/cm, of solutions containing three or four of the alcohols n-pentanol, n-hexanol, n-heptanol, and n-octanol.

[14] E. Schonfeld, R. Sanford, G. Mazzella, D. Gosh, and S. Mook, *The Removal of Strontium and Cesium from Nuclear Waste Solutions by Foam Separation*, Radiation Applications, Inc., July 29, 1960 (NYO-9577).

Table 17.3. Evaluation of the Gibbs-Langmuir Model for Surface Active Agents

Solution	$10^{10} \times \Gamma_m$, moles/cm^2		$10^3 \times \Gamma/c$, cm	
	Calculated from Surface Tension Measurements	Observed in Foam Column Experiments	Calculated from Surface Radioactivity Measurements	Observed in Foam Column Experiments
RWA-100 in H_2O	2.4–3.1	2.5–2.9		
RWA-100 in 0.1 *M* $NaNO_3$	3.0	2.8–3.2		
RWA-100 in $H_2O + Ca^{++}$			2.5–3.0	2.5–3.0

Calculated surface tensions of the multicomponent solutions were based on values of α and Γ_m of the individual alcohols in water.

Kinetic Effects

With aged solutions of RWA-100 (a butyl phenyl phenol sodium sulfonate) in water or 0.1 *M* $NaNO_3$, values of Γ_m calculated from surface tension measurements and values of Γ/c calculated from surface radioactivity measurements agreed with values determined from foam column experiments. Surface tensions decreased as much as 10% as the age of the surface prior to measurement increased from 0 to 24 hr, but beyond this time were essentially constant. These comparisons of Γ_m indicate that the foam in the column attained at least 90% of the surface monolayer concentration, even though the bubbles of gas are in contact with solution only a few seconds.

Screening of Foaming Agents

Standard tests were established to measure the solubilities, critical micelle concentrations, foamabilities, and the separation of cesium, strontium, and cerium from aqueous solutions at pH 1, 7, or 12. Included in the approximately 100 surfactants tested were sulfonates, sulfates, amino acids, and phosphates, most of which were anionic, but a few of which were nonionic or amphoteric. With a few exceptions, solubilities exceeded 0.5 g/liter; in some cases solubilities exceeded 100 g/liter. Most of these surfactants gave stable foams under one or more of the pH test conditions. Critical micelle concentrations, which also are approximately equal to concentrations of maximum foam stability, were primarily in the range 0.1–10 g/liter, or $\sim 2 \times 10^{-4}$ to $\sim 2 \times 10^{-2}$ *M* at pH 7.

The best results of separations tests, in terms of the distribution coefficient, Γ/c, were: (a) $(\Gamma/c)_{Cs} = 1.5 \times 10^{-3}$ cm with Igepon T43 at pH 7; (b) $(\Gamma/c)_{Sr} = 3 \times 10^{-3}$ cm with RWA-100 at pH 7; (c) $(\Gamma/c)_{Ce} = 1.8 \times 10^{-3}$ cm with RWA-100 at pH 2. Igepon T43 is a sodium N-Methyl-N oleoyl taurate.

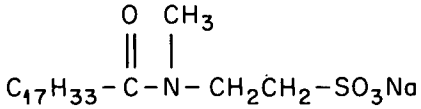

IGEPON T43

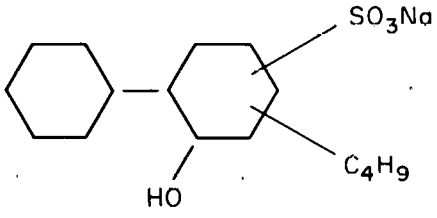

RWA–100

The screening tests suggest that sulfonates be used for strontium in the pH range 2 to 11, for rare earths at pH $\sim$2, and for cesium at pH $\sim$7. Sulfates may be useful in strontium removal at pH 7 to 11. Amino acids should be useful in strontium removal at pH 7 to 11. Amino acids should be useful in strontium and rare earth removal at pH >4 even in the presence of large amounts of sodium, 1 to 5 *M*. In the presence of a large concentration of sodium, cesium is best separated by the surfactant sodium tetraphenyl boron.

Foam-Froth Decontamination of ORNL Low-Activity Waste

Before being drained into White Oak Creek, ORNL low-activity waste is held up in a basin for settling of solids, which contain most of the Cs^{137} of the waste stream. The possible utility of foam-froth decontamination was tested by adding ~200 mesh Illite clay to low-activity waste, adjusting the pH to ~12 with sodium hydroxide, and then adding sodium lauryl sulfate. Within 20 sec of starting a foaming operation with nitrogen gas, the solution was free of all visible quantities of solid. Analyses after 2 min of foaming showed 97 to 99% cesium removal and ~50% strontium removal. The average distribution coefficient, K_D, of Cs^{137} between the Illite clay and solution was 10^5 ml of solution per gram of Illite.

18. RADIATION EFFECTS ON CATALYSTS

18.1 CONVERSION OF CYCLOHEXANOL TO CYCLOHEXENE WITH $MgSO_4$-Na_2SO_4 AS CATALYST

The catalytic activity of $MgSO_4$-Na_2SO_4 in converting cyclohexanol to cyclohexene at 400°C is increased twofold by incorporating 25.9 mc of S^{35} per gram of catalyst in the sulfate radicals and aging the catalyst several hours.[1-3] In further studies the percentage conversion was not affected by exposing the aged catalyst bed to ~118 rad/min of either 180- or 300-kv x rays during the reaction (Fig. 18.1). This dose rate is equivalent to incorporation of 67 mc of S^{35} per gram of catalyst. In these experiments the unused nonradioactive catalysts were characterized by BET surface area measurements (with nitrogen and argon), crystallite size, pore size distribution, and toluene, helium, and tap densities, which was not done in earlier work.[2,3]

In the past, reliable surface areas on aged catalysts could not be obtained since exposure to the atmosphere during transfer of the material from the reaction tube to the surface area sample holders (BET bulbs) is sufficient to make the subsequently determined area a function of out-gassing treatment. Results were reproducible with freshly prepared material when the BET bulbs were loaded in an evacuated system with no exposure to air subsequent to final drying of the catalyst. A system is now under development to permit surface area measurements of used catalysts without removing them from the reaction tube.

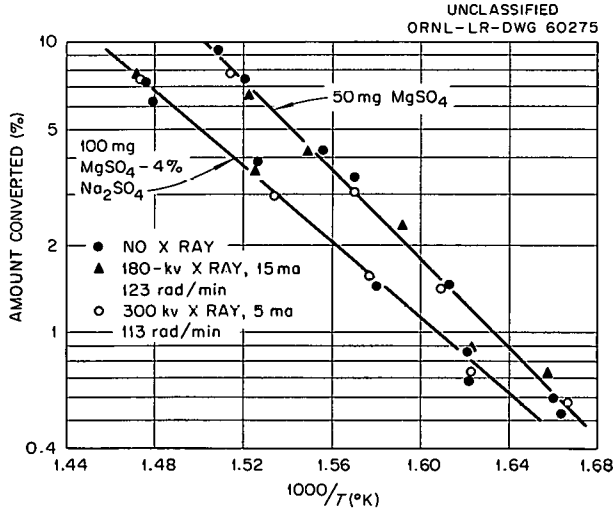

Fig. 18.1. Conversion of Cyclohexanol to Cyclohexene. (*a*) 50 mg of $MgSO_4$; (*b*) 100 mg of $MgSO_4$–4% $NaSO_4$.

[1] A. A. Balandine *et al.*, *Doklady Nauk SSSR* **121**, 495 (1958).

[2] A. A. Balandine *et al.*, Paper No. 68, *Second International Conference on Catalysis*, Paris, July 1960.

[3] *Chem. Tech. Ann. Progr. Rept. Aug. 31, 1960*, ORNL-2993, chap 17.

18.2 DEHYDROGENATION OF METHYLCYCLOHEXANE ON PROMOTED CHROMIA-ALUMINA CATALYSTS

In further work on the effect of incorporating Pm^{147} in the previously described chromia-alumina catalysts, addition of up to 51 mc of Pm^{147} per gram of catalyst had little if any effect on the catalytic activity and did not change the activation energy. The reaction was tentatively established as zero order under the experimental conditions.

19. ION EXCHANGE TECHNOLOGY

The Ion Exchange Technology Program included work on the radiation stability of a cation exchange resin and on the kinetics of uranyl sulfate anion exchange.

19.1 RADIATION DAMAGE TO ION EXCHANGE RESINS

Considerable work has been done on radiation degradation of resins, but most of it has been in static systems, in which degradation products accumulate. In a system in which demineralized water was circulated through Dowex 50W resin being exposed in a Co^{60} source, 0.85×10^9 r (2.3 whr per gram of dry resin) decreased the specific resin capacity 30%, the resin volume 20%, and the moisture content from its original 42.7% to 38.6% (Table 19.1). A dose of 3.9×10^9 r (10.6 whr per gram) decreased the specific capacity 60% and volume 85% and increased the moisture content to 55.1%. These latter values do not agree with analytically determined values[1]

[1] *Chem. Tech. Ann. Progr. Rept. Aug. 31, 1960*, ORNL-2993, chap. 18.

Table 19.1. Summary of Data on Irradiated Dowex 50W X-8 (20–50 mesh) Resin*

	Original Resin	After One Week Irradiation	After One Month Irradiation
Radiation dose, r		0.85×10^9	3.9×10^9
Watt-hr/g dry resin		2.3	10.6
Resin density, g dry resin/ml wet resin	0.386	0.418	0.25
Weight loss (dry basis), %		12	95.7
Moisture content, wt %	42.7	38.6	55.1
Sulfur content, wt %	15.7	12.9	7.0
Capacity, meq/g dry resin			
By titration	4.96	2.89	1.89
By sulfur analysis	4.90	4.03	2.18
Resin volume lost, vol %		20	85
Sulfur recovered as SO_4^{--} from anion resin, meq		4.9	17.8
Sulfur recovery, %		80	64

*Radiation density 0.014 watt/g dry resin.

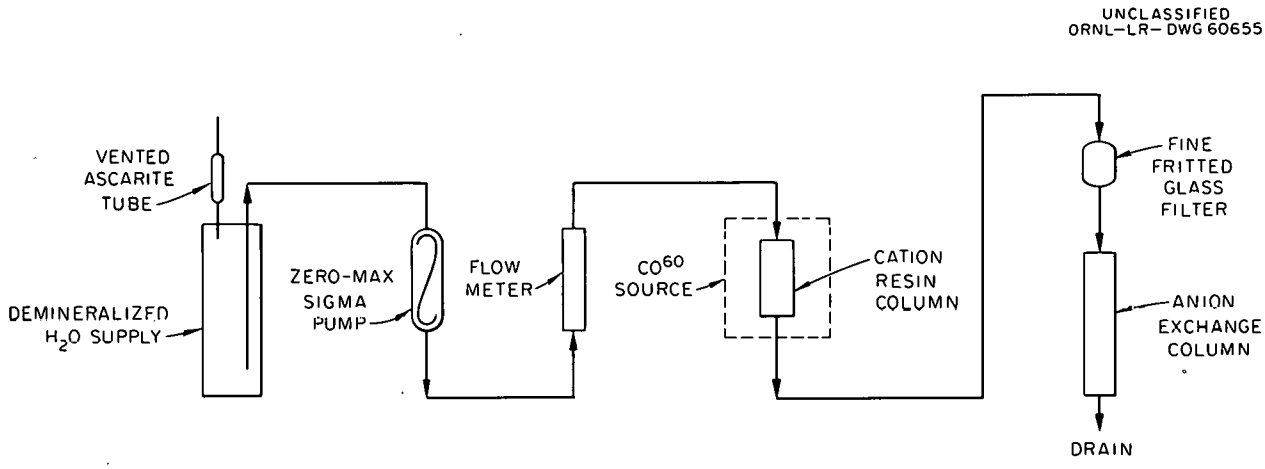

Fig. 19.1. Flow Diagram of Ion Exchange Resin Radiation Experiment.

for Dowex 50W X-12 (100 to 200 mesh), which, with a calculated dose of 12 to 13 whr/g irradiation, lost no capacity and increased in moisture content from 40% to 70%.

In each experiment, a bed of Dowex 50W X-8 (20–50 mesh) resin in the hydrogen form was placed in a stainless steel container and inserted into a 10,000-curie Co^{60} source. Demineralized water, of specific resistance > 10 megohm/cm, was circulated through the container at a rate of 5 to 10 ml/min. The effluent stream was passed through a sintered glass disk to filter out particulate matter and then into a column of dyed anion exchange resin in the hydroxide form to sorb soluble degradation products (Fig. 19.1). Qualitative analysis of the effluent stream prior to entering the anion resin column indicated the presence of sulfate and polybasic organic acids.

19.2 KINETICS OF URANYL SULFATE ANION EXCHANGE

Values of uranium, sulfate, and chloride self-diffusion coefficients (Table 19.2), obtained with the submerged-pump contactor,[2] were used to make calculations for evaluating a mathematical model describing uranyl sulfate anion exchange rates. The consistent ability of these calculations to predict the loading rate adds considerable weight to this model.

[2] *Ibid.*, Fig. 18.3.

Table 19.2. Uranium and Sulfate, Self-Diffusion Coefficients in Dowex 21K

Resin Particle Dia (μ)	Self-Diffusion Coefficient (10^7 cm^2/sec)	
	Uranium	Sulfate
1200	0.443	25.0
960	0.250	12.0
820	0.127	8.75

Earlier information[1] obtained by determining the rate of uranyl sulfate loading on an individual bead of sulfate-equilibrated Dowex 21K showed that the rate is very nearly independent of the uranium and sulfate concentrations, although the experimental conditions caused large changes in the concentrations of the various uranyl sulfate complexes. This observation implied that the distribution of uranium between the various uranyl sulfate complexes did not change within the resin.

It seemed most likely that essentially all the uranium formed the complex of highest SO_4^{--}/U ratio, since the resin can be pictured as a concentrated sulfate solution. If it assumed that all the uranium exists only as a single ion, it should be possible to predict the loading rates by calculating the rate of counterdiffusion of the three ions involved – a uranyl sulfate complex, sulfate, and in some cases chloride ions.

The diffusion of an ion, j, at point i, can be described by the Nernst-Planck flux equation:[3]

$$\phi_{j,i} = -D_j[\text{grad } C_{j,i} + Z_j C_{j,i} (F/RT) \text{ grad } \phi_i] \quad (1)$$

where

D_j = self diffusion coefficient of ion j

$C_{j,i}$ = concentration of ion j at i

Z_j = valence of ion j

ϕ_i = electric potential at i

$\phi_{j,i}$ = flux of ion j at i.

The first term of Eq. 1 is the same as the one obtained from Fick's law diffusion, and the second term represents the effect of electric fields on the ions.

The rates of uranyl sulfate loading on sulfate-equilibrated Dowex 21K were calculated from the model by considering uranyl sulfate ions to be diffusing into a sphere occupied by relatively mobile sulfate ions (D_{SO_4}/D_U = 40 to 80). Results for all three size fractions of Dowex 21K available agreed well with experimental loading curves (e.g., Fig. 19.2) when the uranium was assumed to exist as $UO_2(SO_4)_2^{--}$. Rates calculated on the assumption that the uranium was in the $UO_2(SO_4)_3^{4-}$ state were higher than those observed.

[3]F. Helfferich and M. S. Plesset, *J. Chem. Phys.*, 28 (1958) 418.

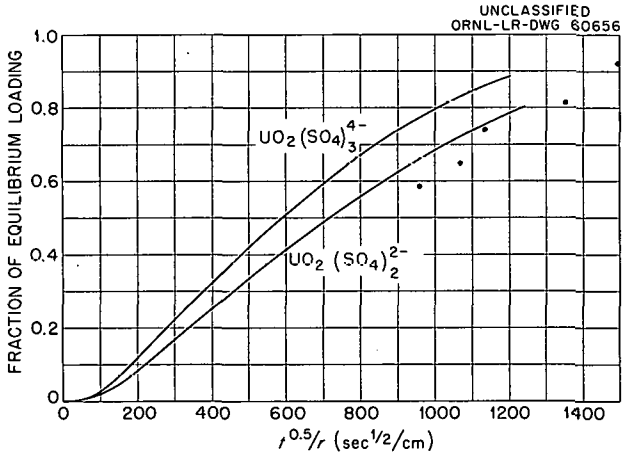

Fig. 19.2. Calculated (–) and Measured (●) Uranyl Sulfate Loading on Sulfate-Equilibrated 820-μ Dowex 21 K.

19.3 FISSION PRODUCT RECOVERY

A previously reported cation exchange scheme[3] for recovering strontium from Purex waste did not appear to be competitive because the resin capacity for strontium was at least 100-fold less than that for other cations in the waste. A direct head-end precipitation-redissolution step to obtain a more concentrated strontium solution suitable for ion exchange processing was considered possible from solubility studies of the nitrates of strontium and the chief Purex cationic impurities, Al^{3+} and Fe^{3+}, in 50 to 80% HNO_3. These data indicated that >90% of the strontium could be precipitated in 80% HNO_3 with <20% of the aluminum and <1% of the iron. However, it was found that the presence of 1 *M* sulfate in Purex interfered with the above predicted quantative recovery of strontium. On a laboratory scale, >85% of this sulfate was precipitated by adding excess ferric ion to Purex waste and diluting with fuming nitric acid to 50 to 55% HNO_3. The extent of strontium recovery from this nearly sulfate-free filtrate will be determined by how closely the solution approaches nitrate system conditions at 80 to 85% HNO_3. These fields may be created by the motions of the ions that they affect. If the motion of several ions is considered and it is required that the net charge at each point in the resin (taking into account the resin capacity) and the net flux of charge at all points is zero, the electric potential term can be evaluated:

$$(F/RT) \text{ grad } \phi_i = \frac{\sum_j D_j \text{ grad } C_{j,i}}{\sum_j Z_j^2 D_j C_{j,i}}. \quad (2)$$

These equations were programmed for the IBM-7090 to calculate the radial diffusion rates of up to three ions into or out of a spherical bead of ion exchange resin. Numerical solutions to these equations have been reported in the literature[3] for only two ions and for a limited range of diffusion coefficient ratios.

19.4 PLUTONIUM RECOVERY

The plutonium flushed from the Pilot Plant during cleanup after the evaporator explosion (Chap. 6) was recovered by ion exchange with losses of only 1%. Plutonium solutions of concentration

>0.01 g/liter were adjusted to 0.1 *M* aluminum to complex fluoride and evaporated to 33% of the original volume. The nitric acid was adjusted to 7.0 *M* and the plutonium was reduced to Pu(III) with ferrous sulfamate and then reoxidized with sodium nitrite at elevated temperature. In a 5-in.-dia by 5-ft-high ion column containing 23 liters of Permutit SK resin, the maximum loading was 34 g of plutonium per liter of resin. The plutonium on the bed was scrubbed with 7.2 *M* HNO_3–0.005 *M* HF at 60°C to remove fission product activity and ionic contaminants, and eluted with 0.6 *M* HNO_3 at 60°C. The overall decontamination factor from fission products was 5200, which was sufficient to reduce the gamma activity of the product to 3.5×10^3 c min^{-1} mg^{-1}.

20. CHEMICAL ENGINEERING RESEARCH

20.1 BOTTOM INTERFACE CONTROL FOR PULSED COLUMN

A bottom interface control device based on differential levels in water-purged head pots was satisfactorily demonstrated on a 24-ft-high nozzle-plate pulsed column. This type of controller is suitable for a direct maintenance radioactive facility because there are no parts in contact with radioactive solutions which require maintenance. The most critical design feature of the device is the necessity of providing surge capacity in the horizontal portion of the transmission lines so that an increase in column pressure does not force either organic or aqueous salt solutions into the vertical runs of pipe, thereby adversely affecting the differential level in the head pots. The lag in indicated interface was less than 0.5 in. and recovery time was about 5 min after a linear increase or decrease of interface level of 4 in./min.

20.2 INTERFACIAL VISCOSIMETER

Previous studies on the water–uranyl nitrate–tributyl phosphate system indicate that in solvent extraction contactors the rate-limiting process for the extraction of uranyl nitrate is diffusive and convective transport of the molecular species concerned to and from the interface. The presence of surface-active agents increases interfacial viscosity, and an interfacial viscosimeter was designed (Fig. 20.1) to measure this property. It is essentially a modified two-dimensional Brookfield viscosimeter. A stationary ring, suspended in the interface by a fine wire of known torsional spring constant is surrounded by another ring, with a known clearance, which is rotated at constant velocity. From the torque produced in the stationary ring by the shear in the interface, the interfacial viscosity can be calculated. Momentum transfer from the rotating to the stationary ring is minimized by appropriate baffles, and can be separately measured and corrections applied.

20.3 STACKED CLONE CONTACTOR

A larger model, MK II, of the stacked clone contactor[1] was constructed and partly tested (Fig. 20.2) on the system Amsco–0.08 *M* HNO_3–benzoic acid. The MK II contactor, compared to MK I, has hydroclone stages twice the diameter (1.5 vs 0.75 in.), half the length (2 vs 4 in.), and larger overflow and underflow ports. Throughputs of both phases are 6 liters/min compared to 1.2 liters/min for MK I, and the holdup of both phases per stage is 203 ml compared to 192 ml.

Tested stage efficiencies for MK II range from 10 to 30% compared to 30 to 90% for MK I. These lower efficiencies for MK II are attributed to backmixing of one or both phases. Lithium chloride tracer injection studies, in which LiCl solution is injected into a stage and the concentration profile through the contactor is measured, show aqueous backmixing of 50 to 150% of the aqueous throughput under various conditions. Studies are in progress of the effect of variations of appropriate equipment dimensions, and of the effect of stage pump recycle flow on the backmixing ratio and on the stage efficiency.

[1] MK I was described in ORNL-2993.

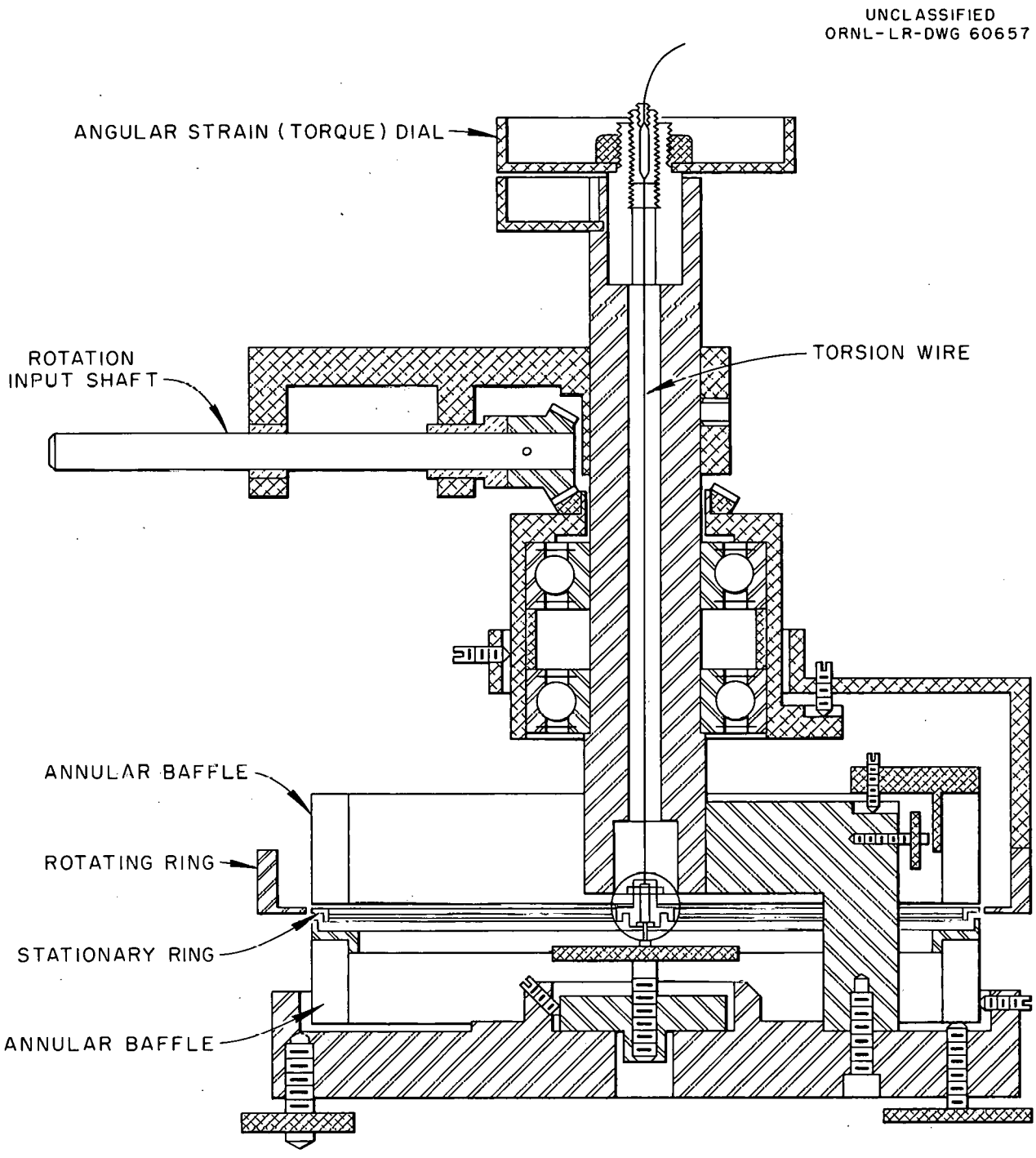

Fig. 20.1. Interfacial Viscosimeter.

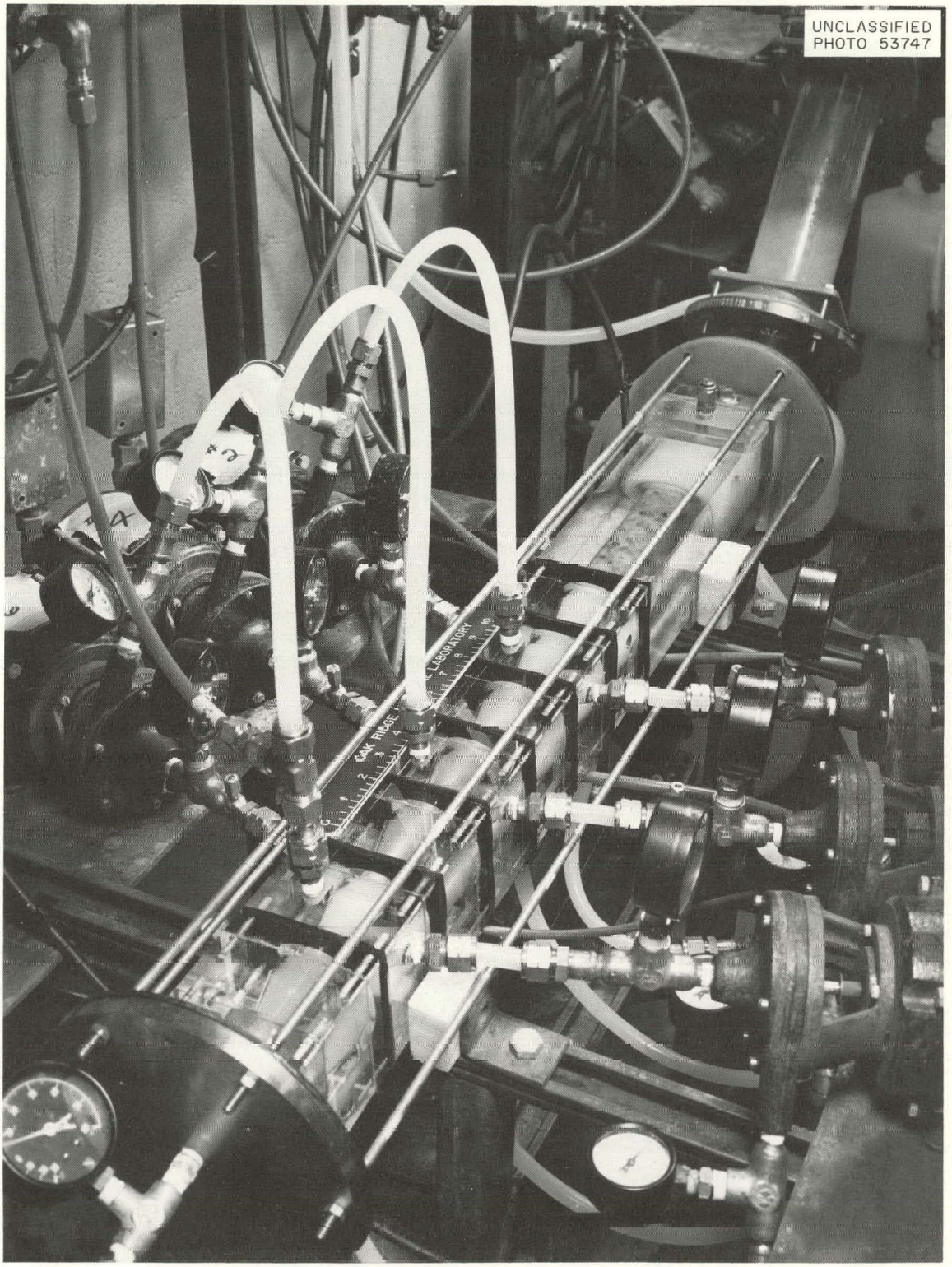

Fig. 20.2. MK II Contactor in Operation.

20.4 THERMAL DIFFUSION

Thermal diffusion of electrolytes is being studied to advance the basic understanding of this relatively new chemical engineering unit operation. Soret coefficient measurements on three samples of aqueous solutions of $LiNO_3$ showed no measurable isotopic enrichment by thermal diffusion. Soret coefficient measurements on a uranyl sulfate–water solution with composition essentially that of the aqueous Homogeneous Reactor fuel (10 g/liter of U, 25% excess sulfate as H_2SO_4) were not reproducible (Table 20.1), but no high-temperature inversion (concentration of salt in the hot region) was indicated. The lack of reproducibility is caused primarily by the small concentration changes produced by thermal diffusion. Since the concentration ratios between hot and cold sides are close to 1, small analytical uncertainties can lead to large errors in the logarithm of the ratios used in calculating the Soret coefficients.

Negative Soret coefficients obtained for the $ZrO(NO_3)_2$-H_2O and $HfO(NO_3)_2$-H_2O systems indicated that both salts concentrate at the hot wall of the cell (inversion) (Table 20.1). However, preliminary calculations indicate that this observed effect may be almost entirely due to a thermo-osmotic transfer of water across the membrane rather than to thermal diffusion. The solubilities of both salts were found to be quite small. Both salts are believed to be only partially ionized in solution, and to show colloidal behavior.

Theoretical studies of the thermal diffusion of electrolytes were started but results are still very preliminary. The results will be tested largely in the $Ni(NO_3)_2$-$Co(NO_3)_2$-H_2O system due to its convenience for spectrophotometric analysis.

20.5 INTERMEDIATE-SCALE MIXER-SETTLER PERFORMANCE

The intermediate-scale mixer-settler solvent extraction contactors to be installed in the IMMI Facility in Building 4507 were extensively tested with the standard Purex flowsheet. Three banks of mixer-settlers are racked vertically to provide gravity flow of the solvent effluent from bank A, the extraction-scrub bank, to B, the partitioning bank, and finally to C, the stripping bank. A and B banks each contain 17 stages; C bank has 11. With proper control of the interfaces, aqueous holdup in the mixing and adjacent settling chamber is 20 and 120 ml, respectively; the corresponding organic holdup is 20 and 80 ml. The C bank is oversized by a volumetric factor of 2.25, compared to banks A and B. Aqueous flow through the tanks is controlled by the motor-driven pump-mix impellers which pull aqueous into the bottom of each mixing chamber and discharge the organic-aqueous emulsions through the mixed-phase discharge ports into each settling chamber. The organic stream moves countercurrently from the settling to the mixing chamber via overflow ports.

In the test runs the extraction-scrub and partitioning bank total throughputs were each 280 ml/min at an impeller speed of 1200 rpm; the stage efficiency for uranium extraction was 95%, at 85% of flooding. In the stripping bank total flow at 95% of flooding was 578 ml/min at an impeller speed of 950 rpm. The uranium stripping stage efficiency was 93%. Actually, the stripping bank, where uranium is stripped from the solvent, was limiting to aqueous throughput which is near maximum at 350 ml/min. At 375 ml/min, sporadic flooding occurred by aqueous backing up and eventually flowing out the solvent outlet from

Table 20.1. Soret Coefficients for Salt Systems

System	Mean Cell Temperature (°C)	Temperature Difference (°C)	Mean Soret Coefficient ($°C^{-1}$)
UO_2SO_4-H_2O	32	55	$1.9 \pm 0.4 \times 10^{-3}$
10 g/liter of U	27	44	$1.1 \pm 0.3 \times 10^{-3}$
25% excess H_2SO_4	21	33	$-0.5 \pm 0.8 \times 10^{-3}$
$ZrO(NO_3)_2$-H_2O	32	55	-2.65×10^{-2}
$HfO(NO_3)_2$-H_2O	32	55	-2.03×10^{-2}

the bank, but at the stable operating total flow rates of 578 ml/min, the Purex flowsheet could be operated at an aqueous throughput of 75 liters of aqueous feed per day, corresponding to a uranium throughput of 24 kg/day.

As the aqueous throughput was increased, the impeller speed was necessarily increased to provide greater pumping action with attendant improvement in stage mixing efficiency. Maximum stage efficiencies for uranium extraction and stripping were at 85 to 95% of flooding capacity.

In the A and B banks, where the aqueous flow is small relative to the organic, stainless steel disks were attached to the bottom of the impellers to restrict the aqueous pumping from stage to stage. In the C bank, where the aqueous flow is relatively large, the disks were omitted to realize maximum aqueous pumping.

21. INSTRUMENTATION

A method was devised for measuring the densities of aqueous solutions at measured temperatures and pressures up to the solution critical points. The liquid volume of a weighed solution of known composition is determined in an autoclave of suitable material, and an x-ray photograph is made to show the position of the vapor-liquid interface in a calibrated section of the autoclave (Fig. 21.1).

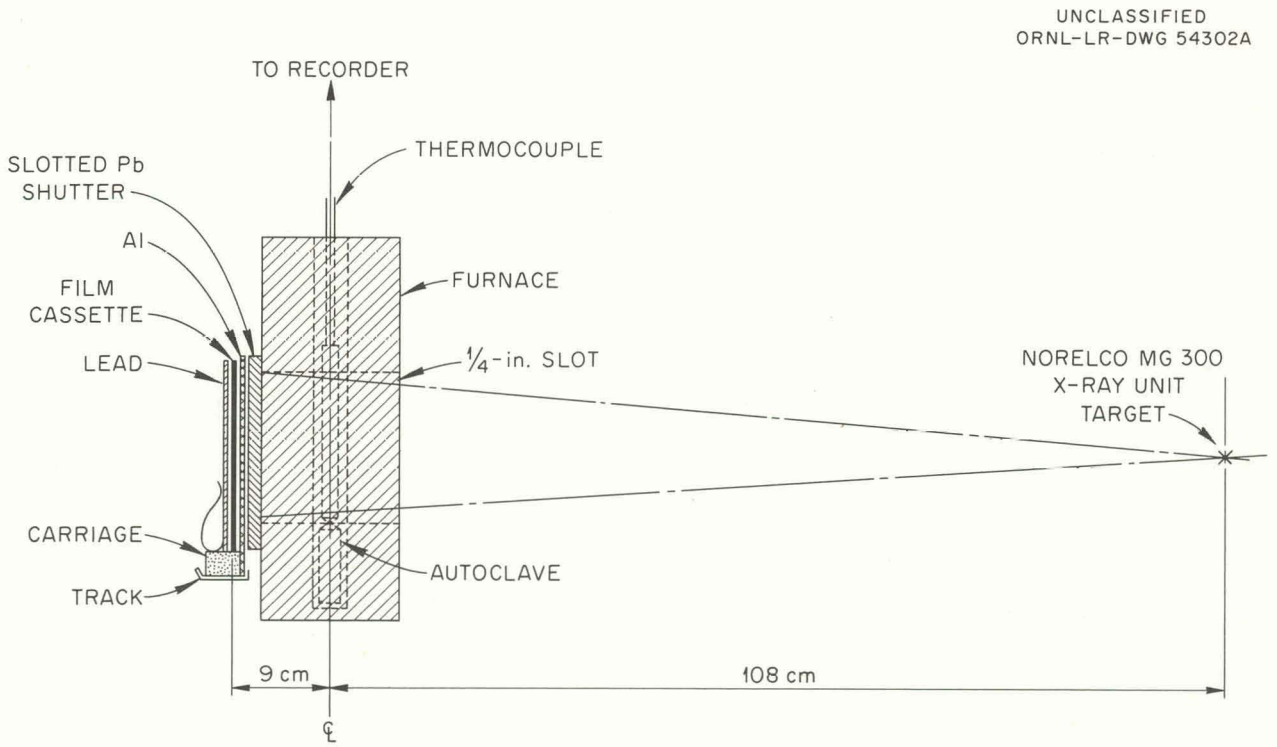

Fig. 21.1. Apparatus for Making X-ray Photograph of Vapor-Liquid Interface for Use in Density Determinations.

The density is determined from the weight of solution and the location of the interface. The feasibility of the method was established[1] by the close agreement of experimentally determined densities of a uranyl sulfate solution with those reported for a very similar solution over the temperature range 20 to 300°C.

[1]N. A. Krohn and R. G. Wymer, *A Method for Measuring Liquid Densities at High Temperatures and Pressures*, ORNL CF-61-1-47, (Jan. 11, 1961).

22. HIGH-TEMPERATURE CHEMISTRY

Design of a high-temperature high-pressure spectrophotometer system was completed.[1] The spectrophotometer system, based on the Cary Model 14 PM spectrophotometer, is designed for use with highly radioactive aqueous solutions at temperatures up to 330°C and at pressures up to 3000 psi.

[1]By Applied Physics Corporation under contract.

An auxiliary system was developed by the ORNL Instrumentation and Controls Division to produce a digital output from the wavelength and absorbency information provided by the spectrophotometer system. The digitized information is fed to a standard IBM 26 printing card punch, which is programmed to produce cards suitable for computer processing.

23. CHEMICAL APPLICATION OF NUCLEAR EXPLOSIONS (CANE)

The Chemical Technology Division efforts in the CANE program are a small part of other investigations, centered primarily at Livermore, to explore the feasibility of producing desirable isotopes or chemical reactions with the effects of contained thermonuclear explosions. Rock salt is considered a good containment medium, the major impurities in which are calcium and magnesium sulfates. Exploratory chemical studies at high temperature have been made to define the nature of the reactions of hydrogen and tritium with minerals in the containment medium; a sequential sampler for the gas phase detonation products from the Gnome event is being designed.

23.1 CHEMICAL STUDIES

The stoichiometry and kinetics of the reactions of hydrogen with $CaSO_4$ and $MgSO_4$ at temperatures up to 900°C and isotopic exchange of tritium between molecular hydrogen and water catalyzed by sulfates at 400 to 700°C were studied.

Reduction of Sulfates by Hydrogen

Calcium sulfate was reduced by hydrogen in the 800 to 900°C temperature range according to the

reaction

$$CaSO_4 + 4H_2 \rightarrow (1 - x)CaS + xCaO + xH_2S + (4 - x)H_2O$$

where x = mole fraction of $CaSO_4$ reacting to form H_2S or CaO. Direct measurement of the H_2S formed after complete reduction of the $CaSO_4$ showed 12 to 18 mole % reduced to CaO and the remainder to CaS. The CaO and H_2S were formed by hydrolysis of CaS. The reduction rate of $CaSO_4$ was independent of H_2 pressure above 200 mm Hg under static conditions. The instantaneous reduction rate at 700°C was 2.43×10^{-7} mole m^{-2} min^{-1} and the apparent activation energy was 39 kcal $mole^{-1}$.

Magnesium sulfate was reduced completely to MgO with the formation of H_2O, H_2S, and S in the 700 to 800°C temperature range. The mechanism of free sulfur formation is not known. At 800°C $CaSO_4$ was reduced about 5-fold more rapidly than $MgSO_4$.

Tritium Exchange

The exchange rate was investigated for the reaction

$$HTO + H_2 \rightleftharpoons H_2O + HT$$

catalyzed by pure $CaSO_4$ and by impure anhydrite. Conditions were chosen so that the exchange would be limited by diffusion, a condition which probably is typical of the reaction conditions following a nuclear detonation. The net exchange was measured after a gaseous mixture of H_2-H_2O-HTO had been passed over layers of $CaSO_4$ at initial flow rates, in moles per minute, of 6.5×10^{-3} for H_2, 4.5×10^{-4} for H_2O, and 4.1×10^{-11} for HTO. The exchange rate apparently depended most strongly on the temperature and the residence time of the gases at temperature; there was little noted effect of $CaSO_4$ and surface area even with finely divided powders. The maximum tritium exchange at 600°C under steady-state conditions was 25.8% for a residence time of 45 sec when the gas stream was in contact with 12.0 g of $CaSO_4$ (10.0 m^2/g). Anhydrite samples obtained from the Gnome drill hole in bedded salt were only 25% as effective as pure $CaSO_4$ for catalyzing the exchange, and pure NaCl was only 1% as effective. Decreasing the total gas flow rate by a factor of 2 increased the exchange by a factor of 1.5. Further decrease in flow rate did not increase the exchange, which indicated that the exchange was adsorption- or mass-transfer-controlled. The net exchange was never more than 25% of the calculated equilibrium value. Arrhenius plots gave an apparent activation energy 8.8 ± 0.08 kcal for the exchange.

Since only 1% tritium exchange was observed in gas samples from the Tamalpais nuclear explosion in tufted rock, these laboratory results strongly suggest that tritium from the detonation either did not contact any H_2O or any reducible oxygen bearer at elevated temperatures, or the contact was for a very short time.

23.2 ENGINEERING STUDIES

Equipment was designed[1] for taking seven samples in a predetermined time sequence of the gaseous product of the proposed Project Gnome event during the expansion of the cavity and for taking samples on a continuing basis after completion of expansion (Fig. 23.1). The design provides for taking samples at millisecond intervals; valves will operate in approximately 50 μsec. Samples of the expanding gas streams moving at velocities of possibly 90 km/sec will be taken.

In co-operation with Frankford Arsenal a hypervelocity jet sampler is being studied for possible use in removing irradiation targets from the damage zone of a contained nuclear detonation prior to the onset of damage. Its purpose is to irradiate and then to instantly and quantitatively recover a target material before the shock wave produced by the explosion destroys the target and exit tubes. Specimen cones for use with shaped charges of conventional explosives were submitted to Lawrence Radiation Laboratory and Frankford Arsenal for experiments with this type of sampler.

Considerable study was devoted to sampling the chamber developed by the nuclear device for long periods after the explosion. This requires that a hole from the shot zone to the ground surface be kept open. The best system so far conceived proposes the use of a very heavy-walled steel pipe, with an outer diameter-to-inner diameter ratio of ¾, partially filled with water and protected from ground shock by a gas blanket produced by a conventional explosive.

[1] J. W. Landry, "CANE Sequenced Sampler for Project Gnome: Design Proposal," ORNL CF-61-3-101 (Mar. 15, 1961).

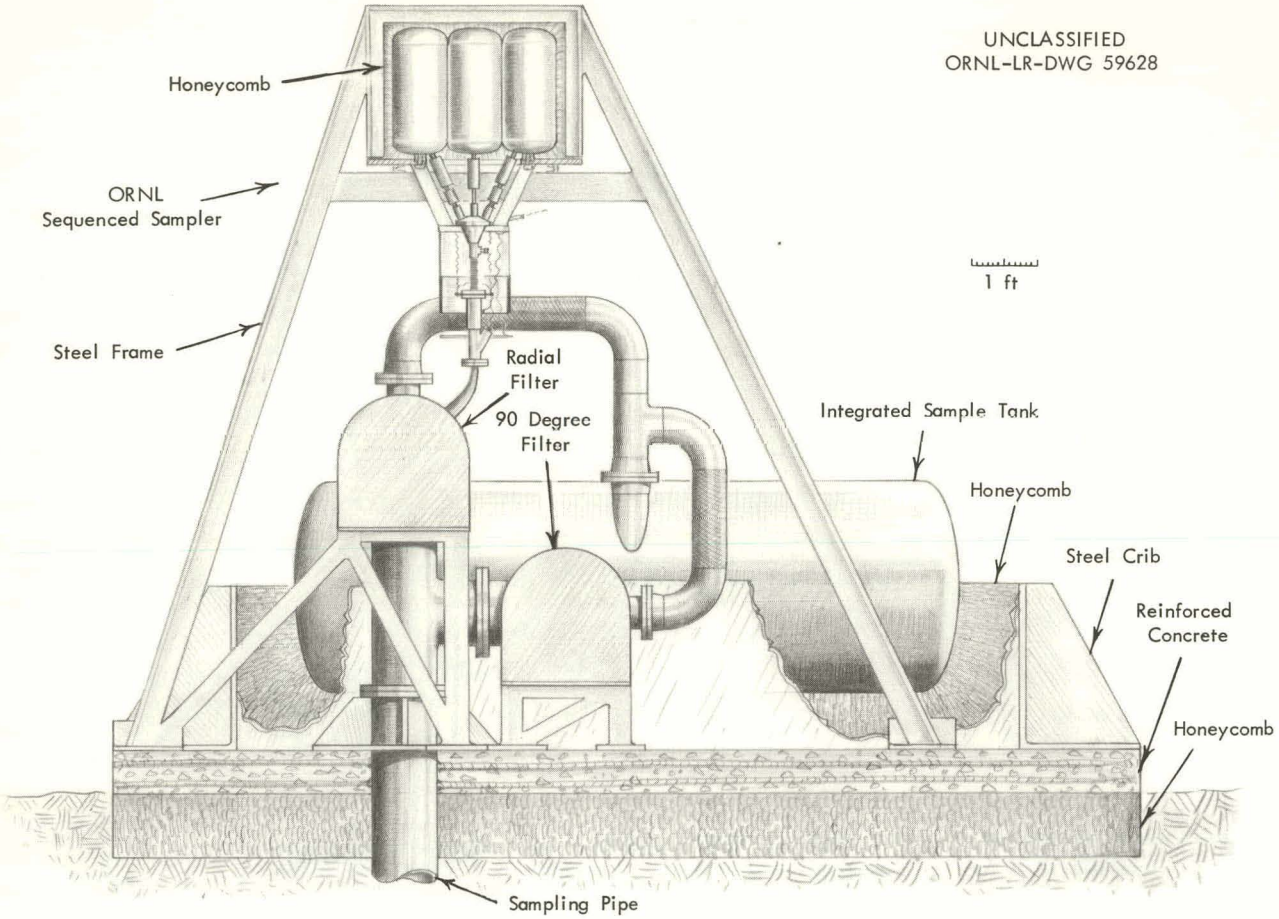

Fig. 23.1. ORNL Sequenced Sampler, Design Proposal: Assembly, Schematic.

24. REACTOR EVALUATION STUDIES

24.1 HEAT TRANSFER FROM SPENT FUELS DURING SHIPPING

The dissipation of radioactive decay heat from spent fuel elements inside shielded carriers is a major problem in the shipping of fuels from the reactor to the processor. In order to avoid melting or other damage that could result in release of radioactive materials, the carriers must be designed to maintain temperatures within safe limits under any conditions. Since the rate of heat removal may limit the carrier capacity, accurate methods of predicting temperature rises are needed for safe and economical carrier design.

Initial measurements of temperature rise were made in stainless steel tubes internally heated with Nichrome resistance wire assembled into mock fuel bundles inside a 12-in.-i.d. stainless steel cylinder with transite flanges for air-filled carriers and heat generation rates expected with reactor fuels. They indicated that 30% or more of the heat transfer will be by radiation. Since

this type of transfer can be analyzed mathematically with relatively few data, initial analytical effort has been in this direction. In a simple experiment with two concentric tubes of different diameters separated by a near vacuum, the emissivity of the stainless steel tube was found to be approximately 0.55. Calculated configuration factors for radiation are shown in Fig. 24.1, to adjacent tubes in curve a and to diagonal tubes in curve b, as a function of the tube spacing to radius ratio, S. Because of the tight spacing of power reactor fuel elements, each tube can see no more than four adjacent tubes, four diagonal tubes, and eight other tubes adjacent to the diagonals. Factors for the diagonal tubes need be calculated for values of S up to only $2\sqrt{2}$ since for greater spacings there is no shadowing of the radiant flux by the adjacent tube. Under these conditions, configuration factors for diagonal tubes and $S > 2\sqrt{2}$ may be obtained from Fig. 24.1a since the tubes appear as adjacents with spacing $S\sqrt{2}$. The configuration factor for other tubes adjacent to the diagonal may be obtained by noting that the factor for radiation from one surface to all enclosing surfaces is 1. Then the factor for this case is $\frac{1}{8} - \frac{1}{2}(F_{adj} + F_{diag})$.

24.2 SHIELDING DESIGN CALCULATION CODE[1]

A code for the IBM 7090 was written to perform at least 90% of the basic shielding calculations required for fuel-handling facilities.[2] The time saving is indicated by the completion in 2 min of a problem that required 2 to 8 hr by hand calculation. The code will handle the following materials as options for the structure of the shielding, cladding material, and the material constituting a volume source: (1) water, (2) aluminum, (3) iron, (4) lead, (5) uranium, (6) ordinary concrete, (7) barytes concrete, (8) magnatite concrete, (9) ferrophos concrete, (10) window glass, (11) 3.2 g/cc density glass, and (12) 6.3 g/cc density glass. Space has also been allotted for five optional materials which may be added. Three different calculations involving laminated shields can be performed.

[1] In co-operation with Betty F. Maskewitz, Central Data Processing, K-25.

[2] E. D. Arnold and Betty F. Maskewitz, *SDC: A Shielding Design Calculation Code for Fuel Handling Facilities,*" ORNL-3041 (to be published).

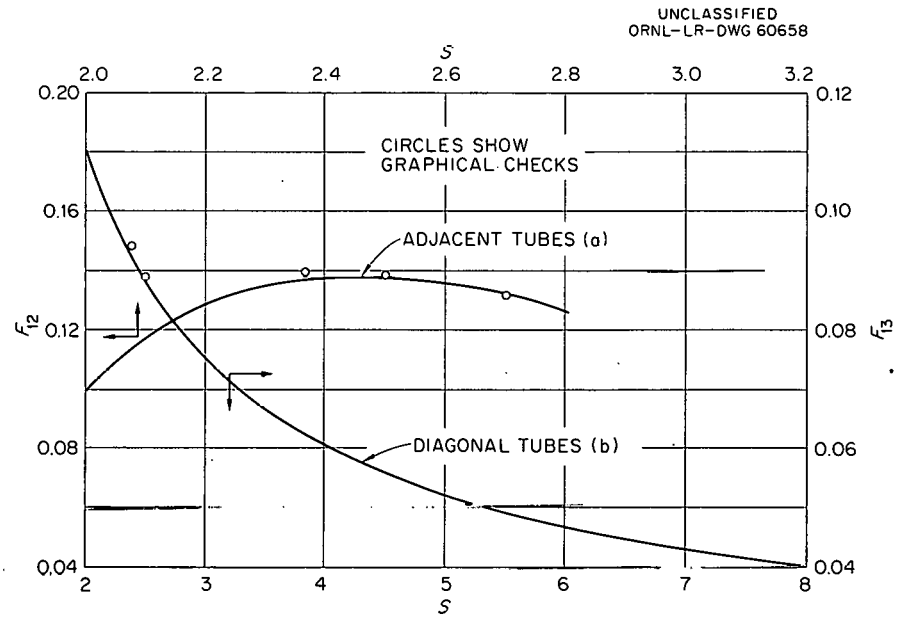

Fig. 24.1. Configuration Factors for Adjacent Tubes and Diagonal Tubes.

The code calculates shield requirements as determined by the basic equations for the various geometries given by Etherington.[3] The geometry source options covered are: (1) point, (2) line, (3) disk, (4) plane, (5) slab, (6) cylinder with shield at side, (7) cylinder with shield at end, (8) sphere, (9) ring, (10) rod cluster, (11) skew line, (12) annular cylinder with shield at side, (13) annular cylinder with shield at end, (14) line with cosine source distribution, (15) cylinder with shield at side and cosine source distribution, (16) rod cluster with cosine source distribution. Equations for geometry options (10) and (12) through (16) were written by the authors.

The code supplies many calculational features as built-in data. These include E and F functions as subroutines: self-absorption coefficients for large distances from source (both cylinders and spheres) were evaluated from the data in the Nuclear Engineering Handbook and fitted to a polynominal by the method of least squares, and coefficients for small distances from the source were obtained from the curves in the Nuclear Engineering Handbook. These values were tabulated and a double interpolation subroutine was written to evaluate intermediate values of the self-absorption coefficient: total linear attenuation coefficients were taken from the Nuclear Engineering Handbook and other sources for the listed material options (linear interpolation is used to find intermediate values from these tables), and build-up factors were obtained either directly or extrapolated from other data in the literature. Again, double interpolation is used to obtain intermediate values. A method is incorporated to obtain a flux-averaged build-up factor for all penetrations that are not perpendicular to the shield surface.

The code has been used successfully to evaluate shield thickness and/or dose rates for several design jobs.

[3] H. Etherington, *Nuclear Engineering Handbook*, McGraw-Hill, New York, 1958.

25. ASSISTANCE PROGRAMS

25.1 EUROCHEMIC ASSISTANCE

ORNL's contribution to the Eurochemic assistance program consisted in coordination of the program and review and exchange of pertinent technical information on radiochemical processing of irradiated fuels. About 210 USAEC-originated documents and 40 miscellaneous items were sent to Eurochemic,. 11 Eurochemic documents were reproduced and distributed, and an additional 25 Eurochemic documents were received and are now being processed for distribution.

The preproject study (scope) by St. Gobain for the Eurochemic chemical processing plant has been essentially completed and contracts have been signed with eight special architect-engineering firms for various phases of the plant and supporting facilities. Project effort has started on the low-activity waste lines for the plant and research laboratory, on the research laboratory, and on the fuel reception and storage canal. Site layout has been frozen, and the administration building and the connecting canal bridge have been completed. The main process building currently envisioned is about 260 ft long, 90 ft wide, and 90 ft high. Two dissolver systems are included, one for fuels up to 1.6% enrichment and one for remaining fuels of <5% enrichment. Consideration is being given to processing of intermediate-enrichment and fully enriched uranium. Dissolution procedures include the Sulfex process for stainless steel–clad fuels, the Zirflex process for Zircaloy-clad fuels, caustic or dilute sulfuric acid for aluminum-clad fuels, dilute sulfuric acid for magnesium-clad fuels, and nitric acid for uranium, UO_2, and uranium-molybdenum alloy fuels. Other processes includes feed preparation and storage facilities, a solvent-extraction partitioning cycle, a solvent-extraction second cycle, an unspecified (ion exchange or TLA extraction)

second plutonium cycle, a silica gel system, two solvent recovery systems, waste evaporation and acid recovery facilities, and rework facilities.

25.2 O^{17} PILOT PLANT

A pilot plant was designed for the Reactor Chemistry Division to separate 50% pure O^{17} by water distillation and thermal diffusion of oxygen gas. The water distillation cascade is rated at a product rate of 1.5 g/day, the product containing ~3.6% O^{17}. This water will be electrolyzed and gaseous oxygen separated as 50% O^{17} in two 35-mg/day streams, one rich in O^{16} and the other in O^{18}.

The pilot plant was fabricated and installed in the high bay area of Bldg. 4501. Installation is complete and shakedown tests are being made.

25.3 U^{233} METALLURGICAL DEVELOPMENT LABORATORY

Design criteria and a preliminary cost estimate are being prepared for a shielded facility to be used by the Metallurgy Division for developing economic systems for fabrication of U^{233} into power reactor fuel elements. Because U^{232} is formed in small amounts along with U^{233} by neutron irradiation of thorium, U^{233} is accompanied by penetrating radiation, the most energetic being the 2.6 Mev gamma of Th^{212}. Rapid refabrication after purification can minimize but cannot eliminate the need for shielding. The initial effort in the proposed U^{233} facility will be to develop a remotely operable technique for production and vibratory compaction of very dense thorium-uranium oxide particles into tubular fuel rods; the facility design will be such that these techniques can be tried.

The physical plant will consist of three cells shielded by 4 ft of normal concrete and required supporting areas. The largest cell (20 × 48 × 18 ft high) will be used for oxide preparation and experimental fuel element fabrication on a small scale. A second cell (9 × 16 ft) is to be used for decontamination and remote repair of equipment. These two cells will be joined by a shielding, sealing door; both cells will be completely sealed to prevent the escape of alpha active materials. A third cell (9 × 16 ft) is to be provided for inspection of the finished fuel elements but will not have to be leaktight because all radioactive material will be contained in sealed metal tubes. Viewing will be through zinc bromide windows, by periscopes, and by television. Manipulation will be by sealed master-slaves and by rectilinear manipulators. A powered hoist will be provided for transport of heavy objects.

25.4 HIGH RADIATION LEVEL ANALYTICAL LABORATORY

Design criteria were provided for the Analytical Chemistry Division's High Radiation Level Analytical Laboratory. The HRLAL will be located across the street from and west of Bldg. 3019 on the site of the old physics building and will be approximately 130 × 85 ft with a second story 110 × 73 ft. It will contain one storage cell 8 × 12 × 8 ft high, one unloading cell 6 × 8 × 11 ft high, six work cells 6 × 6 × 11 ft high, an operating area, a radioactive servicing area, a decontamination area, three 24- × 24-ft standard laboratories, and supporting change room, offices, and loading facilities. The storage cells will be built from 4 ft of barytes concrete and will be equipped with standard-duty model 8 manipulators and cerium glass windows; the work cells will be built with 4 ft of standard concrete and will be equipped with standard model 8 manipulators, zinc bromide windows, and roll-out shield doors. The unloading cell will be built with 4 ft of standard concrete and will be equipped with zinc bromide windows on front and rear faces, standard- and heavy-duty manipulators, and a double-door carrier entrance system. This facility will be used both as a service facility for the Laboratory's high-activity-level analytical requirements and for research and development on analytical techniques and equipment in high radiation fields.

25.5 BUILDING 4507 ADDITION

An addition to Bldg. 4507 to be located immediately west of the existing 4507 building and immediately south of Bldg. 4505 was designed. It will be 93 × 56 ft and will include four work cells 8 ft 6 in. × 8 ft × 11 ft high, a storage and an unloading cell each 8 ft 6 in. × 6 ft × 12 ft high, a nonradioactive operating area, and a cell-servicing area on the ground floor. A makeup area will be at the second level over the servicing area and an air-tight crane bay will be installed over the top of the cells. Barytes concrete shielding will be used on the fronts of all cells and the backs of the storage and unloading cell; normal

concrete will be used on the backs of the work cells and on the roofs of all cells. Each cell will be equipped with a cerium glass window, a Model 8 manipulator, a roll out back door, and full opening roofs slabs. The unloading cell will be used for receiving and unloading carriers and doing simple operations on preparation of samples for storage and for use in the work cells. The storage cell will be used to store radioactive materials prior to use in the work and for storing radioactive solid wastes prior to disposal to the burial ground. The work cells will be used to demonstrate various radiochemical processes and operations on a small, full-activity-level scale.

25.6 CONTAINMENT MODIFICATIONS

Laboratory standards require that all facilities handling $\geq$1000 curies of β-γ activity and/or 1 g of plutonium be fully contained. There will be a primary containment zone in which the radioactive material is handled and a secondary containment zone surrounding the primary. The flow of air will be always from the general environment to the secondary zone to the primary, with special precautions to minimize backflow in the event of fire, explosion, or other catastrophe. Air leaving the primary area will be cleaned prior to release through the plant stacks. Similar provisions are also applied to the discharge of liquid and solid waste from the primary zones.

A thorough review of the containment requirements for the PRFP complex in Bldgs. 3019 and 3505 led to the conclusion that Bldg. 3019 should be fully contained but that Bldg. 3505 could be eliminated from fuel processing use by moving the plutonium processing function to Bldg. 3019. The cost of modifying Bldg. 3019 for both containment and processing improvements and additions was estimated to be $1,000,000. As a result of the AEC decision to pilot plant the PRFP processes at ICPP, the program for upgrading the Bldg. 3019 process equipment was abandoned and the containment changes were limited to those necessary for safe operation of the Volatility Pilot plant in cells 1 and 2. A filter and ion exchange system were to be installed on the Metal Recovery Canal as soon as possible; however, these plans were abandoned in favor of installing a temporary filter since the canal will be drained, cleaned, and abandoned as soon as the 30 tons of BNL slugs has been removed and shipped to SRP.

Containment changes at Bldg. 3019 included installation of an off-gas scrubber for cells 1 and 2 to remove all F_2 or HF in the event of a leak in any of the process equipment. The HF or F_2 would be scrubbed with KOH to prevent their entering the main building duct and possibly destroying the absolute filters at the 3039 stack, resulting in release of collected activity. All holes in cells 1 and 2 were sealed with duct seal or equivalent, vestibules were installed to the operating and sampling areas, bulkhead doors at the cell entries, and absolute filters and backflow preventers on the cell air inlets. All holes and windows in the crane bay area over the cells were sealed. Automatic instrumentation was installed to reset airflow patterns during an emergency, and neutron, γ, and air monitors were installed as needed to provide radiation data for personnel protection.

New equipment is being installed in cell 3 of Bldg. 3019 for storage of U^{233}, which is now stored in three infinitely safe tanks in the pipe tunnel. The new storage tank will be a 225-gal conventional tank filled with boron glass raschig rings for criticality control (Sec. 1.9). This tank and its associated piping will be unit shielded in cell 3.

Room 211 in Bldg. 3019, which formerly contained the ion exchange equipment for U^{233} isolation and concentration, is being re-equipped as a plutonium process development laboratory. The old equipment was removed and the room stripped of its conventional laboratory furniture. A vestibule was installed for radiation control, and a new stainless steel floor was put down to simplify future decontamination. New or decontaminated used laboratory furniture and four glove boxes will be installed to complete the renovation.

At Bldg. 4507 an airtight structure was built over the cell roof and Gantry crane, including an airtight telescoping door at the west end of the new structure. Vestibules were constructed at both existing entrances, all cell holes were sealed, especially the 6- × 6-ft back door openings and roof plugs, the Argonne Model 8 manipulators were double-booted, and filters and backflow preventers were installed on all cell air inlets and

individual filters on all cell off-gas outlets. Instrumentation similar to that at Bldg. 3019 was provided for personnel protection.

Containment modifications similar to those for Bldg. 4507 were also made at Bldg. 3026. In addition, the area above the cells was enclosed by a concrete block housing and equipped for use as a GM manipulator and general maintenance area. Because NaK is to be handled in cell A during the SRE fuel mechanical processing program, special fire protection systems were provided in the cell, including bags of graphite powder to be used for smothering of small fires and a rate-of-rise instrumented CO_2 extinguisher system for larger fires. Both systems were thoroughly checked out.

New off-gas filter houses were installed to handle the low-activity-level exit air from the laboratory and analytical radioactive cell area of Bldg. 3019 and the combined cell exhausts from Bldgs. 4501, 4505, and 4507. The former is located north of Bldg. 3019 and west of the 3039 stack. The latter is about 100 yards east of the main plant stack.

25.7 PLANT AQUEOUS WASTE SYSTEM

Modifications to existing ORNL liquid waste system needed to decrease radioactive discharges at the Laboratory to ≤ 0.1 mpc_w were studied. The proposed modifications emphasize containment of activity through storage of high-activity wastes in new stainless steel tanks, evaporation of intermediate-activity wastes, and decontamination of low-activity wastes by either ion exchange or lime-soda softening and vermiculite sorption. Conceptual designs were completed for a storage tank and evaporator facility and for a system for collecting and pumping wastes produced in Melton Valley to the Main Laboratory waste system in Bethel Valley.

Two high-level waste storage tanks of 50,000 gal capacity each, with approximate dimensions 10 ft dia by 85 ft long, will be equipped with cooling coils on their outer surfaces for removal of a maximum of 300,000 Btu/hr of decay heat and will be supported inside a concrete vault for containment. The evaporator and a feed tank will be installed inside a cell shielded with 5 ft of concrete and will process mainly intermediate-activity waste supernatant from the concrete waste tanks, but will be able to evaporate high-activity waste as well. Two additional cells for the condenser and other off-gas equipment will be housed with the evaporator cell in a building with an operating area and sampling gallery.

The proposed new waste collection and transfer system in Melton Valley will provide for collection of intermediate-activity waste from each facility in that valley in a central station composed of two 15,000-gal stainless steel tanks. These tanks would be evacuated through a 2-in.-dia underground cast iron line to the concrete tank farm in Bethel Valley. The low-activity wastes requiring decontamination before discharge would be pumped from retention basins at the various facilities through 6-in.-dia cast-iron lines to the equalization basin in Bethel Valley. As an alternative, either waste stream may, in an emergency, be routed to the existing 3,000,000-gal impoundment basin or to the seepage trenches in lower Melton Valley.

The decision as to how to best modify the low-activity waste treatment facilities to afford decontamination factors as great as 10^3 on 750,000 gal/day of waste will await results of pilot plant studies being carried out with ion exchange using synthetic phenolic resins and with vermiculite and natural zeolites.

26. APPENDIX. LIST OF PUBLICATIONS AND SPEECHES

POWER REACTOR FUEL PROCESSES

Bradley, M. J., and L. M. Ferris, "Recovery of Uranium and Thorium from Graphite Fuel Elements. I. Grind-Leach Process," *Nuc. Sci. Eng.* 8, 432 (1960).

Bradley, M. J., and L. M. Ferris, "Recovering Uranium from Graphite Fuel Elements," *Ind. Eng. Chem.* 53, 279 (1961).

Ferris, L. M., "Ammonium Fluoride-Uranyl Fluoride-Water System," *J. Chem. Eng. Data* 5, 241 (1960).

Ferris, L. M., and A. H. Kibbey, "Sulfex-Thorex and Darex-Thorex Processes for the Dissolution of Consolidated Edison Power Reactor Fuel: Laboratory Development," ORNL-2934 (Oct. 26, 1960).

Ferris, L. M., "Zirflex Process for PWR Blanket Fuel. II. Revised Flowsheet," ORNL-2940 (Oct. 26, 1960).

Ferris, L. M., J. W. Ullmann, A. H. Kibbey and J. F. Land, "Three-Minute Irradiation at Variable Power Density of Prototype CETR Fuel Pellets," ORNL-2999 (Sept. 28, 1960).

Ferris, L. M., "Aqueous Processes for Dissolution of Uranium-Molybdenum Alloy Reactor Fuel Elements," ORNL-3068 (in press).

Finney, B. C., and B. A. Hannaford, "Sulfex Process: Engineering-Scale Semicontinuous Decladding of Unirradiated Stainless Steel-Clad UO_2 and UO_2-ThO_2," ORNL-3072 (Mar. 21, 1961).

Gens, T. A., and R. L. Jolley, "New Laboratory Developments in the Zircex Process," ORNL-2992 (Apr. 10, 1961).

Gens, T. A., "New Developments in Uranium-Zirconium Alloy Fuel Reprocessing," *Nuc. Sci. Eng.* 9, 488 (1961).

Gens, T. A., "An Oxyhydrochlorination Process for Preparing Uranium-Molybdenum Reactor Fuels for Solvent Extraction: Laboratory Development," ORNL-3019 (May 8, 1961).

Gens, T. A., "Measurement of Hazardous Components of Darex Process Off-Gas," ORNL-3022 (Apr. 17, 1961).

Gens, T. A., "Consolidated Edison Fuel Losses on Exposure to Irradiated and Aerated Sulfex and Darex Decladding Solutions," ORNL-3023 (Apr. 18, 1961).

Goode, J. H., and J. R. Flanary, "Laboratory Development of a Tributyl Phosphate Solvent Extraction Process for Processing 20% Enriched Uranium Alloy Fuel," ORNL-2855 (May 16, 1961).

Guthrie, C. E., "Radiochemical Reprocessing Costs in an Expanding Nuclear Economy," *Nuclear Engineering. Part VIII*, Vol. 56, No. 28, p 30, 1960.

McDuffee, W. T., "Power Reactor Fuel Processing Pilot Plant: Brookhaven Fuel Program," ORNL-3013 (Dec. 1, 1960).

Messing, A. F., and O. C. Dean, "Removal of Silica from Darex Dissolver Solutions," ORNL-3000 (Dec. 27, 1960).

Rainey, R. H., and J. G. Moore, "Laboratory Development of the Acid Thorex Process for Recovery of Thorium Reactor Fuel," *Nuc. Sci. Eng.* (in press).

Rainey, R. H., and J. G. Moore, "Laboratory Development of the Acid Thorex Process for the Recovery of Consolidated Edison Thorium Reactor Fuel," ORNL-3155 (in press).

Warren, K. S., "Survey of Potential Vapor-Phase Explosions in Darex and Sulfex Processes," ORNL-2937 (Dec. 27, 1960).

Watson, C. D., G. A. West, W. F. Schaffer, B. B. Klima, and J. B. Adams, "Mechanical Dejacketing of SRE Fuel," TID-7599, Book 2, 8th Hot Laboratory and Engineering Conference, San Francisco, Dec. 13–15, 1960, p 337.

FUSED SALT–FLUORIDE VOLATILITY PROCESS

Carr, W. H., "Volatility Processing of the ARE Fuel," *Nuclear Engineering. Part VIII*, Vol. 56, No. 28, 57 (1960).

Groves, F. R., Jr., "Measurement of Dissociation Pressure of Molybdenum Fluoride–Sodium Fluoride Complex," ORNL-3088 (Mar. 28, 1961).

Milford, R. P., S. Mann, J. B. Ruch, and W. H. Carr, Jr., "Recovering Uranium Submarine Reactor Fuels," *Ind. Eng. Chem.* **53**, 357 (1961).

HOMOGENEOUS REACTOR FUEL PROCESSING

Chilton, J. M., and R. E. Leuze, "Development of Processing Methods for the Uranyl Sulfate Blanket Solution of a Homogeneous Reactor," *Nuclear Engineering. Part VIII*, Vol. 56, No. 28, 62 (1960).

WASTE TREATMENT AND DISPOSAL

Hancher, C. W., H. W. Godbee, J. T. Roberts, and J. J. Perona, "Solidification of Radioactive Liquid Waste by Pot Calcination," TID-7599, 8th Hot Laboratory and Engineering Conference, San Francisco, Dec. 13–15, 1960.

Roberts, J. T., and H. W. Godbee, "Laboratory Development of a Pot Calcination Process for Converting Liquid Wastes to Solids," ORNL-2986 (in press).

Roberts, J. T., and R. R. Holcomb, "A Phenolic Resin Ion Exchange Process for Decontaminating Low-Radioactivity-Level Process Water Wastes," ORNL-3036 (Mar. 17, 1961).

FUEL CYCLE DEVELOPMENT

Dean, O. C., W. S. Ernst, D. E. Ferguson, P. A. Haas, and K. H. McCorkle, "Preparation of High-Density Oxides and Vibratory Compaction in Fuel Tubes," ORNL-2965 (Jan. 27, 1961).

"Fuel Cycle Development: Semiannual Progress Report for Period Mar. 31, 1961," ORNL-3142 (in press).

SOLVENT EXTRACTION TECHNOLOGY

Arnold, W. D., and D. J. Crouse, "Further Evaluation of Amines as Extractants for Uranium from Sulfate Liquors," ORNL-3030 (Dec. 28, 1960).

Coleman, C. F., F. A. Kappelmann, and B. Weaver, "Solvent Extraction Recovery of Technetium, Neptunium, and Uranium from Fluorination Plant Residues," *Nuc. Sci. Eng.* 8, 507 (December 1960).

Davis, W., Jr., "Solubilities of Uranyl and Iron(III) Dibutyl and Monobutyl Phosphates in TBP Solvent Extraction Studies," ORNL-3084 (Mar. 1, 1961).

Horner, D. E., and C. F. Coleman, "Plutonium Extraction from Nitrate and Sulfate Solutions by Amines and Organophosphorus Compounds," ORNL-3051 (Feb. 23, 1961).

Hurst, F. J., and D. J. Crouse, "Recovery of Uranium from Amine Extractants with Ammonium Carbonate," ORNL-3064 (Feb. 15, 1961).

McDowell, W. J., and K. A. Allen, "Thorium Extraction by Di-*n*-decylamine Sulfate in Benzene," *J. Phys. Chem.* **65** (1961). (To be published in August).

Peterson, S., "The Reaction Between Thenoyltrifluoroacetone and its Uranyl Complex in Benzene," *J. Inorg. Nucl. Chem.* **14**, 126 (1960).

Ryon, A. D., "McCabe-Thiele Graphical Solution of Uranium-Thorium Partitioning from 30% TBP-Amsco Solvent," ORNL-3045 (Jan. 17, 1961).

Seeley, F. G., and D. J. Crouse, "Recovery of Uranium from Amines by the High Nitrate–Water Stripping Method," ORNL-3071 (May 25, 1961).

Weaver, B., and D. E. Horner, "Distribution Behavior of Neptunium and Plutonium Between Acid Solutions and Some Organic Extractants," *J. Chem. Eng. Data* **5**, 260 (1960).

CHEMICAL ENGINEERING RESEARCH

Bresee, J. C., F. S. Patton, Jr., M. W. Rosenthal, and M. E. Whatley, "Chemical Engineering Problems: Nuclear Engineering. II," Am. Inst. of Chemical Engineers, New York, 1960.

Chester, C. V., and J. S. Newman, "Interfacial Area Measurement in Liquid-Liquid Systems by Radioisotopes. II. The Use of a Liquid Scintillator," ORNL-3018 (Jun. 19, 1961).

Chester, C. V., "An Investigation of the Transfer of Uranyl Nitrate Across the Water–Tributyl Phosphate Interface Using the Method of Photographic Photometry," ORNL-3109 (May 25, 1961).

INSTRUMENTATION

Mackey, T. S., "Inline Densimeter for Pulsed Column Liquid Density, Pulse Amplitude, and Pulse Frequency Measurements," ORNL-3129 (in press).

MISCELLANEOUS

"Chemical Technology Division Annual Progress Report for Period Ending Aug. 31, 1960," ORNL-2993 (Sept. 23, 1960).

Baybarz, R. D., "Recovery of Np^{237} by an Oxidation-Reduction Fluoride Precipitation Method," ORNL-3055 (Mar. 21, 1961).

Baybarz, R. D., "Preparation of Americium Dioxide by Thermal Decomposition of Americium Oxalate in Air," ORNL-3003 (Dec. 5, 1960).

Bresee, J. C., review of the book by the Franklin Institute and the American Nuclear Society, *Gas-Cooled Reactors*, J. Franklin Inst. Philadelphia, 1960, reviewed for *J. Nucl. Energy*, Pergamon Press, London.

Bresee, J. C., "Redox Dissolver Incident: Comprehensive Report (Hanford)," to be published in *Nuclear Safety*.

Carr, W. H., "Decontamination Hazards," *Nuclear Safety* **2**, No. 2, 48 (1960).

Davis, W., Jr., W. H. Baldwin, and A. B. Meservey, "Chemistry of the Intercycle Evaporator Incident of November 20, 1959," ORNL-2979 (Nov. 9, 1960).

Dean, O. C., "Production of Uranium Metal from UF_6 by Direct Reduction with Lithium or Sodium Amalgam," ORNL-2770 (Apr. 18, 1961).

Ferris, L. M., "Lead Nitrate-Nitric Acid-Water System," *J. Chem. Eng. Data* **5**, 242 (1960).

King, L. J., and W. T. McCarley, "Plutonium Release Incident of November 20, 1959," ORNL-2989 (Feb. 1, 1961).

Scott, C. D., J. B. Adams, and J. C. Bresee, "Fluorox Process: Production of UF_6 in a Fluidized Bed Reactor," ORNL-2797 (Oct. 13, 1960).

Scott, C. D., "Direct Reduction of Uranium Hexafluoride to Uranium Metal by Sodium (Druhm Process)," ORNL-3012 (May 10, 1961).

Scott, C. D., "Kinetics of the Catalyzed Oxidation of Hydrogen, Carbon Monoxide, and Methane by Oxygen in a Flowing Stream of Helium," ORNL-3043 (Jan. 7, 1961).

MONTHLY PROGRESS REPORTS

Chemical Technology Division Chemical Development Section B Monthly Progress Reports:

For August 1960, ORNL-CF-60-9-108

For September 1960, ORNL-CF-60-10-91

For October 1960, ORNL-CF-60-11-87

For November 1960, ORNL-CF-60-12-99

For December 1960, ORNL-CF-60-12-100

For January 1961, ORNL-CF-61-2-61

For February 1961, ORNL-CF-61-3-50

For March 1961, ORNL-CF-61-4-108

Chemical Technology Division Chemical Development Section C Monthly Progress Reports:

For August–September 1960, ORNL-CF-60-9-119

For October–November 1960, ORNL-CF-60-11-126

For December 1960–January 1961, ORNL-CF-61-1-106

For February–March 1961, ORNL-CF-61-3-141

Chemical Technology Division Process Design Status Reports:

For August 1960, ORNL-CF-60-9-92

For September 1960, ORNL-CF-60-10-121

For October 1960, ORNL-CF-60-11-116

For November 1960, ORNL-CF-60-12-95

For December 1960, ORNL-CF-61-1-80

For January 1961, ORNL-CF-61-3-54

For February 1961, ORNL-CF-61-4-92

For March 1961, ORNL-CF-61-5-20

Chemical Technology Division Unit Operations Section Monthly Reports:

For August 1960, ORNL-CF-60-8-86

For September 1960, ORNL-CF-60-9-43

For October 1960, ORNL-CF-60-10-49

For November 1960, ORNL-CF-60-11-38

For December 1960, ORNL-CF-60-12-28

For January 1961, ORNL-CF-61-1-27

For February 1961, ORNL-CF-61-2-65

SPEECHES

IAEA Conference, Vienna, Austria, Sept. 5–9, 1960

Ullmann, J. W., "Some Major Fuel Cycle Problems" (ORNL-CF-60-7-75).

ACS Meeting, New York, New York, Sept. 11–16, 1960

Allen, K. A., and W. J. McDowell, "The Thorium Sulfate Complexes from Di-*n*-decylamine Sulfate Extraction Equilibria," (ORNL-CF-60-5-46).

Blake, C. A., A. T. Gresky, and J. M. Schmitt, "New Studies of Chemical and Radiation Effects on Recovery of TBP Process Solvents" (ORNL-CF-60-5-37).

Bond, W. D., "Thermogravimetric Study of the Kinetics of the Reduction of Cupric Oxide by Hydrogen" (ORNL-CF-60-5-61).

Bradley, M. J., and L. M. Ferris, "Recovery of Uranium from Graphite Fuel Elements. III. Disintegration and Leaching with 90% Nitric Acid" (ORNL-CF-60-3-65).

Holcomb, R. R., and J. T. Roberts, "A Phenolic Resin Ion Exchange Process for Decontaminating Low-Radioactivity-Level Process Water Wastes" (ORNL-CF-60-8-103).

McDowell, W. J., and K. A. Allen, "Thorium Extraction by Di-*n*-decylamine Sulfate in Benzene" (ORNL-CF-60-5-42).

Milford, R. P., S. Mann, J. B. Ruch, and W. H. Carr, Jr., "Modifications to the Oak Ridge Fluoride Volatility Pilot Plant for Recovering Uranium from Irradiated Submarine Reactor Fuel Elements" (ORNL-CF-60-5-81).

Wischow, R. P., and D. E. Horner, "Recovery of Strontium and Rare Earths from Purex Wastes by Solvent Extraction with D2EHPA" (ORNL-CF-60-5-36).

AIChE Meeting, Sept. 25–28, 1960, Tulsa, Oklahoma

Culler, Vaughn (Corning Glass Works), C. D. Watson, and G. A. West (ORNL), "Gamma Radiation Effects on Corning Code 7740 and Code 7900 Glasses" (ORNL-CF-60-3-112).

E. E. Stansbury (Univ. of Tennessee), W. C. Yee, and G. H. Jenks (ORNL), "Fission Fragment Recoil Effects on Zirconium Oxidation" (ORNL-CF-60-3-45).

Second AEC Working Meeting, Fixation of Radioactive Wastes in Stable, Solid Media, Idaho Falls, Idaho, Sept. 27–29, 1960

Blomeke, J. O., "Conversion of Waste to Solids by Pot Calcination" (ORNL-CF-60-9-41).

Clark, W. E., "Corrosion Problems in Pot Calcination of High-Level Radioactive Wastes," (ORNL-CF-60-9-38).

Perona, J. J., "Particulate Attenuation in a Packed Distillation Tower," (ORNL-CF-60-9-33).

Perona, J. J., and M. E. Whatley, "Calculation of Temperature Rise in Deeply Buried Radioactive Cylinders" (ORNL-CF-60-9-39).

Roberts, J. T., "Off-Gas Problems in Pot Calcination" (ORNL-CF-60-9-45).

Mathematical Analyses of Atomic Energy Operations, Meeting Held in Germantown, Maryland, Dec. 2, 1960

Whatley, M. E., and L. E. McNeese, "Use of Electronic Computers in Nuclear Chemical Engineering Problems" (ORNL-CF-60-11-100).

AIChE Symposium on Nuclear Chemical Plant Safety, Washington, D.C., December 4–7, 1960

Blomeke, J. O., and L. B. Shappert, "Radiochemical Processing: Off-Site Transportation and Ultimate Storage Problems" (ORNL-CF-60-7-95).

ANS Meeting, San Francisco, California, Dec. 12–15, 1960

Bresee, J. C., and L. J. King, "Plutonium Release Incident at Oak Ridge National Laboratory" (ORNL-CF-60-9-57).

Dean, O. C., and A. F. Messing (Argonne National Lab), "Hermex Process: The Solubilities of Selected Metals in Mercury" (ORNL-CF-60-8-107).

Gens, T. A., and R. E. Blanco, "Modified Zirflex Process for Dissolution of 1–10% U-Zr Alloy Fuels in Aqueous NH_4F-NH_4NO_3-H_2O_2" (ORNL-CF-60-8-112).

Hancher, C. W., H. W. Godbee, J. T. Roberts, J. J. Perona, and J. O. Blomeke, "Solidification of Radioactive Liquid Waste by Pot Calcination" (ORNL-CF-60-8-89).

McCorkle, K. H., O. C. Dean, and C. E. Schilling, "Preparation of Dense Thorium and Thorium-Uranium Oxide Particles for Vibratory Compaction Loading of Fuel Elements" (ORNL-CF-60-8-111).

Moore, J. G., and R. H. Rainey, "Chemical Feasibility of Nuclear Poisons in Uranium-Thorium Fuel Processing Systems" (ORNL-CF-60-8-115).

Rainey, R. H., and J. G. Moore, "Extraction of Thorium and Uranium from Spent Reactor Fuel Solutions by Tributyl Phosphate-Amsco Using Nitric Acid as the Salting Agent" (ORNL-CF-60-8-110).

Watson, C. D., G. A. West, W. F. Schaffer, B. B. Klima, and J. B. Adams, "Mechanical Dejacketing of SRE Fuel" (ORNL-CF-60-5-56).

ACS Meeting, St. Louis, Mo., Mar. 28, 1961

Allen, K. A., and A. L. Myers, "A Vapor Pressure Apparatus for Organic Solutions" (ORNL-CF-60-11-33).

10th Annual AEC Corrosion Symposium, San Diego, California, May 8–11, 1961

Clark, W. E., "Materials of Construction for Multi-Purpose Aqueous Fuel Reprocessing Plants" (ORNL-CF-61-4-64).

6th Nuclear Congress: Symposium on Thorium Fuel Cycle, Rome, Italy, June 13–15, 1961

Blanco, R. E., L. M. Ferris, and D. E. Ferguson, "Aqueous Processing of Thorium Fuels" (ORNL-CF-61-6-14).

Ferguson, D. E., E. D. Arnold, and W. S. Ernst, Jr., "Preparation and Fabrication of ThO_2 Fuels" (ORNL-CF-61-6-114)

SEMINARS

1960

Sept. 6	Effects of Radiation on Catalysts	N. A. Krohn, R. G. Wymer
Oct. 11	Problems in the Transuranium Program	R. D. Baybarz, M. H. Lloyd
Oct. 18	Computer Simulation of Solvent Extraction Columns	T. J. Walsh, Case Inst. Tech.
Oct. 25	Clean-up of the HILAC Incident	J. E. Rainey, U. Calif., Berkeley
Nov. 1	Report on Vienna Conference	J. W. Ullmann
Nov. 8	Digital Computer Simulation of Thorium Dioxide Pellet Dissolution	M. E. Whatley
Nov. 15	Conversion of Enriched UF_6 to Metal	F. M. Tench, Y-12 Tech. Div.
Dec. 6	Methods for Evaluating Radiochemical Facility Hazards	J. P. Nichols
Dec. 13	High-Temperature Corrosion of Some Metals and Ceramics in Fluorinating Atmospheres	C. F. Hale, ORGDP Tech. Div.

Dec. 20	The Role of XO_4^{n-} Inhibitors in Passivation	G. H. Cartledge, Chem. Div.
Dec. 27	Alkyl Amines as Extractants in Nitrate Systems	V. C. Vaughen
1961		
Jan. 10	Shielding Design Calculation Code	E. D. Arnold
Jan. 17	Speculations on Nature's Laws and the Universal Constants	A. T. Gresky
Jan. 24	Transuranium Laboratory: General Introduction	W. E. Unger
	Bldg. 4507 Process Development Cubicle	B. B. Klima
	Preliminary Design Description	B. F. Bottenfield
Jan. 31	O^{17} Pilot Plant: General Introduction	J. S. Drury, Chem. Div.
	Design	H. O. Weeren
Feb. 7	Recovery of Unirradiated Scrap	J. R. Barkman, J. S. Reece, Y-12 Chem. Operations
Feb. 14	Power Plants for Ion Propulsion of Space Vehicles	A. P. Fraas, Reactor Projects
Feb. 21	Direct Energy Conversion	R. G. Wymer
	Potable Water Production from Saline Water	W. K. Eister
Feb. 28	Status of the Volatility Pilot Plant: Introduction	R. B. Lindauer
	Process and Equipment Performance	W. H. Carr, Jr.
	Analysis of Data	E. C. Moncrief
Mar. 7	Genetic Effects of Radiation on Plants	M. J. Constantin, U.T. Ag. Farm
Mar. 14	Final Cycle Plutonium Extraction by Amines	C. F. Coleman
Mar. 21	Transuranium Program: Operating Philosophies	E. J. Frederick
	Mechanical Design Program	F. L. Hannon
	Equipment Development Program	G. K. Ellis
Mar. 28	Transuranium Process Development: HFIR Target Development	E. S. Bomar, Metallurgy
	Anion Exchange	M. H. Lloyd
	Solvent Extraction	R. D. Baybarz
Apr. 11	Low-Level Waste Treatment by Scavenging-Ion Exchange	R. R. Holcomb
	Design of Pilot Plant	J. M. Holmes
Apr. 18	Preparation of Thorium and Thorium-Uranium Oxides	O. C. Dean
	Laboratory Compaction Status Report	W. S. Ernst, Jr.
Apr. 25	Fixation of High-Level Wastes in Solid Media: Ruthenium by Phosphite Addition	W. E. Clark

	Optimization of Solid Product	H. W. Godbee
May 2	New Solvent Studies and Extraction Performance of Degraded Process Extractants	C. A. Blake
May 16	Gas Recombination Catalysis in Aqueous Reactor Slurries: Introduction and Status	J. P. McBride
	Experimental Method	W. L. Pattison
	Reaction Kinetics	L. E. Morse
May 23	Foam Separation Process	W. Davis, Jr. E. Schonfeld
May 29	Modified Zirflex Process for Dissolution of Zirconium-Uranium Alloy Fuels	T. A. Gens, F. G. Kitts

THIS PAGE

WAS INTENTIONALLY

LEFT BLANK

CHEMICAL TECHNOLOGY DIVISION

F. L. CULLER, DIRECTOR
VIRGINIA WELLS, SECRETARY
NANCY ELLISON, SECRETARY
W. K. EISTER, TECHNICAL ASSISTANT†
LUCRETIA REED, SECRETARY
MARTHA GERRARD, REPORTS EDITOR

LONG RANGE PLANNING COMMITTEE
A. T. GRESKY
E. D. ARNOLD
C. E. GUTHRIE, RADIATION OFFICER
J. T. ROBERTS
J. W. ULLMANN
FRANCES QUILLEN, SECRETARY
TECHNICIAN
P. P. HAYDON

C. W. SCHERSTEN, ADMINISTRATIVE ASSISTANT TO DIRECTOR†
RUTH TEMPLIN, SECRETARY
H. B. GRAHAM, ADMINISTRATIVE ASSISTANT
LUCILLE KUYKENDALL, SECRETARY
W. O. GREEVER, PROCUREMENT
J. W. CLARK, PROCUREMENT†

APPLIED RESEARCH GROUP
R. G. WYMER
N. A. KROHN
TECHNICIAN
D. M. HELTON

CHEMICAL DEVELOPMENT SECTION A

D. E. FERGUSON, SECTION CHIEF
JOANNE MAYES, SECRETARY
IMOGENE LOOPE, SECRETARY
C. F. KECK, TECHNICIAN

THORIUM OXIDE STUDIES
J. P. McBRIDE, GROUP LEADER
L. E. MORSE
W. L. PATTISON

ALPHA-ACTIVE MATERIALS PROCESSING
R. E. LEUZE, GROUP LEADER
R. D. BAYBARZ, PROBLEM LEADER, *TRANSURANICS*
M. H. LLOYD
J. M. CHILTON, *U^{232} PREPARATION*
TECHNICIANS
R. L. HICKEY
S. J. MOTTEN
O. K. TALLENT
J. T. WIGGINS

EQUIPMENT DECONTAMINATION
A. B. MESERVEY, PROBLEM LEADER
TECHNICIAN
D. H. NEWMAN

FLUORIDE VOLATILITY PROCESSING
G. I. CATHERS, GROUP LEADER
R. L. JOLLEY, PROBLEM LEADER, *HOT CELL OPERATIONS*
D. O. CAMPBELL, PROBLEM LEADER, *MSR FUEL PROCESSING*
M. R. BENNETT
H. F. SOARD
TECHNICIANS
T. E. CRABTREE
C. J. SHIPMAN

FUEL CYCLE STUDIES AND THORIUM BLANKET STUDIES
O. C. DEAN, GROUP LEADER
A. T. KLEINSTEUBER
K. H. McCORKLE
C. E. SCHILLING
TECHNICIAN
C. W. GREENE

CHEMICAL DEVELOPMENT SECTION B

R. E. BLANCO, SECTION CHIEF
RUTH WILLIAMS, SECRETARY
PHYLLIS MARKS, SECRETARY
J. E. FARMER, DRAFTSMAN
J. R. FLANARY,* *HOT CELL SUPERVISOR*
J. A. McLAREN,† SPECIAL ASSIGNMENT

MECHANISMS OF SEPARATION METHODS, ION EXCHANGE, FOAM SEPARATION
W. DAVIS, JR., PROBLEM LEADER
ERNESTO SCHONFELD[1]
W. C. YEE
J. FLINT[2]
TECHNICIAN
C. T. THOMPSON

WASTE TREATMENT AND DISPOSAL
W. E. CLARK,* PROBLEM LEADER
H. W. GODBEE
H. H. HOLCOMB
TECHNICIANS
G. D. DAVIS
W. E. SHOCKLEY

CANE
W. D. BOND, PROBLEM LEADER
TECHNICIAN
J. F. TALLEY

POWER REACTOR FUEL PROCESSING
J. R. FLANARY,* PROBLEM LEADER, *FLOWSHEET DEMONSTRATION ON RADIOACTIVE FUELS*
J. H. GOODE
C. P. JOHNSTON†
TECHNICIANS
L. A. BYRD
R. C. SHIPWASH
G. E. WOODALL

L. M. FERRIS, PROBLEM LEADER, *HEAD END PROCESSING*
M. J. BRADLEY
T. A. GENS
A. H. KIBBEY
K. S. WARREN
TECHNICIANS
E. R. JOHNS
J. F. LAND

W. E. CLARK,* PROBLEM LEADER, *CORROSION STUDIES*
R. H. RAINEY, PROBLEM LEADER, *SOLVENT EXTRACTION STUDIES*
J. G. MOORE
M. K. T. NAIR[2]
T. AOCHI[2]
TECHNICIAN
R. C. LOVELACE

CHEMICAL DEVELOPMENT SECTION C

K. B. BROWN, SECTION CHIEF
MABLE GUINN, SECRETARY

PROCESSING OF URANIUM AND THORIUM ORES AND CONCENTRATES
D. J. CROUSE, GROUP LEADER
W. D. ARNOLD
F. J. HURST
F. G. SEELEY

SOLVENT EXTRACTION TECHNOLOGY
K. A. ALLEN,** GROUP LEADER, *FUNDAMENTAL CHEMISTRY*
W. J. McDOWELL
A. L. MYERS[1]
TECHNICIAN
G. N. CASE

C. A. BLAKE, GROUP LEADER, *PROPERTIES AND BEHAVIOR OF REAGENTS AND DILUENTS IN RADIOCHEMICAL PROCESSING*
(A. T. GRESKY* ASSISTING)
J. M. SCHMITT
R. G. MANSFIELD††
TECHNICIAN
W. E. OXENDINE

C. F. COLEMAN, GROUP LEADER, *PLUTONIUM PROCESSING AND SPECIAL ASSIGNMENTS*
F. A. KAPPELMANN

B. S. WEAVER, GROUP LEADER, *TRANSURANIUMS AND OTHER METAL SEPARATIONS*
TECHNICIANS
J. P. EUBANKS
J. A. COLLINS

FISSION PRODUCT RECOVERY
R. P. WISCHOW,* GROUP LEADER
D. E. HORNER
TECHNICIANS
M. J. BARTLETT
W. R. HOWERTON

UNIT OPERATIONS SECTION

M. E. WHATLEY, SECTION CHIEF
C. V. CHESTER, SPECIAL ASSIGNMENT
L. J. KING, SPECIAL ASSIGNMENT
J. J. PERONA, LONG-TERM WASTE STUDIES
J. T. LONG, BOOK PREPARATION
PAULA P. MAYS, SECRETARY
MARTHA M. DAWSON, SECRETARY
MILDRED I. SWANK, SECRETARY

FUEL CYCLE STUDIES AND THORIUM UTILIZATION
P. A. HAAS,* GROUP LEADER
J. W. SNIDER
S. D. CLINTON
C. C. HAWS, JR.
TECHNICIAN
R. D. ARTHUR

TRANSURANICS
P. A. HAAS,* GROUP LEADER
T. S. MACKEY
G. K. ELLIS†

FLUORIDE VOLATILITY PROCESS
R. W. HORTON, GROUP LEADER
L. E. McNEESE
W. W. PITT
J. D. MOTTLEY[1]
R. J. McNAMEE††
S. H. STAINKER††
TECHNICIANS
J. BEAMS
V. L. FOWLER
T. D. NAPIER††
F. N. McLAIN†

SOLVENT EXTRACTION DEVELOPMENT AND FISSION PRODUCT RECOVERY
A. D. RYON, GROUP LEADER
F. L. DALEY
R. S. LOWRIE
W. M. WOODS
M. G. BAILLIE[2]
A. N. PRASAD[2]
TECHNICIANS
G. JONES, JR.
F. G. KILPATRICK
K. LADO
C. H. TIPTON

GAS COOLED REACTOR PURIFICATION STUDIES
J. C. SUDDATH,* GROUP LEADER
C. D. SCOTT
TECHNICIANS
R. O. PAYNE
W. G. SISSON

ION EXCHANGE
J. C. SUDDATH,* GROUP LEADER
S. H. JURY[2]
J. S. WATSON
TECHNICIAN
D. A. McWHIRTER

WASTE PROCESSING STUDIES
J. C. SUDDATH,* GROUP LEADER
C. W. HANCHER
TECHNICIAN
J. S. TAYLOR

POWER REACTOR FUEL PROCESSING
C. D. WATSON, GROUP LEADER
B. C. FINNEY, *MECHANICAL PROCESSING*
G. A. WEST
J. B. ADAMS††

F. G. KITTS, *CHEMICAL HEAD-END*
B. A. HANNAFORD
H. F. JOHNSON[4]
TECHNICIANS
J. C. ROSE
D. K. WILLIS††
G. B. DINSMORE
F. L. ROGERS

PROCESS DESIGN SECTION

H. E. GOELLER, SECTION CHIEF
W. E. UNGER,* ASSISTANT SECTION CHIEF
E. M. SHANK, *EUROCHEMIC ASSISTANCE*
W. M. SPROULE, TECHNICIAN
J. W. LANDRY, *CANE PROJECT*
A. M. ROM, *BUILDING 4507 CONTAINMENT*
W. G. STOCKDALE, *ECONOMIC STUDIES*
A. R. IRVINE, *U^{233} METALLURGICAL DEVELOPMENT LABORATORY*
W. G. STOCKDALE,* *CHEMICAL DEVELOPMENT HOT CELLS ADDITION*
W. R. WINSBRO, *HIGH RADIATION LEVEL ANALYTICAL LABORATORY*
MAY BERGEN, STENOGRAPHER
NELLINE ROSS, SECRETARY
ALICE McWILLIAMS, SECRETARY
BEVERLY CANTRELL, SECRETARY

POWER REACTOR FUEL PROCESSING
E. L. NICHOLSON, *PROBLEM LEADER AND LIAISON WITH ICPP*
W. F. SCHAFFER, *MECHANICAL PROCESSING OF FUELS*
I. R. SHAPPERT, *FUEL SHIPPING STUDY*
A. N. SINGHAL[2]

FLUORIDE VOLATILITY PROCESS
R. P. MILFORD, PROBLEM LEADER
TECHNICIANS
R. L. BOLES
M. O. SMITH

TRANSURANIUM PROGRAM
W. E. UNGER,* GROUP LEADER
B. F. BOTTENFIELD,* *BUILDING 7511 DESIGN*
G. B. BERRY
E. J. FREDERICK, *PROCESS STUDIES*
F. L. HANNON, *MECHANICAL STUDIES*
B. B. KLIMA, *TEST EQUIPMENT DESIGN*
J. P. NICHOLS, *SHIELDING AND RADIATION STUDIES*

WASTE STUDIES
J. O. BLOMEKE, PROBLEM LEADER
J. M. HOLMES, *ION EXCHANGE PILOT PLANT AND CALCINATION PILOT PLANT*
F. C. McCULLOUGH†
R. C. WADHWA[2]
S. FUJII[2]
W. R. WHITSON
F. N. BROWDER, *MELTON VALLEY WASTES*
H. O. WEEREN, *WASTE TANKS AND EVAPORATOR*
F. E. HARRINGTON, *WASTE TANKS AND EVAPORATOR*

PROJECT ENGINEERING
B. F. BOTTENFIELD,* PROBLEM LEADER
P. L. ROBERTSON

DRAFTSMEN
J. H. MANNEY, CHIEF
EVELYN BRIDGES
J. W. DAY
J. D. CLIPP
W. L. ELLISON
H. W. FALLON
A. J. FARMER
L. C. HUBBARD
R. R. MANIGOLD
A. B. OLDHAM
J. D. PHILLIPS
J. H. THOMPSON
J. N. WHEELER

PILOT PLANT SECTION

J. C. BRESEE, SECTION CHIEF
W. H. LEWIS,* ASSISTANT SECTION CHIEF
R. B. LINDAUER[5]
BOBBIE HOYLE, SECRETARY
L. M. JOHNSON, SECRETARY†
P. G. PARKER, CLERK††
R. B. WATERS, DRAFTSMAN

HOMOGENEOUS REACTOR FUEL PROCESSING
W. D. BURCH, GROUP LEADER, *HRT CHEMICAL PLANT*
U. U. TARBIU
R. J. SHANNON
TECHNICIANS
W. T. BOSTIC
E. W. BROWN
W. A. LINDSEY

POWER REACTOR FUEL PROCESSING
J. L. MATHERNE,* GROUP LEADER, *ENGINEERING*
R. H. VAUGHAN†
C. D. HYLTON††
G. S. SADOWSKI††
R. E. BROOKSBANK, GROUP LEADER, *OPERATIONS*
J. R. PARROTT††
W. I. McDUFFEE
W. T. McCARLEY††
W. A. SHANNON, SUPERVISOR
D. E. SPANGLER†
D. H. SUMMERS
C. E. WADDELL††
B. J. STRADER††
TECHNICIANS
R. E. PURKEY
J. H. WALKER
OPERATORS
J. E. BACON††
J. V. BROCK†
H. D. CROSS††
R. M. DUFF†
W. DUNCAN†
B. G. DEVALL††
J. R. EBLEN†
J. M. GLASGOW†
W. K. GOODMAN†
C. T. RANKIN††
C. L. SHEPERD††
F. H. WATSON†

FLUORIDE VOLATILITY PROCESS
W. H. LEWIS,* GROUP LEADER
W. H. CARR, *OPERATIONS*
S. MANN
F. MILES
E. L. YOUNGBLOOD
J. L. MATHERNE*
E. C. MONCRIEF
R. G. NICOL
J. B. RUCH
TECHNICIANS
M. C. HILL
H. C. THOMPSON
OPERATORS
C. W. BOATMAN
E. C. BRANTLEY
J. H. BROCK
W. J. BRYAN
H. S. CALDWELL
J. H. GIBSON†
C. H. JONES
Z. R. McNUTT††
J. W. MEADE†
G. R. THOMPSON
A. V. WILDER††

	SCIENTIFIC	TECHNICAL	ADMINISTRATIVE AND CLERICAL	TOTAL
AVG. FOR FY 1961	147	95	29	271
JUNE 1, 1961	136	83	24	243

*DUAL CAPACITY
**DECEASED
†TERMINATED
††TRANSFERRED
[1]RESEARCH PARTICIPANT
[2]FOREIGN RESEARCH PARTICIPANT
[3]EMPLOYEE OF RADIATION APPLICATIONS, INC.
[4]CONSULTANT, U.T.
[5]ON LOAN TO MOLTEN SALT REACTOR PROJECT

THIS PAGE

WAS INTENTIONALLY

LEFT BLANK

INTERNAL DISTRIBUTION

1. C. E. Center
2. Biology Library
3–5. Central Research Library
6. Reactor Division Library
7–126. Laboratory Records Department
127. Laboratory Records, ORNL R.C.
128. A. M. Weinberg
129. J. P. Murray (K-25)
130. R. G. Jordan (Y-12)
131. J. A. Swartout
132. E. D. Shipley
133–134. F. L. Culler
135. W. H. Jordan
136. A. H. Snell
137. A. Hollaender
138. K. Z. Morgan
139. T. A. Lincoln
140. C. S. Harrill
141. C. E. Winters
142. H. E. Seagren
143. F. R. Bruce
144. M. E. Whatley
145. R. S. Livingston
146. C. D. Susano
147. H. E. Goeller
148. R. N. Lyon
149. R. B. Briggs
150. C. W. Hancher
151. R. E. Blanco
152. W. E. Unger
153. D. E. Ferguson
154. A. T. Gresky
155. G. E. Boyd
156. J. L. Gabbard
157. M. J. Skinner
158. J. S. Drury
159. E. D. Arnold
160. C. E. Guthrie
161. J. W. Ullmann
162. K. B. Brown
163. J. C. Bresee
164. T. H. Pigford (consultant)
165. D. L. Katz (consultant)
166. H. Worthington (consultant)
167. C. E. Larson (consultant)
168–169. ORNL – Y-12 Technical Library, Document Reference Section

EXTERNAL DISTRIBUTION

170. Sylvania Electric Products, Inc.
171. Division of Research and Development, AEC, ORO
172–681. Given distribution as shown in TID-4500 (16th ed., Rev.) under Chemical Separations Processes for Plutonium and Uranium category (75 copies – OTS)

Reports previously issued in this series are as follows:

ORNL-268	Period Ending May 31, 1949
ORNL-467	Period Ending August 31, 1949
ORNL-530	Period Ending November 30, 1949
ORNL-663	Period Ending February 28, 1950
ORNL-763	Period Ending May 31, 1950
ORNL-846	Period Ending August 31, 1950
ORNL-936	Period Ending November 20, 1950
ORNL-1000	Period Ending February 20, 1951
ORNL-1061	Period Ending May 20, 1951
ORNL-1141	Period Ending August 20, 1951
ORNL-1311	Period Ending February 10, 1952
ORNL-1328	Period Ending May 20, 1952
ORNL-1385	Period Ending August 20, 1952
ORNL-1448	Period Ending November 20, 1952
ORNL-1494	Period Ending February 20, 1953
ORNL-1561	Period Ending September 30, 1953
ORNL-1708	Period Ending March 31, 1954
ORNL-1800	Period Ending September 30, 1954
ORNL-1881	Period Ending March 31, 1955
ORNL-2000	Period Ending September 30, 1955
ORNL-2079	Period Ending March 31, 1956
ORNL-2169	Period Ending August 31, 1956
ORNL-2392	Period Ending August 31, 1957
ORNL-2576	Period Ending August 31, 1958
ORNL-2788	Period Ending August 31, 1959
ORNL-2993	Period Ending August 31, 1960